000

000 0156

TABLE OF CONTENTS

14. SAFETY ANALYSIS

Section		Page
14.1	CORE AND COOLANT BOUNDARY PROTECTION ANALYSIS	14.1-1
14.1.1	ABNORMALITIES	14.1-1
14.1.2	ANALYSIS OF EFFECTS AND CONSEQUENCES	14.1-2
14.1.2.1	Uncompensated Operating Reactivity Changes	14.1-2
14.1.2.1.1	Identification of Cause	14.1-2
14.1.2.1.2	Analysis and Results	14.1-3
14.1.2.2	Startup Accident	14.1-3
14.1.2.2.1	Identification of Cause	14.1-3
14.1.2.2.2	Methods of Analysis	14.1-4
14.1.2.2.3	Results of Analysis	14.1-4
14.1.2.3	Rod Withdrawal Accident From Rated Power Operation	14.1-6
14.1.2.3.1	Identification of Cause	14.1-6
14.1.2.3.2	Methods of Analysis	14.1-6
14.1.2.3.3	Results of Analysis	14.1-7
14.1.2.4	Moderator Dilution Accident	14.1-8
14.1.2.4.1	Identification of Cause	14.1-8
14.1.2.4.2	Analysis and Results	14.1-9
14.1.2.5	Cold Water Accident	14.1-10
14.1.2.6	Loss-of-Coolant Flow	14.1-10
14.1.2.6.1	Identification of Cause	14.1-10
14.1.2.6.2	Methods of Analysis	14.1-11
14.1.2.6.3	Results of Analysis	14.1-11
14.1.2.7	Stuck-Out, Stuck-In, or Dropped-In Control Rod	14.1-13
14.1.2.7.1	Identification of Cause	14.1-13
14.1.2.7.2	Analysis and Results	14.1-13
14.1.2.8	Loss of Electric Power	14.1-13
14.1.2.8.1	Identification of Cause	14.1-13
14.1.2.8.2	Results of "Blackout" Conditions Analysis	14.1-14
14.1.2.8.3	Analysis Results of Complete Loss of All Plant Power	14.1-15
14.1.2.9	Steam Line Failure	14.1-16
14.1.2.9.1	Identification of Cause	14.1-16
14.1.2.9.2	Analysis and Results	14.1-16
14.1.2.10	Steam Generator Tube Failures	14.1-19
14.1.2.10.1	Identification of Accident	14.1-19
14.1.2.10.2	Analysis and Results	14.1-19
14.2	STANDBY SAFEGUARDS ANALYSIS	14.2-1
14.2.1	SITUATIONS ANALYZED AND CAUSES	14.2-1
14.2.2	ACCIDENT ANALYSES	14.2-1
14.2.2.1	Fuel Handling Accidents	14.2-1
14.2.2.1.1	Identification of Accident	14.2-1
14.2.2.1.2	Analysis and Results	14.2-2

000 0157

00

14.2.2.2	Rod Ejection Accident	14.2-2
14.2.2.2.1	Identification of Accident	14.2-2
14.2.2.2.2	Method of Analysis	14.2-5
14.2.2.2.3	Analysis and Results	14.2-5
14.2.2.3	Loss-Of-Coolant Accident	14.2-8
14.2.2.3.1	Identification of Accident	14.2-8
14.2.2.3.2	Accident Bases	14.2-8
14.2.2.3.3	Accident Simulation	14.2-11
14.2.2.3.4	Accident Analysis	14.2-16
14.2.2.4	Maximum Hypothetical Accident	14.2-39
14.3	ENVIRONMENTAL CONSEQUENCES OF HYPOTHETICAL ACCIDENTS	14.3-1
14.3.1	GENERAL APPROACH	14.3-1
14.3.2	STEAM GENERATOR TUBE FAILURE	14.3-1
14.3.3	LOSS OF ELECTRIC POWER	14.3-1
14.3.4	STEAM LINE FAILURE	14.3-3
14.3.5	FUEL HANDLING ACCIDENT	14.3-4
14.3.6	ROD EJECTION ACCIDENT	14.3-4
14.3.7	WASTE GAS TANK RUPTURE	14.3-4
14.3.8	LOSS-OF-COOLANT ACCIDENT	14.3-5
14.3.8.1	Environmental Consequences	14.3-5
14.3.8.2	Effects of Reactor Building Purging	14.3-6
14.3.9	MAXIMUM HYPOTHETICAL ACCIDENT	14.3-6
14.3.9.1	The Source Term	14.3-6
14.3.9.2	Thyroid Dose	14.3-7
14.3.9.3	Direct Dose from Containment Building	14.3-7
14.3.9.4	Whole-Body Dose From the Cloud	14.3-8
14.3.9.5	Effects of Radiation Source From Pump Leakage During Maximum Hypothetical Accident	14.3-8
14.3.9.6	Rainout	14.3-8
14.3.9.7	Doses in the Control Room Following the MHA Accident	14.3-9
14.3.10	IODINE REMOVAL SENSITIVITY ANALYSIS	14.3-10
14.3.11	POPULATION DENSITY CONSIDERATIONS	14.3-12
14.4	REFERENCES	14.4-1

000 0158

000

LIST OF TABLES

Table Number	Title	Page
14.1-1	Abnormalities Affecting Core and Coolant Boundary	14.1-1
14.1-2	Uncompensated Reactivity Disturbances	14.1-3
14.2-1	Situations Analyzed and Causes	14.2-1
14.2-2	Core Flooding Tank Performance Data	14.2-20
14.2-3	Tabulation of Loss-of-Coolant Accident Characteristics for Spectrum of Hot Leg Rupture Sizes	14.2-25
14.2-4	Tabulation of Loss-of-Coolant Accident Characteristics for Spectrum of Cold Leg Rupture Sizes	14.2-26
14.2-5	Reactor Operating Conditions for Evaluation	14.2-29
14.2-6	Reactor Building Structure Data for Analysis of Time-Dependent Building Pressure	14.2-31
14.2-7	Summary of Reactor Building Pressure Analysis	14.2-33
14.3-1	Summary of Maximum Estimated Doses in Rems	14.3-2
14.3-2	Summary of the Sensitivity Analysis of Iodine Removal Showing the Effects of Parameter Variations	14.3-13
14.3-3	SMUD Site Population Distribution and Integrated Man-Rem Exposures	14.3-14

00

000 0159

LIST OF FIGURES

Figure Number	Title
14.1-1	Startup Accident from 10^{-9} Rated Power Using a 1.2% $\Delta k/k$ Rod Group; High Pressure Reactor Trip Is Actuated
14.1-2	Startup Accident from 10^{-9} Rated Power Using All Rods with a Worth of 10% $\Delta k/k$; High Flux Reactor Trip is Actuated
14.1-3	Peak Thermal Power versus Rod Withdrawal Rate for a Startup Accident from 10^{-9} Rated Power
14.1-4	Peak Neutron Power versus Rod Withdrawal Rate for a Startup Accident from 10^{-9} Rated Power
14.1-5	Peak Thermal Power versus Trip Delay Time for a Startup Accident Using a 1.2% $\Delta k/k$ Rod Group at 5.8×10^{-5} $(\Delta k/k)$ /sec from 10^{-9} Rated Power
14.1-6	Peak Thermal Power versus Doppler Coefficient for a Startup Accident Using a 1.2% $\Delta k/k$ Rod Group at 5.8×10^{-5} $(\Delta k/k)$/ sec from 10^{-9} Rated Power
14.1-7	Peak Thermal Power versus Trip Delay Time for a Startup Accident Using All Rods at 5.8×10^{-4} $(\Delta k/k)$/sec from 10^{-9} Rated Power
14.1-8	Peak Thermal Power versus Doppler Coefficient for a Startup Accident Using All Rods at 5.8×10^{-4} $(\Delta k/k)$/sec from 10^{-9} Rated Power
14.1-9	Peak Pressure versus Trip Delay Time for a Startup Accident Using All Rods at 5.8×10^{-4} $(\Delta k/k)$/sec from 10^{-9} Rated Power
14.1-10	Peak Pressure versus Tripped Rod Worth for a Startup Accident Using All Rods at 5.8×10^{-4} $(\Delta k/k)$/sec from 10^{-9} Rated Power
14.1-11	Peak Pressure versus Doppler Coefficient for a Startup Accident Using All Rods at 5.8×10^{-4} $(\Delta k/k)$/sec from 10^{-9} Rated Power
14.1-12	Peak Pressure versus Moderator Coefficient for a Startup Accident Using All Rods at 5.8×10^{-4} $(\Delta k/k)$/sec from 10^{-9} Rated Power
14.1-13	Rod Withdrawal Accident from Rated Power Using a 1.2% $\Delta k/k$ Rod Group at 5.8×10^{-5} $(\Delta k/k)$/sec; High Pressure Reactor Trip Is Actuated

000 0160 00

Figure Number	Title
14.1-14	Peak Pressure versus Rod Withdrawal Rate for a Rod Withdrawal Accident from Rated Power
14.1-15	Peak Pressure versus Trip Delay Time for a Rod Withdrawal Accident from Rated Power Using a 1.2% $\Delta k/k$ Rod Group; High Pressure Reactor Trip is Actuated
14.1-16	Peak Pressure versus Doppler Coefficient for a Rod Withdrawal Accident from Rated Power Using a 1.2% $\Delta k/k$ Rod Group
14.1-17	Maximum Neutron and Thermal Power for an All-Rod Withdrawal Accident from Various Initial Power Levels
14.1-18	Peak Fuel Temperature in Average Rod and Hot Spot for an All-Rod Withdrawal Accident from Various Initial Power Levels
14.1-19	Percent Reactor Coolant Flow as a Function of Time after Loss of Pump Power
14.1-20	Minimum DNBR Which Occurs during the Coastdown for Various Initial Power Levels
14.1-21	Reactor System Cooling Rate for a Steam Line Break of 4 $in.^2$
14.2-1	Percent Core Experiencing DNB as a Function of Ejected Control Rod Worth at Ultimate Power
14.2-2	Zr-H_2O Reaction as a Function of Ejected Control Rod Worth at Ultimate Power
14.2-3	Reactor Neutron Power Variation with Ejected Control Rod Worth
14.2-4	Reactor Thermal Power as a Function of Ejected Control Rod Worth
14.2-5	Enthalpy Increase to Hottest Fuel Rod versus Ejected Control Rod Worth
14.2-6	Effect on Reactor Neutron Power of Varying the Doppler Coefficient - Rod Ejection at 10^{-9} Ultimate Power
14.2-7	Effect on Reactor Neutron Power of Varying the Moderator Coefficient - Rod Ejection at 10^{-9} Ultimate Power
14.2-8	Effect on Reactor Thermal Power of Varying the Doppler Coefficient - Rod Ejection at 10^{-9} Ultimate Power

000 0161 000

Figure Number	Title
14.2-9	Effect on Reactor Thermal Power of Varying the Moderator Coefficient - Rod Ejection at 10^{-9} Ultimate Power
14.2-10	Reactor Thermal Power versus Trip Delay - Rod Ejection at Ultimate Power
14.2-11	Enthalpy Increase to the Hottest Fuel Rod versus Trip Delay Time - Rod Ejection
14.2-12	LOFT Semiscale Blowdown Test No. 546 - Vessel Pressure versus Time
14.2-13	Predicted Percent Mass Remaining versus Time - LOFT Test No. 546
14.2-14	Neutron Power versus Time for a 36-in. ID, Double-Ended, Hot Leg Pipe Rupture at Ultimate Power Without Trip
14.2-15	Reactivity versus Time for a 36-in. ID, Double-Ended, Hot Leg Pipe Rupture at Ultimate Power Without Trip
14.2-16	Integrated Power versus Break Size for a Spectrum of Rupture Sizes
14.2-17	Core Flow versus Time for a 36-in. ID, Double-Ended, Hot Leg Pipe Rupture
14.2-18	Hot Channel Clad Surface Heat Transfer Coefficient after DNB versus Time for a 36-in. ID, Double-Ended, Hot Leg Pipe Rupture
14.2-19	Reactor Vessel Water Volume versus Time for a 36-in. ID, Double-Ended, Hot Leg Pipe Rupture for 600 psig Core Flooding Tank Operating Pressure
14.2-20	Reactor Vessel Water Volume versus Time for a 36-in. ID, Double-Ended, Hot Leg Pipe Rupture for 400 psig and 1,000 psig Core Flooding Tank Operating Pressures
14.2-21	Core Flooding Tank Analysis; Maximum Clad Temperature versus Time to Quench for a 36-in. ID, Double-Ended Hot Leg Pipe Rupture
14.2-22	Maximum Hot Spot Clad Temperature versus Maximum Heat Transfer Coefficient after DNB for a 36-in. ID, Double-Ended, Hot Leg Pipe Rupture
14.2-23	Maximum Hot Spot Clad Temperature as a Function of Time to Reach DNB for a 36-in. ID, Double-Ended, Hot Leg Pipe Rupture

000 0162

Figure Number	Title
14.2-24	Hot Spot Clad Temperature versus Time for a 36-in. ID, Double-Ended, Hot Leg Pipe Rupture and Variable Quench Coefficient
14.2-25	Hot Spot Clad Temperature as a Function of Full-Power Seconds Resulting from Void Shutdown for a 36-in. ID, Double-Ended Hot Leg Pipe Rupture
14.2-26	Hot Spot Clad Temperature versus Time for 36-in. ID, Double-Ended, Hot Leg Pipe Rupture and Variable Sink Temperature
14.2-27	Mass Released to Reactor Building for the Spectrum of Hot Leg Ruptures
14.2-28	Reactor Coolant Average Pressure for the Spectrum of Hot Leg Ruptures
14.2-29	Hot Line Ruptures - Reactor Vessel Water Volume versus Time Including Effects of Boiloff and Injection
14.2-30	Hot Spot Cladding Temperature versus Time for Spectrum Hot Line Leaks
14.2-31	Reactor Coolant Average Pressure - Spectrum of Cold Leg Rupture Sizes
14.2-32	Cold Line Ruptures - Reactor Vessel Water Volume versus Time, Including Effects of Boiloff and Injection
14.2-33	Hot Spot Clad Temperature versus Time for Spectrum of Cold Leg Ruptures
14.2-34	Emergency Core Cooling Systems Capability
14.2-35	Reactor Building Pressure versus Time After a 14.1 ft^2 Hot Leg Pipe Rupture
14.2-36	Reactor Building Pressure versus Time for a 14.1 ft^2 Hot Leg Pipe Rupture with and without Cooling of the Recirculated Spray Water
14.2-37	Reactor Building Atmosphere and Sump Coolant Temperatures Following a 14.1 ft^2 Hot Leg Pipe Rupture
14.2-38	Reactor Building Pressure versus Time after Rupture (8.5 ft^2)
14.2-39	Reactor Building Pressure versus Time after Rupture (3.0 ft^2)
14.2-40	Reactor Building Pressure versus Time after Rupture (1.0 ft^2)

000 0163 00

Figure Number	Title
14.2-41	Reactor Building Pressure versus Time after Rupture (0.4 ft^2)
14.2-42	Reactor Building Energy Inventory for 14.1 ft^2 Hot Leg Pipe Rupture
14.2-43	Reactor Building Energy Inventory for 3.0 ft^2 Rupture
14.2-44	Reactor Building Vapor and Sump Temperatures versus Time after a 14.1 ft^2 Hot Leg Pipe Rupture
14.2-45	Reactor Building Vapor and Sump Temperatures versus Time after a 3.0 ft^2 Rupture
14.2-46	Criterion 49 for a 14.1 ft^2 Hot Leg Pipe Rupture
14.2-47	Reactor Building Zr Reaction Capability for 59 psig Design Pressure
14.2-48	Reactor Building Pressure versus Time after a 14.1 ft^2 Hot Leg Pipe Rupture with One and Two Core Flooding Tanks Operating
14.2-49	Reactor Building Pressure versus Time after Rupture (8.5 ft^2) with Operation of Core Flooding Tanks
14.2-50	Reactor Building Pressure versus Time after Rupture (3.0 ft^2) with Operation of Core Flooding Tanks
14.3-1	Thyroid Dose from Loss-Of-Coolant Accident
14.3-2	Thyroid Dose from the Maximum Hypothetical Accident
14.3-3	Reactor Building Direct Dose Following MHA
14.3-4	Whole-Body Cloud Dose Following MHA
14.3-5	Iodine Removal Time Constant
14.3-6	Cloud Concentration Reduction Factor as a Function of Droplet Size
14.3-7	Thyroid Dose at the Site Boundary

000 0164

000

14. SAFETY ANALYSIS

14.1 CORE AND COOLANT BOUNDARY PROTECTION ANALYSIS

14.1.1 ABNORMALITIES

In previous sections of this report both normal and abnormal operations of the various systems and components have been discussed. This section summarizes and further explores abnormalities that are either inherently terminated or require the normal protection systems to operate to maintain integrity of the fuel and/or the reactor coolant system. These abnormalities have been evaluated for rated power of 2,452 Mwt. Whenever a fission product release to the environment is postulated, the release is based upon the fission product inventory associated with the ultimate reactor core power level of 2,568 Mwt. Fission product dispersion in the atmosphere is assumed to occur as predicted by the dispersion models developed in 2.3. Table 14.1-1 summarizes the potential abnormalities studied.

TABLE 14.1-1
ABNORMALITIES AFFECTING CORE AND COOLANT BOUNDARY

Event	Cause	Effect
Uncompensated Operating Reactivity Changes	Fuel depletion or xenon build-up	Reduction in reactor system average temperature. Automatic reactor trip if uncompensated. No equipment damage or radiological hazard.
Startup Accident	Uncontrolled rod* withdrawal	Power rise terminated by negative Doppler effect, reactor trip from short period, high reactor coolant system pressure, or overpower. No equipment damage or radiological hazard.
Rod Withdrawal Accident at Rated Power	Uncontrolled rod withdrawal	Power rise terminated by overpower trip or high pressure trip. No equipment damage or radiological hazard.
Moderator Dilution Accident	Equipment malfunction or operator error	Slow change of power terminated by reactor trip on high temperature or pressure. During shutdown a decrease in shutdown margin occurs, but criticality does not occur. No radiological hazard.

000 0165 00

TABLE 14.1-1 continued

Event	Cause	Effect
Loss of Coolant Flow	Mechanical or electrical failure of reactor coolant pump(s)	None. Core protected by reactor low-flow trip. No radiological hazard.
Stuck-Out, Stuck-In, or Dropped-In Control Rod	Mechanical or electrical failure	None. Subcriticality can be achieved if one rod is stuck-out. If stuck-in or dropped-in, continued operation is permitted if effect on power peaking not severe. No radiological hazard.
Loss of Electric Power	Miscellaneous faults	Possible power reduction or reactor trip depending on condition. Environmental effects described in 14.3.3 and Table 14.3-1.
Steam Line Failure	Pipe failure	Reactor automatically trips if rupture is large. Environmental effects indicated in Section 14.3.4 and Table 14.3-1.
Steam Generator Tube Failure	Tube failure	Reactor automatically trips if leakage exceeds normal makeup capacity to reactor coolant system. Environmental effects described in 14.3.? and Table 14.3-1.

*Control rod, rod, and control rod assembly (CRA) are used interchangeably in this section and elsewhere in the report.

A control rod group consists of a symmetrical arrangement of four or more control rod assemblies. See 7.2.2.1.2.

14.1.2 ANALYSIS OF EFFECTS AND CONSEQUENCES

14.1.2.1 Uncompensated Operating Reactivity Changes

14.1.2.1.1 Identification of Cause

During normal operation of the reactor, the overall reactivity of the core changes because of fuel depletion and changes in fission product poison concentration. These reactivity changes, if left either uncompensated,

000 0166 00

or overcompensated, can cause operating limits to be exceeded. In all cases, however, the reactor protective system prevents safety limits from being exceeded. No damage occurs from these conditions.

14.1.2.1.2 Analysis and Results

During normal operation, the automatic reactor control system senses any reactivity change in the reactor. Depending on the direction of the reactivity change, the reactor power increases or decreases. Correspondingly, the reactor coolant system average temperature increases or decreases, and the automatic reactor control system acts to restore reactor power to the power demand level and to re-establish this temperature at its set point. If manual corrective action is not taken or if the automatic control system malfunctions, the reactor coolant system average temperature changes to compensate for the reactivity disturbance. Table 14.1-2 summarizes these disturbances.

TABLE 14.1-2
UNCOMPENSATED REACTIVITY DISTURBANCES

Cause	Maximum Reactivity Rate, $(\Delta k/k)/sec$	Rate of Average Temperature Change (Uncorrected), F/sec
Fuel Depletion	-6×10^{-9}	-0.0006
Xenon Buildup	-3×10^{-8}	-0.003

These results are based on $+6 \times 10^{-5}$ $(\Delta k/k)/F$ moderator coefficient and -1.14×10^{-5} $(\Delta k/k)/F$ Doppler coefficient. The nominal value of $+6 \times 10^{-5}$ $(\Delta k/k)/F$ is representative of the moderator coefficient at the beginning of core life for an equilibrium cycle. This value is also valid at BOL for the first cycle after 15 days. A higher value [$+10 \times 10^{-5}$ $(\Delta k/k)/F$] exists at the start of the first core cycle. However, the effect of this slightly higher value has been shown to be of minor importance by the evaluation of the sensitivity of the reactor to moderator coefficient variations. These reactivity changes are extremely slow and allow the operator to detect and compensate for the change.

14.1.2.2 Startup Accident

14.1.2.2.1 Identification of Cause

The objective of a normal startup is to bring a subcritical reactor to the critical or slightly supercritical condition, and then to increase power in a controlled manner until the desired power level and system operating

000 0167 00

temperatures are obtained. During a startup, an uncontrolled reactivity addition could cause a nuclear excursion. This excursion is terminated by the strong negative Doppler effect if no other protective action operates.

The following design provisions minimize possibility of inadvertent continuous rod withdrawal and limit the potential power excursion:

a. The control system is designed so that only one control rod group can be withdrawn at a time, except that there is a 25 percent overlap in travel between two successive rod groups. This overlap occurs at the minimum worth for each group since one group is at the end of travel and the other is at the beginning of travel. The maximum worth of any single control rod group is 1.2% $\Delta k/k$ when the reactor is critical as specified in 7.2.2.1.3.

b. Control rod withdrawal rate is limited to 25 in./min.

c. A short-period withdrawal stop and alarm are provided in the source range.

d. A short-period withdrawal stop, alarm, and trip are provided in the intermediate range.

e. A high flux level and a high pressure trip are provided in the power range.

The reactor protection system is designed to limit (a) the reactor thermal power to 114 percent of rated power to prevent fuel damage, and (b) the reactor coolant system pressure to 2,515 psia.

14.1.2.2.2 Methods of Analysis

An analog model of the reactor core and coolant system was used to determine the characteristics of this accident. This analog model used full reactor coolant flow, but no heat transfer out of the system and no sprays in the pressurizer. The rated-power Doppler coefficient [-1.14×10^{-5} $(\Delta k/k)/F$] was used although the Doppler is much larger than this for the principal part of the transient. The rods were assumed to be moving along the steepest part of the rod-worth vs rod-travel curve. A reactor trip on short period was not incorporated in the analysis. The nominal values of the principal parameters used were: 0.3 sec trip delay, $+6 \times 10^{-5}$ $(\Delta k/k)/F$ moderator coefficient, and -1.14×10^{-5} $(\Delta k/k)/F$ Doppler coefficient. The total worth of all the control rods inserted into the reactor core following any trip is 8.4% $\Delta k/k$ without a stuck control rod, or 5.4% $\Delta k/k$ (the nominal case in this study) with a stuck rod.

14.1.2.2.3 Results of Analysis

Figure 14.1-1 shows the results of withdrawing the maximum worth control rod group at a rod speed of 25 in./min from 1 percent subcritical. This

000 0168 000

group has a maximum worth of 1.2% $\Delta k/k$. This rod velocity and worth result in a maximum reactivity addition rate of 5.8×10^{-5} $(\Delta k/k)$/sec. The Doppler effect begins to slow the neutron power* rise, but the heat to the coolant increases the pressure past the trip point, and the transient is terminated by the high pressure trip.

Figure 14.1-2 shows the results of withdrawing all 69 control rod assemblies (with a total worth of 10.0% $\Delta k/k$) at the maximum speed from 1 percent subcritical. This results in a maximum reactivity addition rate of 5.8×10^{-4} $(\Delta k/k)$/sec. About 15.3 sec after passing through criticality, the neutron power peaks at 147 percent, where the power rise is stopped by the negative Doppler effect. The high neutron flux trip takes effect 0.25 sec after the peak power is reached and terminates the transient. The peak thermal heat flux is only 16 percent of the rated power heat flux.

A sensitivity analysis was performed on both of these startup accidents to determine the effect of varying several key parameters. Figures 14.1-3 through 14.1-6 show typical results for the single group, 1.2% $\Delta k/k$ startup accident.

Figures 14.1-3 and 14.1-4 show the effect of varying the reactivity addition rate on the peak thermal power and peak neutron power. This reactivity rate was varied from one order of magnitude below the nominal single rod group case (1.2% $\Delta k/k$) to more than an order of magnitude above the rate that represents all rods (10.0% $\Delta k/k$) being withdrawn at once. The slower rates - up to about 0.5×10^{-3} $(\Delta k/k)$/sec - will result in the pressure trip being actuated, whereas only the very fast rates actuate the high neutron flux level trip.

Figures 14.1-5 and 14.1-6 show the peak thermal power variation as a function of a wide range of trip delay times and Doppler coefficients for the 1.2% $\Delta k/k$ rod group. Only a small change in power is noted. Figures 14.1-7 and 14.1-8 are the corresponding results from the withdrawal of all rods (10.0% $\Delta k/k$). Since this transient inserts reactivity an order of magnitude faster than does the single control rod group case, there is considerably more variation in the peak thermal power over these wide ranges. At high values of the Doppler coefficient, the neutron power rise is virtually stopped before reaching the high flux trip level. Reactor power generation continues until sufficient energy is transferred to the reactor coolant to initiate a high pressure trip. This results in a higher peak thermal power.

Figures 14.1-9 through 14.1-12 show the peak pressure response to variations in several key parameters for the case where all rods are withdrawn. It is seen that the safety valve is opened when these parameters are changed considerably from the nominal values, except in the case of the moderator coefficient which has little effect because of the short duration of the transient. Again for a high Doppler coefficient, the high pressure trip is relied upon.

---

*Neutron power is defined as the total sensible energy release from fission.

000 0169

None of these postulated startup accidents, except for reactivity addition rates greater than 2×10^{-3} $(\Delta k/k)$/sec, which is three times greater than for withdrawal of all rods at once, causes a thermal power peak in excess of 40 percent rated power or a nominal fuel rod average temperature greater than 1,715 F. The nominal 1.2% $\Delta k/k$ rod group withdrawal causes a peak pressure of 2,515 psia, the safety valve set point. The capacity of the safety valves is adequate to handle the maximum rate of coolant expansion resulting from this startup accident. The 10.0% $\Delta k/k$ withdrawal - using all 69 rods - causes a peak pressure of only 2,465 psia because the flux trip is actuated prior to the pressure trip.

It is concluded that the reactor is completely protected against any startup accident involving the withdrawal of any or all control rods, since in no case does the thermal power approach 114 percent, and the peak pressure never exceeds 2,515 psia.

14.1.2.3 Rod Withdrawal Accident From Rated Power Operation

14.1.2.3.1 Identification of Cause

A rod withdrawal accident presupposes an operator error or equipment failure which results in accidental withdrawal of a control rod group while the reactor is at rated power. As a result of this assumed accident, the power level increases; the reactor coolant and fuel rod temperatures increase; and if the withdrawal is not terminated by the operator or protection system, core damage would eventually occur.

The following provisions are made in the design to indicate and terminate this accident.

a. High reactor coolant outlet temperature alarms

b. High reactor coolant system pressure alarms

c. High pressurizer level alarms

d. High reactor coolant outlet temperature trip

e. High reactor coolant system pressure trip

f. High power level trip

14.1.2.3.2 Methods of Analysis

An analog computer model was used to determine the characteristics of accident. A complete kinetics model, pressure model, average fuel rod model, steam demand coastdown model to 15 percent of rated load, coolant transport model, and a simulation of the instrumentation for pressure and flux trip were included. The initial conditions were normal rated power operation without automatic control. Only the moderator

000 0170

000

and Doppler coefficient of reactivity were used as feedback. The nominal values used for the main parameters were 0.3 sec trip delay time, -1.14×10^{-5} $(\Delta k/k)/F$ Doppler coefficient, $+6 \times 10^{-5}$ $(\Delta k/k)/F$ moderator coefficient, 25 in./min control rod speed, and 1.2% $\Delta k/k$ control rod group worth. The total worth in all the control rods inserted into the reactor core following any trip is 8.4% $\Delta k/k$ without a stuck control rod, or 5.4% $\Delta k/k$ (the nominal value used) with a stuck rod.

The foregoing rod speed and group rod worth give a maximum reactivity addition rate of 5.8×10^{-5} $(\Delta k/k)/sec$, which is the nominal case. The reactor protection system is designed to limit (a) the reactor power to 114 percent of rated power to prevent fuel damage, and (b) the coolant system pressure to 2,515 psia to prevent reactor coolant system damage.

14.1.2.3.3 Results of Analysis

Figure 14.1-13 shows the results of the nominal rod withdrawal from rated power using the 1.2% $\Delta k/k$ rod group at 5.8×10^{-5} $(\Delta k/k)/sec$. The transient is terminated by a high pressure trip, and reactor power is limited to 108 percent, much less than the design overpower of 114 percent of rated power. The changes in the parameters are all quite small, e.g., 5 F average reactor coolant temperature rise and 200 psi system pressure change.

A sensitivity analysis of important parameters was performed around this nominal case, and the resultant reactor coolant system pressure responses are shown in Figures 14.1-14 through 14.1-16.

Figure 14.1-14 shows the pressure variation for a very wide range of rod withdrawal rates - more than an order of magnitude smaller and greater than the nominal case. For the very rapid rates, the neutron flux level trip is actuated. This is the primary protective device for the reactor core; it also protects the system against high pressure during fast rod withdrawal accidents. The high pressure trip is relied upon for the slower transients. In no case does the thermal power exceed 108 percent rated power.

Figures 14.1-15 and 14.1-16 show the pressure response to variations in the trip delay time and Doppler coefficient. For the higher values of the Doppler coefficient, the pressure trip is always actuated, and, therefore, the pressure levels off.

An analysis has been performed extending the evaluation of the rod withdrawal accident for various fractional initial power levels up to rated power. This evaluation has been performed assuming simulated withdrawal of all 69 control rods giving a maximum reactivity addition of rate of 5.8×10^{-4} $(\Delta k/k)/sec$. This rate is a factor of ten higher than used in the cases evaluated at rated power. The results of this analysis are shown in Figure 14.1-17 and Figure 14.1-18.

As seen in Figure 14.1-17 the peak thermal power occurs for the rated power case and is well below the maximum design power of 114 percent. The peak neutron power for all cases is approximately 117 percent of rated

000 0171 000

power and represents a slight overshoot above the trip level of 114 percent. Figure 14.1-18 shows that the maximum fuel temperature reached in the average rod and the hot spot are well below melting. Even in the most severe case at rated power, the average fuel temperature only increases by 26 F. It is therefore readily concluded that no fuel damage would result from simultaneous all-rod withdrawal from any initial power level.

This analysis shows that the high pressure trip and the high flux level trip adequately protect the reactor against any rod withdrawal accident from rated power.

14.1.2.4 Moderator Dilution Accident

14.1.2.4.1 Identification of Cause

The reactor utilizes boric acid in the reactor coolant to control excess reactivity. The boron content of the reactor coolant is periodically reduced to compensate for fuel burnup. The dilution water is supplied to the reactor coolant system by the makeup and purification system. This system is designed with several interlocks and alarms to prevent improper operation. These are as follows:

a. Flow of dilution water to the makeup tank must be initiated by the operator. The dilution water addition valve can be opened only when the control rods have been withdrawn to the preset position (95 percent) and the timing device to limit the integrated flow has been set. Dilution water is added at flow rates up to 70 gpm.

b. Flow of dilution water is automatically stopped when either the flow has integrated to a preset value or when the rods have been inserted to a preset position (at about 75 percent full stroke).

c. A warning light is on whenever dilution is in progress.

2| The makeup and purification system normally has one pump in operation which supplies up to 70 gpm to the reactor coolant system and the required flow to the reactor coolant pump and control drive seals. Thus, the total makeup flow available is limited to 70 gpm unless the operator takes action to increase the amount of makeup flow to the reactor coolant system. When the makeup rate is greater than the maximum letdown rate of 70 gpm, the net water makeup will cause the pressurizer level control to close the makeup valves.

The nominal moderator dilution accident considered is the pumping of water with zero boron concentration from the makeup tank to the reactor coolant system by the makeup pump.

It is also possible, however, to have a slightly higher flow rate during transients when the system pressure is lower than the nominal value and the pressurizer level is below normal. This flow might be as high as 100 gpm.

In addition, with a combination of multiple valve failures or maloperations, plus more than one makeup pump operating and reduced reactor coolant system pressure, the resulting inflow rate can be as high as 500 gpm. This constitutes the maximum dilution accident. A reactor trip would terminate unborated water addition to the makeup tank, and total flow into the coolant system would be terminated by a high pressurizer level. 2

The criteria of reactor protection for this accident are:

a. The reactor power will be limited to less than the design overpower of 114 percent rated power to prevent fuel damage.

b. The reactor protection system will limit the reactor coolant system pressure to less than the system design pressure of 2,500 psig.

c. The reactor minimum subcriticality margin of 1% $\Delta k/k$ will be maintained.

d. Administrative procedures will be imposed to monitor and control the relationship of control rod regulating group patterns and boron concentrations in the reactor coolant over the operating life of the core. 2

14.1.2.4.2 Analysis and Results

The reactor is assumed to be operating at rated power with an initial boron concentration (1,800 ppm), in the reactor coolant system. The dilution water is uniformly distributed throughout the reactor coolant volume. Uniform distribution results from a discharge rate of 70-500 gpm into a reactor coolant flow of 88,000 gpm. A change in concentration of 100 ppm produces a 1% $\Delta k/k$ reactivity change. The effects of these three dilution rates on the reactor are as follows: 1

Dilution Water Flow, gpm	Reactivity Rate, $(\Delta k/k)$/sec	Average Reactor Coolant System Temp. Change, F/sec
70	$+2.5 \times 10^{-6}$	0.3
100	$+3.6 \times 10^{-6}$	0.3
500	$+1.8 \times 10^{-5}$	0.4

1

The fastest rate of dilution can be handled by the automatic control system, which would insert rods to maintain the power level and reactor coolant system temperature. If an interlock failure occurred while the

000 0173

OC

reactor was under manual control, these reactivity additions would cause a high reactor coolant temperature trip or a high pressure trip. In the case of high pressure trip without any automatic or manual control, the reactor will be shut down in less than 20 seconds, at which time less than 0.05% Δk/k would have been added, which is not even 10% of the total rod worth available for trip with a stuck rod. In any event the thermal power will not exceed 114 percent rated power, and the system pressure will not exceed the design pressure of 2,500 psig. Therefore moderator dilution accidents will not cause any damage to the reactor system.

During refueling or maintenance operations when the reactor closure head has been removed, the sources of dilution water makeup to the makeup tank - and therefore to the reactor coolant system - are locked closed, and the makeup pumps are not operating. At the beginning of core life when the boron concentration is highest, the reactor is about 9.5% Δk/k subcritical with the maximum worth rod stuck out. To demonstrate the ability of the reactor to accept moderator dilution during shutdown, the consequences of accidentally filling the makeup tank with dilution water and starting the makeup pumps have been evaluated. The entire water volume from the makeup tank could be pumped into the reactor coolant system (assuming only the coolant in the reactor vessel is diluted), and the reactor would still be 6.5% Δk/k subcritical.

14.1.2.5 Cold Water Accident

The absence of individual loop isolation valves eliminates the potential source of cold water in the reactor coolant system. Therefore, this accident is not credible in this reactor.

14.1.2.6 Loss-of-Coolant Flow

14.1.2.6.1 Identification of Cause

A reduction in the reactor coolant flow rate occurs if one or more of the reactor coolant pumps should fail. A pumping failure can occur from mechanical failures or from a loss of electrical power. With four independent pumps available, a mechanical failure in one pump will not affect operation of the others.

Each reactor coolant pump receives electrical power from one of the two electrically separate buses of the 6,900-volt system discussed in 8.2.2.4. Faults in an individual pump motor or its power supply could cause a reduction in flow, but a complete loss of flow is extremely unlikely.

In spite of the low probability of a complete loss of power to all reactor coolant pumps, the nuclear unit has been designed so that such a failure would not lead to core damage.

The reactor protection criterion for loss-of-coolant-flow conditions starting at rated power is that the reactor core will not reach a departure from nucleate boiling ratio (DNBR) smaller than the DNBR in the hot channel at the steady state design overpower. This corresponds to a DNBR of 1.38 at 114 percent rated power (Table 3.2-1).

00 0174

14.1.2.6.2 Methods of Analysis

The loss-of-coolant-flow accident is analyzed by a combination of analog and digital computer programs. Analog simulation is used to determine the reactor flow rate following loss of pumping power. Reactor power, coolant flow, and inlet temperature are input data to the digital program which determines the core thermal characteristics during the flow coastdown.

The analog model used to determine the neutron power following reactor trip includes six delayed neutron groups, control rod worth and rod insertion characteristics, and trip delay time. The analog model used to determine flow coastdown characteristics includes description of flow-pressure drop relations in the reactor coolant loop. Pump flow characteristics are determined from manufacturers' zone maps. Flow-speed, flow-torque, and flow-head relationships are solved by affinity laws.

A transient, thermal-hydraulic, B&W digital computer program is used to compute channel DNBR continually during the coastdown transient. System flow, neutron power, fission product decay heat, and core entering enthalpy are varied as a function of time. The program maintains a transient inventory of stored heat which is determined from fuel and clad temperatures beginning with the initial steady state conditions. The transient core pressure drop is determined for average channel conditions. The representative hot channel flows and corresponding DNBR are obtained by using the average core pressure drop. The hot channel DNBR as a function of time is compared with the design DNBR at maximum overpower to determine the degree of heat transfer margin.

The loss-of-coolant-flow analysis has been carried out in the power range between 102 and 114 percent rated power. Conditions utilized in the analysis are as follows:

a. Initial core inlet temperature for given power level is assumed to be plus 2 F in error.

b. Initial system pressure is assumed to be minus 65 psi in error.

c. Trip delay time, i.e., time for sensor detection for low flow condition until initial downward movement of control rod, is 300 milli-seconds.

d. The percent of initial reactor neutron power as a function of time after loss of pumps is as shown in Figure 3.2-6.

e. The pump inertia is 70,000 lb-ft^2.

14.1.2.6.3 Results of Analysis

The results of this analysis show that the reactor can sustain a loss-of-coolant-flow accident without damage to the fuel. The results of the evaluation are presented in Figures 14.1-19 and 14.1-20. Figure 14.1-19

000 0175

shows the percent reactor flow as a function of time after loss of all pump power. Figure 14.1-20 shows the minimum DNBR's which occur during the coastdown for various initial power levels. The degree of core protection during coastdown is indicated by comparing the DNBR for the coastdown with the design value of 1.38 at 114 percent rated power. This DNBR (1.38) in the representative hot channel corresponds to a 99 percent confidence that 99.5 percent of the core will not experience a departure from nucleate boiling under steady state conditions at the design overpower (3.2.3.1).

Under normal conditions, the maximum indicated reactor power level from which a loss-of-coolant-flow accident could occur is 102 percent rated power (as indicated by reactor instrumentation). This power level represents an allowance of plus 2 percent rated power for transient overshoot. This power level also represents the maximum power demand that will be permitted to the reactor control system. The 102 percent rated power is an instrument-indicated value and is subject to the following maximum errors: (a) ± 2 percent heat balance and (b) ± 4 percent nuclear instrumentation. The true power level could be as high as 108 percent at 102 percent indicated power. As shown in Figure 14.1-20, however, the DNBR at 108 percent is 1.44, which is significantly larger than the design DNBR.

The reactor coolant system is capable of providing natural circulation flow after the pumps have stopped. The natural circulation characteristics of the reactor coolant system have been calculated using conservative values for all resistance and form loss factors. No voids are assumed to exist in the core or reactor outlet piping. The following tabulation and Figure 9.5-2 show the natural circulation flow capability as a function of the decay heat generation.

Time After Loss of Power, sec	Decay Heat Core Power, %	Natural Circulation Core Flow Available, % Full Flow	Flow Required for Heat Removal, % Full Flow
0.36×10^2	5	4.1	2.3
2.2×10^2	3	3.3	1.2
1.2×10^4	1	1.8	0.36
1.3×10^5	1/2	1.2	0.20

The flows above provide adequate heat transfer for core cooling and decay heat removal by the reactor coolant system.

The reactor is protected against reactor coolant pump failure(s) by the protection system and the integrated control system. The integrated control system initiates a power reduction on pump failure to prevent reactor power from exceeding that permissible for the available flow. The reactor is tripped if insufficient reactor coolant flow exists for the power level. The operating limits for less than four pumps in operation have been presented in 4.3.7.

000 0176 00

14.1.2.7 Stuck-Out, Stuck-In, or Dropped-In Control Rod

14.1.2.7.1 Identification of Cause

The control rod drives have been described in 3.2.4.3. The results of continuous control rod withdrawal have been analyzed in 14.1.2.2 and 14.1.2.3. In the event that a control rod cannot be moved because of electrical faults or mechanical seizure, localized power peaking and subcritical margin must be considered.

14.1.2.7.2 Analysis and Results

Adequate hot subcritical margin is provided by requiring a subcriticality of 1% $\Delta k/k$ subcritical with the control rod of greatest worth fully withdrawn from the core. The nuclear analysis reported in 3.2.2 demonstrates that this criterion can be satisfied.

In the event that an unmovable control rod is partially or fully inserted in the core or a single rod is dropped during operation, its location and effect on local power distribution determine whether continued power operation is permissible. The location of a stuck rod in the core will be studied further to define permissible conditions of operation. The criteria for these studies are (a) operation with a stuck rod will not increase the DNB probability above the probability specified for design conditions, and (b) a hot subcritical margin of 1% $\Delta k/k$ will be maintained with the stuck rod in its inoperative position and the operating rod of greatest reactivity worth in the fully withdrawn position.

If a control rod is dropped into the core during power operation, the same consideration of localized power peaking as for a stuck rod will apply.

14.1.2.8 Loss of Electric Power

14.1.2.8.1 Identification of Cause

The Rancho Seco Plant is designed to withstand the effects of loss of electric load or electric power. Two types of power losses are considered:

a. A "blackout" condition, caused by severe interconnected grid upset.

b. A hypothetical condition resulting in a complete loss of all plant power.

The reactor protection criteria for these conditions are that fuel damage will not occur from an excessive power-to-flow ratio and that the reactor coolant system pressure will not exceed design pressure.

000 0177

00

14.1.2.8.2 Results of "Blackout" Conditions Analysis

The net effect of a "blackout" condition on the nuclear unit would be opening of all 230 kv breakers, thus disconnecting the plant from the entire transmission system. When this occurs on the nuclear unit, a runback signal on the integrated master controller causes an automatic power reduction to 15 percent reactor power. Other actions that occur are as follows:

a. All vital electrical loads, including reactor coolant pumps, condenser circulating water pumps, condensate and other auxiliary equipment, will continue to obtain power from the unit generator. Feedwater is supplied to the steam generators by steam-driven feed pumps.

b. As the electrical load is dropped, the turbine generator accelerates and closes the governor valves, and interceptor valves. The unit frequency will peak at less than the overspeed trip point and decay back to set frequency in 40-50 sec.

c. Following closure of the turbine governor valves and interceptor valves, steam pressure increases to the turbine bypass valve set point and may increase to the steam system safety valve set point. Steam is relieved to the condenser and to the atmosphere. Steam venting to the atmosphere occurs for about 2 minutes following blackout from 100 percent rated power until the turbine bypass can handle all excess steam generated. The capacity of the modulating turbine bypass valve is 15 percent of the valves wide open (VWO) steam flow, and that of the safety valves is 100 percent of VWO steam flow. The first safety valve banks are set at 1,050 psig with additional banks set at pressures up to 1,104 psig (5 percent above design pressure as allowed by code). Steam venting permits energy removal from the reactor coolant system to prevent a high pressure reactor trip. The initial power runback is to 15 percent power which is greater than the unit auxiliary load. This allows sufficient steam flow for regulating turbine speed control. Excess power above the unit auxiliary load is rejected by the turbine bypass valve to the condenser.

d. During the short interval while the turbine speed is high, the vital electrical loads connected to the unit generator will undergo speed increase in proportion to the generator frequency increase. All motors and electrical gear so connected are designed for the increased frequency.

e. After the turbine generator has been stabilized at auxiliary load and set frequency, the plant operator may reduce reactor power to the auxiliary load as desired.

000 0178

000

The blackout accident does not produce any fuel damage or excessive pressures on the reactor coolant system. There is no resultant radiological hazard to plant operating personnel or to the public from this accident, since only secondary system steam is discharged to the atmosphere.

14.1.2.8.3 Analysis Results of Complete Loss of All Plant Power

The second power loss considered is the hypothetical case where all plant power except the plant batteries is lost. The sequence of events and the evaluation of consequences relative to this accident are given below:

a. A loss of power results in gravity insertion of the control rods.

b. The steam generator safety valves actuate after the turbine trips and prevent excessive temperatures and pressures in the reactor coolant system.

c. The reactor coolant system flow decays without fuel damage occurring. Decay heat removal after coastdown of the reactor coolant pumps is provided by the natural circulation characteristics of the system. This capability is discussed in the loss-of-coolant-flow evaluation (14.1.2.6).

d. A turbine-driven or motor-driven emergency feedwater pump is provided to supply feedwater any time the main feed pumps cannot operate. The emergency feed pump takes suction from the condensate storage. The emergency pumps supply feedwater to the steam generators. The turbine-driven emergency feed pump is driven by steam from either or both steam generators. The motor-driven emergency feed pump can be powered from the diesel generator.

   The controls and auxiliary systems for the emergency feed pumps operate on d-c power from the plant batteries.

   A recirculation line from the emergency pumps' discharge back to the condensate storage tank is provided to permit periodic testing.

e. The condensate storage tank provides cooling water in the unlikely event that all power is lost. The minimum condensate inventory is 250,000 gallons. This inventory provides sufficient water for decay heat cooling (assuming infinite irradiation at 2,568 Mwt) for a period of approximately one day.

The features described above permit decay heat cooling of the nuclear unit for an extended period of time following a complete loss of electric p

000 0179 00

The foregoing evaluation demonstrates the design features incorporated in the design to sustain loss of power conditions with just the plant batteries to operate system controls. Immediate operation of the emergency feedwater pump is not of critical nature. The reactor can sustain a complete electric power loss without emergency cooling for about 25 minutes before the steam volume in the pressurizer is filled with reactor coolant. These 25 minutes are derived as follows:

a.	Steam generators evaporate to dryness	10 minutes
b.	Pressurizer safety valves open	5
c.	Pressurizer fills with water (due to reactor coolant system expansion)	10
		25 minutes

Beyond this time reactor coolant will boil off, and an additional 90 minutes will have elapsed before the boiloff will start to uncover the core. The emergency feedwater pump can be actuated within this period of time. Accordingly, core protection is ensured for the unlikely condition of total loss of plant electric power.

14.1.2.9 Steam Line Failure

14.1.2.9.1 Identification of Cause

Analyses have been performed to determine the effects and consequences of loss of secondary coolant due to failures in the steam lines between the steam generators and the turbine.

The criteria for plant protection and the release of fission products to the environment are as follows:

a. The reactor shall trip and remain subcritical without boron addition until a controlled rate of system cooldown can be effected.

b. The potential environmental consequences from radioactivity in the secondary coolant system shall not exceed those specified by 10 CFP 100. 3

14.1.2.9.2 Analysis and Results

The rate of reactor system cooling following a steam line break accident is a function of the area of the failure and the steam generator water inventory available for cooling. The steam generator inventory increases with power level. The inventory at rated power is 46,000 lb and decreases linearly to 20,000 lb at 15 percent power. The steam line break accident analysis is performed at ultimate power in order to determine maximum cooling and inventory release effects. 2

The immediate effect of any steam line break accident is a reduction in steam pressure and a reduction in steam flow to the turbine. These effects initially cause the reactor control system to act to restore steam pressure and load generation.

A steam line rupture of a small area causes a relatively slow decrease in steam pressure. This places a demand on the control system for increased feedwater flow. In addition, the turbine control valves will open to maintain power generation. Increased feedwater flow causes the average reactor coolant temperature to decrease, and the resulting temperature error calls for control rod withdrawal. The limiting action in this condition is the 102 percent limit on power demand to the rod drive control system. If the moderator temperature coefficient of reactivity is small or slightly positive, the reactor power will decrease when the control system reaches the power demand limit because of continuing temperature decrease. The reactor will then trip on low reactor coolant system pressure. A reactor trip will initiate a reduction in the feedwater flow to the steam generators.

When the moderator temperature coefficient is negative, the reactor power will tend to increase with decreasing average coolant temperature. This will cause control rod insertion to limit reactor power to 102 percent. With power limited at 102 percent, additional cooling causes a reduction in reactor coolant pressure, and the reactor trips on low reactor coolant pressure. Turbine trip occurs when the reactor trips. Upon turbine trip, the unaffected steam line is isolated by the turbine stop valves as shown in Figure 10.2-1. The unit with the ruptured steam line continues to blow down to the atmosphere.

The maximum cooldown of the reactor coolant system would be that resulting from the blowdown from one steam generator. A typical cooling rate following reactor trip for a steam line rupture of 4 $in.^2$ is shown in Figure 14.1-21.

The tabulation below lists the approximate time required to blow down the contents of the steam generator with a ruptured steam main.

Leak Area, $in.^2$	Blowdown Time, sec
4	860
32	110
128	27

A steam line failure of large area results in high steam flow with resulting rapid pressure decrease in the reactor coolant system and steam system. The reactor trips on low reactor coolant system pressure or high flux. Reactor trip causes turbine trip and reduction in feedwater flow to decay heat level. The turbine trip closes the turbine stop valves which isolate the steam lines and prevent blowdown of the steam generator whose secondary side does not have a pipe rupture. The steam generators are

000 0181

00

designed to maintain reactor system integrity upon loss-of-secondary-side pressure. Therefore, this accident will not lead to a reactor coolant system failure.

Assuming the blowdown from one steam generator results from a secondary steam system rupture, the maximum cooling rate during this accident occurs during the first 10 sec after the break. The maximum cooling rate is approximately 3 F/sec and a low pressure or high flux trip occurs. The net cooldown of the reactor coolant system, assuming total blowdown of one steam generator and accounting for transfer of core stored heat and decay heat, is less than 50 F. This results in an average coolant temperature of 530 F which is about 10 F lower than the normal zero power average coolant temperature.

The minimum shutdown margin at 540 F with the most reactive rod stuck out is 2.9% $\Delta k/k$. The reduction in reactivity shutdown margin associated with cooling the moderator temperature 10 F below its normal shutdown temperature of 540 F would be 0.30% $\Delta k/k$. Using the maximum negative value for the moderator temperature coefficient (-3.0×10^{-4} $\Delta k/k/F$), the shutdown margin at 530 F would be 2.6% $\Delta k/k$, which is adequate to prevent return to criticality.

In addition, high pressure injection can be actuated during the cooldown period following a large area steam line failure. This system supplies borated water to the reactor coolant system to increase the shutdown margin further. Boron addition to the reactor coolant during the controlled cooling of the system to atmospheric pressure will prevent criticality at lower temperatures.

The effect of a steam line rupture inside the reactor building has been evaluated by conservatively assuming an instantaneous release to the reactor building of the energy associated with this accident. The mass and energy released per steam generator in this analysis are approximately:

	Mass, lb	Energy Btu x 10^{-6}
Steam Generator	46,000	28.0
Feedwater Flow (6 sec. full flow plus coastdown to 7.5% flow @ 16 sec)	12,800	5.6
Reactor Coolant System Energy Transferred	-	17.6
Total	58,800	51.2

Based upon the above, a single steam generator release would result in approximately 10 psig pressure rise in the reactor building. This is well below the reactor building design pressure of 59 psig.

000 0182 000

14.1.2.10 Steam Generator Tube Failures

14.1.2.10.1 Identification of Accident

In the event of a reactor coolant leak to the secondary system, such as a complete severance of a steam generator tube, the activity contained in the coolant would be released to the secondary system. Radioactive gases and some of the radioactive iodine would be released to the atmosphere through the condenser air removal system.

14.1.2.10.2 Analysis and Results

In analyzing the consequences of this failure, the following sequence of events is assumed to occur:

a. A double-ended rupture of one steam generator tube occurs with unrestricted discharge from each end.

b. The initial leak rate, approximately 435 gpm, exceeds the normal makeup of 70 gpm to the reactor coolant system, and system pressure decreases. No operator action is assumed, and a low reactor coolant system pressure trip will occur in about 8 minutes.

c. Following reactor trip, the reactor coolant system pressure continues to decrease until high pressure injection is actuated at a pressure of 1,800 psig. The capacity of the high pressure injection is sufficient to compensate for the leakage and maintains both pressure and volume control of the reactor coolant system. Thereafter, the reactor is conservatively assumed to be cooled down and depressurized at the normal rate of 100 F per hour.

d. Following reactor trip, the turbine stop valves will close. Since a reactor coolant to secondary system leak has occurred, steam line pressure will increase, opening the steam bypass valves to the condenser. Each bypass valve actuates at a lower pressure than do the safety valves. The reactor coolant that leaks as a result of the tube failure is condensed in the condenser. Only the fission products that escape from the condensate are released to the atmosphere.

e. The affected steam generator would be isolated by the non-return valve in the turbine stop valve when the reactor coolant system pressure falls below the set-point of the secondary system safety valves, i.e., 1,050 psig. Cooldown continues with the unaffected steam generator until the temperature is reduced to 250 F. Thereafter, cooldown to ambient conditions is continued using the decay heat removal system.

000 0183 00 1

f. At the design cooling rate for the pressurizer of 100 F/ hr, depressurization to 1,050 psig requires approximately 1.7 hr. During this time period 1.6×10^8 cc (5,650 ft^3) of reactor coolant leaks to the secondary system. This leakage corresponds to approximately 45,800 curies of xenon-133 and 0.05 curies I-131 release to the atmosphere if the reactor has been operating with 1 percent failed fuel. The amount of iodine released to air in the condenser is based on a liquid-to-gas partition coefficient of 10^4.

2

000 0184

000

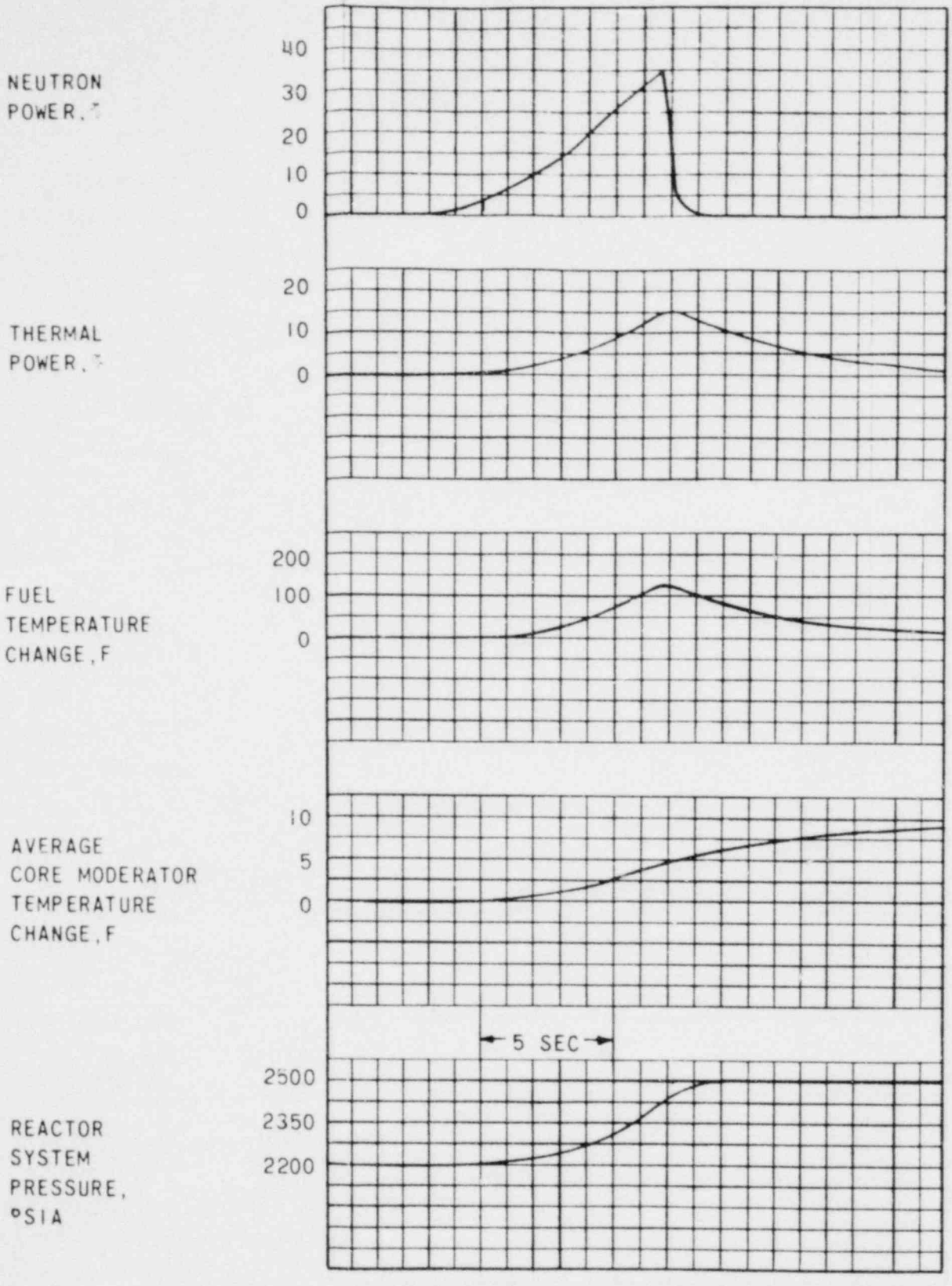

FIGURE 14.1-1
STARTUP ACCIDENT FROM 10^{-9} RATED POWER
USING A 1.2% $\Delta k/k$ ROD GROUP; HIGH
PRESSURE REACTOR TRIP IS ACTUATED

000 0185

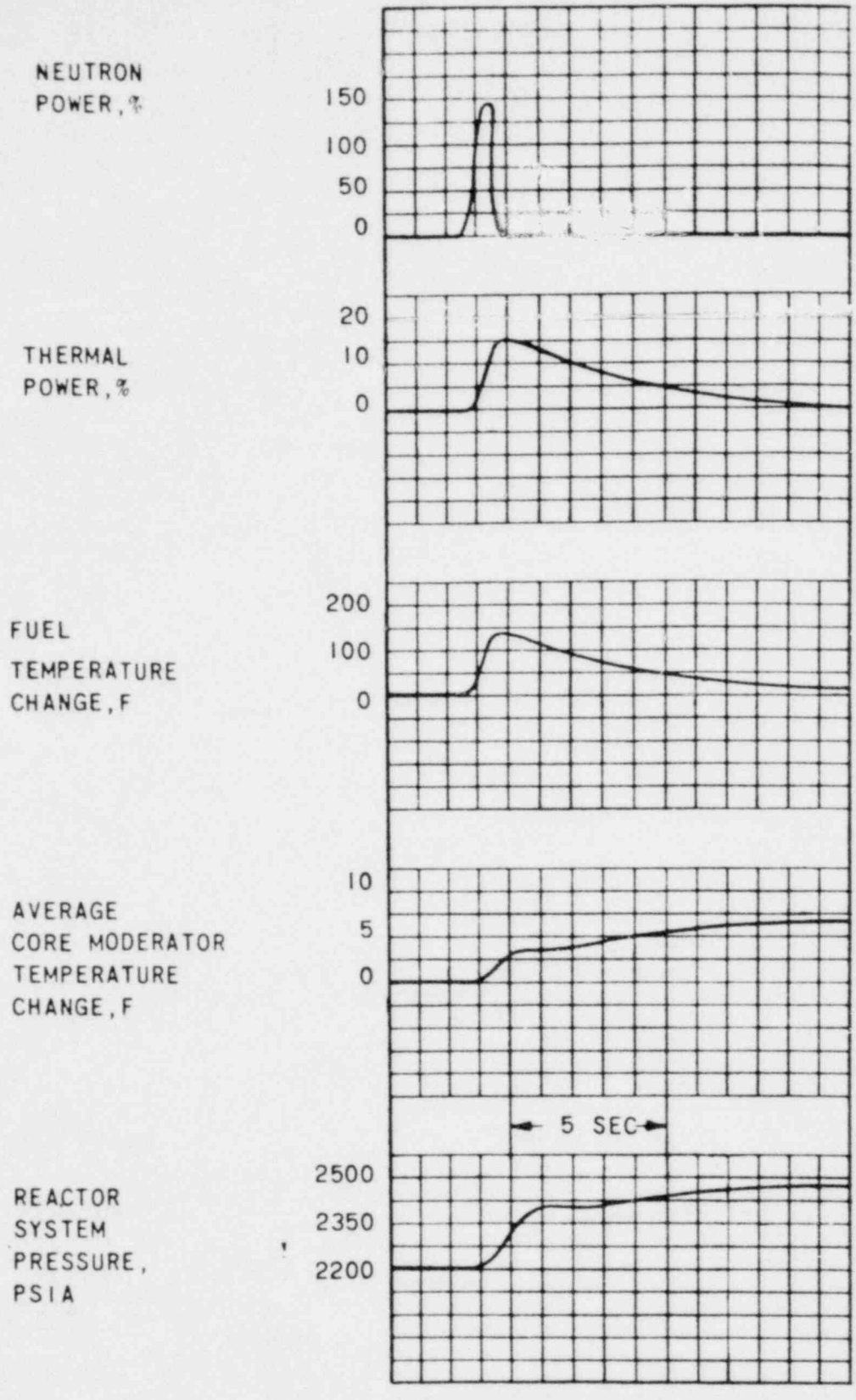

FIGURE 14.1-2
STARTUP ACCIDENT FROM 10^{-9} RATED POWER
USING ALL RODS WITH A WORTH OF 10%
$\Delta k/k$; HIGH FLUX REACTOR TRIP IS ACTUATED

000 0186

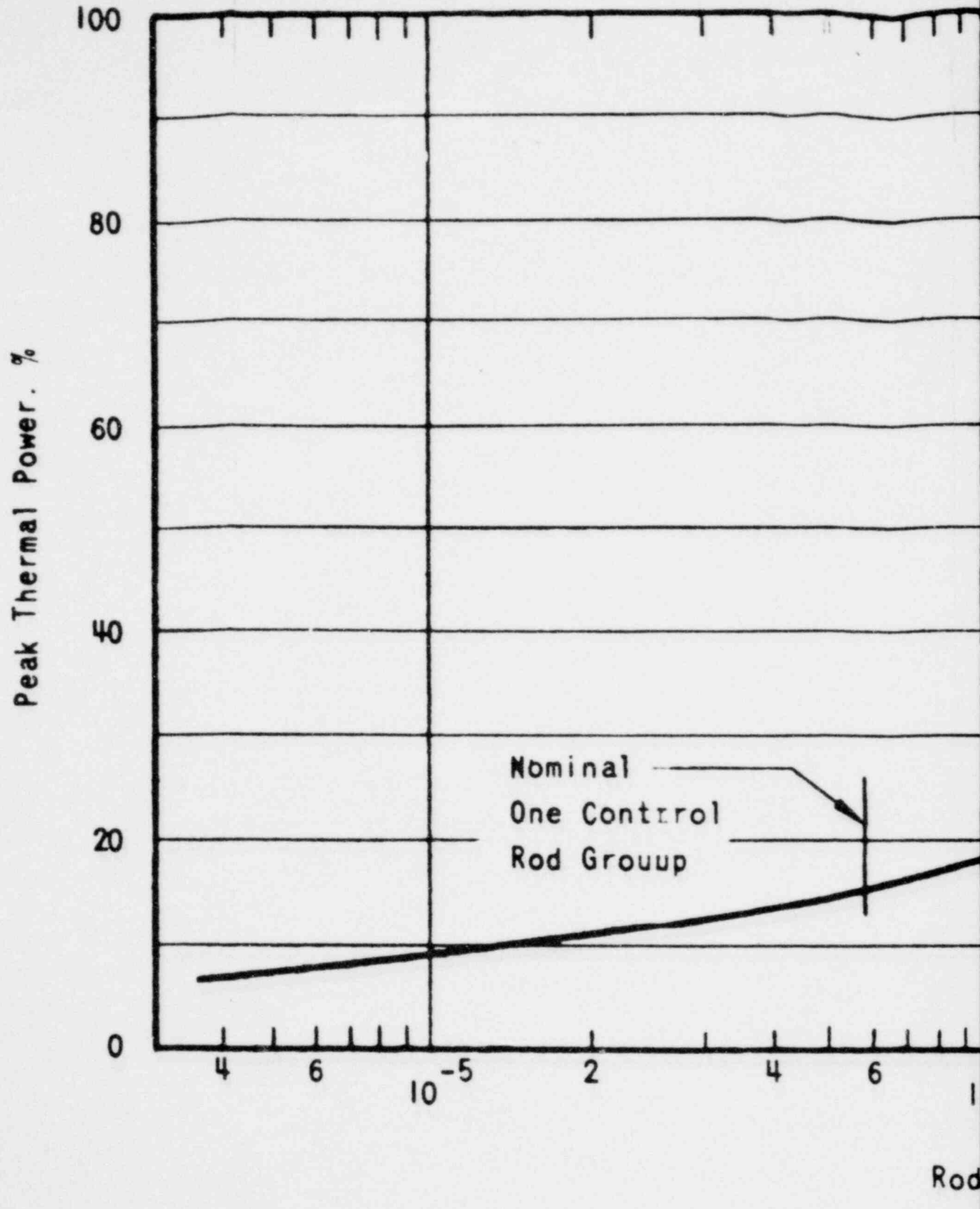
100
80
60
40
20
0
Peak Thermal Power. %
Nominal
One Control
Rod Grouup
4
6
10^-5
2
4
6
Rod

000 0187

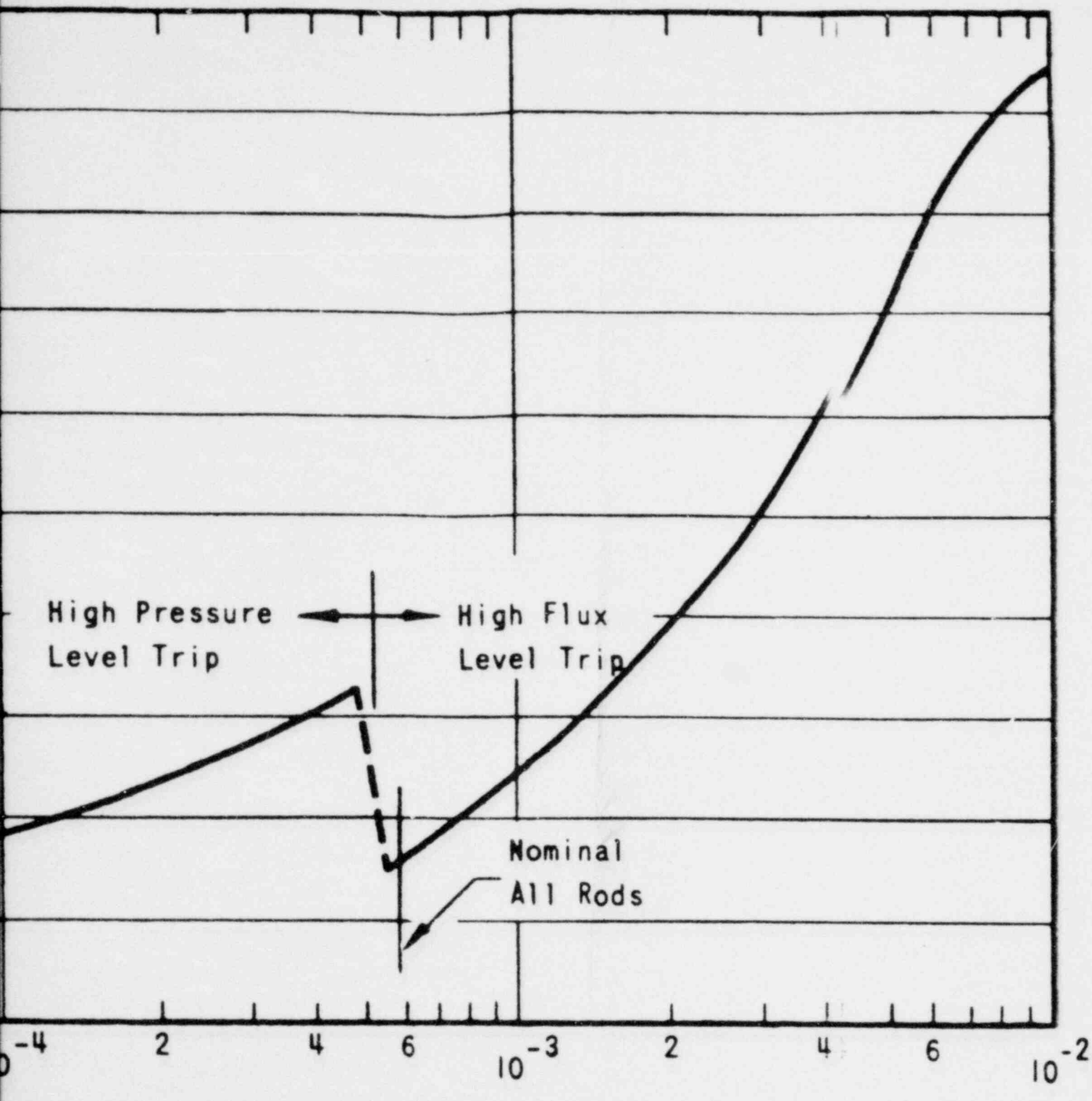

FIGURE 14.1-3
PEAK THERMAL POWER VERSUS ROD WITHDRAWAL RATE FOR A STARTUP ACCIDENT FROM 10^{-9} RATED POWER

SMUD

SACRAMENTO MUNICIPAL UTILITY DISTRICT

000 0188

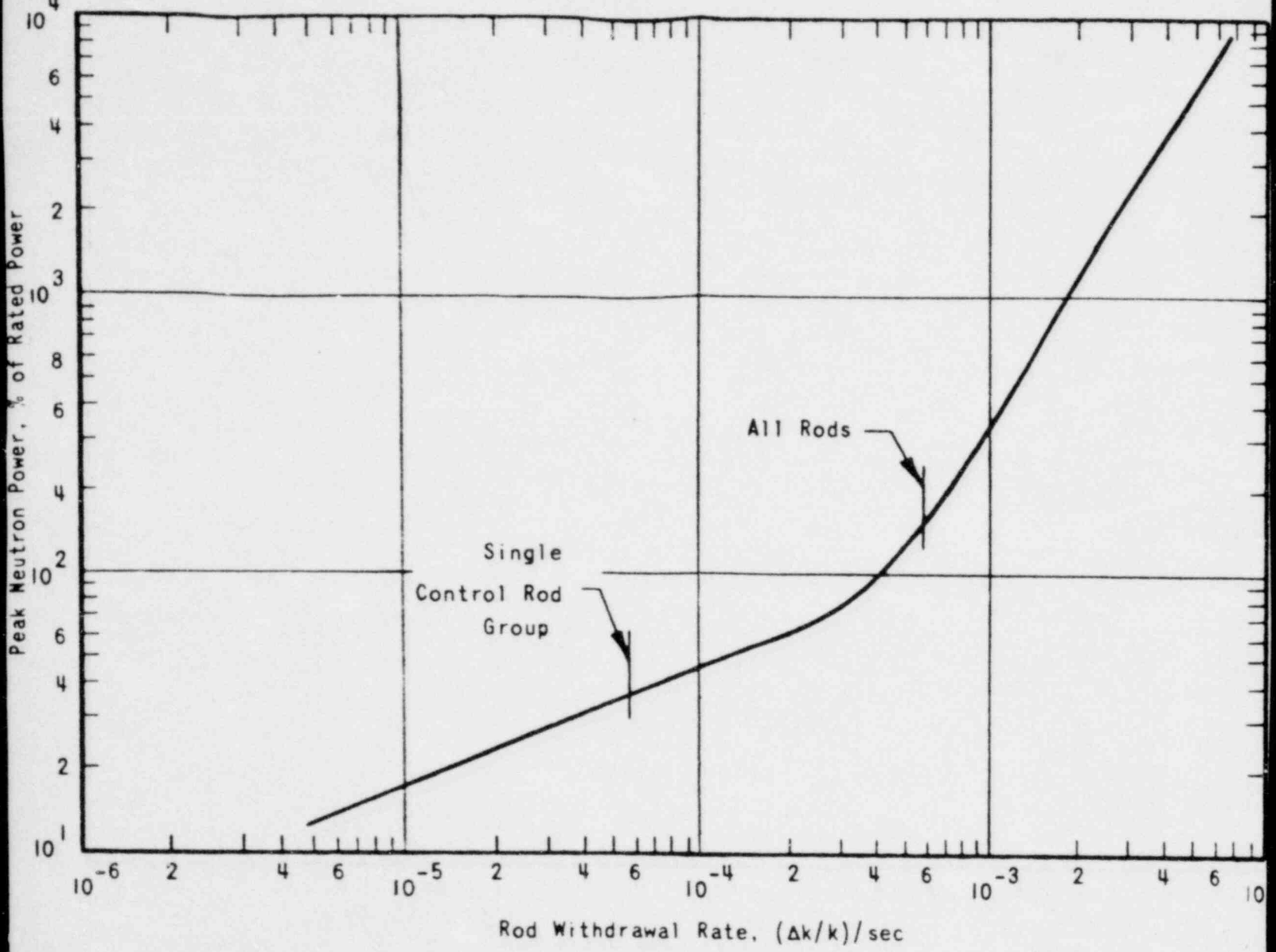

00 +

FIGURE 14.1-4
PEAK NEUTRON POWER VERSUS ROD
WITHDRAWAL RATE FOR A STARTUP
ACCIDENT FROM 10^{-9} RATED POWER

SMUD
SACRAMENTO MUNICIPAL UTILITY DISTRICT

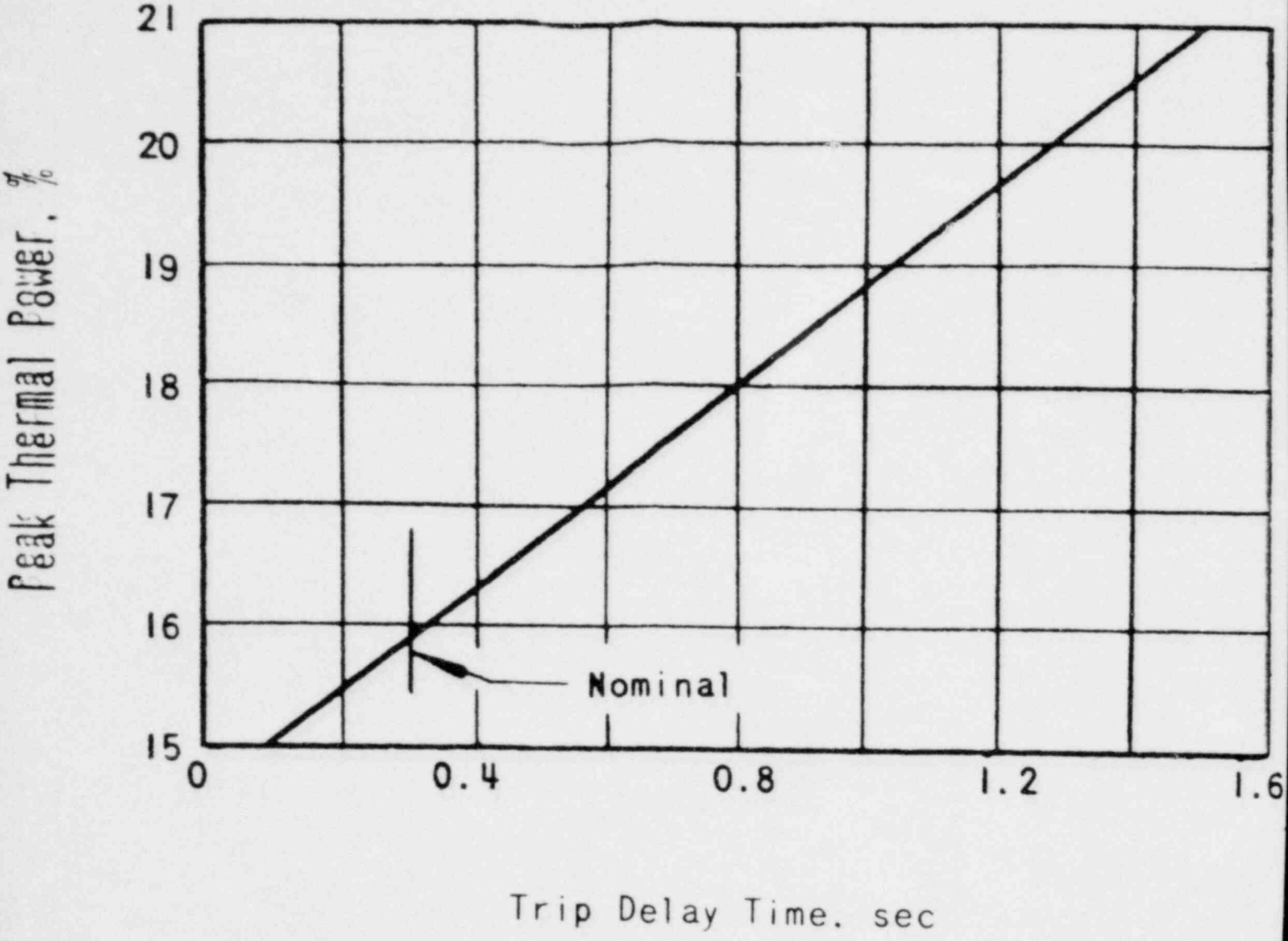

00

FIGURE 14.1-5
PEAK THERMAL POWER VERSUS TRIP DELAY TIME FOR A STARTUP ACCIDENT USING A 1.2% Δk/k ROD GROUP AT 5.8×10^{-5} (Δk/k)/SEC FROM 10^{-9} RATED POWER

SMUD
SACRAMENTO MUNICIPAL UTILITY DISTRICT

000 0190

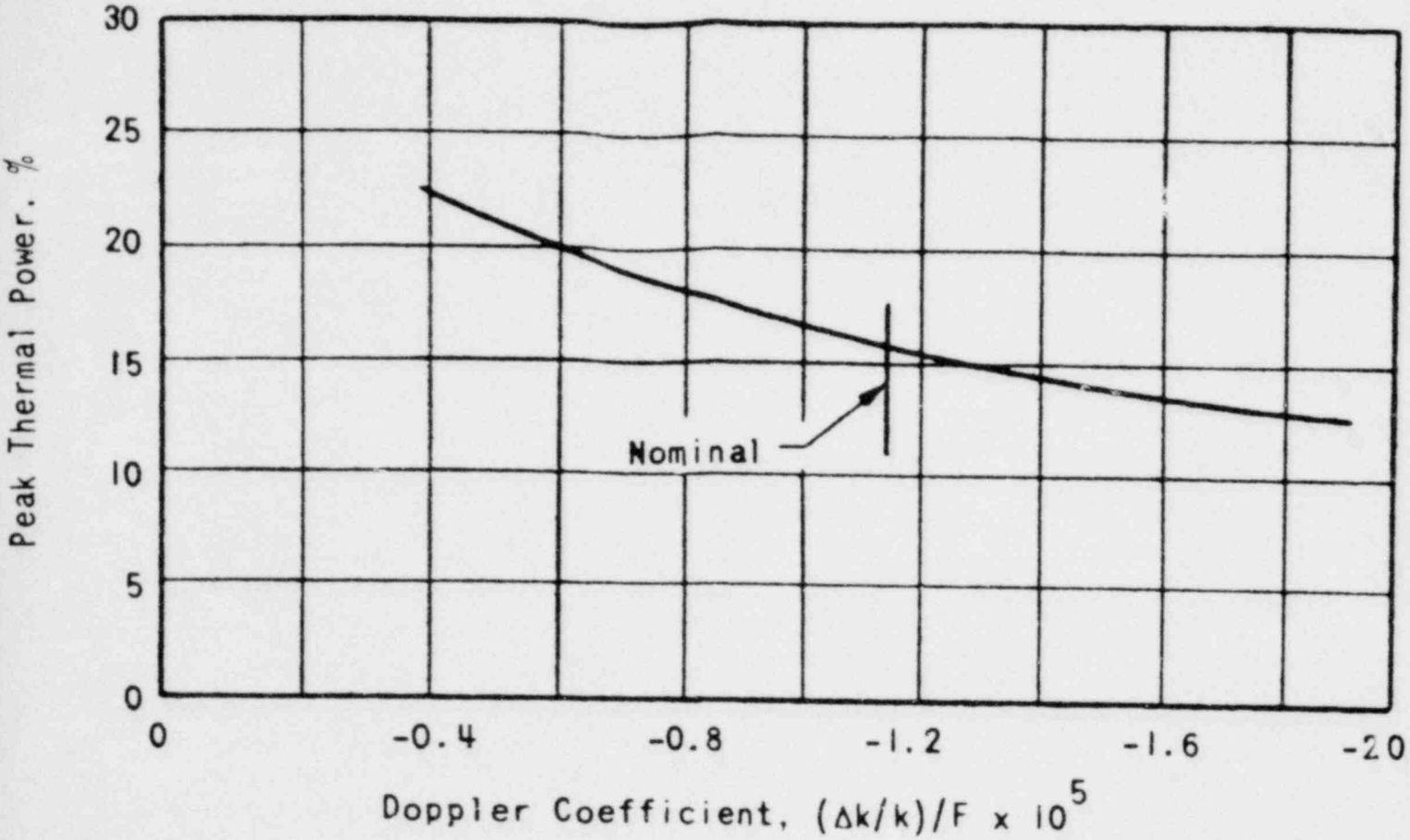

FIGURE 14.1-6
PEAK THERMAL POWER VERSUS DOPPLER COEFFICIENT FOR A STARTUP ACCIDENT USING A 1.2% Δk/k ROD GROUP AT 5.8×10^{-5} (Δk/k)/SEC FROM 10^{-9} RATED POWER

000 0191

SMUD
SACRAMENTO MUNICIPAL UTILITY DISTRICT

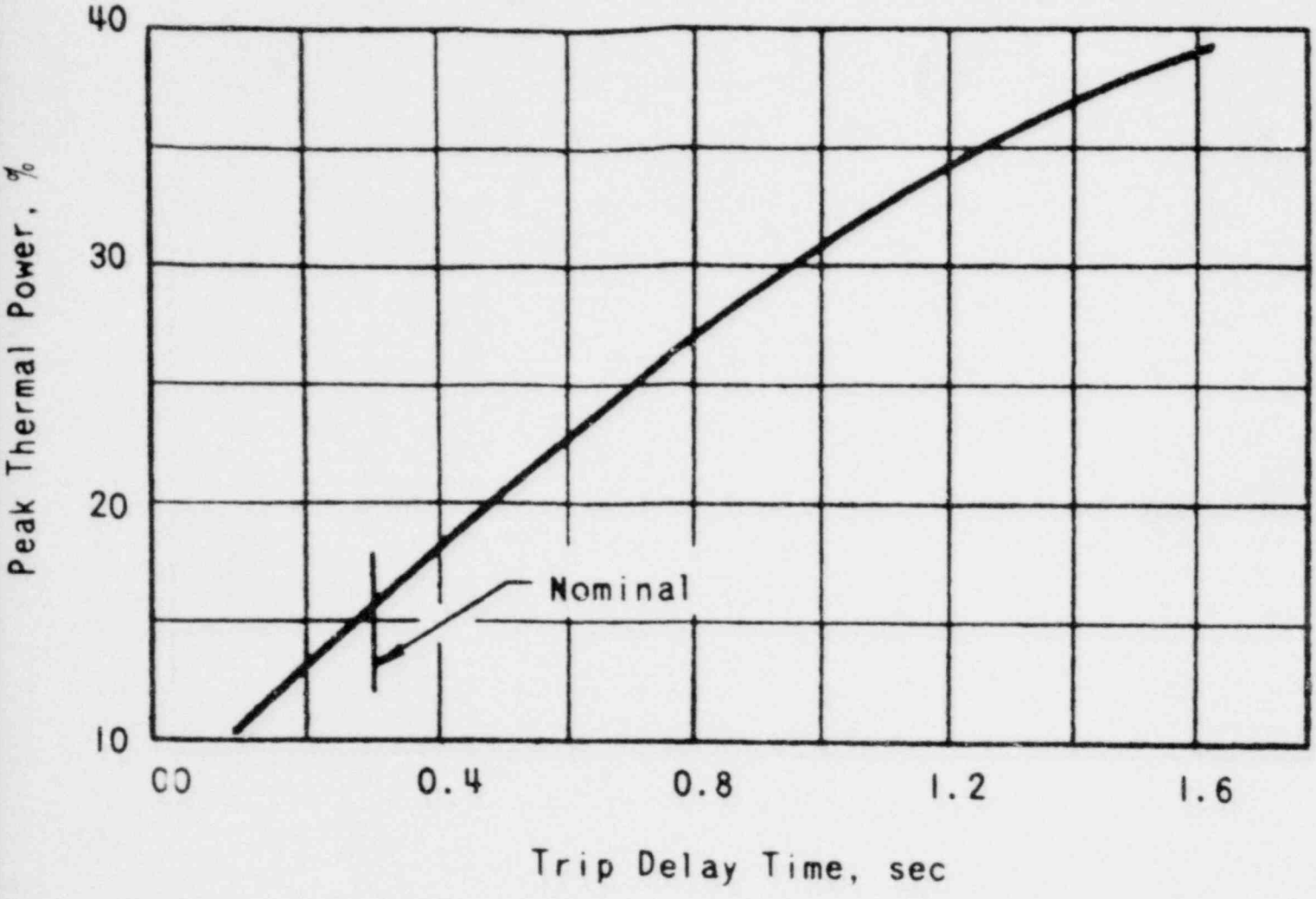

FIGURE 14.1-7
PEAK THERMAL POWER VERSUS TRIP DELAY TIME FOR A STARTUP ACCIDENT USING ALL RODS AT 5.8×10^{-4} ($\Delta k/k$)/SEC FROM 10^{-9} RATED POWER

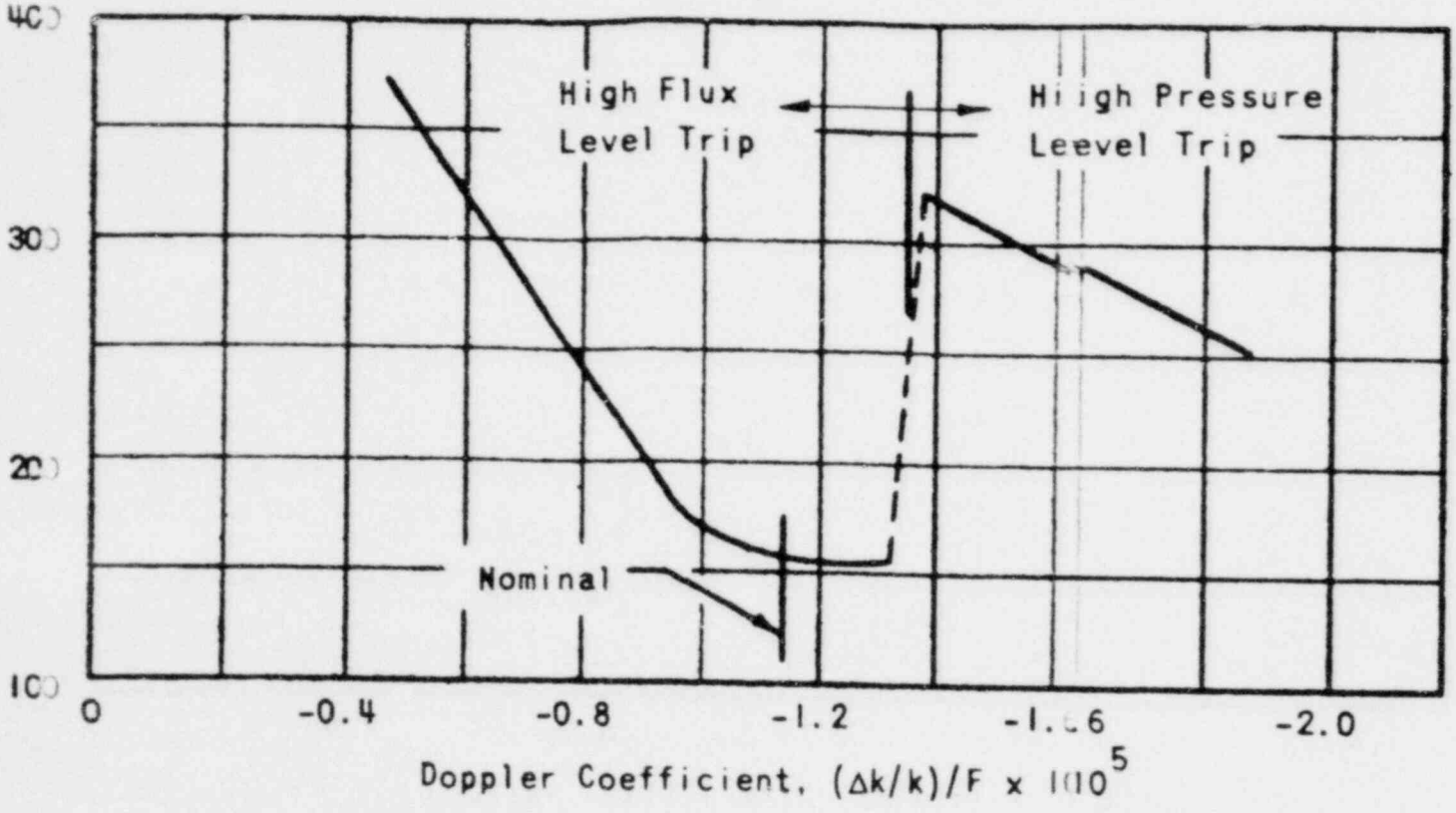

FIGURE 14.1-8
PEAK THERMAL POWER VERSUS DOPPLER
COEFFICIENT FOR A STARTUP ACCIDENT USING
ALL RODS AT 5.8 X 10^{-4} (Δk/k)/SEC
FROM 10^{-9} RATED POWER

0193

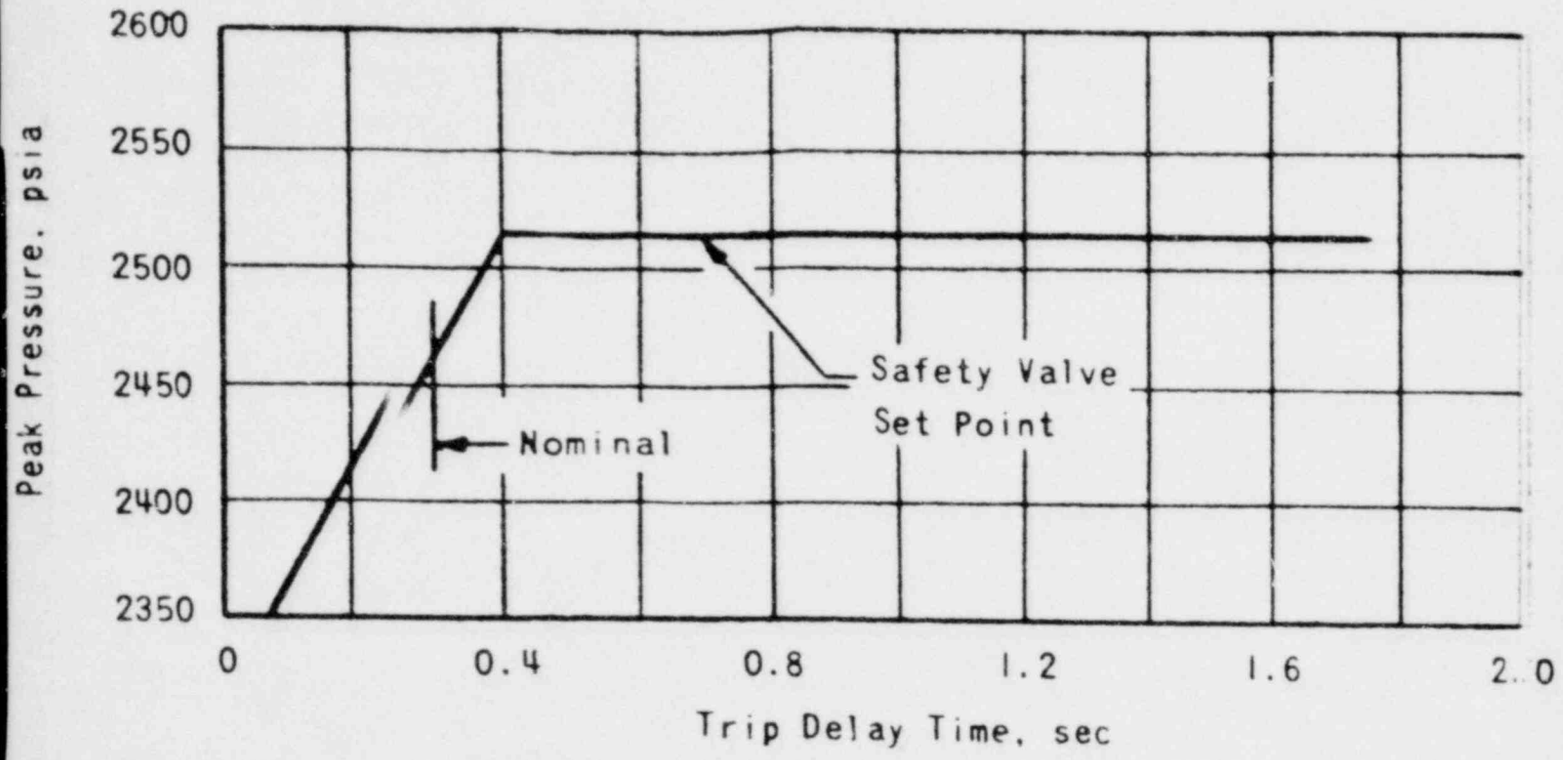

FIGURE 14.1-9
PEAK PRESSURE VERSUS TRIP DELAY TIME
FOR A STARTUP ACCIDENT USING ALL RODS AT
5.8×10^{-4} $(\Delta k/k)$/SEC FROM 10^{-9} RATED POWER

000 0194

SMUD
SACRAMENTO MUNICIPAL UTILITY DISTRICT

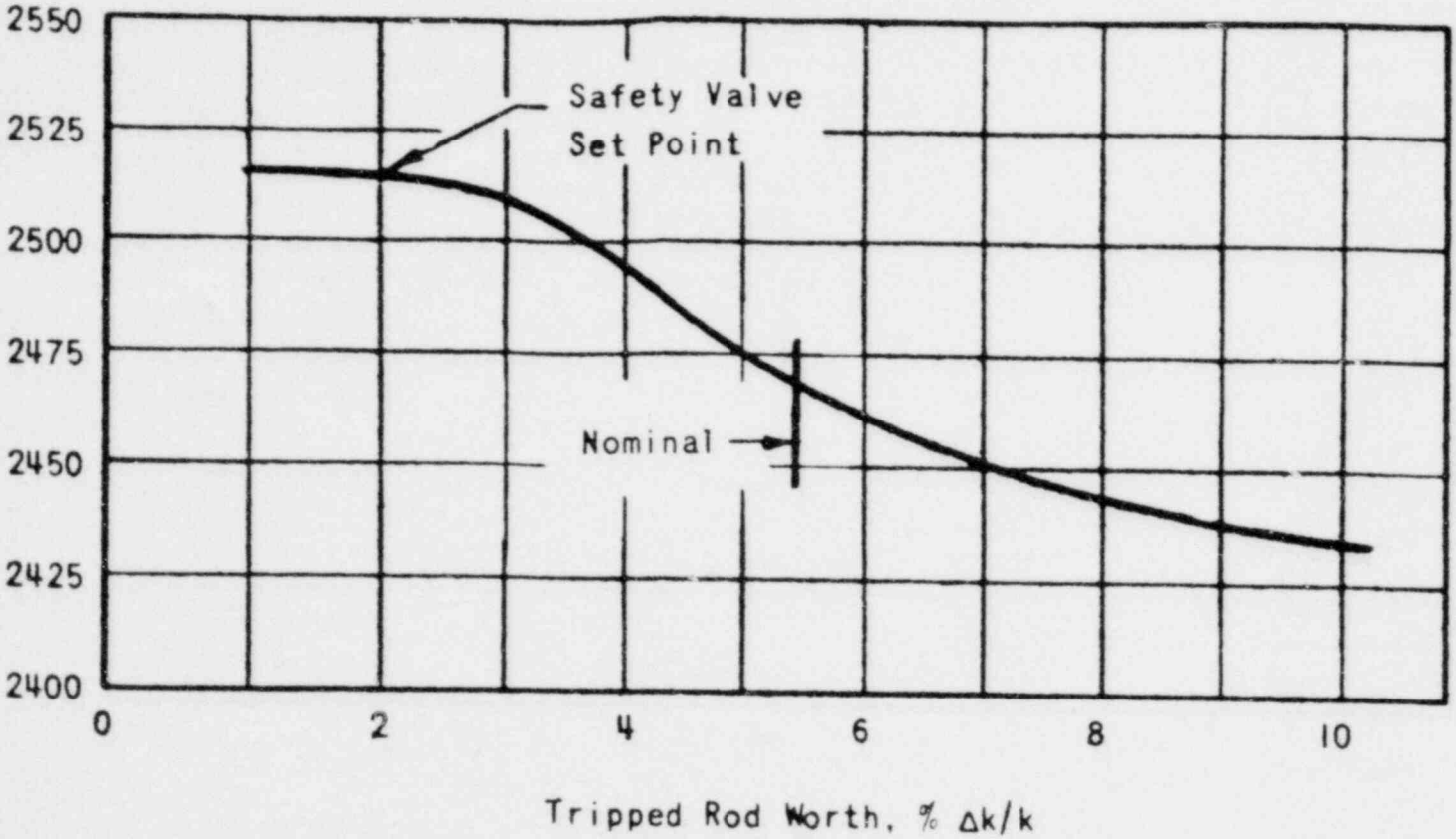

FIGURE 14.1-10
PEAK PRESSURE VERSUS TRIPPED ROD WORTH
FOR A STARTUP ACCIDENT USING ALL
RODS AT 5.8×10^{-4} $(\Delta k/k)$/SEC
FROM 10^{-9} RATED POWER

000 0195

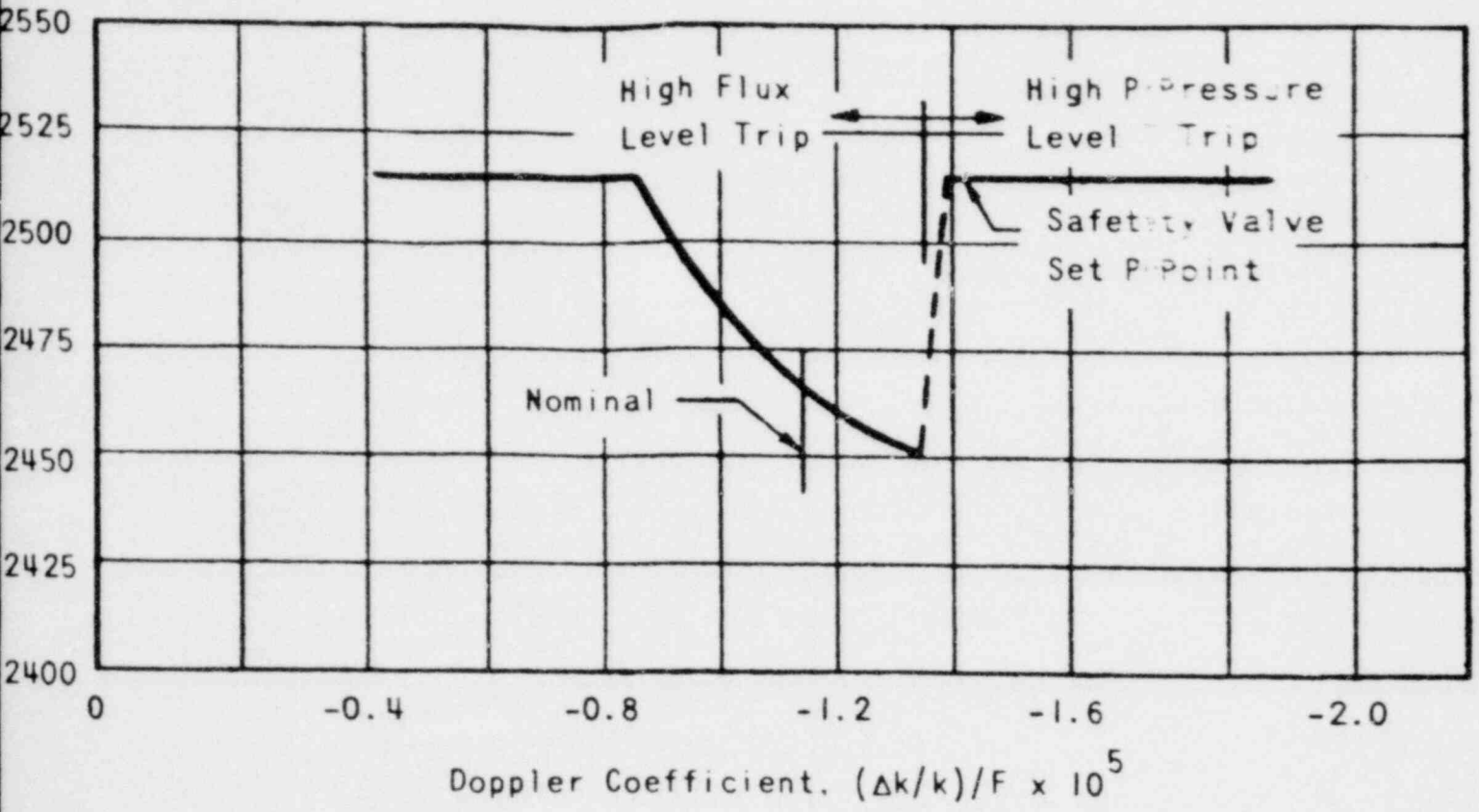

FIGURE 14.1-1111
PEAK PRESSURE VERSUS DOPPLER COEFFICIENT
FOR A STARTUP ACCIDENT USING ALL RODS
AT 5.8 X 10^{-4} (Δk/k)/SEC
FROM 10^{-9} RATED POWER

000 0196

SMUD
SACRAMENTO MUNICIPAL UTILITY DISTRICT

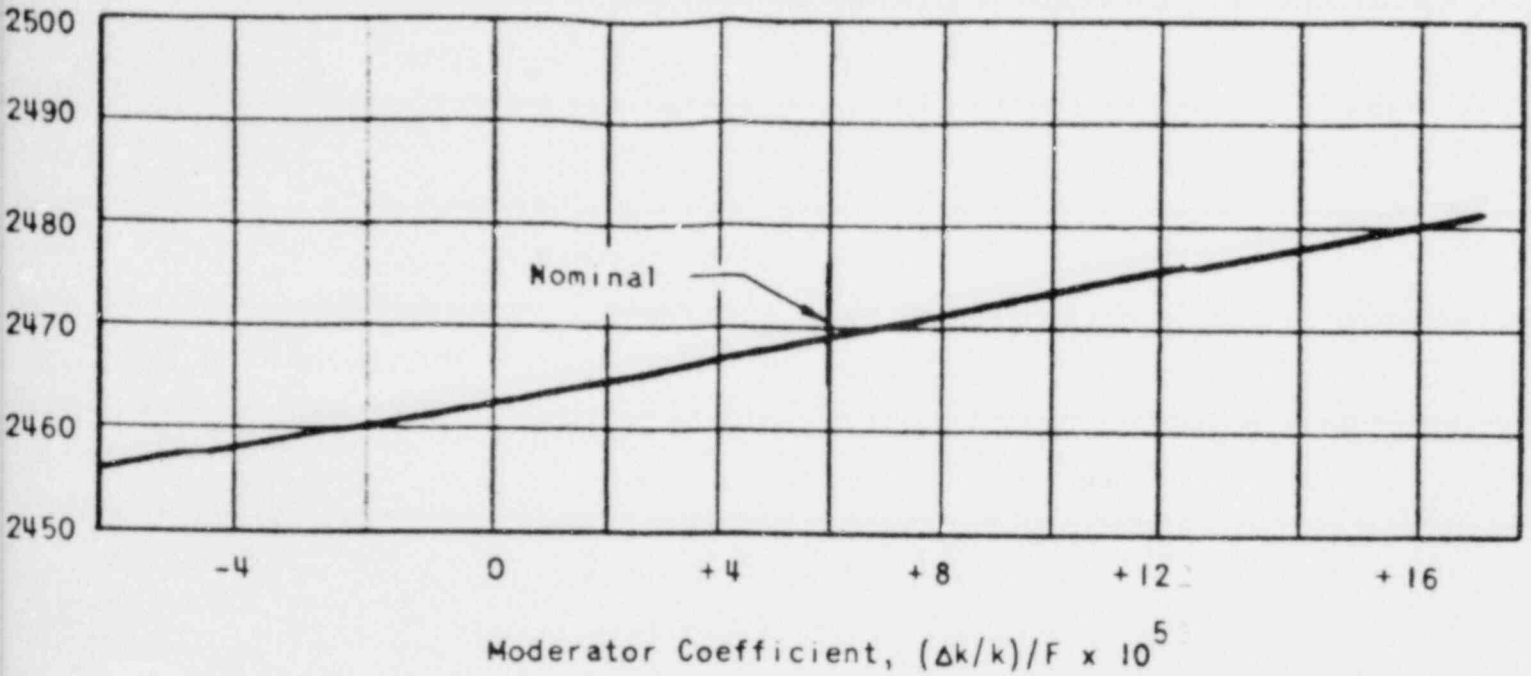

FIGURE 14.1-112
PEAK PRESSURE VERSUS MODERATOR
COEFFICIENT FOR A STARTUP ACCIDENT
USING ALL RODS AT 5.8 X 10^{-4}
(Δk/k)/SEC FROM 10^{-9} RATED POWER

000 0197

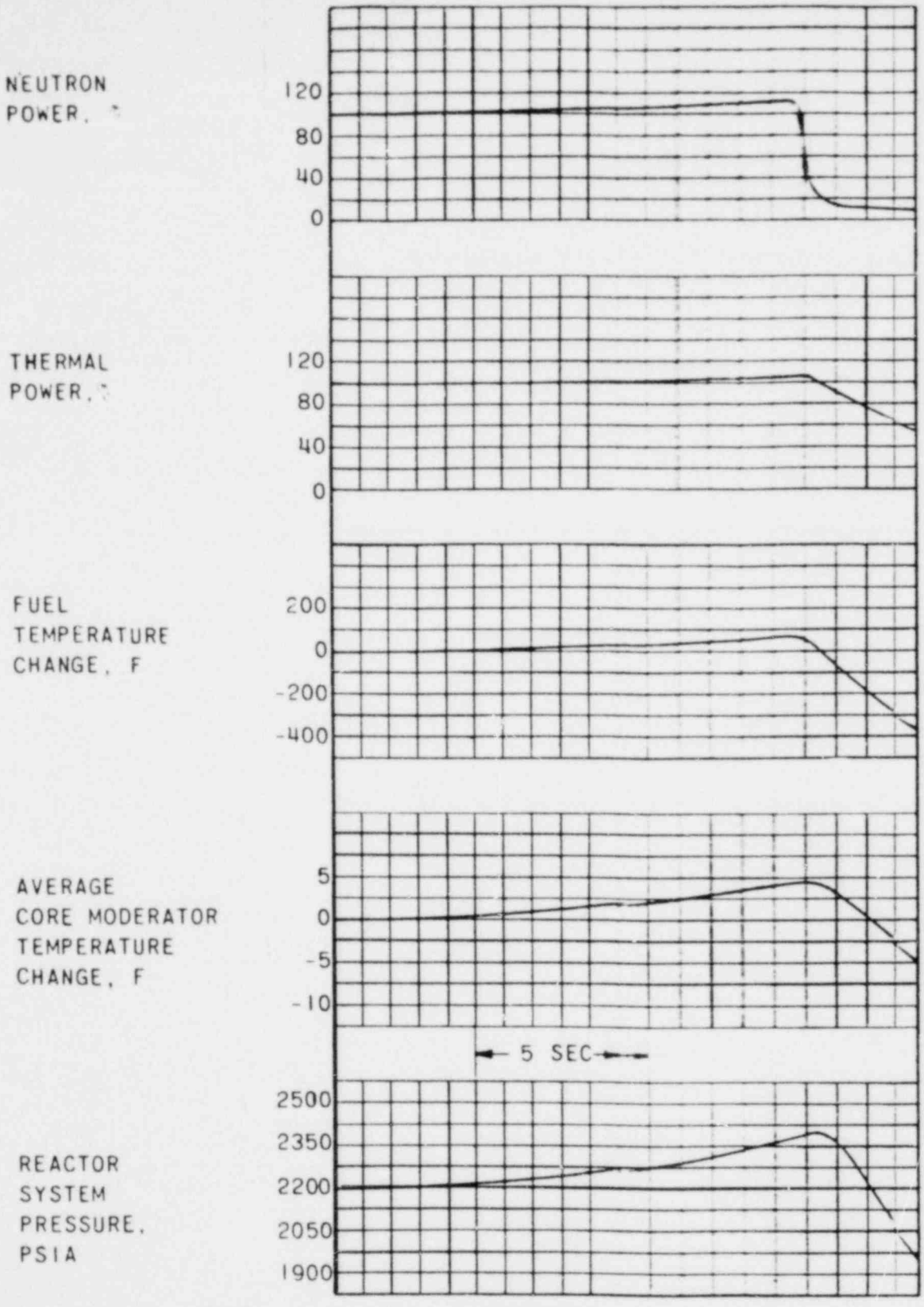

FIGURE 14.1-13
ROD WITHDRAWAL ACCIDENT FROM RATED POWER USING A 1.2% Δk/k ROD GROUP AT 5.8 X 10^{-5} (Δk/k)/SEC; HIGH PRESSURE REACTOR TRIP IS ACTUATED

SMUD
SACRAMENTO MUNICIPAL UTILITY DISTRICT

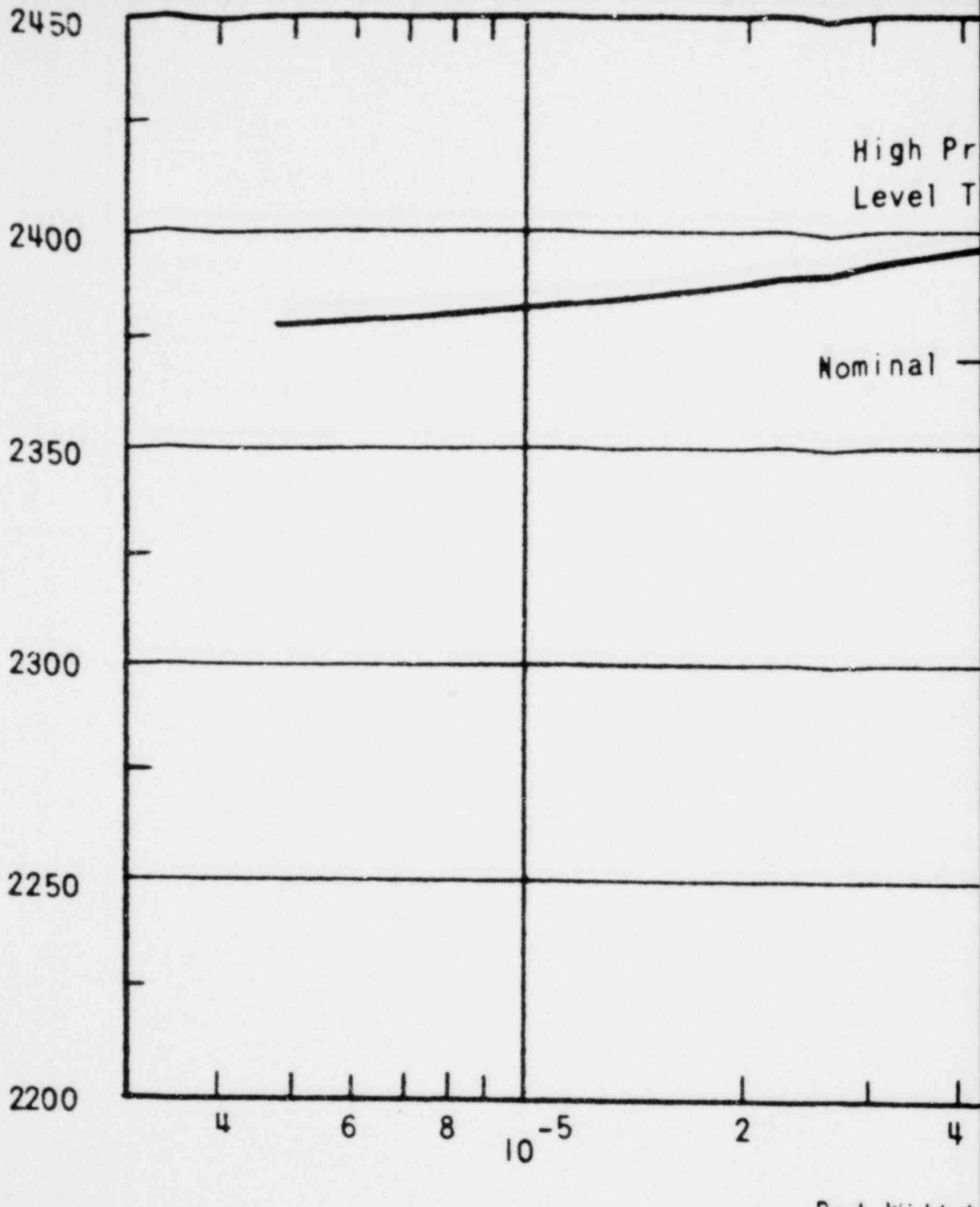
2450
2400
2350
2300
2250
2200
High Pr
Level T
Nominal
4
6
8
10^{-5}
2
4
Rod Withd

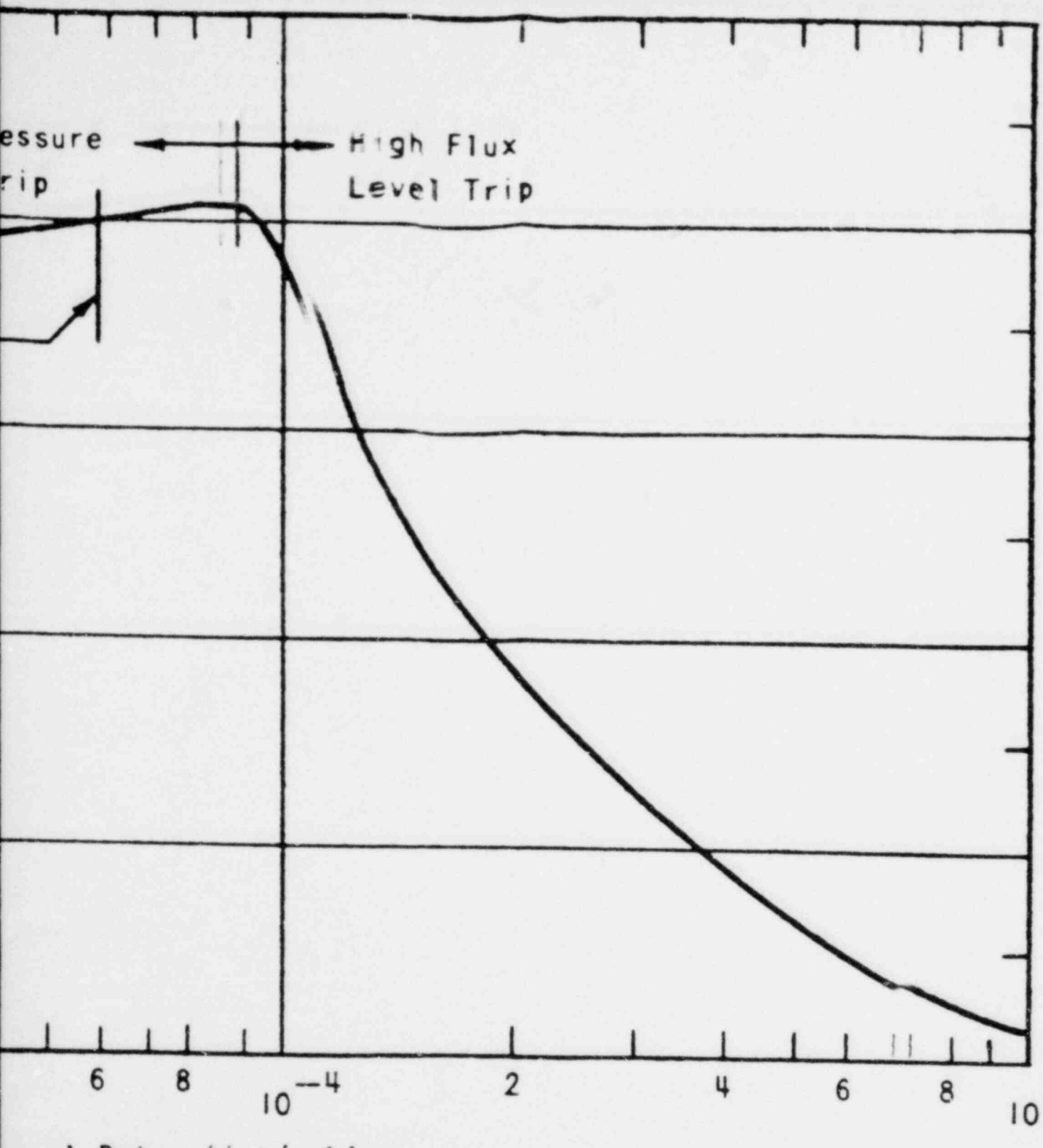

FIGURE 14.1-14
PEAK PRESSURE VERSUS ROD WITHDRAWAL RATE FOR A ROD WITHDRAWAL ACCIDENT FROM RATED POWER

SMUD

SACRAMENTO MUNICIPAL UTILITY DISTRICT

000 0200

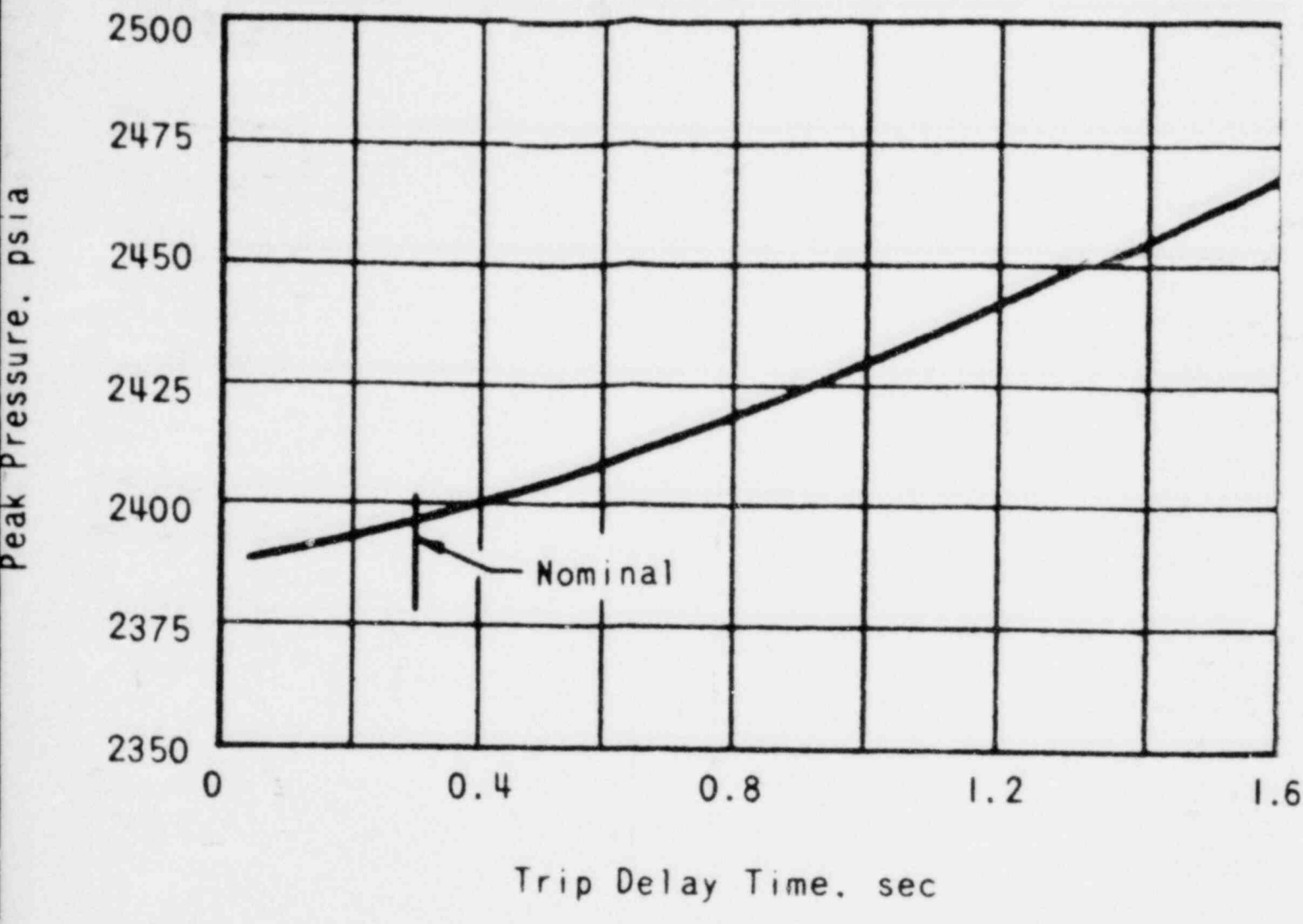

FIGURE 14.1-15
PEAK PRESSURE VERSUS TRIP DELAY TIME FOR A ROD WITHDRAWAL ACCIDENT FROM RATED POWER USING A 1.2% Δk/k ROD GROUP; HIGH PRESSURE REACTOR TRIP IS ACTUATED

SMUD
SACRAMENTO MUNICIPAL UTILITY DISTRICT
000 0201

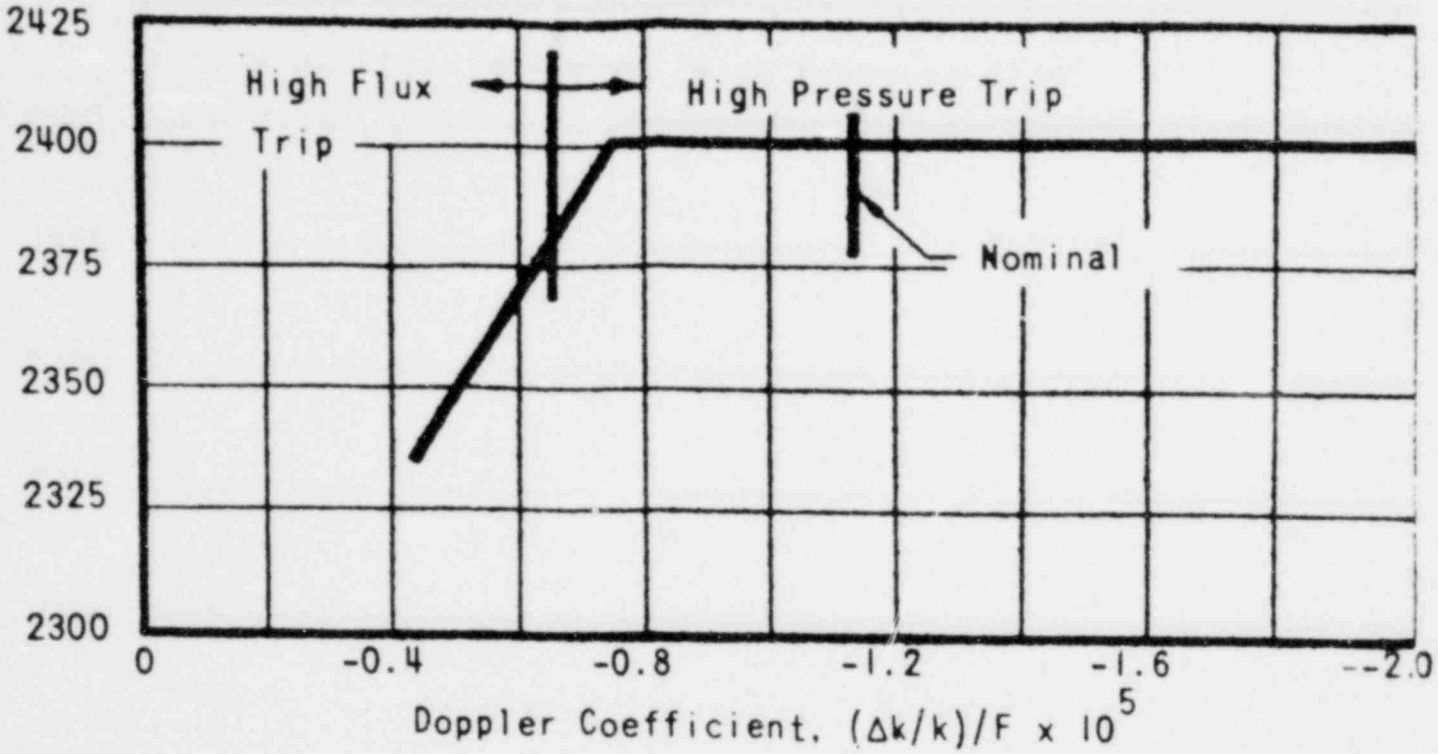

FIGURE 14.1-16
PEAK PRESSURE VERSUS DOPPLER COEFFICIENT
FOR A ROD WITHDRAWAL ACCIDENT FROM RATED
POWER USING A 1.2% Δk/k ROD GROUP

SMUD

SACRAMENTO MUNICIPAL UTILITY DISTRICT

000 0202

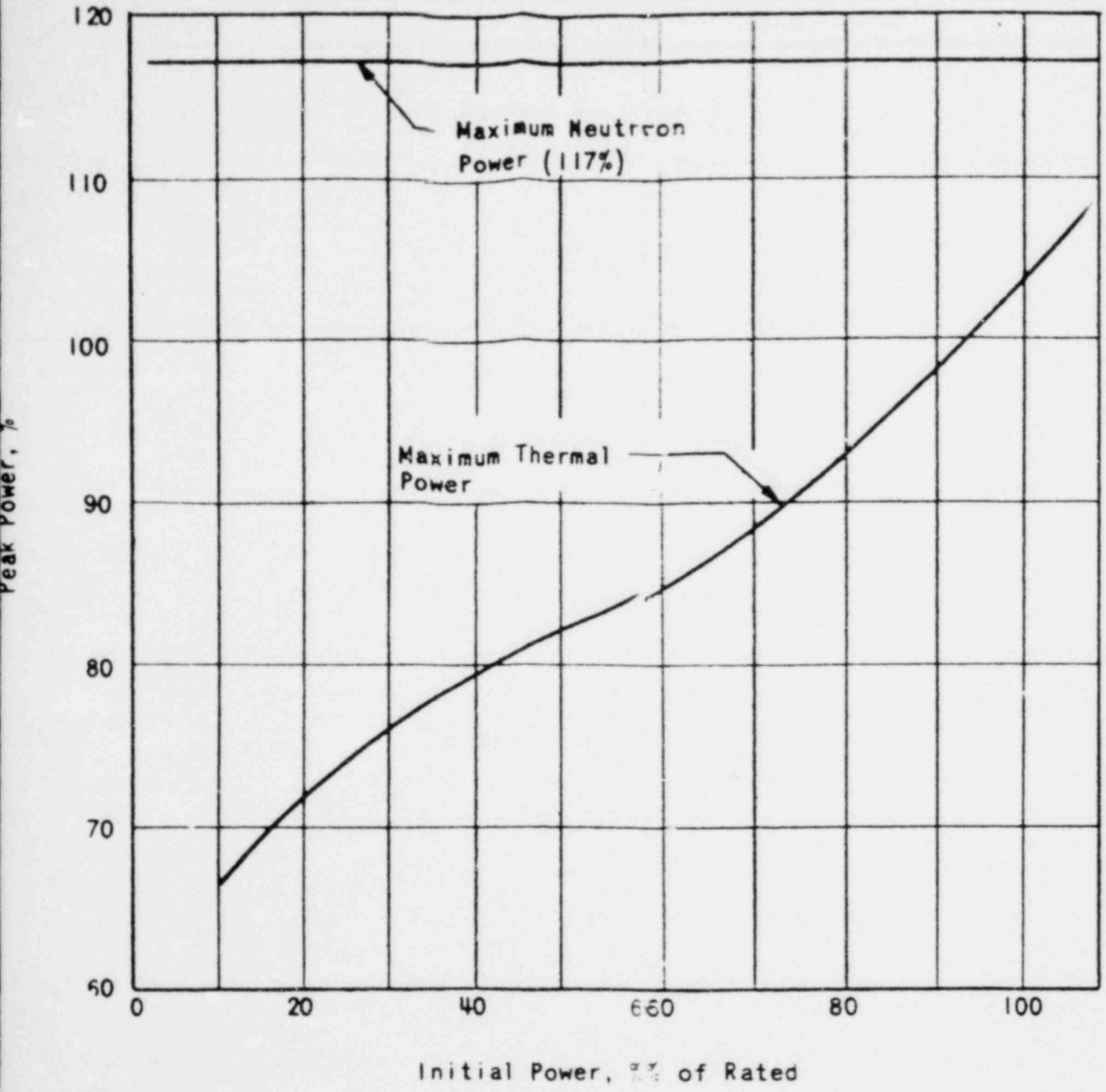

FIGURE 14.1-17
MAXIMUM NEUTRON AND THERMAL POWER
FOR AN ALL-ROD WITHDRAWAL ACCIDENT
FROM VARIOUS INITIAL POWER LEVELS

SMUD
SACRAMENTO MUNICIPAL UTILITY DISTRICT
000 0203

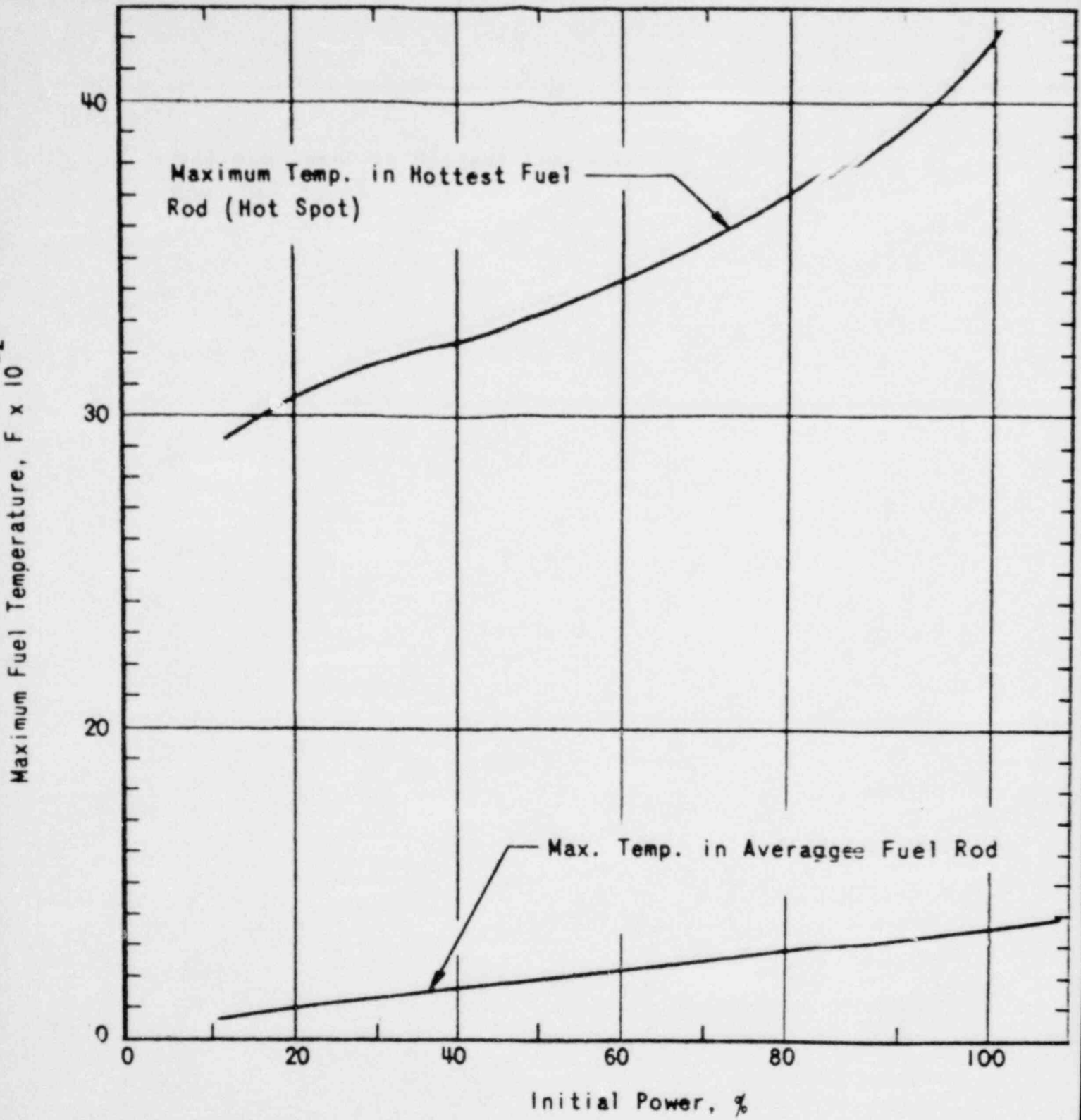

FIGURE 14.[illegible]-18
PEAK FUEL TEMPERATURES IN AVERAGE ROD AND HOT SPOT FOR AN ALL-ROD WITHDRAWAL ACCIDENT FROM VARIOUS INITIAL POWER LEVELS

SMUD
SACRAMENTO MUNICIPAL UTILITY DISTRICT

000 0204

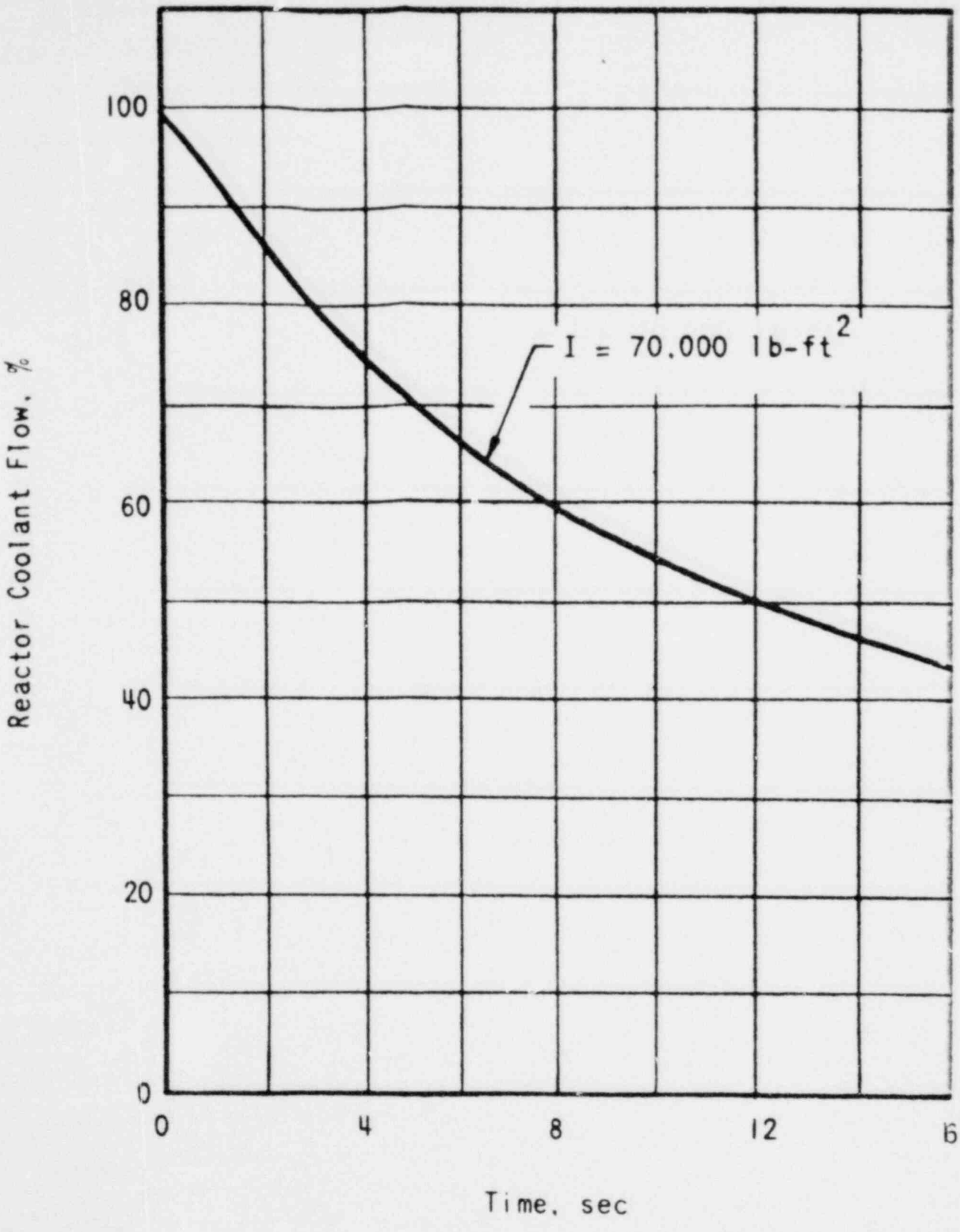

FIGURE 14.1-19
PERCENT REACTOR COOLANT FLOW AS A
FUNCTION OF TIME AFTER
LOSS OF PUMP POWER

SMUD
SACRAMENTO MUNICIPAL UTILITY DISTRICT

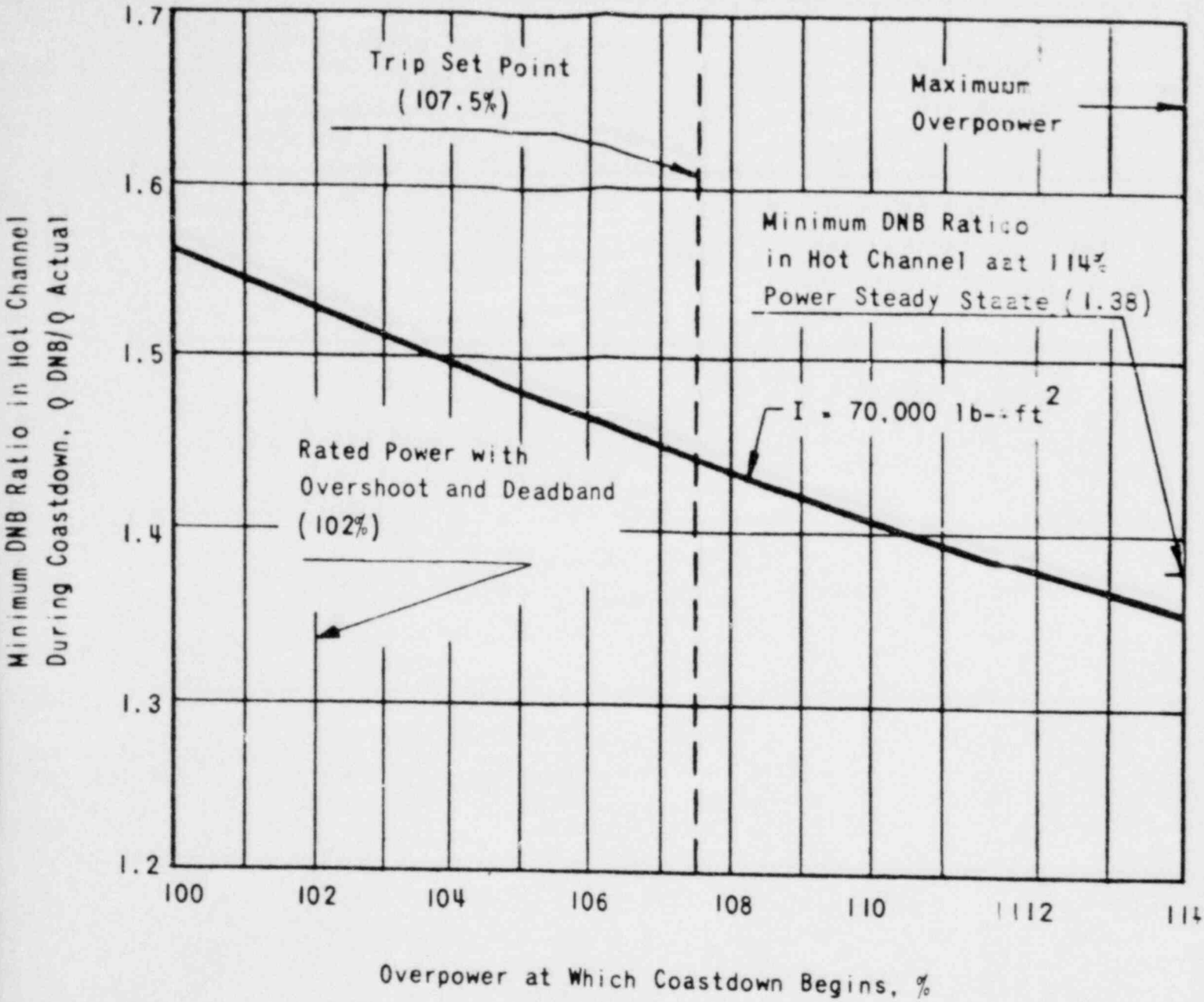

FIGURE 14.1-20
MINIMUM DNBR WHICH OCCURS
DURING THE COASTDOWN FOR
VARIOUS INITIAL POWER LEVELS

SMUD 00

SACRAMENTO MUNICIPAL UTILITY DISTRICT

000 0206

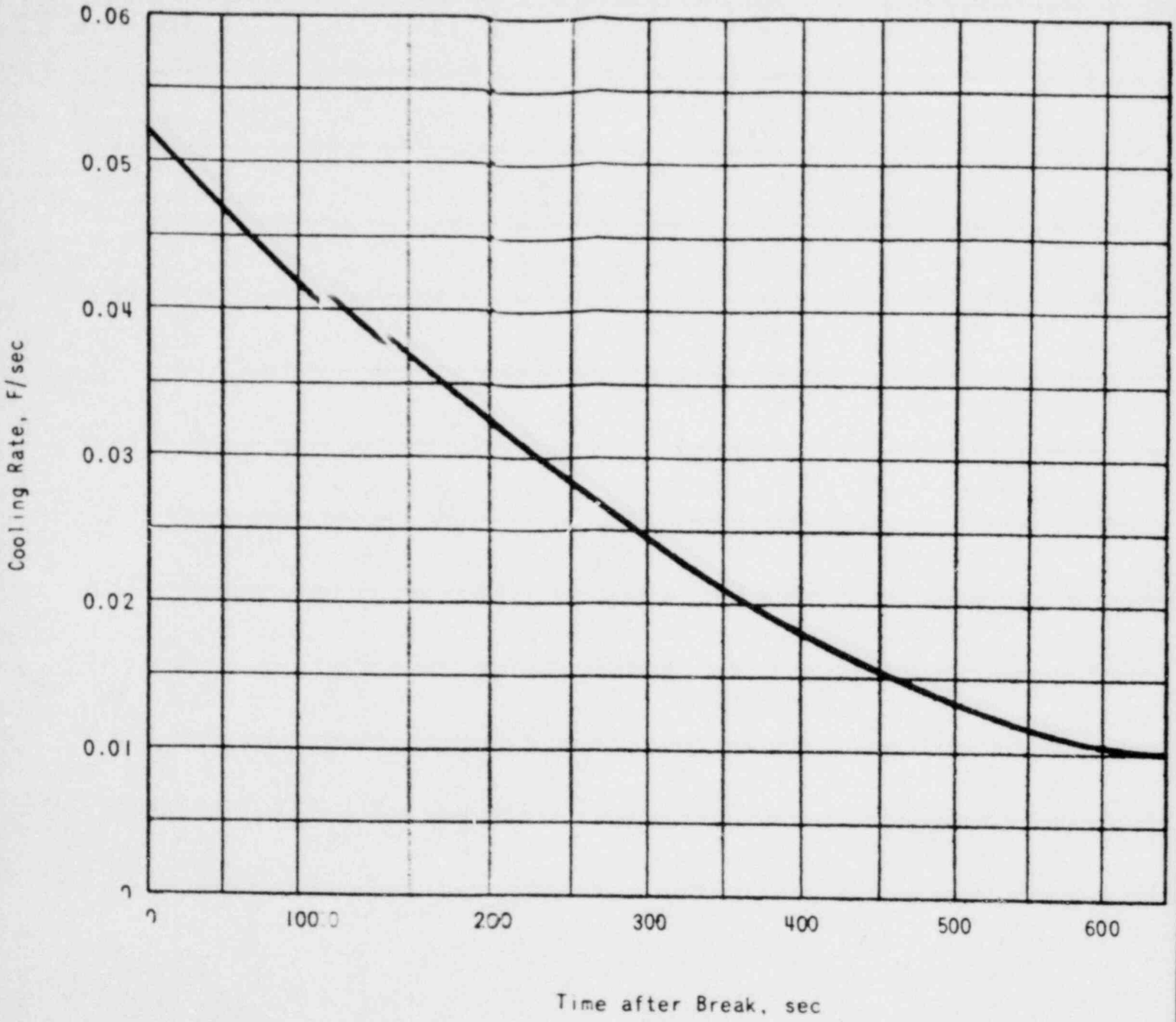

FIGURE 14.1-21
REACTOR SYSTEM COOLING RATE FOR
A STEAM LINE BREAK OF 4 IN.^{2}

00.

SMUD
SACRAMENTO MUNICIPAL UTILITY DISTRICT

14.2 STANDBY SAFEGUARDS ANALYSIS

14.2.1 SITUATIONS ANALYZED AND CAUSES

In this section accidents are analyzed in which one or more of the protective barriers are not effective and standby safeguards are required. All accidents evaluated are based on the ultimate power level of 2,568 Mwt rather than the rated power level of 2,452 Mwt. Table 14.2-1 summarizes the potential accidents studied.

TABLE 14.2-1
SITUATIONS ANALYZED AND CAUSES

Event	Cause	Effect
Fuel Handling Accidents	Mechanical damage during transfer.	Gap activity released. Environmental consequences discussed in 14.3.5
Rod Ejection Accident	Failure of control rod drive pressure housing.	Some clad failure. Environmental consequences discussed in 14.3.6
Loss-of-Coolant Accident	Rupture of reactor coolant system.	No clad melting. Environmental consequences evaluated in 14.3.8
Maximum Hypothetical Accident	Release from core of 100% noble gases, 50% iodine, and 1% solid fission products.	Environmental consequences shown in 14.3.9

14.2.2 ACCIDENT ANALYSES

14.2.2.1 Fuel Handling Accidents

14.2.2.1.1 Identification of Accident

Spent fuel assemblies are handled entirely under water. Before refueling, the reactor coolant and the fuel transfer canal water above the reactor are increased in boron concentration so that, with all control rods removed, the k_{eff} of a core is no greater than 0.98. In the spent fuel storage pool, the fuel assemblies are stored under water in storage racks having an eversafe geometric array. Under these conditions, a criticality accident during refueling is not considered credible. Mechanical damage to the fuel assemblies during transfer operations to the auxiliary building is possible but improbable. This type of accident is considered the maximum potential source of activity release during refueling operations.

000 0208 00

14.2.2.1.2 Analysis and Results

The fuel assembly is conservatively assumed to have operated at 29 Mwt, twice the power level of an average fuel assembly. The reactor is assumed to have been shut down for 24 hours, which is the minimum time for reactor cooldown, reactor closure head removal, and removal of the first fuel assembly. It is further assumed that the entire outer row of fuel rods, 56 of 208, suffers damage to the cladding. Since the fuel pellets are cold, only the gap activity is released. The fuel rod gap activity is calculated using the escape rate coefficients and calculational methods discussed in 11.1.1.3. 2

The gases released from the fuel assembly pass through the spent fuel storage pool water prior to reaching the auxiliary building atmosphere. As a minimum, the gases pass through 10 feet of water. Although there is experimental evidence that a portion of the noble gases will remain in the water, no retention of noble gases is assumed. Based on pertinent data,[3,4] 99 percent of the iodine released from the fuel assembly is assumed to remain in the water. The total activity released to the building atmosphere is therefore:

Iodine	28.4 curies
Noble gases	2.79×10^4 curies

14.2.2.2 Rod Ejection Accident

14.2.2.2.1 Identification of Accident

Reactivity excursions initiated by uncontrolled rod withdrawal (14.1) were shown to be safely terminated without damage to the reactor core or reactor coolant system integrity. In order for reactivity to be added to the core at a more rapid rate, physical failure of the control rod drive housing or control rod drive nozzle must occur. Failure in the drive upper pressure housing can cause a pressure differential to act on a control rod assembly and rapidly eject the assembly from the core region. The power excursion due to the rapid increase in reactivity is limited by the Doppler effect and terminated by reactor protection system trips.

The criterion for reactor protection, should this condition occur, is that the reactor will be operated in such a manner that a control rod ejection accident will not further damage the reactor coolant system.

a. Accident Bases

The bases for the rod ejection accident are as follows:

Worth of ejected rod	0.3% Δ k/k
Rod ejection time	0.150 sec
Ultimate power level	2568 Mwt
Reactor trip delay	0.3 sec

0

000 0269

The severity of the rod ejection accident is dependent upon the worth of the ejected rod and the reactor power level. The control rod group of greatest worth is the first of the entire rod pattern to be withdrawn from the core. The worth of the ejected rod can be as high as 30 percent of the total pattern worth of 10.0% $\Delta k/k$, i.e., 3% $\Delta k/k$. However, the 3% $\Delta k/k$ value exists only when the reactor is subcritical. The details of control rod worth calculations and the methods of selecting the number of control rods in each group are presented in 3.2.2 and 7.2.2.1.2.

When the reactor is subcritical, the boron concentration is maintained at a level whereby the reactor is at least 1 percent subcritical with the control rod of greatest worth fully withdrawn from the core. Therefore, rod ejection, when the reactor is subcritical and all other rods are in the core, does not cause a nuclear excursion. As criticality is approached, the worth of the remaining control rods decreases. At criticality, rod ejection would result in a maximum reactivity addition of 0.56% $\Delta k/k$. 1

At rated power, but before equilibrium xenon is established, the total rod pattern worth remaining in the core is 2.8% $\Delta k/k$. At equilibrium xenon the pattern worth is 1.8% $\Delta k/k$. Before establishing equilibrium xenon, the greatest single control rod worth is 0.46% $\Delta k/k$. A single rod worth of up to 0.7% $\Delta k/k$ has been used in the analysis of this accident. 1

In order for any one rod to have this much worth, it would necessarily be fully inserted in the core. Assuming that a pressure housing failure occurs in such a manner that it no longer offers any restriction for rod ejection, the time and therefore the rate of reactivity addition can be calculated. Further assuming that there is no viscous drag force limiting the rate of ejection, control rod travel time to the top of the active region of the core is calculated to be 0.176 sec. To account for the S-shaped reactivity worth versus position of the rod, an ejection time of 0.150 sec (75 percent of active core height) is used in the analysis.

b. Fuel Rod Damage Criteria

Power excursions caused by reactivity disturbances of the order of magnitude occurring in rod ejection accidents could lead to three potential modes of fuel rod failure. First, for very rapid and large transients in

which there is insufficient time for heat transfer from fuel to cladding, fuel melting followed by vaporization can generate destructive internal pressures without increasing cladding temperatures significantly. The second mode occurs when the internal vapor pressure is not sufficient to cause cladding rupture, but subsequent heat transfer raises the temperature of the cladding and weakens it until failure occurs. The third mode occurs when the nuclear excursion has insufficient energy to cause melting of the fuel, but subsequent heat transfer to clad from fuel may cause excessive cladding temperatures. In all three cases there is a possible occurrence of metal-water reactions. However, only very rapid and large transients will generate a rapid pressure buildup in the reactor coolant system.

The energy required to initiate UO_2 fuel melting is 220 to 225 cal/gm, based on an initial temperature of 68 F.[5] The heat of fusion requires an additional 60 cal/gm. Any further energy addition vaporizes the fuel and produces a buildup of vapor pressure within the fuel rod. The effect of the vapor pressure is dependent upon the temperature and ultimate strength of the cladding. Energy additions of up to 420 cal/gm have been calculated to be necessary before the bursting pressure of cladding is exceeded. The lower limit for producing significant fuel vapor pressure (14.7 psi) is 325 cal/gm.[6] The potential cladding failure is a function not only of the fuel vapor pressure, but also of fission product gas pressure, cladding and fuel irradiation exposure, and zirconium hydriding. At a lower limit, the potential for bursting of cladding and release of molten fuel to the reactor coolant is conservatively set at a fuel enthalpy of 280 cal/gm in this evaluation.

For power excursions with energy bursts below 280 cal/gm, zirconium-water reactions are possible. A correlation of the TREAT experiments presents a method of correlating the potential zirconium-water reaction as a function of fission energy input.[7] These data are based on initially cold (room temperature) fuel rods, but are also correlated as a function of peak adiabatic core temperature. This correlation can be used either by computing the core temperature or by adding the initial steady state fuel enthalpy to the nuclear energy burst and obtaining an equivalent final fuel enthalpy. Accordingly, a zirconium-water reaction requires a minimum fuel enthalpy of 125 cal/gm. Increasing fuel enthalpies cause a linear increase in the percentage of the reaction, which may be approximated by

$$\%Zr\text{-}H_2O \text{ Reaction} = 0.125 \text{ (Final Fuel Enthalpy - 125)}.$$

000 0211

It is assumed that DNB will take place when the clad reaches a heat flux of 6.36×10^5 Btu/hr-ft^2. At this heat flux the hot fuel rod enthalpy would be approximately 140 cal/gm at EOL and 130 cal/gm at BOL. Applying the peaking factors described in 3.2.3 to the results of these analyses, the percent of the core having an enthalpy greater than the values above can be calculated. Any fuel rod exceeding the enthalpy values above is assumed to fail from overheating and releases the gap activity of that fuel rod.

14.2.2.2.2 Method of Analysis

The hypothetical control rod ejection accident was investigated using the exact 1-dimensional WIGL2 digital computer program.[8] It was found that the point kinetics analog model results agreed with the WIGL2 results to within 10 percent for rod worths up to 0.75% $\Delta k/k$. The point kinetics model assumes an initial flux distribution which is undisturbed by local control rod assemblies. The space-dependent model, however, has significant flux depressions in the vicinity of control rods. Although the flux throughout the core begins to increase shortly after the start of the rod ejection, the flux increase in this depressed region rises more quickly so that by the time the average power has reached a level just a few percent above the initial power level, the flux shape has almost no perturbation in the region previously occupied by the ejected rod. The entire reactor flux then rises uniformly until the Doppler effect terminates the excursion. Thus by applying the peak-to-average flux factors of 2.92 for EOL and 3.24 for BOL to the point kinetics results, the peak and integrated flux at any point in the reactor can be accurately assessed.

14.2.2.2.3 Analysis and Results

a. Source Power

A sensitivity study at source level has been done around a single rod worth 0.5% $\Delta k/k$. This analysis was performed with the core 0.5% $\Delta k/k$ sub-critical so that a total rod worth of 1% $\Delta k/k$ was withdrawn in 0.150 sec. The reactor power was initially at 10^{-9} of the ultimate power level. The low pressure trip occurs at 1.7 sec after the ejection starts, and the reactor power is terminated at a peak value of 39 percent ultimate power. This peak neutron power value is not reached until about 15 sec after the rod is ejected because Doppler feedback controls the rate of rise and magnitude of the neutron power. Therefore, a low pressure trip will terminate the accident before significant power is generated owing to the loss of coolant through the rupture. 1

000 0212 0(

An analysis was performed for the accident above without a low pressure trip to demonstrate the capability of the reactor to accept the accident.

In this case the neutron power reaches 1,000 Mwt (39 percent ultimate power), and the peak fuel temperature is 990 F. This is far below the melting temperature of UO_2, and the resultant thermal power is only 16 percent of ultimate power. Hence, no fuel damage would result from the rod ejection accident at source power level.

b. Ultimate Power

1

A sensitivity study at ultimate power level has been done around an assumed single rod worth of 0.3% $\Delta k/k$. The analysis includes rod worths from 0.1-0.7% $\Delta k/k$, however, for the ultimate power case at beginning-of-life (BOL), the ejection of a single control rod worth 0.3% $\Delta k/k$ would result in virtually no Zr-H_2O reaction and approximately 1% of the core experiencing DNB (see Figures 14.2-1 and 14.2-2). The hot fuel rod would reach a peak enthalpy of about 166 cal/gm.

For the end-of-life case (EOL), the reactor neutron power peaks at 6,190 Mwt, 200 milliseconds after the start of ejection of a 0.3% $\Delta k/k$ control rod. The prompt negative Doppler effect terminates the power rise, and control rod insertion from high flux signal terminates the excursion. The total neutron energy burst during the transient is approximately 3,200 Mw-sec. The final fuel enthalpy of the nominal rod is 113 cal/gm, i.e., the enthalpy of the hot rod is 163 cal/gm. This enthalpy is considerably below the minimum range (220 to 225 cal/gm) for central fuel melting. As a result of the excursion, approximately 13.5 percent of the core would have DNB (see Figure 14.2-1).

The power distribution at the beginning of core life, with the higher power peaking factors shown in 3.2.3, was used to determine the distribution of the energy of the excursion. With this distribution of fuel enthalpies, and using the TREAT correlation, 0.53 percent of the zirconium cladding may react (see Figure 14.2-2) to contribute an additional 677 Mw-sec of energy. The resultant temperature increase is spread over a relatively long period of time. Consequently, the metal-water reaction energy is liberated over a long period of time, and no damaging pressure pulses are produced in the system.

As a result of the postulated pressure housing failure, which produces a rupture size of 0.04 sq ft, reactor coolant is lost from the system. The rate of mass and energy input to the reactor building is considerably

lower than that for the 3 sq ft rupture discussed in 14.2.2.3. This lower rate of energy input results in a lower reactor building pressure than that obtained for the 3 sq ft rupture.

The fission product release from this accident is calculated by conservatively assuming that all fuel rods that undergo a DNB will experience a clad failure, subsequently releasing all gap activity. Actually most of the fuel rods will recover from the DNB, and no fission product release will occur. For the case of a 0.3% $\Delta k/k$ rod ejection from ultimate power at the end of life, 13.5 percent of the fuel rods are assumed to fail, releasing 177,000 curie-equivalents of I-131 and 1.45×10^6 curies of noble gases to the containment building. Fission product activities for this accident are calculated using the methods discussed in 11.1.1.3.

c. Sensitivity Analysis

The results of a sensitivity analysis performed on the control rod ejection accident are shown in Figures 14.2-3 through 14.2-11. Figure 14.2-3 shows the variation in the peak neutron power as a function of the worth of the ejected control rod. For the nominal 0.3% $\Delta k/k$ case from ultimate power, the peak neutron power is less than 300 percent, again assuming that a low pressure trip does not occur. The rod ejection from source level results in a Doppler turn-around before the flux trip is reached. Figure 14.2-4 shows the variation in the corresponding thermal power with control rod worth.

Figure 14.2-5 shows the corresponding enthalpy increase of the hot fuel rod versus control rod worth. Note the very small spread in values for the BOL and EOL ultimate power conditions. As expected, the enthalpy increases with rod worth.

Figures 14.2-6 through 14.2-9 show the peak reactor neutron and thermal powers as a function of changes in the positive moderator temperature coefficient and negative Doppler coefficient for the nominal 0.5% $\Delta k/k$ control rod ejection from source level. There was insignificant variation of the peak neutron and thermal power with changes in the two reactivity feedback coefficients.

Figure 14.2-10 shows the change in nominal thermal power with variations in the trip delay time for the nominal 0.3% $\Delta k/k$ rod ejection from ultimate power (the variation from zero power is negligible). The trip delay time

000 0214

does not affect the peak neutron power because the Doppler effect controls the power transient. Figure 14.2-11 shows the corresponding change in the total enthalpy increase of the hot fuel rod versus the trip delay.

The thermal power never exceeds 114 percent ultimate power for any of the variations studied using the nominal rods (0.1% $\Delta k/k$ for ultimate power and 0.5% $\Delta k/k$ for source level). The hot fuel rod average temperature never increases by more than 310 F above the ultimate power peak value (4,090 F). It is therefore concluded that each of these parameter variations has relatively little effect on the nominal results.

14.2.2.3 Loss-of-Coolant Accident

14.2.2.3.1 Identification of Accident

Failure of the reactor coolant system would allow partial or complete release of reactor coolant into the reactor building, thereby interrupting the normal mechanism for removing heat from the reactor core. If all the coolant were not released immediately, the remaining amount would be boiled off owing to residual heat, fission product decay heat, and possible heat from chemical reactions unless an alternate means of cooling were available. In order to prevent significant chemical reactions and destructive core heatup, emergency core cooling equipment rapidly recovers the core and provides makeup for decay heat removal.

14.2.2.3.2 Accident Bases

All components of the reactor coolant system have been designed and fabricated to ensure high integrity and thereby minimize the possibility of their rupture. The reactor coolant system, the safety factors used in its design, and the special provisions taken in its fabrication to ensure quality are described in Section 4.

In addition to the high-integrity system to minimize the possibility of a loss of coolant, emergency core cooling is provided to ensure that the core does not melt even if the reactor coolant system should fail and release the coolant. This emergency core cooling is provided by the core flooding system, the makeup and purification system (high pressure injection), and the decay heat removal system (low pressure injection). These systems are described in detail in Section 6, and their characteristics are summarized in the following paragraphs.

The performance criterion for the emergency cooling equipment is to limit the temperature transient below the clad melting point so that fuel geometry is maintained to provide core cooling capability. This equipment

000 0215

has been conservatively sized to limit the temperature transient to 2,300 F or less as temperatures in excess of this value promote a faster zirconium-water reaction rate, and the termination of the transient near the melting point would be difficult to demonstrate.

The fuel rods may experience cladding failure during the heatup in the loss-of-coolant accident. This could be due to fission gas internal pressure and weakening of the clad due to the increase in clad temperature. The mechanical strength of the Zircaloy cladding is reduced as the temperature exceeds 1,000 F such that the highly-irradiated fuel rods, with high fission gas internal pressure, may fail locally and relieve the gas pressure when the temperature exceeds 1,200 F. Some local ballooning of rods is likely to occur. However, cooling would still be effective since the fuel rods are submerged, and cross-channel flow around the ballooned area will cool the rod. At worst a local hot spot may occur.

It is calculated that a small number of fuel rods operating at peak power will experience a cladding temperature transient to 1,950 F in about 18 sec. The injection of emergency coolant, at a time when the cladding is at a temperature of about 1,950 F, may also cause distortion or bowing between supports. As a result some of the fuel rods may crack and allow relief of internal pressure. However, the cladding is expected to remain sufficiently intact to retain the solid fuel material and to prevent gross fuel shifting. The transient would be limited to regions of the core which operate at peak power. The major portion of the core will not experience as severe a transient.

Heating of the fuel can and the fuel rod spacer grid requires heat flow from the clad to the structure by conduction and radiation; therefore, the structure temperatures will lag the cladding temperature transient. As the fuel rod temperature rises, the fuel rods are expected to experience some bowing between supports due to the temperature differential existing between the fuel rod and the can. The cans and spacer grids are made from stainless steel and have substantial mechanical strength, even at the maximum expected temperatures. The supporting stainless steel structure will therefore retain sufficient strength to assure spacing between fuel rods to allow emergency coolant to reach them, and will keep the fuel rods in the same location in the core to prevent gross fuel shifting.

The core flooding system has two independent core flooding tanks, each of which is connected to a different reactor vessel injection nozzle by a line containing two check valves and a normally open, remotely operated isolation valve. Since these tanks and associated piping are missile-protected and are connected directly to the reactor vessel, a rupture of reactor coolant system piping will not affect their performance. These tanks provide for automatic flooding when the reactor coolant system pressure decreases below 600 psi. The flooding water is injected into the reactor vessel and directed to the bottom of the reactor vessel by the thermal shield. The core is flooded from the bottom upward. The combined contents of the two tanks (1,880 ft^3 of borated water) rapidly reflood the core immediately after the blowdown to provide cooling until coolant flow can be established by low pressure injection.

000 0216

Or

2 High pressure injection, supplies coolant at pressures up to the design pressure of the reactor coolant system and at a rate up to 1,000 gpm. Low pressure injection supplies coolant at pressures below 200 psig and at a rate up to 6,000 gpm. Both of these systems can operate at full capacity from the on-site emergency electrical power supply and can be in operation within 25 sec after the accident. In the reactor vessel, decay heat is transferred to the injection water.

Injection water is supplied from the borated water storage tank. When this tank empties, water is circulated from the reactor building sump through heat exchangers and returned to the reactor vessel. About 200,000 gallons, corresponding to top 12 feet of water in the fuel pit can be made available for injection in an emergency.

Engineered safeguards are also provided to cool the reactor building environment following a loss-of-coolant accident and thereby limit and reduce pressure in the building. Reactor building sprays, actuated on a high building pressure signal of 10 psig, deliver 3,000 gpm to the reactor building atmosphere. This spray water reaches thermal equilibrium within the building atmosphere during its passage from the nozzles to the sump. Spray water is supplied from the borated water storage tank until it is emptied. Thereafter, water collected in the sump is recirculated to the sprays. Cooling is also provided by the reactor building emergency cooling system in which recirculating fans direct the steam-and-air mixture through the emergency coolers, where steam is condensed. Heat absorbed in
2 the emergency coolers is rejected to the nuclear service cooling water system. The heat removal capacity of either of these two reactor building cooling systems is adequate to prevent overpressurization of the building during a loss-of-coolant accident.

This analysis demonstrates that in the unlikely event of a failure of the reactor coolant system, both of the other two boundaries that prevent fission product release to the atmosphere, i.e., the reactor core and the reactor building, are protected from failure. Accordingly, the public would be protected against potential radiation hazards.

In order to evaluate this accident, a range of rupture sizes from small leaks up to the complete severance of a 36-in. ID reactor coolant system line has been evaluated. A core cooling analysis is presented for the complete severance of the 36-in. ID reactor coolant piping.

Since the large rupture removes the least amount of stored energy from the core, this represents the minimum temperature margin to core damage and, therefore, places the most stringent requirements on the core flooding system.

000 0217

14.2.2.3.3 Accident Simulation

a. Hydraulic Model

Blowdown of the reactor coolant system following an assumed rupture has been simulated by using a modified version of the FLASH[9] code. This code calculates transient flows, coolant mass and energy inventories, pressures, and temperatures during a loss-of-coolant accident. The code calculates inflow from the emergency cooling and calculates heat transferred from the core to the coolant.

Modifications were made to FLASH to make the model more applicable to this system. The changes are as follows:

(1) The calculation of reactor coolant pump cavitation was based on the vapor pressure of the cold leg instead of the hot leg water.

(2) Core flooding tanks have been added. Water flow from the core flooding tanks is calculated on the basis of the pressure difference between the core flooding tanks and the point of discharge into the reactor coolant system. The line resistance and the inertial effects of the water in the pipe are included. The pressures in the tanks are calculated by assuming an adiabatic expansion of the gas above the water level in the tank.

(3) Additions to the water physical property tables (mainly in the subcooled region) have also been made to improve the accuracy of the calculations.

(4) A change in the steam bubble rise velocity has been made from the constant value in FLASH to a variable velocity as a function of pressure. The bubble velocity term determines the amount of water remaining in the system after depressurization is complete. For large ruptures, this change in velocity shows no appreciable change in water remaining from that predicted by the constant value in the FLASH code. For smaller ruptures, an appreciable difference exists. The variable bubble velocity is based on pertinent data[10] and adjusted to correspond to data from the LOFT semiscale blowdown tests.

Test No. 546 from the LOFT semiscale blowdown tests is a typical case for the blowdown through a small rupture area. A comparison of the predicted and experimentally observed pressures is shown in Figure 14.2-12. Figure 14.2-13 shows the percent mass remaining in the tank versus time as predicted by the code. At the end of blowdown, the predicted mass remaining is 13 percent. The measured mass remaining is approximately 22 percent.

000 0218 0

The FLASH code describes the reactor coolant system by the use of two volumes plus the pressurizer. The system was grouped into two volumes on the basis of the temperature distribution in the system as follows

(1) Volume 1 includes half of the core water volume, the reactor outlet plenum, the reactor outlet piping, and approximately 55 percent of the steam generators.

(2) Volume 2 includes half of the core water volume, the reactor inlet plenum and downcomer section, the reactor inlet piping, pumps, and 45 percent of the steam generators.

(3) Volume 3 represents the pressurizer.

The resistances to flow were calculated by breaking the reactor coolant system into 24 regions and calculating the volume-weighted resistance to flow for a given rupture location based on normal flow resistances. For the double-ended ruptures, all of the leak was assumed to occur in the volume in which that pipe appeared.

The reactor core power was input as a function of time as determined by the CHIC-KIN code in conjunction with the FLASH output. Steam generator heat removal was assumed to cease when the rupture occurred.

The modified FLASH code has the capability of simulating injection flow from the core flooding tanks. The core flooding transient analysis was performed using the reactor vessel pressure as predicted by FLASH to get the flow from the core flooding tanks. Reactor vessel filling was calculated by adding the mass remaining in the vessel as predicted by FLASH to the mass injected from the core flooding tanks. This method of calculation is conservative in that condensation of steam by the cold injection water is not taken into account. A more recent analysis using the FLASH code with condensation effects confirms the conservatism used in this analysis.

Pressure, temperature, mass and energy inventories, and hydraulic characteristics as determined by FLASH are input into the core thermal code (SLUMP) and the reactor building pressure buildup code (COPATTA).

b. Core Thermal Model

The core heat generation and heat transfer to the fluid are dependent upon the blowdown process. The FLASH program includes a core thermal model and the feedbacks of

000 0219 01

heat transfer and flow on each other. While the FLASH thermal model is acceptable for determining the effect of core heat transfer on the blowdown process, a more extensive simulation is necessary for evaluation of the core temperature transient.

Additional analytical models and a digital computer program (SLUMP) were developed to simulate the core thermal transient for the period beginning with the initiation of the leak and ending after the core temperature excursion had terminated.

The model includes the effects of heat generation from neutrons before reactor trip, neutron decay heat, and fission and activation product decay heat; the exothermic zirconium-water reaction based on the parabolic rate law; heat transfer within the fuel rods, limited heat convection from the fuel clad surface to any fluid within the core region, heat transfer from reactor vessel walls and internals to the coolant, and heat transfer from fuel rods to the steam necessary to sustain a metal-water reaction; and all emergency injection flow and boiloff.

The basic model structure provides 50 equal-volume core regions with input provisions to allow any choice of power distribution. The model may be used to simulate the entire core or any subdivision of the core. Therefore, the core geometry may be detailed to the degree consistent with the results desired.

The following parabolic law for the zirconium-water reaction equation (11) with the following constants is simulated for each of the regions:

$$-\frac{dr}{dt} = \frac{K}{(r_o - r)} \exp -\frac{\Delta E}{RT}$$

where

r = radius of unreacted metal in fuel rod

r_o = original radius of fuel rod

t = time

K = rate law constant (0.3937 cm^2/sec)

ΔE = activation energy (45,500 cal/mole)

R = gas constant (1.987 cal/mole K)

T = temperature, K

300 0220 0

The zirconium-water reaction heat is assumed to be generated completely within the clad node. The heat necessary to increase the steam temperature from the bulk temperature to the reaction temperature is transferred from the clad at the point of reaction. The above equation implies no steam limiting. All heat from neutron, beta, and gamma sources is assumed to be generated within the fuel according to the pre-accident power distribution and infinite irradiation.

Within each of the regions there is a single fuel node and a single clad node with simulation of thermal resistance according to the normal fuel rod geometry. Provision is made to simulate four different modes of heat transfer from the clad node to the fluid sink node by specifying the time-dependent surface coefficient.

The surface heat transfer coefficient input data are determined from calculations which are based on flow and water inventory as furnished from the blowdown and the core flooding tank performance analysis.

In the event that insufficient cooling is provided, the program will allow clad heating to progress to the melting point. At this point the latent heat of zirconium must be added before the clad melts. Provisions are also incorporated to allow the clad to be heated to temperatures above the melting point before slump occurs.

As each region slumps it may be assumed to surrender heat to a water pool or to some available metal heat sink. If water is available an additional 10 percent reaction is assumed to occur.

The program output includes the following (as a function of time unless otherwise specified):

(1) Average fuel temperature of each region.

(2) Average clad temperature of each region.

(3) Percent metal-water reaction in each region.

(4) Time for the clad of each region to reach the metal-water threshold, the beginning and end of melting, and the slump temperatures.

(5) Heat transferred to the reactor building from the core.

000 0221

01

(6) Heat generation by hydrogen and oxygen recombination.

(7) Total zirconium-water reaction.

(8) Total heat stored in metal sinks.

c. Reactor Building Pressure Model

The reactor building pressure - temperature analysis is performed using the digital computer code COPATTA.[17] This code is a Bechtel Corporation modification of the CONTEMPT code originally written by Phillips Petroleum Company in conjunction with the LOFT project. The basic treatment of the problem is very similar to that of the CONTEMPT program but the modified code has been extended to analyze the short-term pressurization of the steam generator compartment during the early part of the blow-down.

In this application of COPATTA, the reactor building is considered divided into two regions: the atmosphere (water vapor and air mixture) and the sump region (liquid water). Each region is assumed to be well mixed and in thermal equilibrium, but the temperature of each region may be different. Mass and energy addition may be made to the appropriate region to simulate primary system blowdown, injection cooling overflow through the rupture, and metal-water reactions including hydrogen recombination. Boiling in the liquid region and condensing in the vapor region are accounted for, when conditions warrant, and provide mass and energy transfers between regions.

The containment building is represented by several heat-conducting segments, thermal behavior can be described by the one-dimensional multi-region transient heat conduction equation. The heat-conducting segments may also be used to describe building internals which act as heat sources or sinks. The program includes the capability of cooling the atmosphere region by air coolers and water sprays, and cooling the sump water being recirculated to the reactor vessel by decay heat coolers.

Calculations are begun by computing initial steady-state atmosphere conditions from the input data obtained from FLASH and SLUMP. Subsequent calculations are performed at specified time steps. Following the rupture, the mass and energy addition to the building atmosphere is determined for each time step. Heat losses or gains due to the heat-conducting segments are calculated. Then the mass, volume, and energy balance equations are solved to determine building pressure, temperature of the liquid and vapor region, and mass transfer between regions.

000 0222

14.2.2.3.4 Accident Analysis

a. Core Flooding Tank-Design Base Accident

The core flooding tank design criteria is based upon the DBA condition such that the 36-in. ID, double-ended pipe rupture produces the fastest blow-down, restricting heat removal from the fuel. This case therefore represents the most stringent emergency core cooling requirements. Results from the modified version of FLASH indicate that the core flooding tank simulation provides for the retention of all injection plus a portion of the original reactor coolant that would otherwise have been released. Thus, the cool injection water provides a cooling and condensing effect which reduces overall leakage. For the present analysis, no credit has been taken for the extra accumulation of water due to the condensing effect.

A detailed analysis of the void shutdown and core response was made with the digital computer program CHIC-KIN. This program accounts for changes in flow, pressure, enthalpy, and void fraction. It also computes axially weighted Doppler and moderator coefficients of reactivity for the kinetics calculation. The Doppler coefficient is input as a nonlinear function of fuel temperature, and the moderator void coefficient is input as a function of void fraction. The parameters describing the coolant were obtained from the digital computer program FLASH, which in turn used the neutron power output from CHIC-KIN. The core is assumed to be initially at the ultimate power level of 2568 Mwt.

Figures 14.2-14 and 14.2-15 show the results of the hot leg, 14.1-ft^2 rupture simulation without trip action. Figure 14.2-14 is the neutron power trace, and Figure 14.2-15 shows the various components of the reactivity feedback.

Figure 14.2-16 shows the total energy generated for the spectrum of leak sizes in the hot leg. Above a 3-ft^2 rupture the blowdown forces on the control rod are greater than the normal core pressure drop so that control rod insertion is not as rapid for the larger break sizes. The dashed portion of the curve represents an estimate of degraded control rod insertion velocity for the intermediate rupture sizes. The blown down forces on the control rods during cold leg rupture do not inhibit rod drop velocity for the complete spectrum of leak sizes. Accordingly, the data presented for the spectrum of cold leg rupture is based upon reactor trip characteristics. The results of this study have been used for determination of hot spot clad temperatures for the loss-of-coolant accident spectrum analysis presented in the following pages under 14.2.2.3.4.b.

000 0225

The transient core flow from the FLASH analysis of the 36 in. ID, double-ended rupture was used to determine the core cooling mechanism used in SLUMP. The very high flow rates during the initial blowdown period provide nucleate boiling conditions. However, the time for Departure from Nucleate Boiling (DNB), especially for the hot regions, is extremely difficult to determine. Therefore, a conservative approach was adopted by assuming DNB at 0.25 sec. Nucleate boiling surface coefficients at high flow rates may exceed 50,000 Btu/hr-ft^2-F. A nucleate boiling surface coefficient of 25,000 Btu/hr-ft^2-F was used in the analysis. However, the series heat transfer from the clad node to the fluid sink is limited to 6,500 Btu/hr-ft^2-F by the relatively low conductance of the clad.

After DNB the surface heat transfer was calculated using the flow provided by FLASH results and Quinn's modified version of the Sieder-Tate[13] correlation:

$$h_{TPF} = 0.023 \frac{k}{D_h} (N_{Re})^{0.8} (N_{Pr})^{1/3} \left[1 + \frac{1 - x}{X} \left(\frac{\rho_B}{\rho_F}\right)\right]^{0.8} \left(\frac{\mu_B}{\mu_W}\right)^{0.14}$$

where

h_{TPF} = two-phase film heat transfer coefficient, Btu/hr-ft^2-F

k = fluid conductivity, Btu/hr-ft^2-F

D_h = hydraulic diameter, ft

N_{Re} = Reynolds number

N_{Pr} = Prandtl number

X = quality

ρ = density

μ = viscosity

subscript B = Bulk

subscript F = Film

subscript W = Wall

000 0224

With this correlation, bulk steam properties are used in the basic form, and the last two bracketed terms are modifiers which correct for quality and different conditions at the wall.

Figure 14.2-17 shows the core flow vs time for the 14.1 ft^2 leak as calculated by FLASH.

Figure 14.2-18 shows the clad surface heat transfer coefficient versus time based on the flow of Figure 14.2-17 and the modified Sieder-Tate equation. The straight line in Figure 14.2-18 indicates the surface heat transfer values which were used in SLUMP, and which are conservative as compared to the results obtained from the Sieder-Tate equation.

In applying the Sieder-Tate equation constant values of bulk steam quality and temperature corresponding to the most conservative assumptions were used.

A sensitivity analysis was made for maximum coefficients in SLUMP ranging from 400 to 2,000 Btu/hr-ft^2-F initially and decreasing to zero at the end of blowdown. Results are discussed below.

After blowdown no core cooling is assumed until after core recovering starts. When the water level reaches the core bottom and starts to rise up on the core, the submerged portion will be cooled by pool boiling, and any steam thus produced will provide some cooling for that portion of the core above the water line. However, in determining peak clad temperatures no cooling is assumed for that portion of the core which is above the water line.

At the point of initial contact of cool water against hot cladding the heat flux and temperature differences will be such that film boiling is the probable mode of heat transfer. This mode provides the lowest surface coefficients which would be in the range of 100 to 300 Btu/hr-ft^2-F. However, in evaluating the core flooding tank design a conservative approach was used by assuming a value of 20 Btu/hr-ft^2-F. This value is adequate for terminating the temperature excursion in the clad.

The core flooding tank analysis incorporated the study of performance sensitivity to three significant core flooding tank parameters: (a) gas pressure (400 to 1,000 psig), (b) ratio of nitrogen gas volume to total volume (1/3 and 1/2), (c) and size of piping between the core

000 0225

flooding tanks and the reactor vessel (12 in. and 14 in. ID). Figure 14.2-19 shows the reactor vessel water level versus time for core flooding tanks operating at 600 psig with different combinations of volume ratio and line size. This figure includes an allowance for boiloff and also shows the effect of the flow provided by high pressure and low pressure injection beginning at 25 sec with emergency power available. Similar curves for 400 psig and 1,000 psig core flooding tanks are shown in Figure 14.2-20. Figure 14.2-21 shows the maximum clad temperature reached by the hot spot and by the 1, 2, 3, 4 and 5 percentiles of the core as a function of quench time.

The quench time for a given percentile is taken as that time when the water level reaches the highest point in the core at which the peaking factor corresponding to that percentile exists. The fact that the same peaking factor may exist at some lower point in the core provides an inherent conservatism in the data as plotted. The axial peaking factor profile for the beginning of core life was used as it imposes the most stringent requirements on the core flooding tank design.

Peak temperatures for the core flooding systems described above are also shown on Figure 14.2-21. These curves demonstrate that all of the systems presented are capable of keeping the peak temperature at the hot spot more than 1,000 F below the melting temperature of the clad. The amount of zirconium-water reaction which occurs for each of these core flooding systems is shown in Table 14.2-2. While this preliminary analysis indicates some difference in the performance of the systems, it is not considered to be a significant difference since the analysis was performed without considering the effects of condensation by the core flooding coolant or of possible bypass to the leak of part of the coolant.

The preliminary core flooding tank design selected is for a 600 psi charge pressure, 940 ft^3 of water, 470 ft^3 of nitrogen, and a 14 in. supply line. The performance of this system in limiting core temperatures is approximately in the center of the range for the systems described. The parameters selected for the final system design will be based on the results of core melting analyses to be conducted as part of the final design of the reactor. For this 600 psi charge pressure, Figure 14.2-21 indicates that the hot spot clad temperature would reach 1,950 F at 17.5 sec and that less than 5 percent of the core would exceed 1,690 F. For this same case calculations indicate less than 0.005 percent total zirconium-water reaction for the whole core.

000 0226

C

TABLE 14.2-2
CORE FLOODING TANK PERFORMANCE DATA

Pressure	Line Size, in.	Nitrogen Volume, % of Total	Total Metal Water Reaction, %
400	14	33	.022
400	14	50	.009
600	14	33	.005
600	14	50	.002
600	12	33	.022
600	12	50	.010
1,000	12	33	.003
1,000	12	50	≈ 0

Additional analysis was performed to evaluate the sensitivity of the maximum clad temperature to three important thermal parameters. All cases discussed below have in common the following parameters

Parameter	Performance
Leak size:	14.1 ft^2
Time of DNB:	0.25 sec
Time at ultimate power:	2 sec
Time that blowdown cooling ends:	9.5 sec
Core region:	Hot spot
Time to initiate quenching:	18 sec
Dependent variable examined:	Clad temperature for hottest 5 percent of core

Figure 14.2-22 shows the clad maximum temperature sensitivity to the initial surface heat transfer coefficient after the 0.25 sec nucleate boiling period. The coefficient is linearly decreased to zero at 9.5 sec. Zero cooling is maintained until quenching is initiated with a clad surface coefficient of 20 Btu/hr-ft^2-F. Previous discussion indicated justification for assuming 1,000 Btu/hr-ft^2-F for the clad surface at 0.25 sec. Figure 14.2-22 shows that a value of 1,000 is not on the most sensitive part of the curve and a 20 percent decrease in h would only result in increasing the peak clad temperature 120 F.

000 0227

The assumption that DNB occurs at 0.25 sec is quite conservative. The duration of the nucleate boiling period has been evaluated to show the sensitivity of the maximum fuel temperature to this parameter. Figure 14.2-23 shows the effect of variation of time to reach a DNB. It should be noted that if DNB occurred at the time of rupture, the peak temperature would only increase about 30 F above 1,950 F.

Figure 14.2-24 shows hot spot clad temperature transients for a range of injection cooling coefficients. All cases have a clad surface coefficient h equal to 1000 Btu/ft^2-F at 0.25 sec, decreasing to zero at 9.5 sec. Heat removal is then zero until the effect of injection cooling is simulated. Figure 14.2-24 shows that without any cooling the temperature reaches the melting point in approximately 50 sec.

The analysis of core cooling has been based upon 2.1 full-power seconds resulting from a void shutdown using the maximum positive moderator temperature coefficient of $+1.0 \times 10^{-4}$ $(\Delta k/k)/F$. The effect of variation of the integrated power on hot spot clad temperature is shown in Figure 14.2-25. The resultant integrated power before a void shutdown occurs could increase to 3.4 full-power seconds before the hot spot clad temperature would reach 2,300 F, the temperature at which 1.0 percent Zr-water reaction occurs.

An h value of 15 stops the fast temperature excursion and allows only a low rate of increase thereafter. Since the continuously increasing depth of coverage provided by the flooding tanks and the pumped flow injection systems provide additional cooling capability with time, an initial cooling value as low as 15 is probably adequate.

An h value of 20 provides immediate quenching action and a slow cooling rate thereafter.

An h value of 100 provides very fast cooling. Even though the 100 is a realistic value for film boiling in a pool - the probable mode for the submerged portion of the core - a more conservative value of 20 has been used as the reference for evaluating core flooding tank performance.

Figure 14.2-26 shows hot spot clad temperature transients for a range of pool fluid sink temperatures. Parameters for heat transfer prior to 18 sec are the same as discussed in the preceding paragraph. At 18 sec a surface

000 0228

coefficient of 20 Btu/hr-ft^2-F was applied with sink temperatures as indicated. All results reported herein previously have had a sink temperature of 280 F during the quenching period. Prior to quenching, the sink temperature in all cases is based on the transient fluid pressure which results from the FLASH analysis. Figure 14.2-26 shows that any sink temperature below approximately 500 F is adequate for holding or reducing the clad temperature which existed at 18 sec. The core flooding tanks will provide a high flow of cool water. Although some heating will occur from contact with hot metal before the injection water reaches the core, the temperature rise could not be over 50 F assuming that the water came in contact with all reactor coolant system metal below the nozzle level before it contacted the core. Using a reference value of 280 F provides an added conservatism to the analysis.

In conclusion, the analysis has shown that the preliminary design of the core flooding system will provide for covering approximately 80 percent of the core at 25 sec after the double-ended rupture of the 36-in. ID pipe first occurs. Beyond this time high pressure and low pressure injection will provide a continuous increase in the water level.

The clad hot spot temperature excursion is terminated at 1,950 F and less than 5 percent of the total cladding exceeds 1,690 F. Only a minute amount (0.005 percent) of zirconium-water reaction occurs, and the maximum temperature is at least 1,400 F below the clad melting point.

The temperature transient in the core can produce significantly higher than normal temperatures in components other than fuel rods. Therefore a possibility of eutectic formation between dissimilar core materials exists. Considering the general area of eutectic formation in the entire core and reactor vessel internals, the following dissimilar metals are present, with major elements being in the approximate proportions shown.

Type 304 Stainless Steel	Control Rod	Zircaloy-4	UO_2
19% Chromium	80% Silver	98% Zirconium	
10% Nickel	15% Indium	1 3/4% Tin	
Palance Iron	5% Cadmium		

All these elements have relatively high melting points, i.e., greater than 2,700 F, except those for silver, cadmium, and indium which, in the case of indium, is as low as approximately 300 F.

000 0229

00 .3

The binary phase diagram indicates that zirconium in the proportion of 75 to 80 percent has a eutectic point with either iron, nickel, or chromium at the temperatures of approximately 1,710, 1,760, and 2,370 F, respectively. If these dissimilar metals are in contact and if these eutectic points are reached, the materials could theoretically melt even though the temperature is below the melting point of either material taken singularly.

One point of such dissimilar metal contact is between Zircaloy-clad fuel rods and stainless steel spacers. The analysis of the performance of the core flooding tanks during a loss-of-coolant accident indicated that only 4 percent of the cladding would ever exceed the zirconium-iron eutectic point. Since the spacers are located at 21 in. intervals along the assembly and each grid has a very small contact area, only a fraction of the 4 percent would be in contact with stainless steel. The approximate time period that the 4 percent of the cladding is above the eutectic point is 30 sec. Because of the relatively small area of contact, the condition could not progress very far and fuel geometry would be maintained. Unless the proper ratio of metals is available, the melting point is higher than the eutectic point.

Another area of dissimilar metal contact is that of a zirconium guide tube with the stainless steel cladding of the control rod. Following blowdown, heat can be generated in the control rods by absorption of gamma rays. Beta ray decay heat will be deposited in the fuel rods where generated. Since gamma decay heat is only about one-half the total decay heat, and the control rod is shielded from the fuel by a guide tube, heat generation rates in control rods will be less than one-half the rates in the fuel. As a result, the peak heat generation rate in control rods adjacent to hot spot fuel would not exceed an estimated one-half times the rate in these fuel rods which have a 3.1 power ratio. The contribution from radiant heat transfer from higher powered fuel rods would be relatively small. The analysis of core melting shows that, with core flooding tanks, fuel rods with a 1.5 power ratio will not exceed 1,500 F. This is well below the eutectic melting point.

The reactor core will remain subcritical after flooding without control rods in the core because the injection water contains sufficient boron (2,270 ppm) to hold the reactor subcritical at reduced temperatures. The most stringent boron requirement for shutdown without any control rods is at the beginning of core life when the

000 0230

reactor is in a cold, clean condition and 1820 ppm boron are required to maintain k_{eff} of 0.99.(See Table 3.2-6, Soluble Boron Levels and Worth.) The concentration existing in the reactor building sump after a loss-of-coolant accident from operating power at the beginning of core life is 2174 ppm boron. This concentration represents a boron margin of 354 ppm above the subcriticality design value margin of 1 percent.

b. Core Cooling Analysis for Spectrum of Leak Sizes

An analysis of the loss-of-coolant accident has been made for a spectrum of leak sizes and locations. This information has been analyzed and is reported according to the following grouping: (1) hot leg ruptures, (2) cold leg ruptures, (3) injection line failures, and (4) injection system capability.

(1) Hot Leg Ruptures

In 14.4.4.5.4a an analysis of the 36-in. ID, double-ended pipe rupture was presented. This accident produced the fastest blowdown and lowest heat removal from the fuel, therefore producing the highest cladding temperatures of any loss-of-coolant accident. This was therefore the basis for design of the core flooding equipment. A decrease in the rupture size assumed results in decreased maximum clad temperature during a loss-of-coolant accident.

Core cooling evaluations have been performed for a spectrum of four additional rupture sizes using the same basic calculational technique and assumptions as for the large rupture case. These rupture sizes are 8.5, 3.0, 1.0, and 0.4 ft^2. The mass released to the reactor building for these ruptures is shown in 14.2-27. The reactor coolant system pressure-time history for these rupture sizes is shown in Figures 14.2-20 and 14.2-28.

The reactor vessel water volume as a function of time after the rupture for the various rupture sizes is shown in Figure 14.2-29. These water volume curves were generated utilizing the flow available from core flooding tanks, one high pressure injection pump, and one low pressure injection pump. The pumping systems were assumed to have a combined capacity of at least 3,500 gpm with a high pressure pump running on emergency power within 25 sec after the rupture, and a low pressure pump delivering 3,000 gpm when the pressure has decayed to 150 psi, or at 25 sec, whichever occurs later.

2

000 0231

Ol

Figure 14.2-30 shows the hot spot clad temperature as a function of time for the various rupture sizes. As can be seen from this figure, the small-sized ruptures yield maximum clad temperatures which are considerably lower than those resulting from the larger sizes. The results of this study are shown in the following Table 14.2-3.

TABLE 14.2-3
TABULATION OF LOSS-OF-COOLANT ACCIDENT CHARACTERISTICS
FOR SPECTRUM OF HOT LEG RUPTURE SIZES

Rupture Size, ft^2	Full-Power Seconds	Minimum Water Level Below Bottom of Core, ft	Hot Spot Max. Temp., F
14.1	2.1	-6.8	1,950
8.5	3.4	-5.2	1,916
3.0	1.5*	-2.2	1,235
1.0	1.5*	+4.7	1,075
0.4	1.5*	+12.0	1,015

* Blowdown forces on control rods are equal to, or less than, normal pressure drop, and control rods will insert with normal velocities. These values are for trip shutdown rather than for a void shutdown, but include void reactivity effects.

(2) Cold Leg Ruptures

A similar analysis of a spectrum of rupture sizes has been made for the cold leg piping. The rupture sizes tabulated are the double-ended, 28-in. ID, inlet pipe, which yields 8.5 ft^2 of rupture area, and the 3.0 ft^2, 1 ft^2, and 0.4 ft^2 sizes of rupture area.

The reactor coolant system average pressure for this spectrum of rupture sizes as a function of time is shown in Figure 14.2-31. The water level as a function of time is shown on Figure 14.2-32. The water level calculation has been based upon uninhibited flooding as the check valves are provided in the core support barrel to equalize pressures and permit the trapped steam above the core to escape out the rupture.

00

The hot spot temperature as a function of time for the spectrum of cold leg leak sizes is shown in Figure 14.2-33. The results of this analysis are shown in the following Table 14.2-4 below.

TABLE 14.2-4
TABULATION OF LOSS-OF-COOLANT ACCIDENT CHARACTERISTICS
FOR SPECTRUM OF COLD LEG RUPTURE SIZES

Rupture Size ft^2	Pipe I.D. In.	Full-Power* Seconds	Minimum Water Level Below Bottom of Core, ft	Hot Spot Max. Temp., F
8.5	28	0.4*	-6.7	1,785
3	16	1.0*	-4.8	1,575
1.0	10	1.8*	+3.6	1,250
0.4	6	1.3*	+7.0	1,090

*Blowdown forces on control rods are equal to, or less than, normal pressure drop, and control rods will insert with normal velocity. These values are for trip shutdown rather than void shutdown, but include reactivity effects.

(3) Evaluation of Emergency Coolant Injection Line Failure

The evaluation of a low pressure injection line failure has been made, and the results of the analysis show that the reactor is protected. The rupture of a pipe which connects a core flooding tank and the low pressure injection flow to the reactor vessel was assumed to fail adjacent to reactor vessel and before the first check valve. (See Figure 6.1-1). This pipe has an internal diameter of 11.5 in., and the resultant rupture area is 0.72 ft^2.

Interpolation of available blowdown calculations has been used to evaluate this rupture size, and the data show that a rupture of this size would result in the core being uncovered several feet below the top of the core. However, the hot spot will never be uncovered, and peak cladding temperatures will be slightly less than that shown in Figure 14.2-33 for the 1.0 ft^2 cold leg rupture.

Since this small rupture size leaves a considerable water inventory in the reactor vessel, the remaining core flooding tank inventory is more than adequate to completely reflood the core.

2

000 0233 00

The other low pressure line can supply 3,000 gpm of water to the reactor vessel and provide coolant to keep the core cooled. The combined capacity of the two high pressure pumps is 1,000 gpm which is in excess of the boiloff rate (680 gpm) due to decay heat immediately after blowdown. With a single 500 gpm high pressure injection pump the excess water above the core is adequate to prevent the core from being uncovered below the three quarter elevation and beyond 300 sec. the water level will begin to increase.

High pressure injection includes two independent strings of flow to supply borated coolant to the system. If a rupture of high pressure injection piping were to occur in one of the four lines between the attachment to the reactor coolant pipe and the check valve, the other string of this system would have adequate capacity to protect the core against this small leak. In the event of a component failure in the second high pressure injection loop, the ruptured flow path can be monitored by the operator and spillage flow can be stopped by isolation of the affected piping. The entire capacity of one pump can then be utilized to handle the small rupture and protect the core. 2

(4) Evaluation of Emergency Core Injection System Performance for Various Rupture Sizes

The loss-of-coolant analysis is based upon the operation of one high pressure injection pump (500 gpm), one low pressure injection pump (3,000 gpm), and the operation of the core flooding tanks. The capability of other combinations of engineered safeguards to provide core protection has been evaluated in a preliminary analysis. This capability is shown on Figure 14.2-34. 2

In this evaluation the core is considered protected if the combination of emergency cooling systems considered will prevent core damage which would interfere with further core cooling.

The high pressure injection equipment with one pump operating can accommodate leaks up to approximately 3 in. in diameter. The preliminary analysis upon which this conclusion is based indicates that one pump will probably have the capability to protect the core for leaks somewhat larger. 2 2

A combination of one high pressure pump and one low pressure injection pump will protect the core up to 2

a 0.4 ft^2 leak. This is equivalent to the rupture of a pressurizer surge line. Two high pressure injection pumps plus two low pressure injection pumps can protect the core up to leak sizes of 3.0 ft^2.

This is considerably in excess of any of the piping connecting to the reactor coolant system. One high pressure injection pump, plus the core flooding tanks and one low pressure injection pump, can protect the core up to 14.1 ft^2 which is a double-ended rupture of the 36-in. ID, hot leg piping.

The core flooding tanks and one low pressure injection pump can protect the core from about a 0.05 ft^2 leak up to the 14.1 ft^2 leak. Figure 14.2-34 demonstrates that high pressure injection system provides core protection for normal operating leakage and for small leaks in which pressure decay of the system may be slow. For intermediate leak sizes, either the core flooding tanks or low pressure injection protects the core following the loss-of-coolant accident. For very large leaks in the category of a double-ended rupture of the reactor coolant piping, the core flooding tanks and low pressure injection together protect the core. For these leaks the core flooding tanks provide immediate protection and can protect the core for several minutes following the rupture. Due to their limited volume, they must be supplemented by the high flow from the low pressure injection pumps within several minutes following the leak in order to prevent the core from again becoming uncovered as a result of boiling off the core flooding tank coolant.

This evaluation of emergency core cooling capability demonstrates that the core is protected for the entire spectrum of leak sizes in both hot and cold leg piping.

c. Reactor Building - Design Base Accident

The basis for this analysis is that the high pressure injection (makeup and purification system) and the low pressure injection (decay heat removal system) are functioning and the core flooding system is not working. It was assumed that the makeup and purification system had one of three pumps in operation and that the decay heat removal system had both pumps available for operation. These systems, operating on emergency power, were assumed to be capable of delivering a total injection to the core of 6,500 gpm within 25 seconds after the accident occurs. The reactor operating conditions used in this analysis are listed in Table 14.2-5. Operation of the core flooding system was not included in any of the building pressure transient analysis.

000 0235

This approach is conservative since any combination of two flooding tank operations and minimum flow from the high and low pressure pumps will provide a lower energy release rate and peak reactor building pressures than those resulting from the 6,500 gpm flow. 2

During blowdown, mass and energy releases to the reactor building are calculated by FLASH. Figure 14.2-27 is a plot of mass released to the reactor building and Figure 14.2-28 is a plot of reactor coolant average pressure, each calculated by FLASH for the spectrum of hot leg ruptures. Following blowdown a 20-region SLUMP model was used to simulate the core thermal transient. This simulation includes fuel heat generation, metal-water reaction, and quenching when the injection water provided cooling by contact with the core. The hydrogen liberated in the metal-water reaction is transported out of the core by the steam and is burned at the rate formed in the reactor building atmosphere.

As any given segment reached the temperature of 4,800 F it was assumed to drop into water below the core and release all heat down to a datum of 286 F. Also, it was assumed that 10 percent additional zirconium-water reaction occurred. When the water covered approximately 25 percent of the core, the surface heat transfer coefficient from all the core clad to the water was assumed to be 100 Btu/hr-ft^2-F. The determination of water level was based on injection flow and included the effects of boiloff.

TABLE 14.2-5
REACTOR OPERATING CONDITIONS FOR EVALUATION

Parameter	Value
Reactor Coolant System Pressure, psig	2,185
Reactor Coolant Average Temperature, F	584
Reactor Power Level (ultimate), Mwt	2,563
Reactor Coolant System Mass, lb	519,173
Initial Reactor Building Temperature, F	120
Initial Reactor Building Relative Humidity, %	50
Initial Reactor Building Pressure, psia	14.7

Assuming a pool boiling coefficient of 100 for the whole core when only 1/4 was covered is conservative for reactor

000 0236

building pressure analysis because it compressed overall energy transport into the shortest credible period.

Heat was also released from the hot metal of reactor coolant system and the reactor vessel internals. During the blowdown period a surface heat transfer coefficient of 1,000 Btu/hr-ft^2-F was used. After blowdown this coefficient was changed to 100 Btu/hr-ft^2-F for the metal below the leak and 5 Btu/hr-ft^2-F above the leak. The coolant sink temperature was provided by FLASH for the blowdown period and assumed to be 286 F thereafter. The internal heat transfer of the metal was based on a multi-layer finite difference model. The whole process of reactor coolant system metal heat transfer was simulated with a digital computer program.

All heat transferred from the core and the reactor coolant system metal was assumed to generate steam without taking credit for the subcooled condition of the injection water (except for that portion which was boiled off) until the reactor vessel was filled to the leak height. Thereafter all energy was removed by the 6,500 gpm injection flow of subcooled water, and the energy release to the reactor building atmosphere terminated. No delay was assumed in transporting steam to the reactor building.

Both reactor inlet (cold) and reactor outlet (hot) line breaks were analyzed with FLASH. However, a complete analysis was made only for the hot line breaks since they provided for the most rapid heat transport from the core. This was true because the hot line breaks had longer blowdown and better heat transfer during blowdown than did the cold line breaks.

In calculating the reactor building pressure, it was conservatively assumed that the average temperature of the building atmosphere and structural materials was 120 F. Upon release of hot reactor coolant, the steel and concrete act as heat sinks which reduce the reactor building pressure. The heat sinks considered in this analysis are specified in Table 14.2-6.

The heat transfer coefficients between the containment atmosphere and the regions exposed to it were patterned after the data of Kolflat and Chittenden.[18] The coefficient for steel surfaces was 620 Btu/hr-ft^2-F at time zero, then stepped down to 40 Btu/hr-ft^2 after a total heat transfer of 110 Btu/ft^2 had been achieved. The coefficient for exposed concrete surfaces was a constant 40 Btu/hr-ft^2-F. For heat transfer from the sump water to the concrete floor a coefficient of 20 Btu/hr-ft^2-F was used. No credit was taken for heat transfer to reinforcing steel in the concrete structures.

TABLE 14.2-6
REACTOR BUILDING STRUCTURE DATA FOR ANALYSIS OF
TIME-DEPENDENT BUILDING PRESSURE

Structure	Measurement
Reactor Building Free Volume, ft^3	1,900,000
Reactor Building Dome	
Liner surface, ft^2	17,100
Cross-section dimensions:	
Steel liner, in.	.25
Concrete, ft	3.25
Reactor Building Cylinder	
Liner surface, ft^2	61,000
Cross-section dimensions:	
Steel liner, in.	.25
Concrete, ft	3.75
Reactor Building Floor Slab	
Exposed surface, ft^2	8,900
Cross-section dimensions:	
Concrete, ft	1.25
Steel liner, in.	.25
Concrete, ft	10.0
Lined Refueling Cavity	
Exposed surface, ft^2	7,700
Cross-section dimensions:	
Steel liner, in.	.1875
Concrete, ft	1.5
Miscellaneous Unlined Concrete	
Exposed surface, ft^2	62,800
Cross-section dimension:	
Concrete, ft	1.5
Structural and Miscellaneous Exposed Steel	
Mass, lb	844,000
Equivalent slab:	
Exposed surface, ft^2	22,000
Thickness, in.	1.0

000 0238

Two complete systems are provided to cool the reactor building following the loss-of-coolant accident: (1) four reactor building cooling units operating in the emergency mode and (2) a 3,000 gpm building spray. Either of these systems can remove 240 x 10^6 Btu/hr at a building atmosphere temperature of 286 F. These systems operate on emergency power and their startup is assumed to be delayed until 35 seconds after the rupture occurred in the pressure transient analysis. A summary of the input parameters and the results for all cases studied are tabulated in Table 14.2-7.

The largest rupture studied was the complete severance of a 36-in. ID reactor coolant system pipe (14.1 ft^2 rupture area). The high pressure and low pressure injection systems were assumed to begin injecting 6,500 gpm of borated water into the reactor coolant system at 25 sec after rupture. Figure 14.2-35 illustrates the resulting reactor building pressure transient for the case where only the four emergency air coolers operate (Case 1 of Table 14.2-7). The peak pressure resulting from this accident occurs 180 sec after the rupture at a value of 56.7 psig.

3

An analysis of the reactor building pressure for the 36-in. ID pipe rupture and spray cooling of the building without the emergency air coolers has also been performed to demonstrate the effectiveness of this system (Case 2 of Table 14.2-7). Initially, water for the building sprays and for injection to the core is taken from the borated water storage tank. When water from the borated water storage tank is exhausted, the water collected in reactor building sump is recirculated through the reactor building sprays and through the decay heat removal coolers to supply the low pressure injection water.

The water temperature in the reactor building sump during the recirculation phase of a loss-of-coolant accident is maintained below saturation temperature by the decay heat removal coolers. These coolers reduce the temperature of water recirculated to the reactor vessel and returned to the reactor building sump. The heat transfer surface of these coolers is set by the normal operating conditions under the decay heat removal operation mode. The cooling capability of this mode of operation will maintain the reactor coolant at 140 F or less at 20 hours after extended rated power operation and is in excess of that required under accident conditions when a higher temperature difference exists between recirculated water and the cooling service water. The performance of these coolers at various inlet temperatures is shown in Figure 6.1-4.

000 0239

Case No.	Size of Break ft^2	
1	14.1	Cor sta coo at
2	14.1	Cor sta sum at 3,0
3	8.5	Cor sta coo sec
4	3.0	Sam
5	1.0	Sam
6	0.4	Sam
7	14.1	(Wi tio 6,5 240 rio
8	14.1	(Wit bui at coo sta inj
9	14.1	Sam
10	8.5	Sam
11	3.0	Sa

TABLE 14.2-7
SUMMARY OF REACTOR BUILDING PRESSURE ANALYSIS

Engineered Safeguards in Effect	Time SIS Starts Sec	Figures Showing Results	Reactor Building		
			Peak Temp. °F	Peak Press psig	
safety injection systems, 6,500 gpm, t at 25 seconds. Emergency building ers, 240 x 10^6 Btu/hr peak duty start 35 seconds	25	14.2-35 14.2-42 14.2-44	2855	56.7	2
e safety injection systems, 6,500 gpm, rt at 25 seconds, begin recirculating o water through decay heat exchangers 2190 seconds. Building spray system, 00 gpm, start at 35 seconds	25	14.2-36 14.2-37	2855	56.2	2
e safety injection systems, 6,500 gpm, rt at 25 seconds. Emergency building lers, 240 x 10^6 Btu/hr, start at 35 onds	25	14.2-38	2853	55.3	2
e as Case 3		14.2-39 14.2-43 14.2-45	2866	57.1	
e as Case 3		14.2-40	2779	51.7	
e as Case 3		14.2-41	2771	45.6	
h maximum credible metal-water reac- n) core safety injection systems, 00 gpm. Emergency building coolers, x 10^6 Btu/hr. (Answer for Crite- n 49.)	—	14.2-46	2886	57.8	2
h variable metal-water reaction rate) lding spray systems, 3,000 gpm, start 35 seconds. Emergency building lers, 240 x 10^6 Btu/hr (peak duty), rt at 35 seconds. Core safety ection systems do not operate.	—	14.2-47	—	59.0	
e as Case 3		14.2-48	2882	53.5	
e as Case 3		14.2-49	2882	53.9	1
e as Case 3		14.2-50	2883	54.4	

0241

flooding tanks do operate, the amount of zirconium-water reaction will be limited to only 0.063 percent for a 36-in. ID pipe rupture, and the potential hydrogen energy release is approximately 57,000 Btu. This amount of energy will not significantly affect reactor building pressure if ignition is delayed or if the hydrogen burns as formed. 1 1

For the case of no core flooding tanks, as used in the above reactor building design pressure evaluation, the amount of metal-water reaction for the 36-inch ID, double-ended rupture is about 8 percent. The reaction begins at 40 sec and stops at 130 sec, by which time the 6,500 gpm of injection flow provides sufficient coolant inventory to the reactor vessel to recover the hot spot and quench the reaction. The steam flow during this period is assumed to provide the transport mechanism for the hydrogen generated. The resultant concentration of hydrogen (at the time of maximum metal-water reaction rate) in the steam leaving the reactor vessel is 7.2 volume percent. This concentration is below the flammability limit. Further dilution will occur as the steam enters the reactor building, and combustion will not occur even as the reactor building is depressurized. 1 3

The effect of core flooding tanks on the reactor building pressure is shown in Figures 14.2-48, 14.2-49, and 14.2-50. In this analysis the minimum high pressure and low pressure injection flow (6600gpm) starts in 25 seconds and the reactor building emergency cooling starts at 35 seconds. Each core flooding tank contains 7,000 gallons of water. For the 36-inch ID, double-ended pipe rupture (Case I of Table 14.2-7) two core flooding tanks limit the zirconium water reaction to 0.063 percent, and the potential hydrogen energy release is approximately 57,000 Btu. In this case a peak building pressure of 53.5 psig is reached. One core flooding tank will limit the zirconium-water reaction to 0.454 percent; however, the peak building pressure will be about the same as with two tanks operating. This happens because the steam released to the building atmosphere during the core recovering appears later in the transient in the case of one core flooding tank and by that time the original high building pressure has subsided due to action of the heat sinks and air coolers. The 8.5 ft^2 and 3.0 ft^2 ruptures with two core flooding tanks operating (Cases 10 and 11 of Table 14.2-7) results in a reactor building pressure of 53.9 psig and 54.4 psig respectively. 1

Although the evaluation of the emergency injection systems demonstrates that only a small amount of metal-water reaction can occur, the case of no injection flow as well as no core flooding has been evaluated (Case 7 of Table

000 0242

1 14.2-7) in response to Criterion 49 of the AEC General Design Criteria. This case assumed that, after blowdown, the reactor vessel would have water up to the bottom of the core. The core was allowed to heat up by decay heat and metal-water reaction heat.

Steam flow-rate limiting of the reaction was not considered so long as any water was assumed to be in the vessel. If and when the clad reached the melting temperature, it was assumed that the whole region slumped into the bottom of the vessel with the attendant reaction of 10 percent more of the remaining zirconium and with the release to the reactor building of all sensible and latent heat above 285 F.

Upon completion of the boiloff, heat input to the reactor building was assumed to cease. Figure 14.2-46 shows a reactor building pressure of 57.8 psig at 220 seconds, the time at which the reactor vessel boils dry. This peak pressure is below the 59 psig design pressure of the reactor building.

d. Reactor Building Zirconium Reaction Capability

In order to determine the theoretical ultimate zirconium reaction capability of the reactor building, a series of hypothetical accidents was investigated (Case 8 of Table 14.2-7).

Blowdown was based on the 14.1 ft^2 leak case. Heat transfer from the core and all reactor coolant system metal below the leak height was assumed to transfer to a 285 F sink based on a surface coefficient of 50,000 Btu/hr-ft^2-F. For reactor coolant system metal above the leak height 5 Btu/hr-ft^2-F was used. Available core heat consisted of the initial stored heat, the equivalent of two full power seconds, decay heat, and metal-water reaction heat, which was added at arbitrary linear rates. The total heat transferred from the core and reactor coolant system metal was assumed to produce steam from water initially at the saturated condition. Hydrogen recombination energy was added to the reactor building as superheat at the rate of hydrogen production from the zirconium-water reaction.

A series of calculations for each of the various cooling capacities was made varying the energy input rate, i.e., Zr-H_2O reaction rate. For example, a 1 percent per second zirconium-water reaction produces 1.173 x 10^6 Btu/sec of

000 0243 06.

metal-water energy and 0.902 x 10^6 Btu/sec hydrogen recombination energy. In all cases the energy was input at a linear rate beginning 10 sec after the rupture. The emergency cooling units and spray coolers were started 35 sec after the rupture. The "time to complete reaction" is the time it takes the reactor vessel to boil dry.

The results of this study are presented in Figure 14.2-47. This amount of allowable zirconium reaction at any time after blowdown depends upon the amount of reactor building cooling in operation. The capability curves show that at approximately 10 sec, when the blowdown pressure peak occurs, the reactor building could accept an instantaneous zirconium-water reaction of 2 percent. This capability increases greatly after the blowdown pressure peak with reactor building cooling equipment in operation.

With four emergency cooling units in operation a 100 percent reaction in 3,300 sec will not exceed the design pressure of 59 psig. With four emergency cooling units and two sprays operating, a 100 percent reaction in 1,200 seconds will not exceed the design pressure.

e. Transient Consequences

Safety injection is designed to prevent significant clad melting in the event of a loss-of-coolant accident. The analyses in the preceding sections have demonstrated that safety injection will prevent clad melting for loss-of-coolant accidents resulting from reactor coolant system ruptures ranging in size from small leaks to the complete severance of a 36-in. ID main coolant pipe. Without clad melting, only the radioactive material in the coolant at the time of the accident plus some gap activity is released to the reactor building.

Consequences of a loss-of-reactor coolant-accident are analyzed by assuming that 1 percent of the fuel rods are defective before the release of reactor coolant to the reactor building. Table 11.1-3 lists the total activity in the coolant. In addition to the coolant activity, the activity associated with the gap of all fuel rods is also assumed to be released. Calculations indicate that 77 percent of the fuel rods will have some point along their lengths with temperatures in excess of 1,200 F at the time of core flooding tank injection. While perforation of fuel cladding will require some time, it is conservatively assumed that all of the fuel rods release their gap activity during the accident.

000 0244 00

The gap activities of various isotopes is indicated below:

Isotope	Total Gap Activity Curies
Kr 85	8.46×10^5
Kr 85m	6.38×10^4
Kr 88	1.14×10^5
Kr 83m	1.35×10^3
Kr 87	3.59×10^4
I 131	1.23×10^6
I 133	3.06×10^5
I 135	9.17×10^4
I 132	1.75×10^5
I 134	1.81×10^4
Xe 131m	7.37×10^4
Xe 133	9.16×10^6
Xe 133m	1.03×10^5
Xe 135	3.27×10^5
Xe 135m	3.25×10^4
Cs 136	4.19×10^3
Cs 137	3.91×10^6

2

000 0245

00

14.2.2.4 Maximum Hypothetical Accident

The analyses in the preceding sections have demonstrated that even in the unlikely event of a loss-of-coolant accident, no core melting will occur. However, to demonstrate that the operation of a nuclear power plant at the proposed site does not present any undue hazard to the general public, a hypothetical accident involving a gross release of fission products is evaluated. No mechanism whereby such a release occurs is postulated since it would require a multitude of failures in the engineered safeguards provided to prevent its occurrence. For the MHA evaluation, fission products are assumed to be released from the core as follows: 100 percent of the noble gases, 50 percent of the halogens, and 1 percent of the solids.

Further, 50 percent of the iodines released to the reactor building are assumed to plate out. In addition, airborne iodine is assumed to be removed by sprays. A spray removal time constant of 25 hr^{-1} is used as indicated and further discussed in Section 14.3.10. Other parameters, such as meteorological conditions, iodine inventory of the fuel, and reactor building leak rate, are the same as those assumed for the loss-of-coolant accident in 14.2.2.3.5. The average integrated iodine inventory, in terms of equivalent curies of iodine-131 available for leakage at different time periods after the accident, is as follows:

0 to 2 hours	1.46×10^6 curies
0 to 24 hours	1.18×10^6 curies
1 to 30 days	0.27×10^6 curies

000 0246

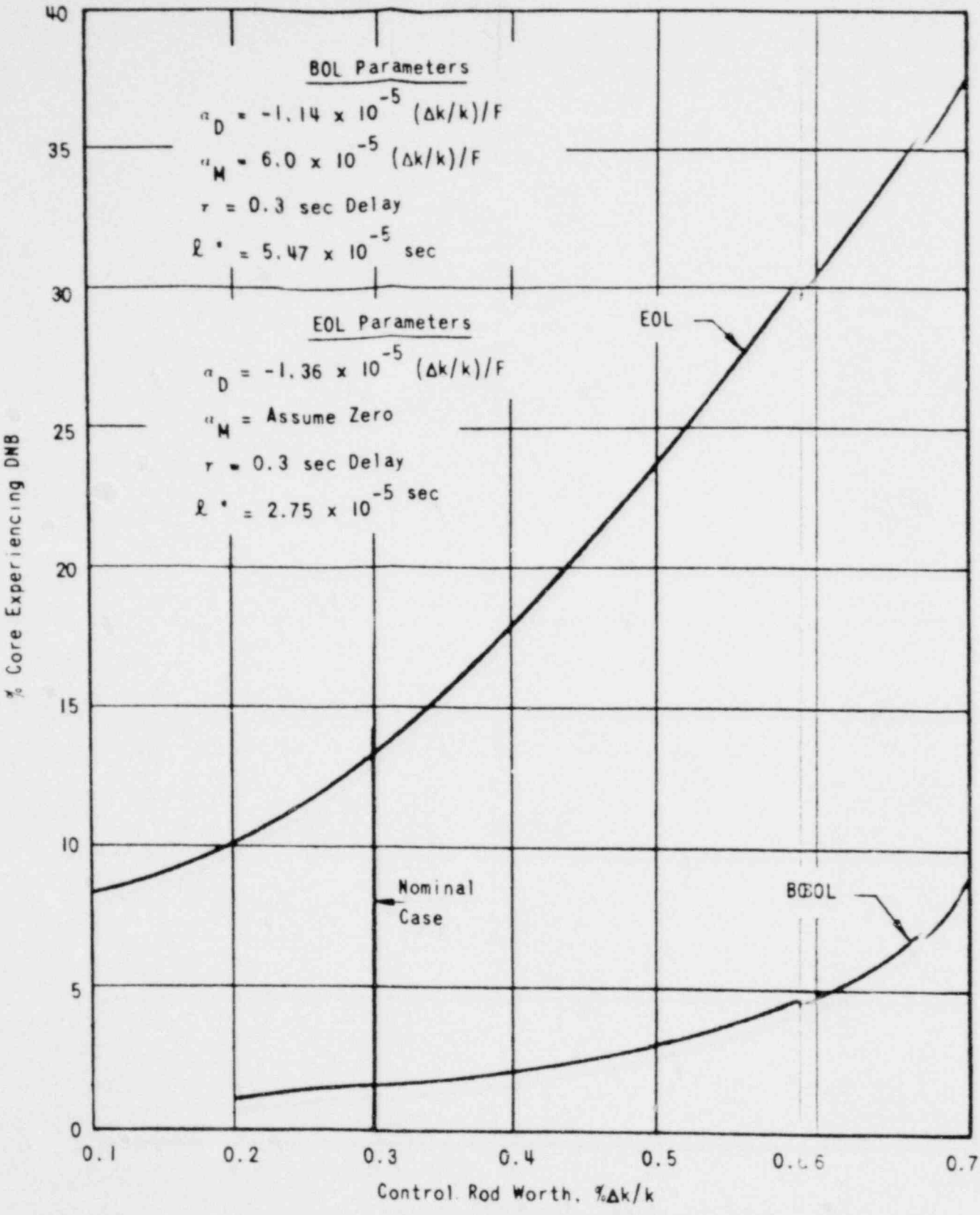

FIGURE 14.2-1
PERCENT CORE EXPERIENCING
DNB AS A FUNCTION OF EJECTED CONTROL
ROD WORTH AT ULTIMATE POWER

000 0247

SMUD

SACRAMENTO MUNICIPAL UTILITY DISTRICT

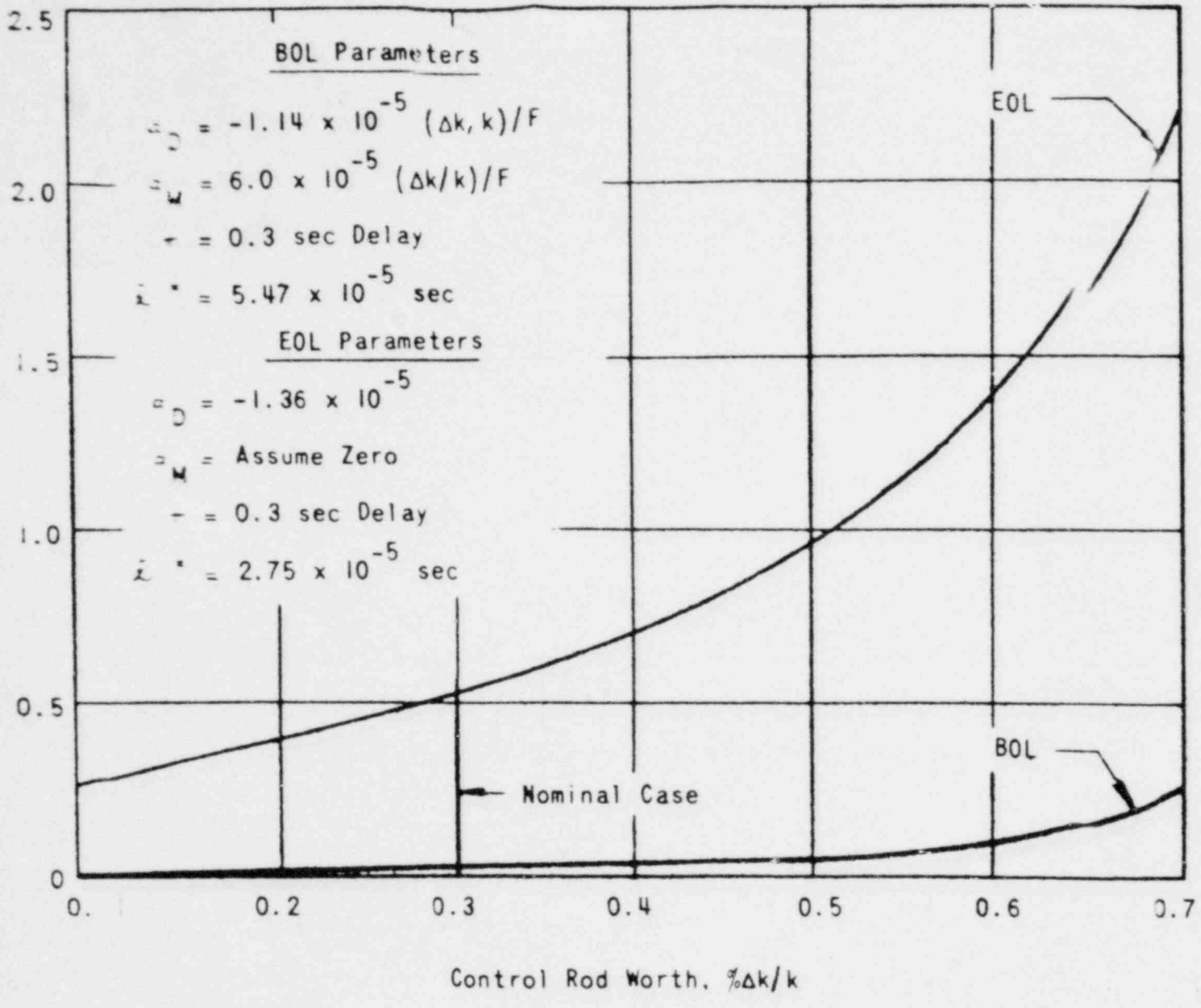

080 0248 00.

FIGURE 14.2-2
ZR-H_2O REACTION AS A FUNCTION
OF EJECTED CONTROL ROD
WORTH AT ULTIMATE POWER

SMUD
SACRAMENTO MUNICIPAL UTILITY DISTRICT

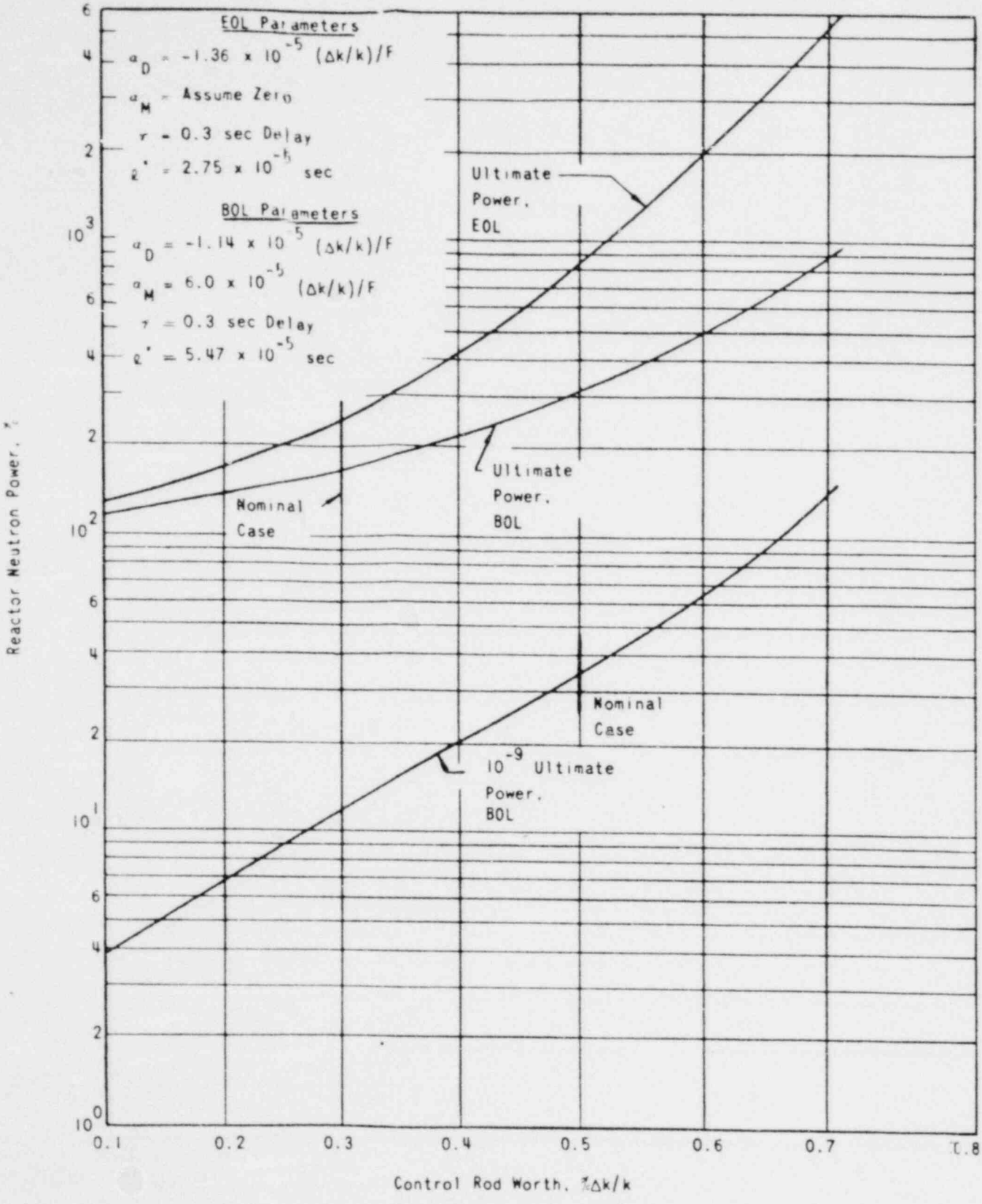

FIGURE 14.2-3
REACTOR NEUTRON POWER VARIATION
WITH EJECTED CONTROL ROD WORTH

00

SMUD
SACRAMENTO MUNICIPAL UTILITY DISTRICT

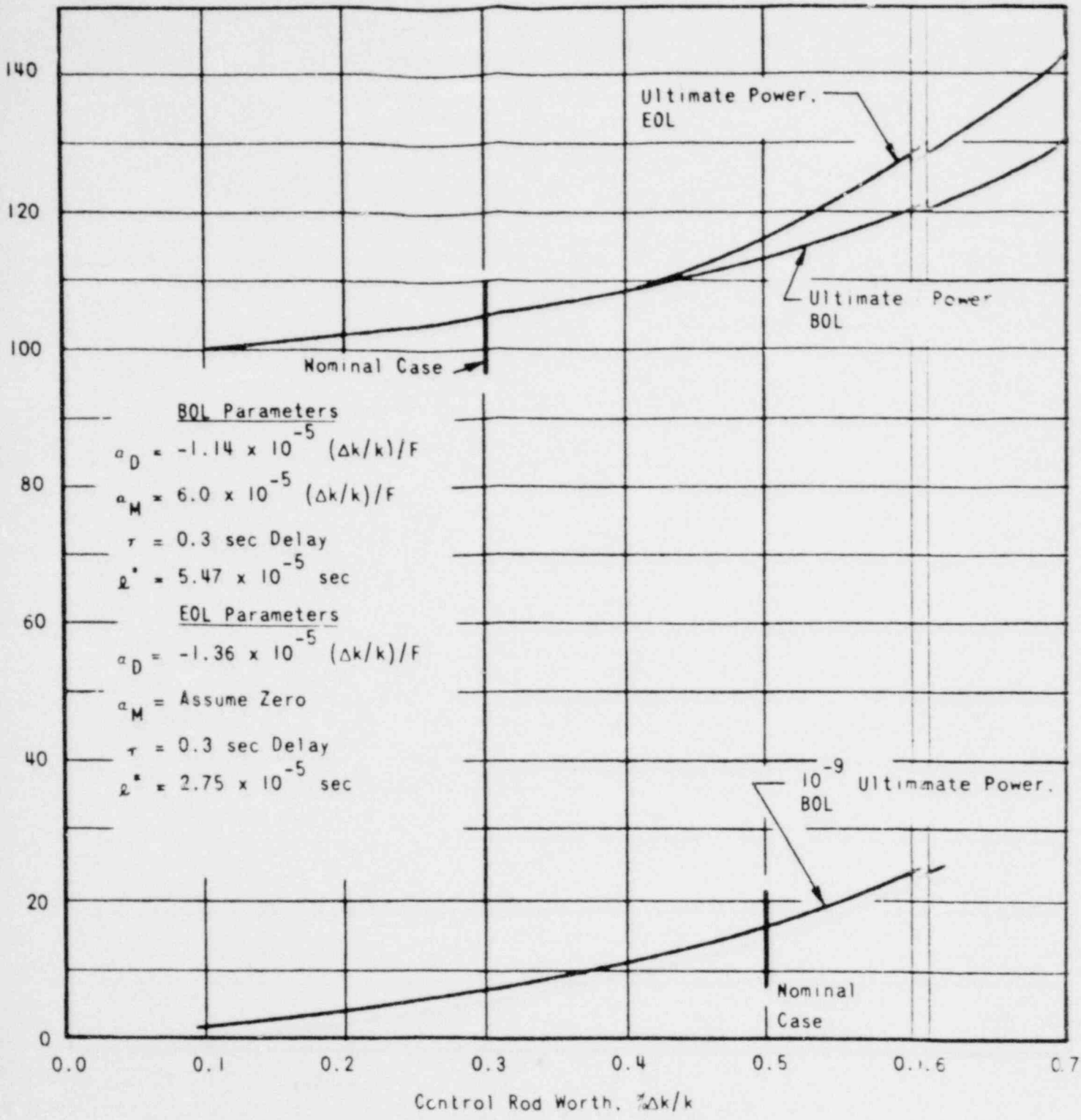

FIGURE 14.2-4
REACTOR THERMAL POWER AS A FUNCTION
OF EJECTED CONTROL ROD WORTH

0250

SMUD

00

SACRAMENTO MUNICIPAL UTILITY DISTRICT

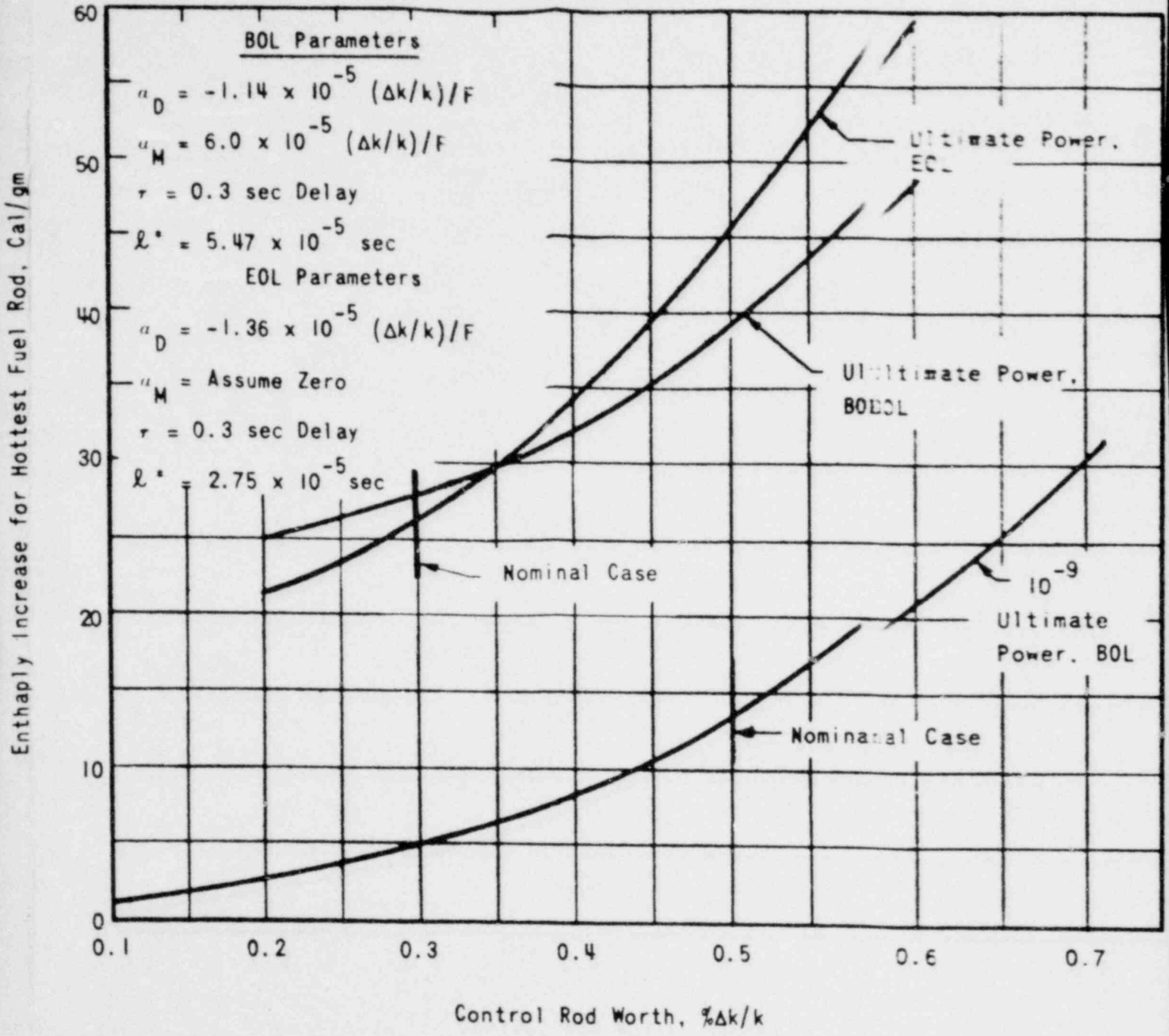

000 0251

FIGURE 1-14.2-5
ENTHALPY INCREASE TO THE HOTTEST FUEL ROD
VERSUS EJECTED CONTROL ROD WORTH

00

SMUD
SACRAMENTO MUNICIPAL UTILITY DISTRICT

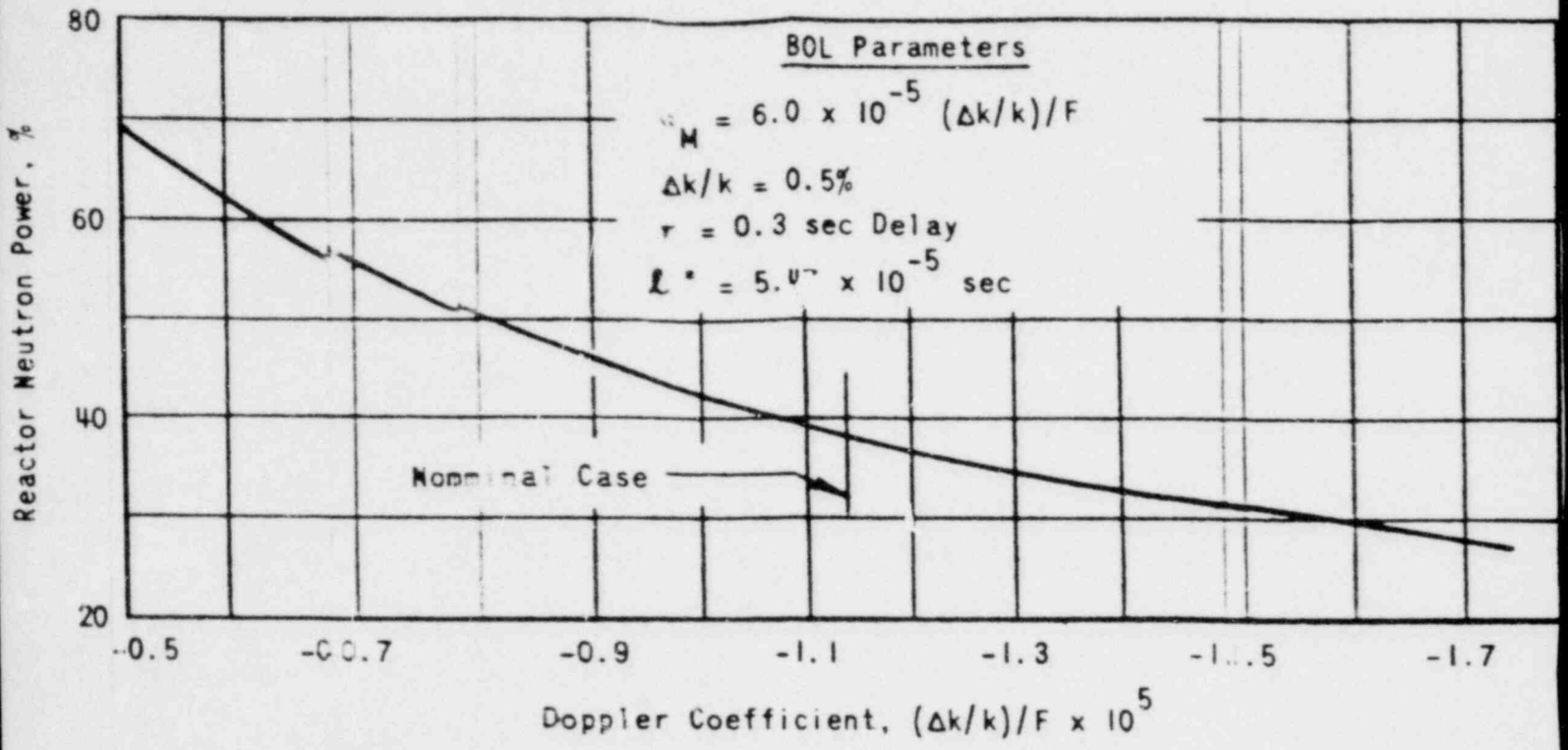

000 0252

FIGURE 14.2.2-6
EFFECT ON REACTOR NEUTRON POWER
OF VARYING THE DOPPLER COEFFICIENT-
ROD EJECTION AT 10-9 ULTIMATE POWER

SMUD
SACRAMENTO MUNICIPAL UTILITY DISTRICT

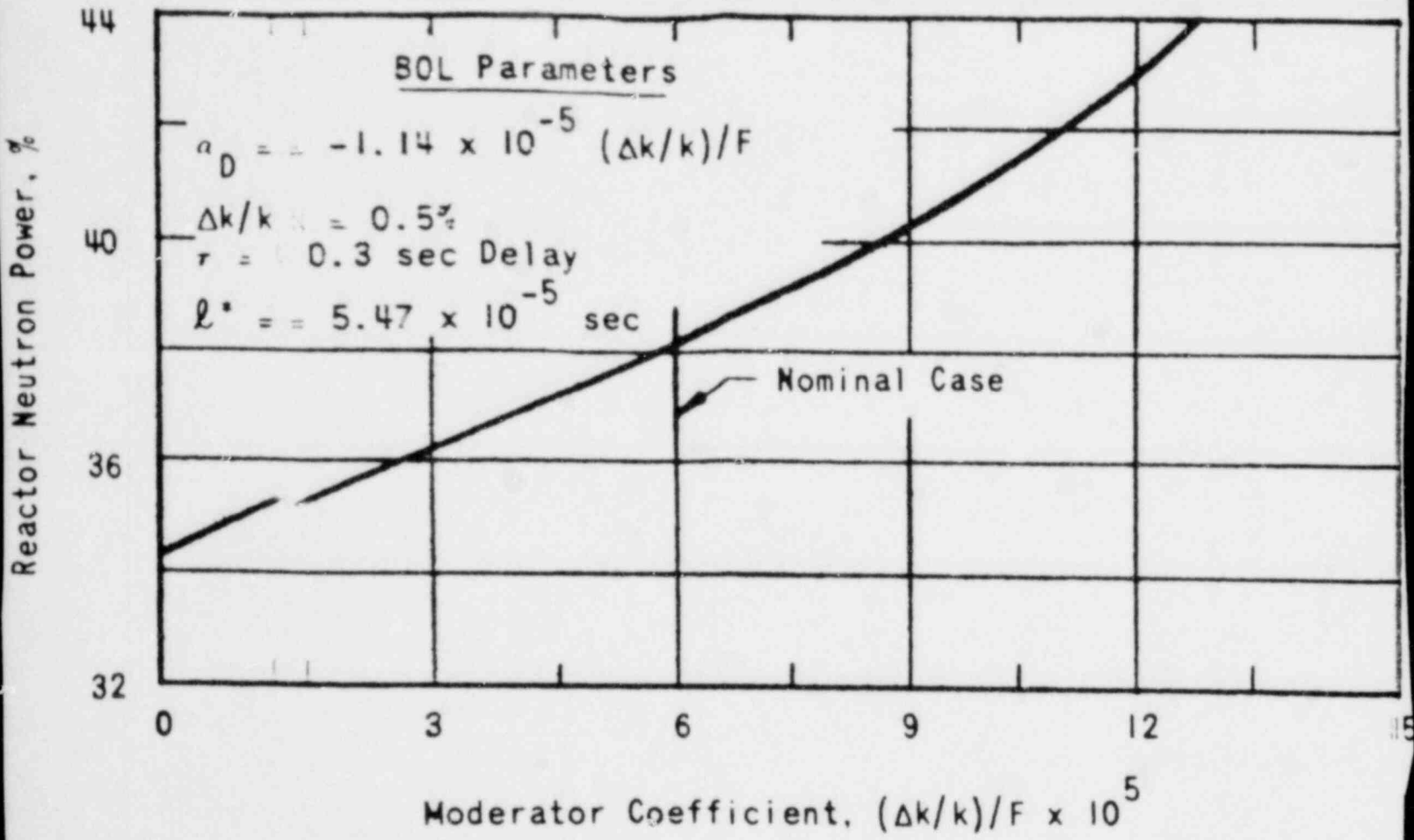

000 0253

FIGURE 14.2-7
EFFECT ON REACTOR NEUTRON POWER
OF VARYING THE MODERATOR COEFFICIENT -
ROD EJECTION AT 10^{-9} ULTIMATE POWER

SMUD
SACRAMENTO MUNICIPAL UTILITY DISTRICT

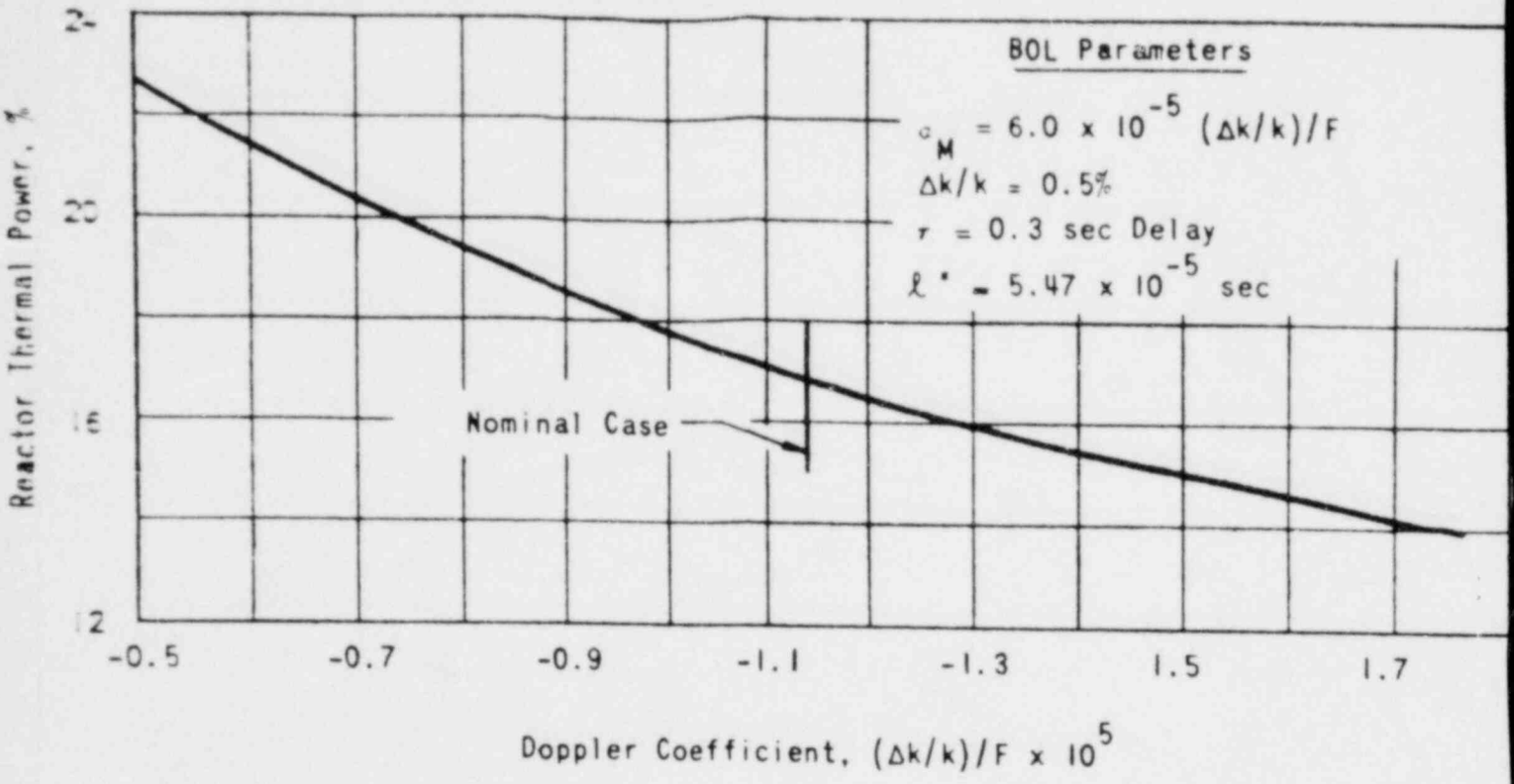

000 0254

FIGURE 14.2-8
EFFECT ON REACTOR THERMAL POWER OF VARYING THE DOPPLER COEFFICIENT -- ROD EJECTION AT 10^{-9} ULTIMATE POWER

SMUD
SACRAMENTO MUNICIPAL UTILITY DISTRICT

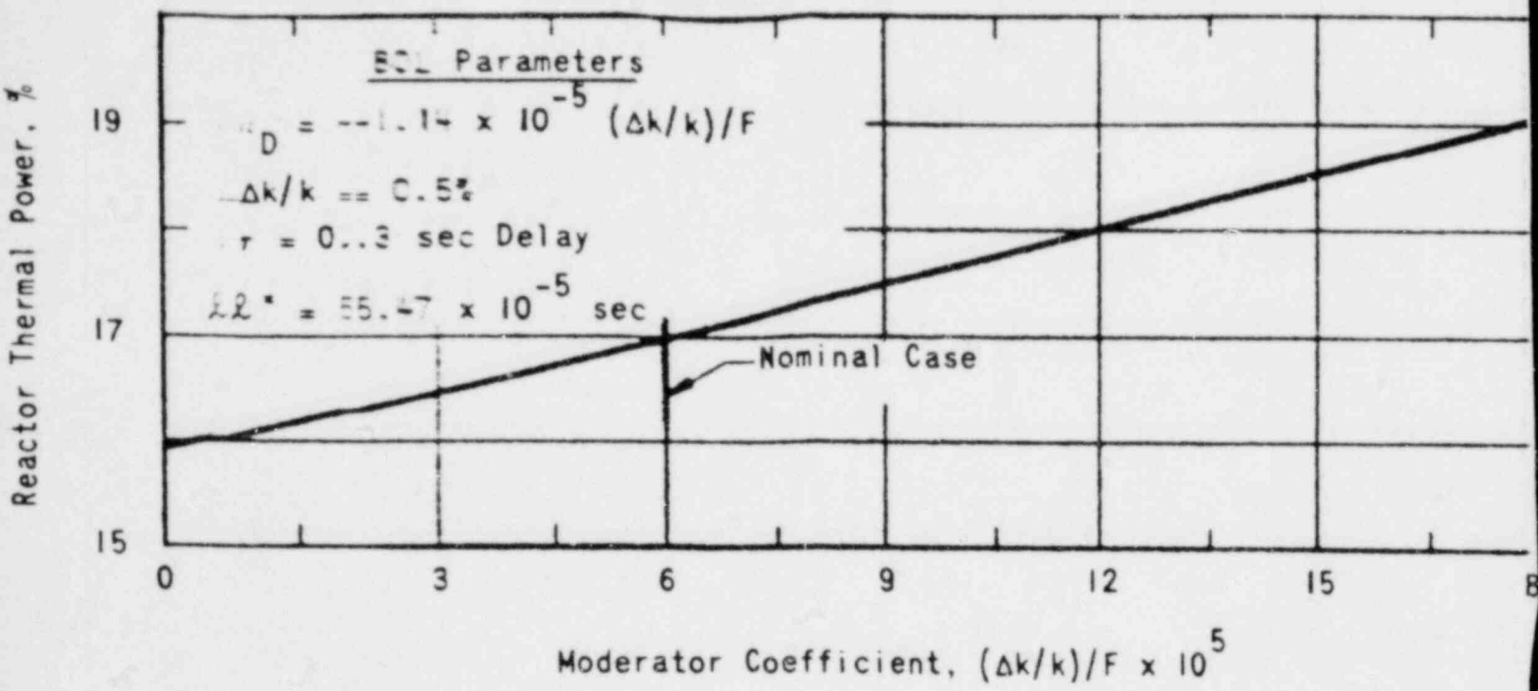

000 0255

FIGURE 14.2-9
EFFECT ON REACTOR THERMAL POWER OF VARYING THE MODERATOR COEFFICIENT-ROD EJECTION AT 10^{-9} ULTIMATE POWER

SMUD 00
SACRAMENTO MUNICIPAL UTILITY DISTRICT

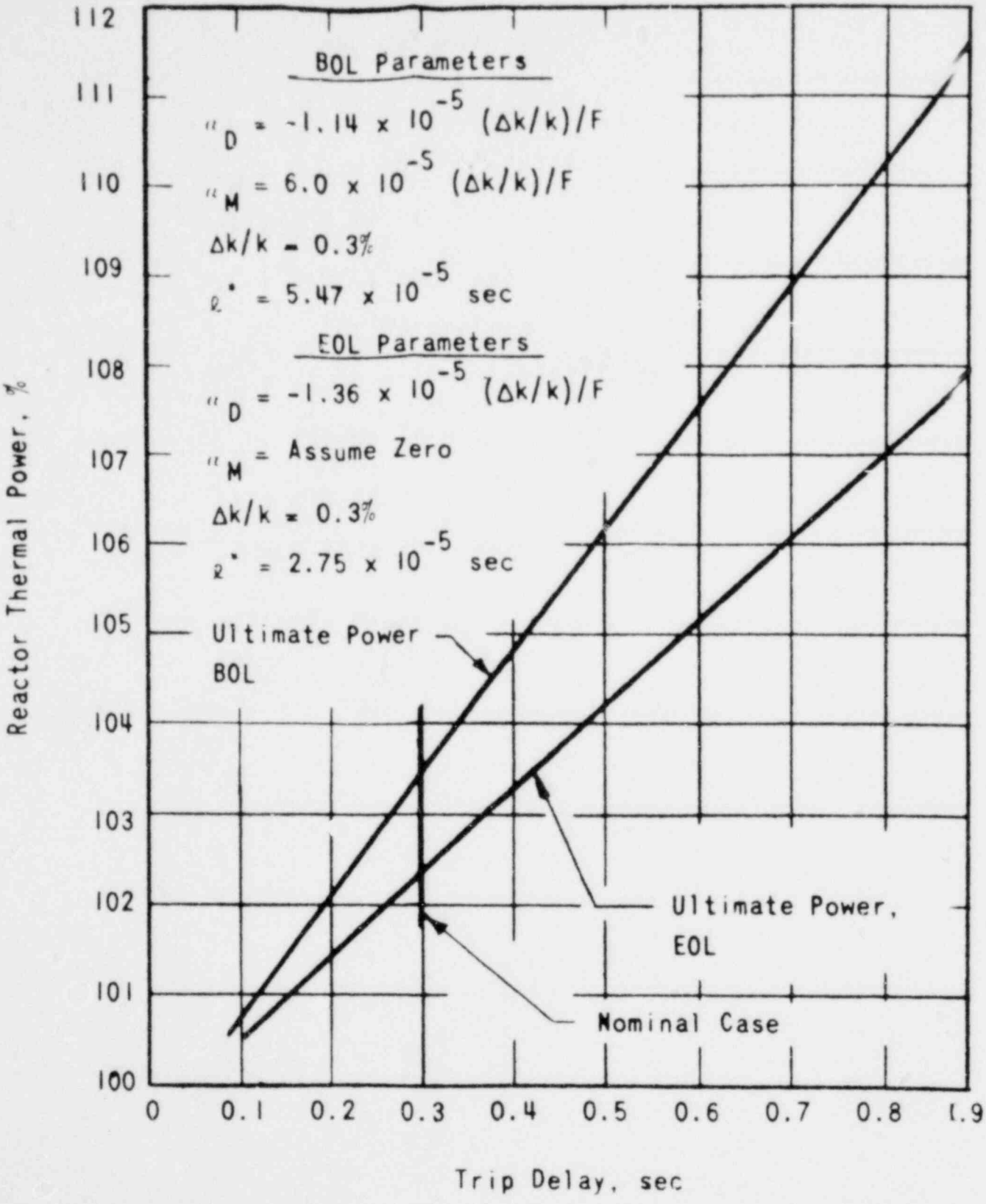

FIGURE 14.2-10
REACTOR THERMAL POWER VERSUS TRIP DELAY - ROD EJECTION AT ULTIMATE POWER

000 0256

SMUD
SACRAMENTO MUNICIPAL UTILITY DISTRICT

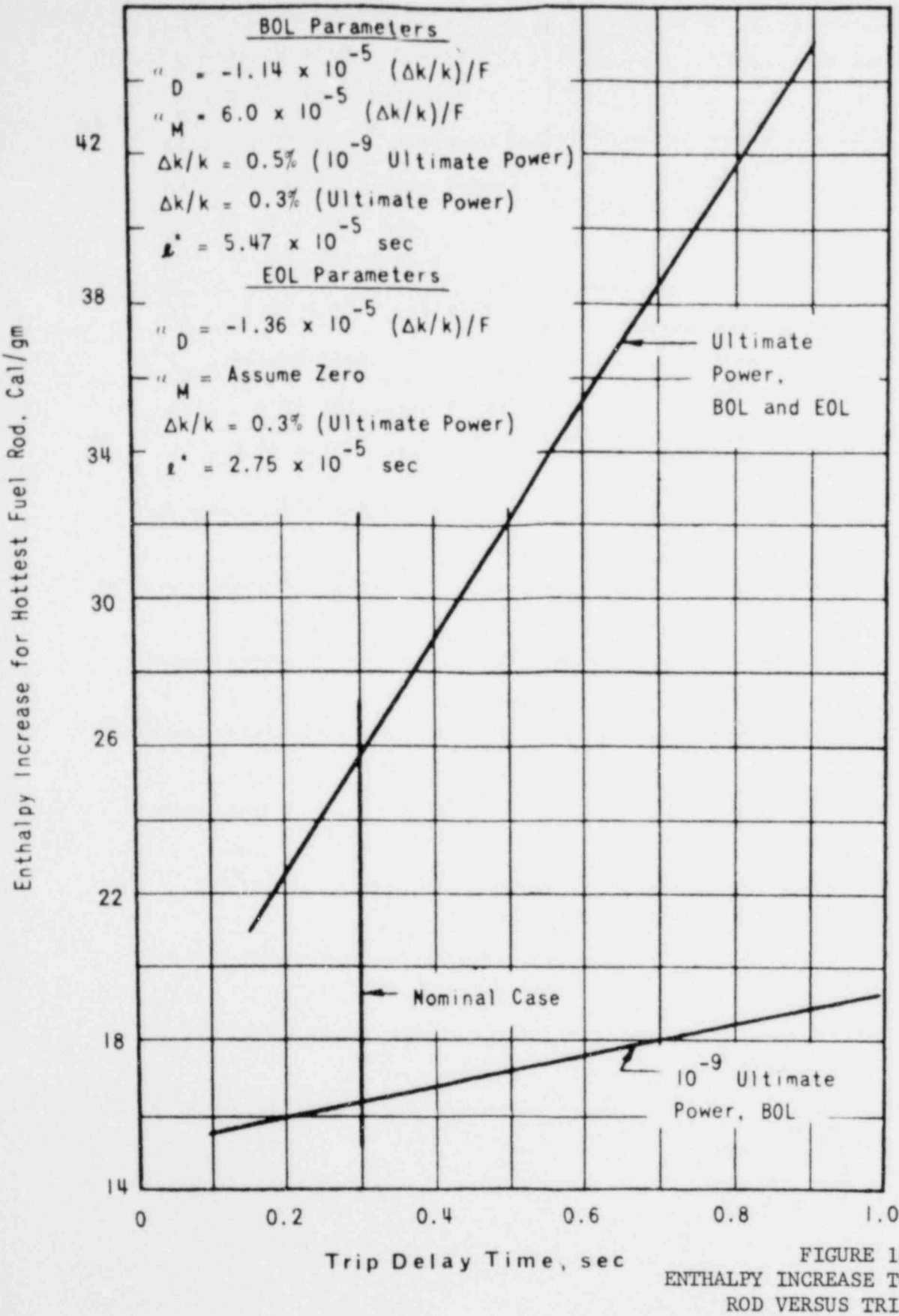

FIGURE 14.2-11
ENTHALPY INCREASE TO THE HOTTEST FUEL ROD VERSUS TRIP DELAY TIME - ROD EJECTION

000 0257

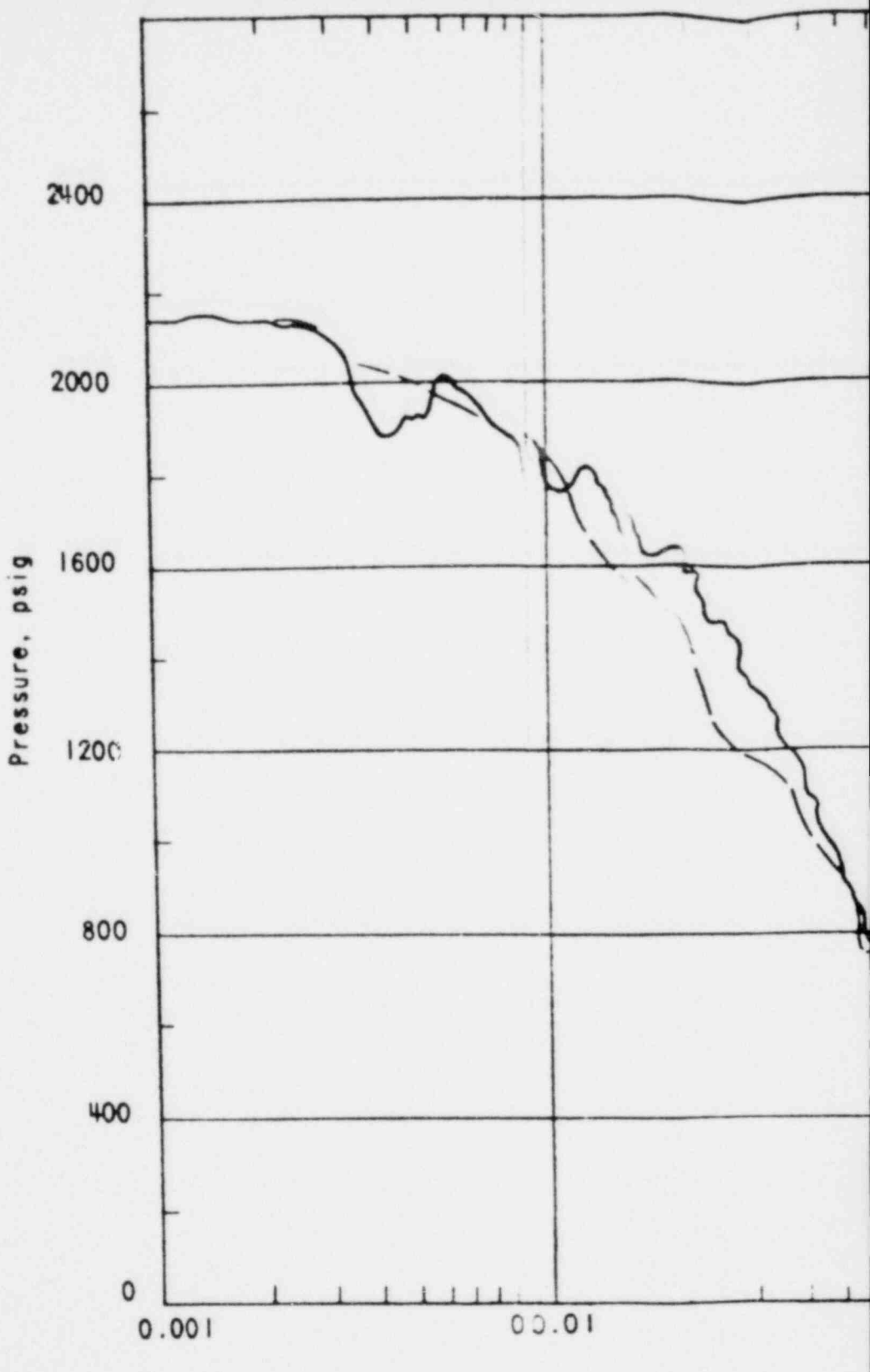
2400
2000
1600
1200
800
400
0
Pressure, psig
0.001
0.01

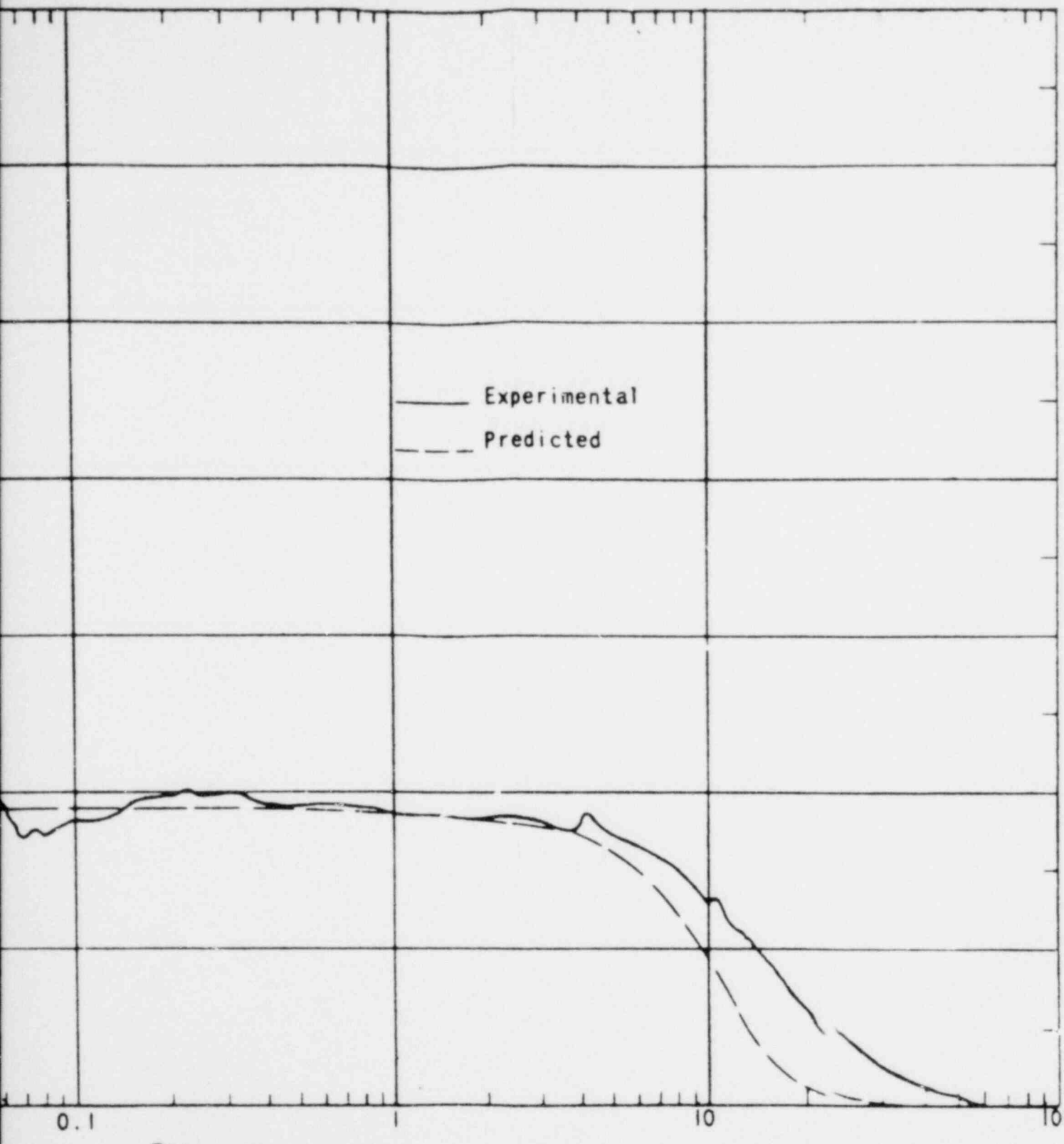

FIGURE 14. .2-12
LOFT SEMISCALE BLOWDOWN TEST NO.
546 - VESSEL PRESSURE VERSUS TIME

(NP) 0259

SMUD
SACRAMENTO MUNICIPAL UTILITY DISTRICT

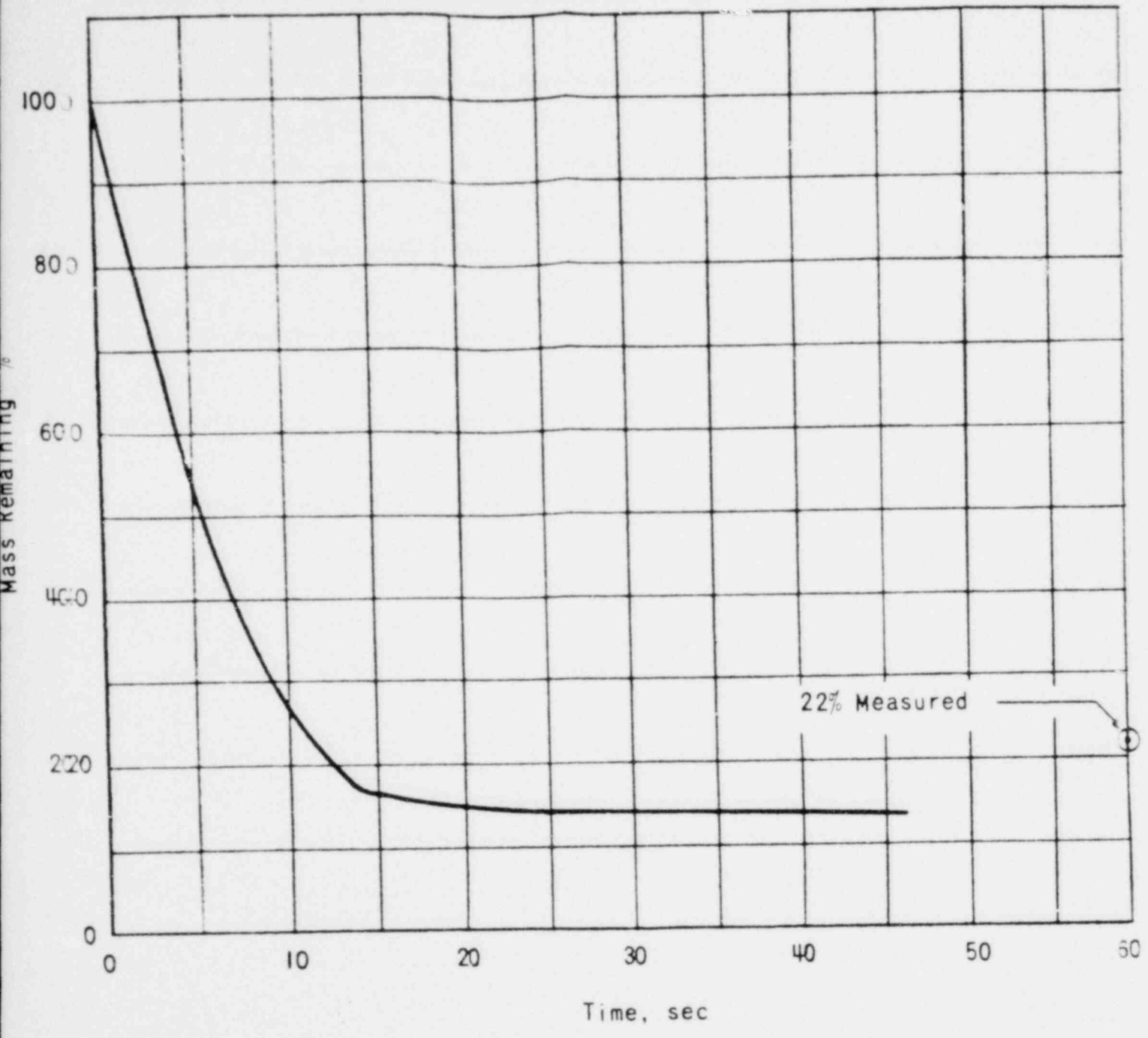

000 0260

FIGURE 14.2-13
PREDICTED PERCENT MASS REMAINING VERSUS
TIME - LOFT TEST NO. 546

SMUD
SACRAMENTO MUNICIPAL UTILITY DISTRICT

001

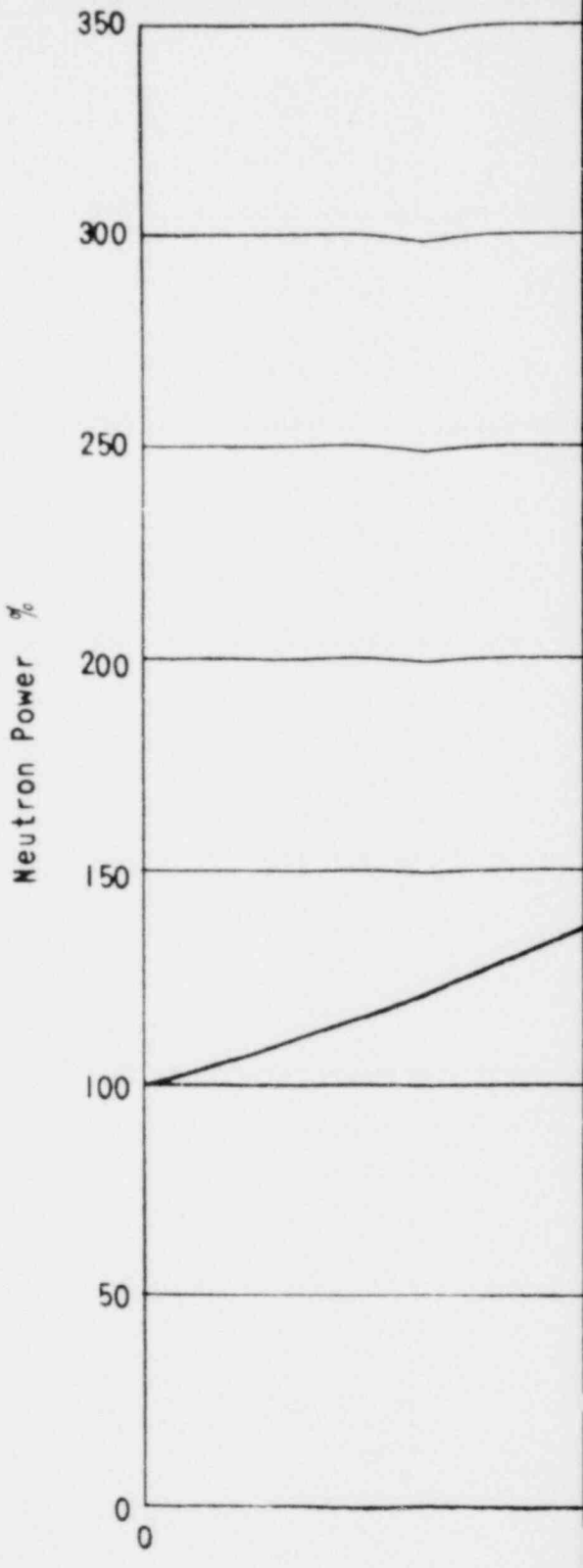

000 0261

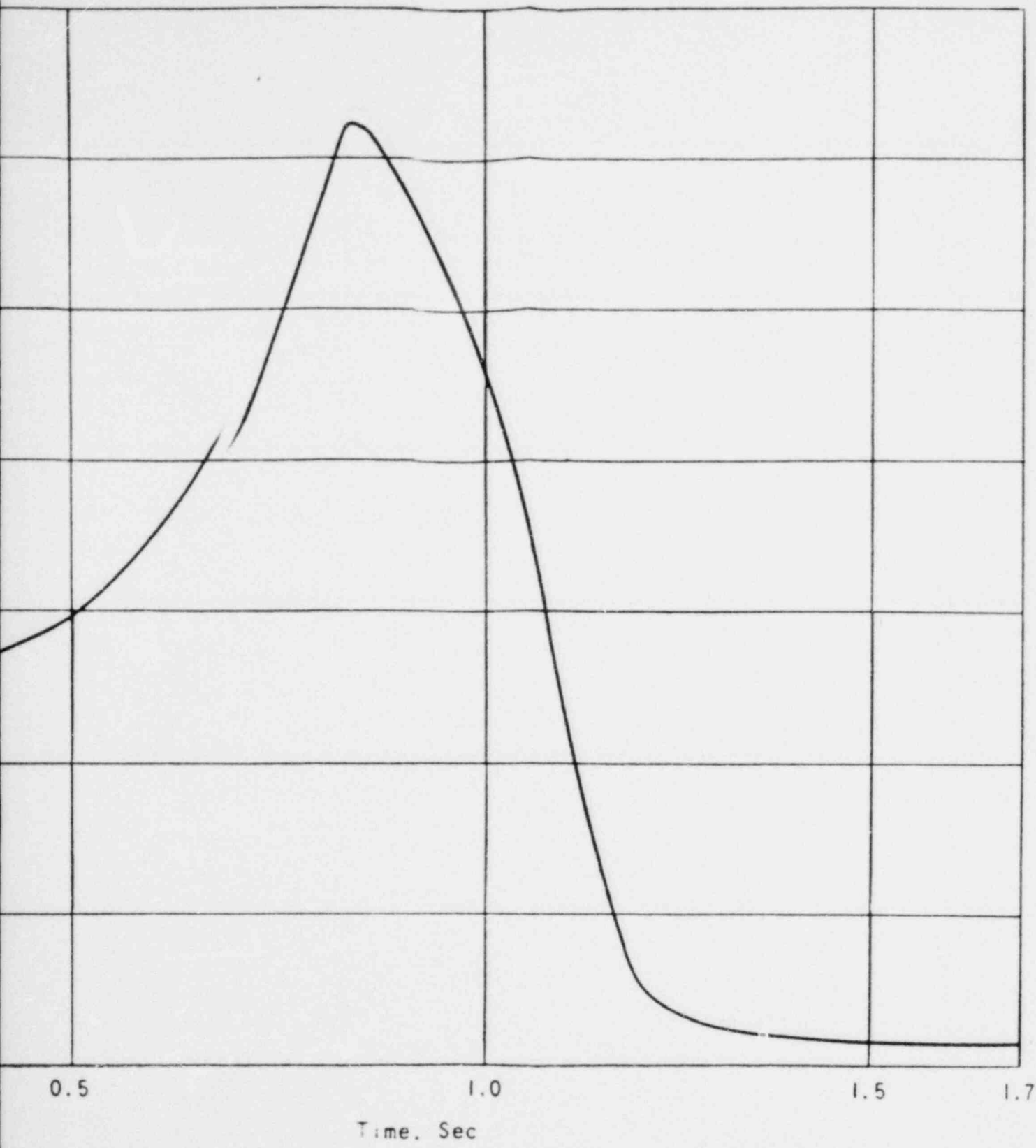

FIGURE 14.2-14
NEUTRON POWER VERSUS TIME FOR A
36-IN. ID, DOUBLE-ENDED, HOT-LEG PIPE
RUPTURE AT ULTIMATE POWER WITHOUT TRIP

000 0262

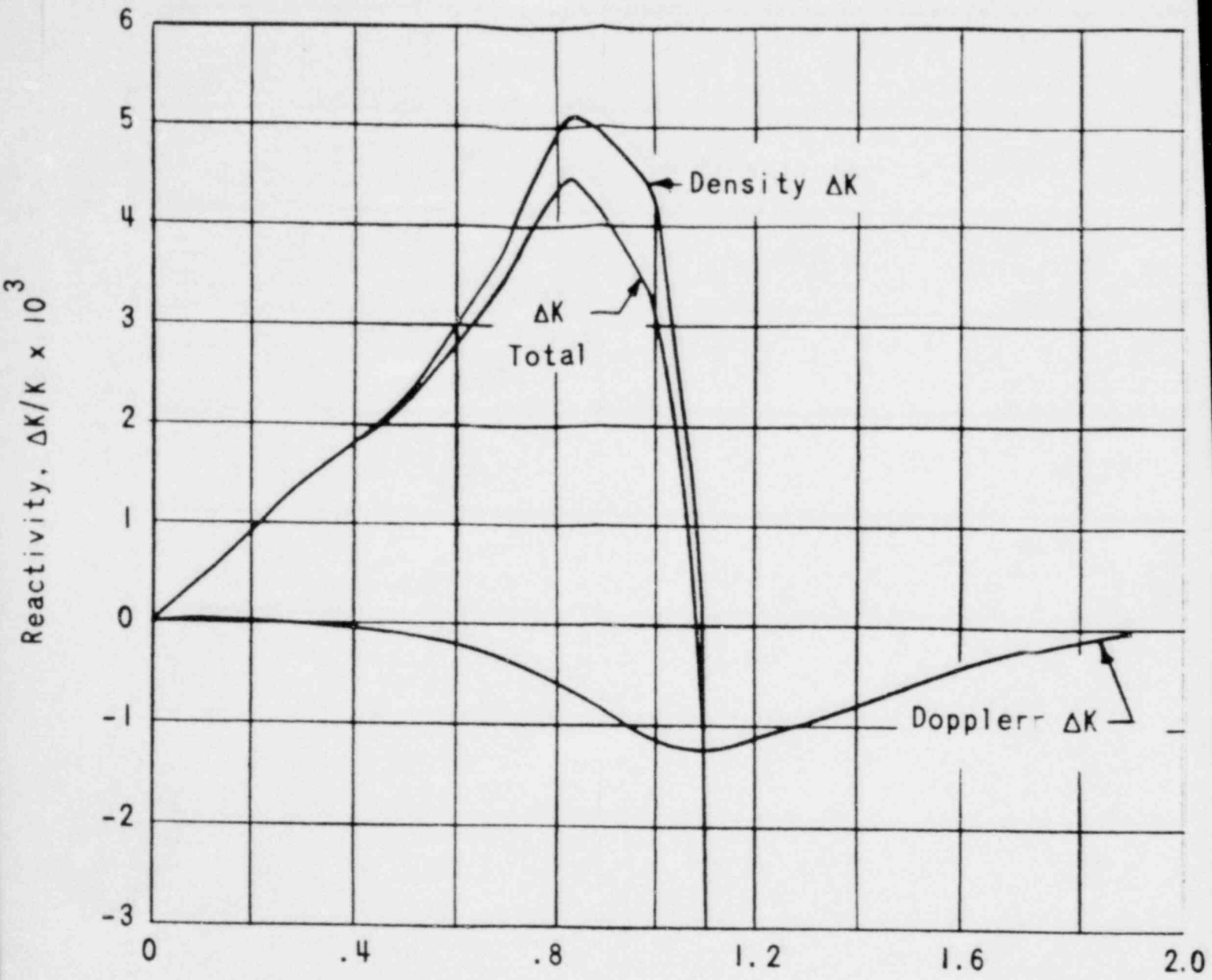

000 0263

FIGURE 14.2-15
REACTIVITY VERSUS TIME FOR A 36-IN. ID, DOUBLE-ENDED, HOT-LEG PIPE RUPTURE AT ULTIMATE POWER WITHOUT TRIP

SMUD

SACRAMENTO MUNICIPAL UTILITY DISTRICT

000 0264

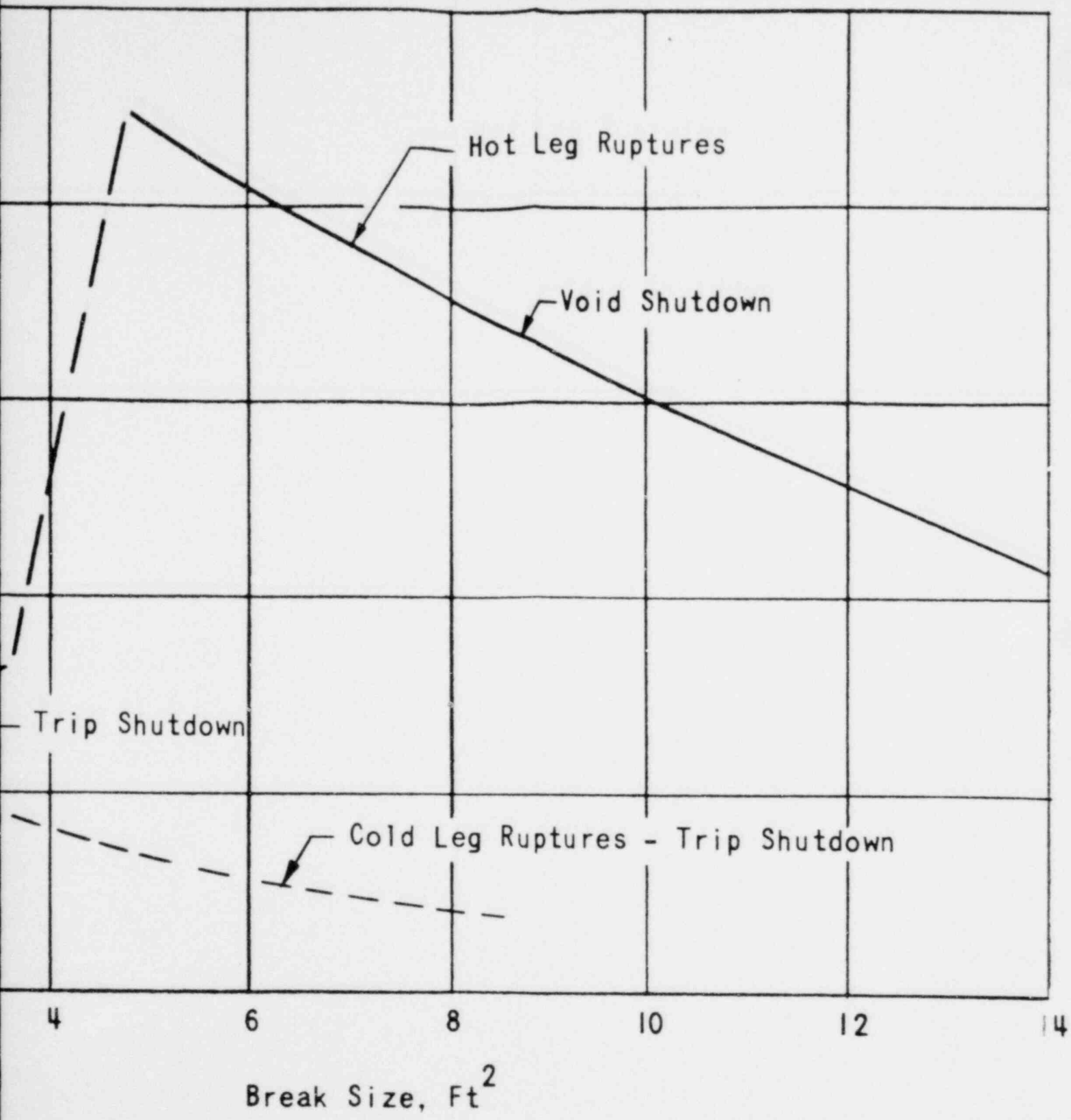

FIGURE 14.2-16
INTEGRATED POWER VERSUS BREAK SIZE
FOR A SPECTRUM OF RUPTURE SIZES

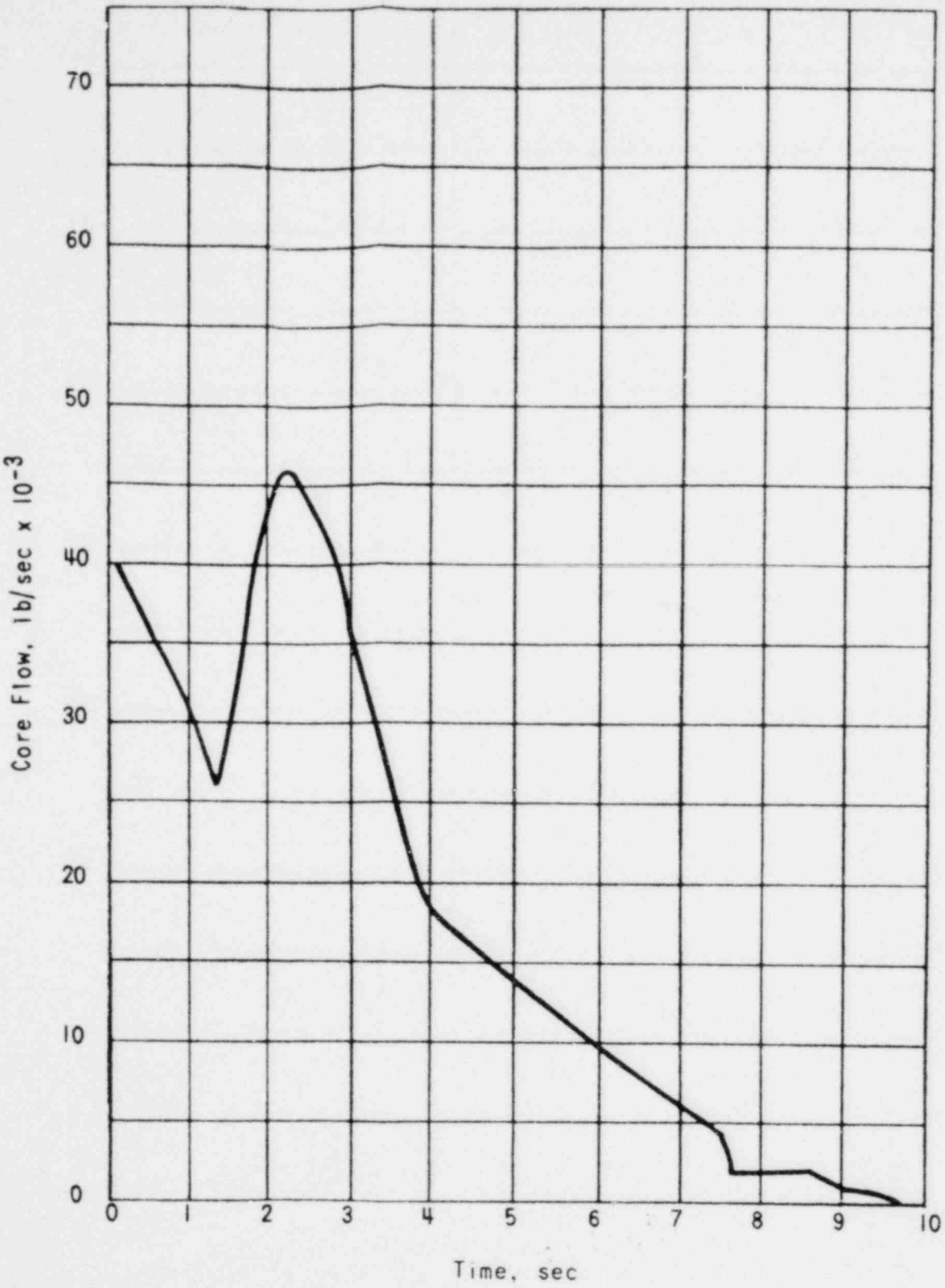

000 0266

FIGURE 14.2-17
CORE FLOW VERSUS TIME FOR A 36-IN. ID, DOUBLE-ENDED, HOT-LEG PIPE RUPTURE

SMUD
SACRAMENTO MUNICIPAL UTILITY DISTRICT

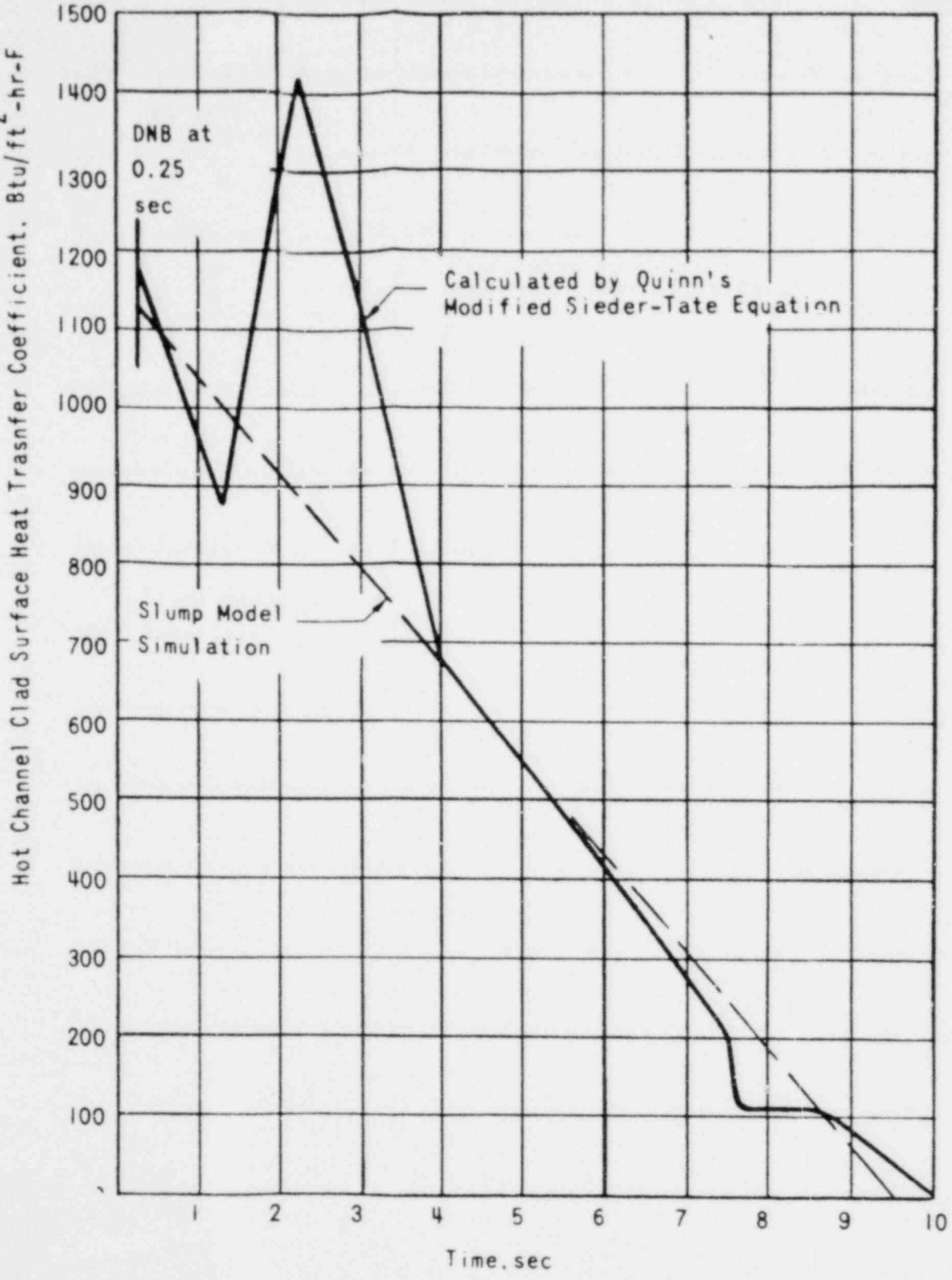

FIGURE 14.2-18
HOT CHANNEL CLAD SURFACE HEAT TRANSFER COEFFICIENT AFTER DNB VERSUS TIME FOR A 36-IN. ID, DOUBLE-ENDED, HOT-LEG PIPE RUPTURE

000 0267

SMUD 00

SACRAMENTO MUNICIPAL UTILITY DISTRICT

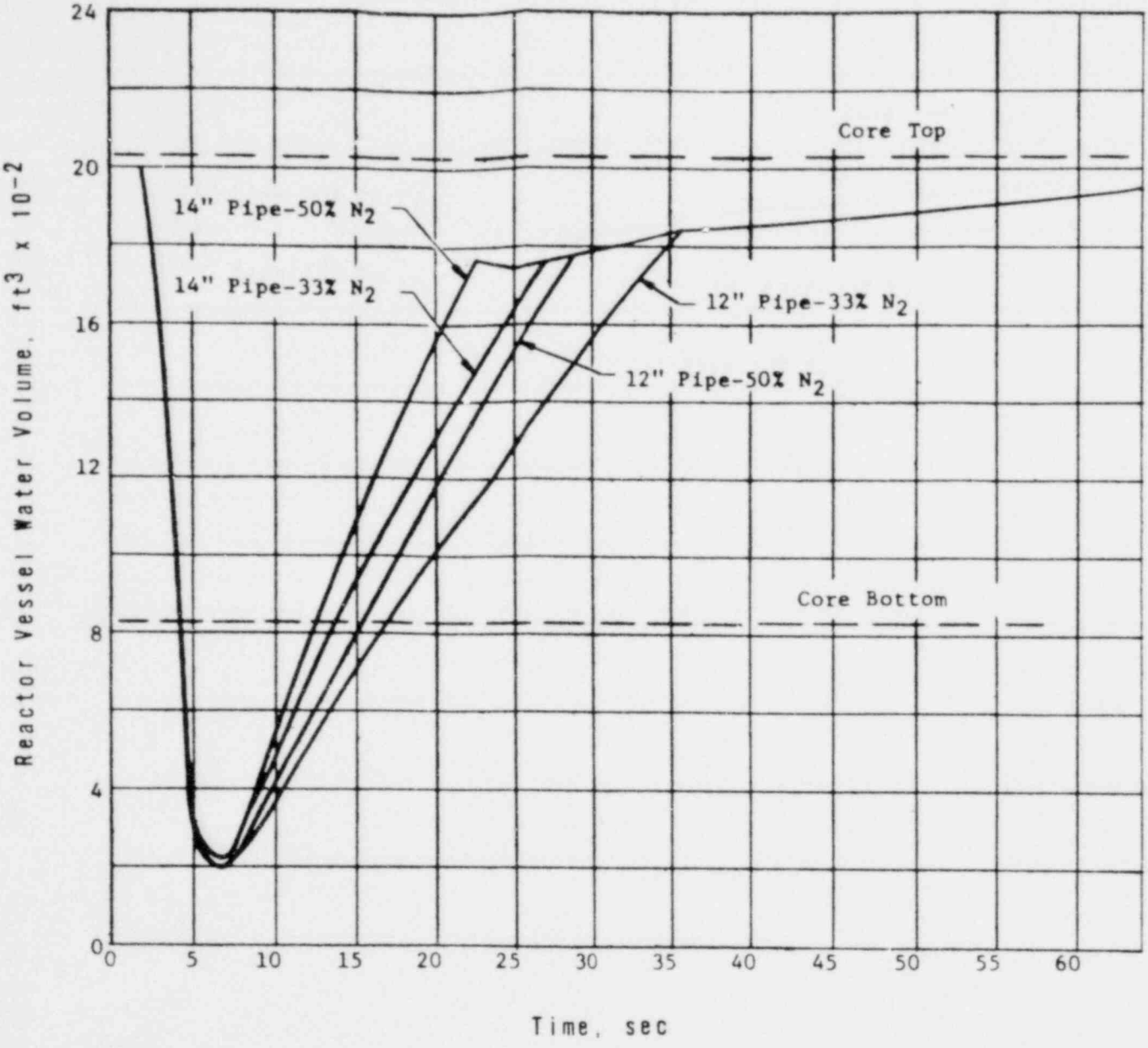

FIGURE 14.2-19
REACTOR VESSEL WATER VOLUME VERSUS TIM
FOR A 36-IN. ID, DOUBLE-ENDED, HOT-LEG
PIPE RUPTURE FOR 600 PSIG CORE FLOODIN
TANK OPERATING PRESSURE

000 0268

SMUD
SACRAMENTO MUNICIPAL UTILITY DISTRICT

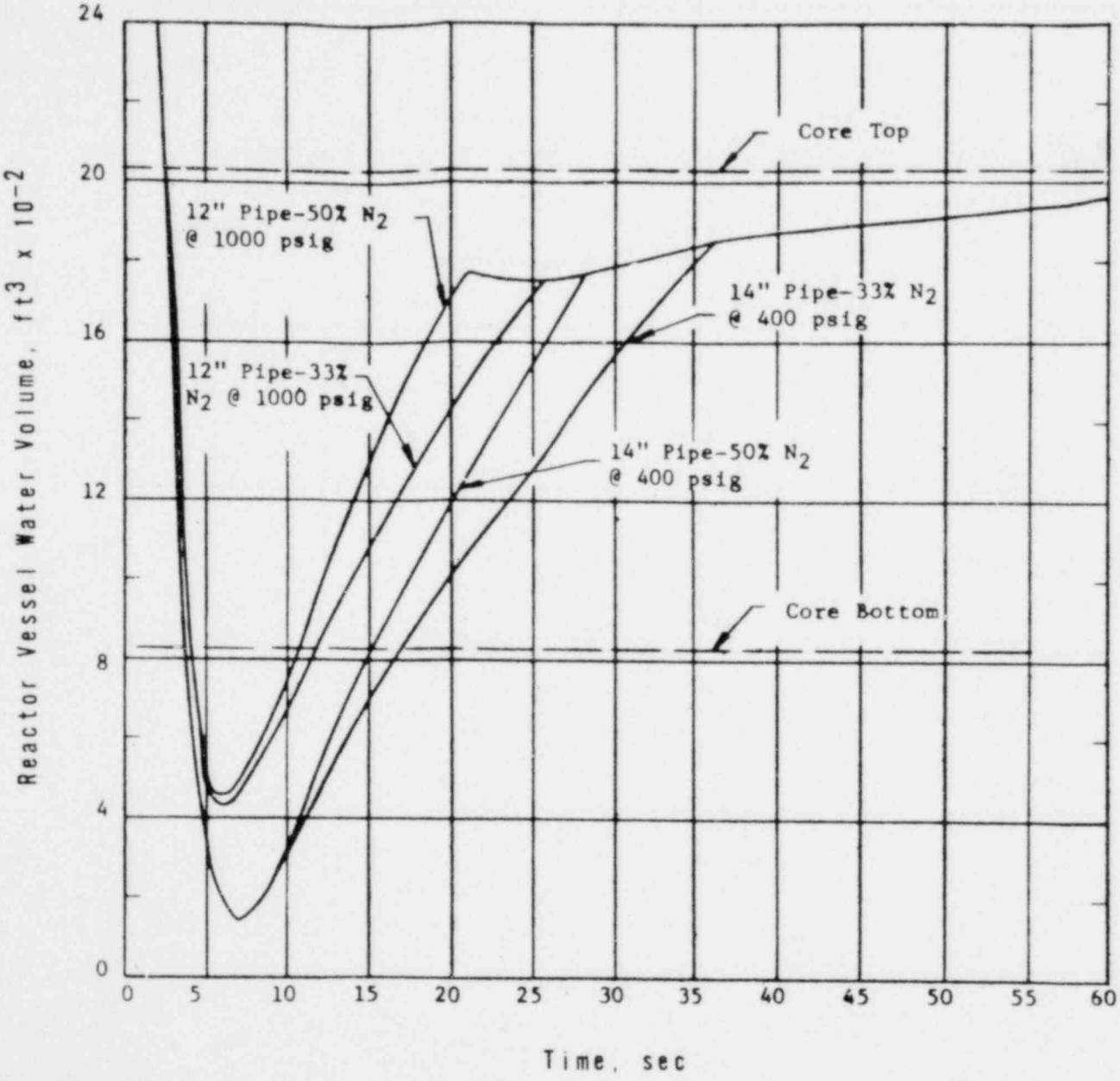

FIGURE 14.2-20
REACTOR VESSEL WATER VOLUME VERSUS TIME
FOR A 36-IN. ID, DOUBLE-ENDED, HOT-LEG
PIPE RUPTURE FOR 400 PSIG AND 1,000
PSIG CORE FLOODING TANK OPERATING PRESSURES

000 0269

SMUD
SACRAMENTO MUNICIPAL UTILITY DISTRICT

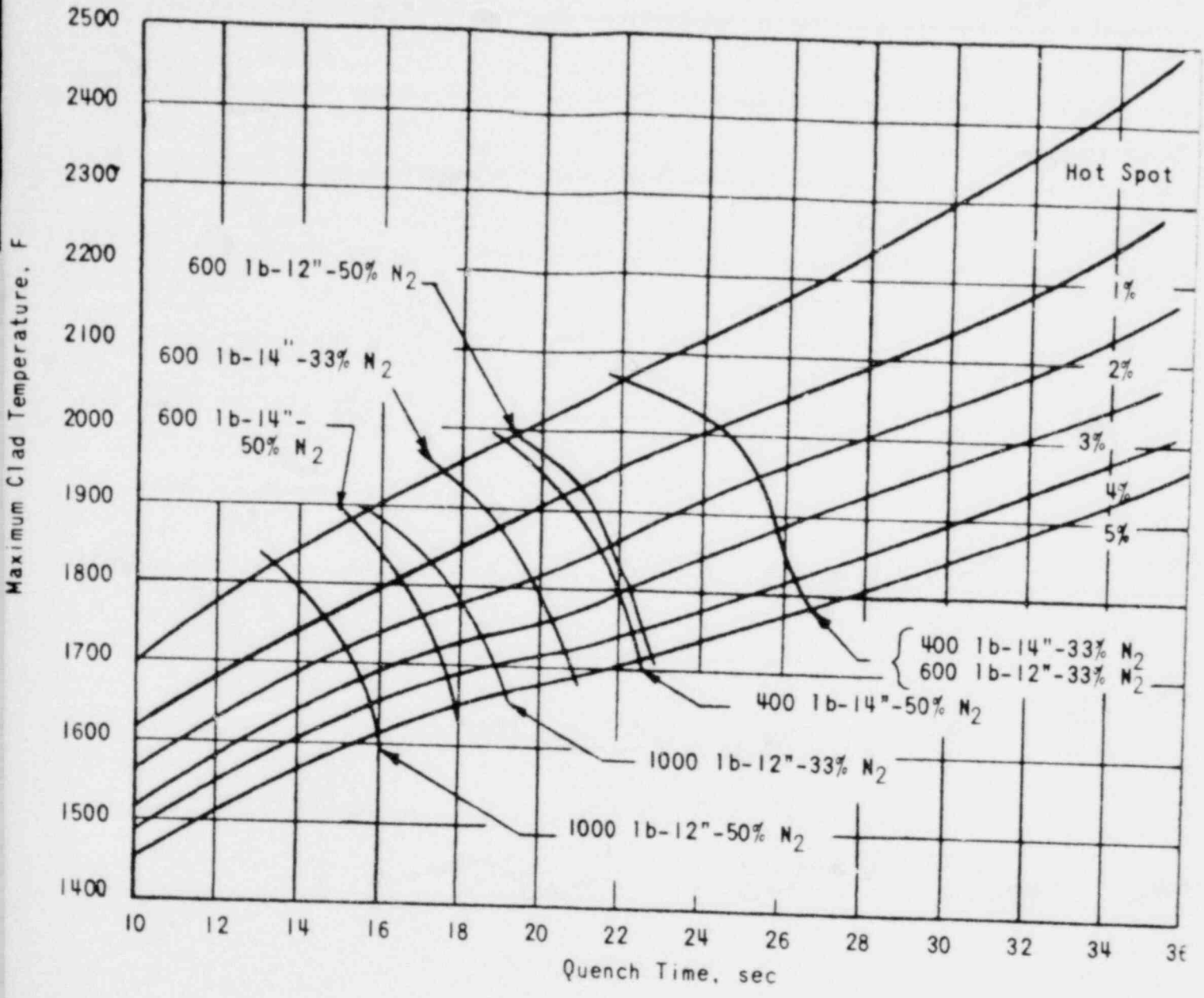

000 270

FIGURE 14.2-21
CORE FLOODING TANK ANALYSIS; MAXIMUM CLAD TEMPERATURE VERSUS TIME TO QUENCH FOR A 36-IN. ID, DOUBLE-ENDED HOT-LEG PIPE RUPTURE

SMUD
SACRAMENTO MUNICIPAL UTILITY DISTRICT

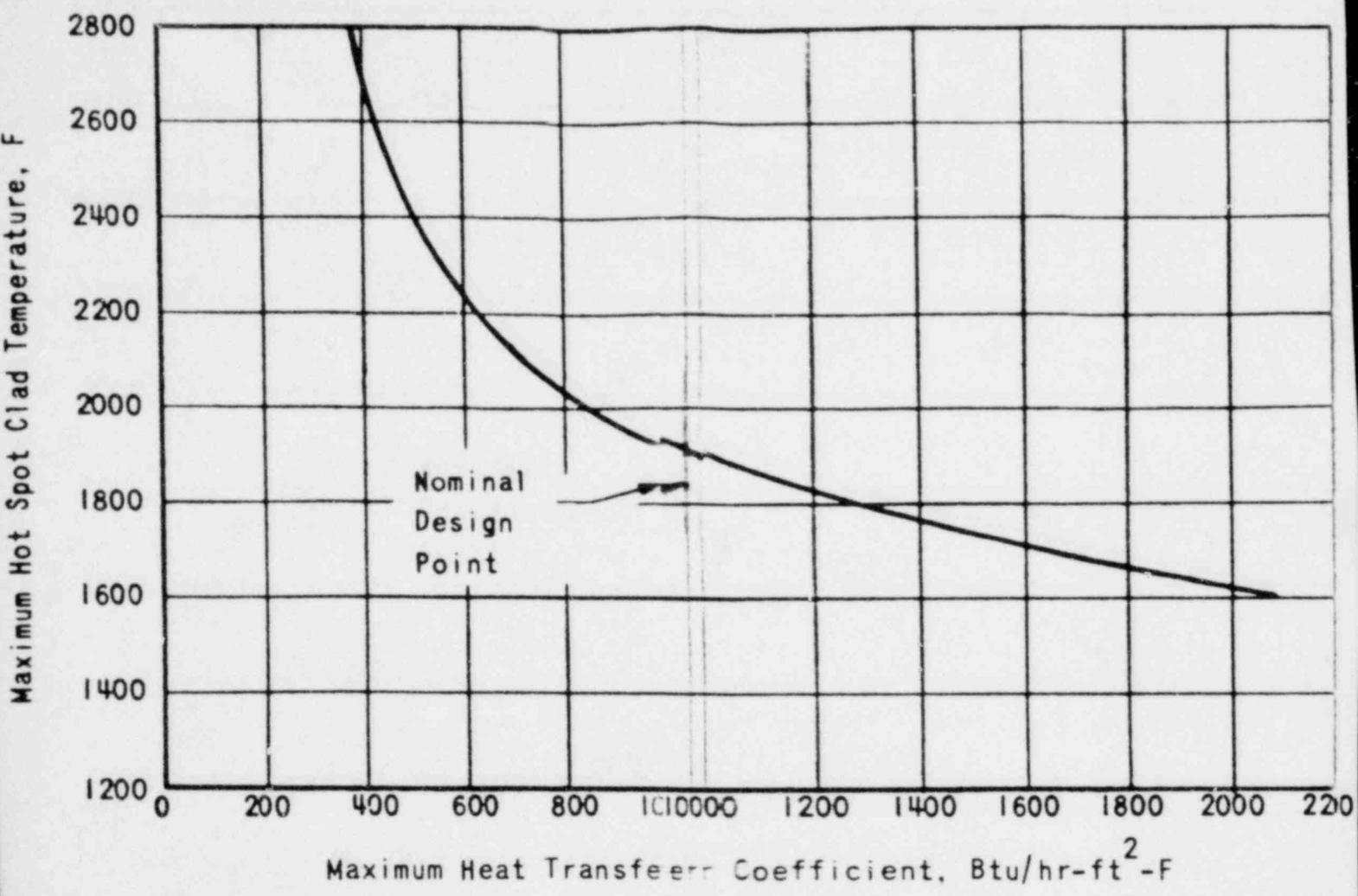

000 0270

0

FIGURE 14.2-22
MAXIMUM HOT SPOT CLAD TEMPERATURE VERSUS
MAXIMUM HEAT TRANSFER COEFFICIENT AFTER
DNB FOR A 36-IN. ID, DOUBLE-ENDED,
HOT-LEG PIPE RUPTURE

SMUD
SACRAMENTO MUNICIPAL UTILITY DISTRICT

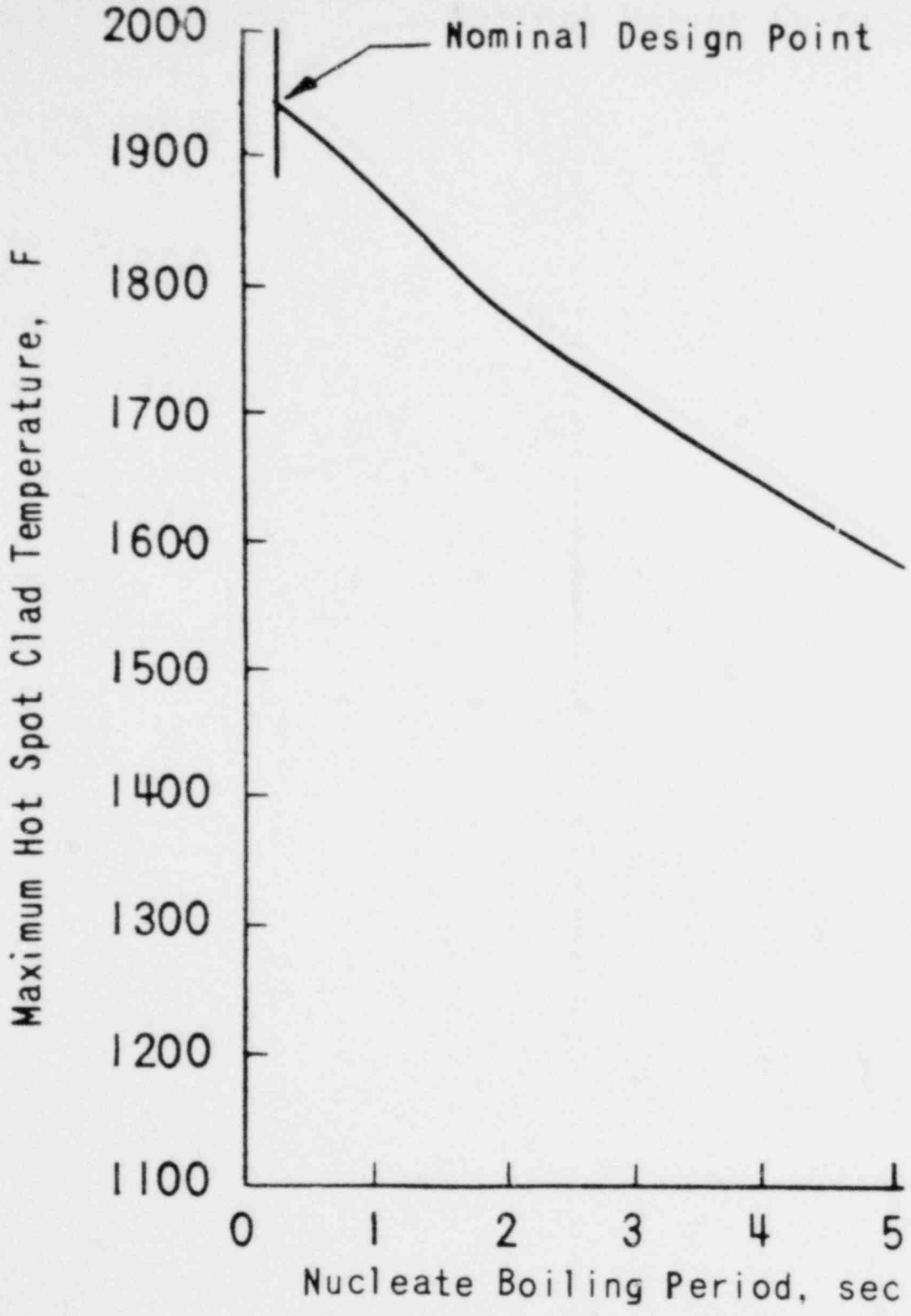

FIGURE 14.2-23
MAXIMUM HOT SPOT CLAD TEMPERATURE AS A
FUNCTION OF TIME TO REACH DNB FOR A
A 36-IN. ID, DOUBLE-ENDED,
HOT-LEG PIPE RUPTURE

000 0272

SMUD
SACRAMENTO MUNICIPAL UTILITY DISTRICT

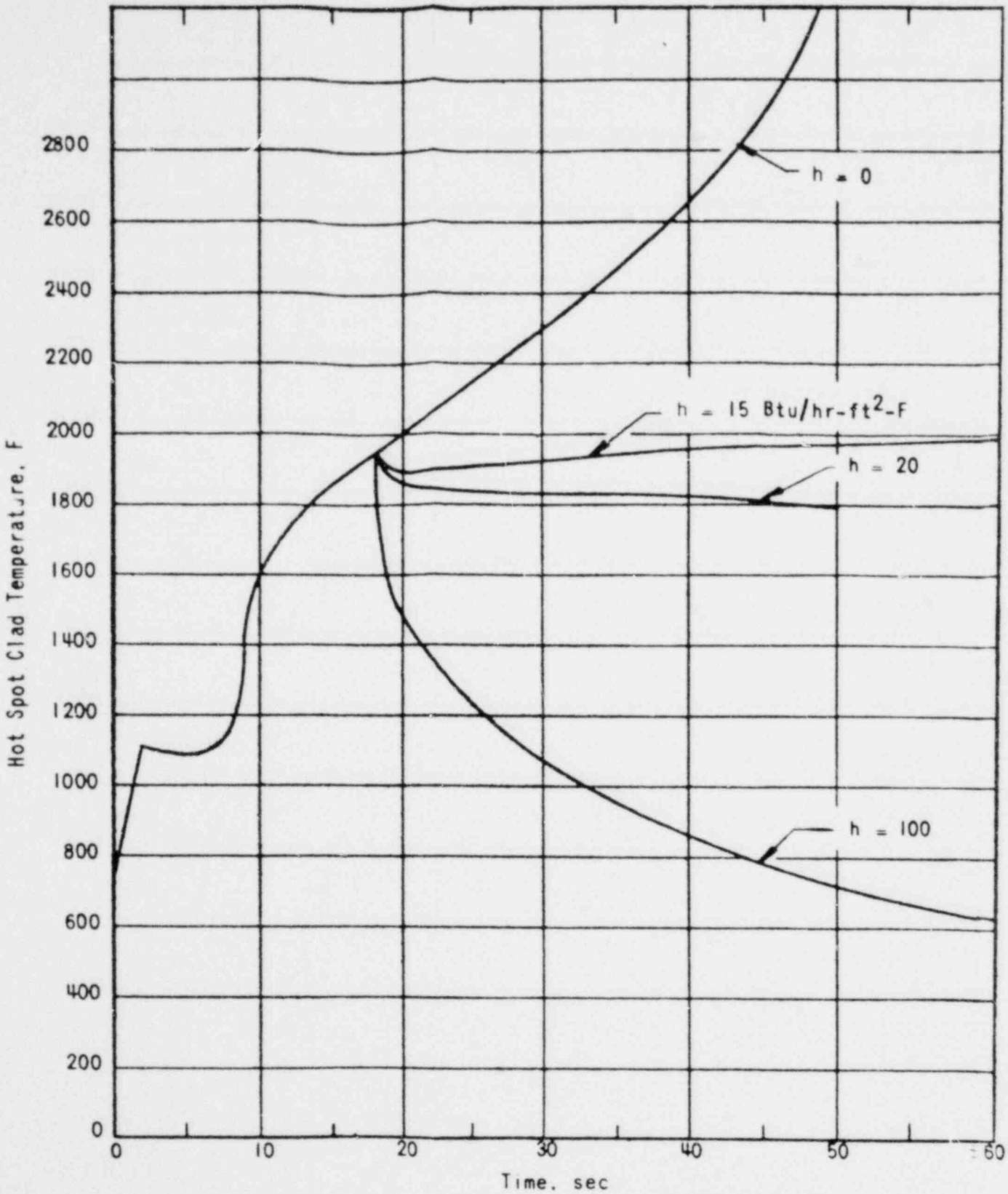

FIGURE 14.2-24
HOT SPOT CLAD TEMPERATURE VERSUS TIME
FOR A 36-IN. ID, DOUBLE-ENDED, HOT-LEG
PIPE RUPTURE AND
VARIABLE QUENCH COEFFICIENT

000 0273

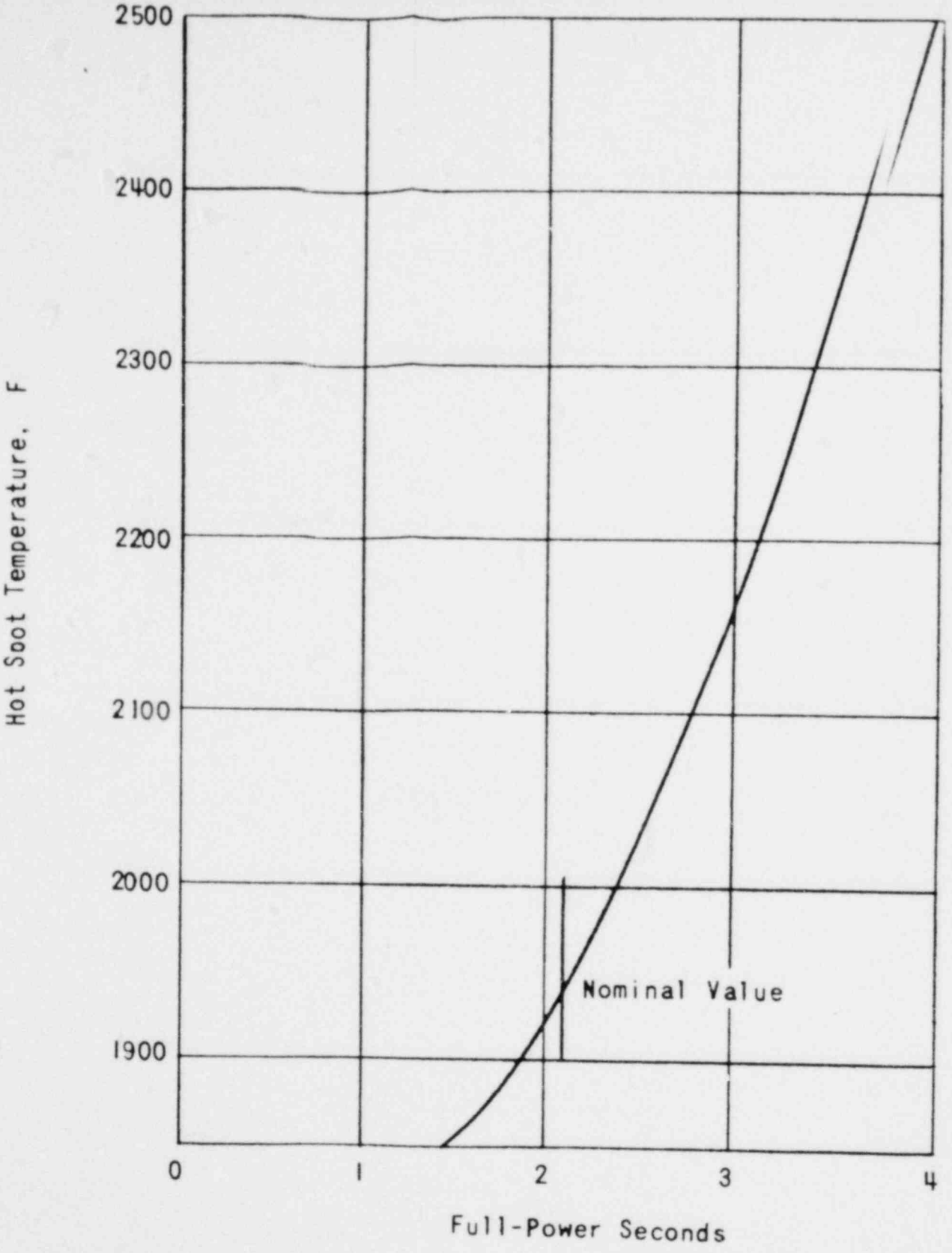

FIGURE 14.2-25
HOT SPOT CLAD TEMPERATURE AS A FUNUNCTION
OF FULL-POWER SECONDS RESULTING I FROM
VOID SHUTDOWN FOR A 36-IN. IID,
DOUBLE-ENDED HOT-LEG PIPE RUPTTURE

000 0274

SMUD
SACRAMENTO MUNICIPAL UTILITY DIDISTRICT

00

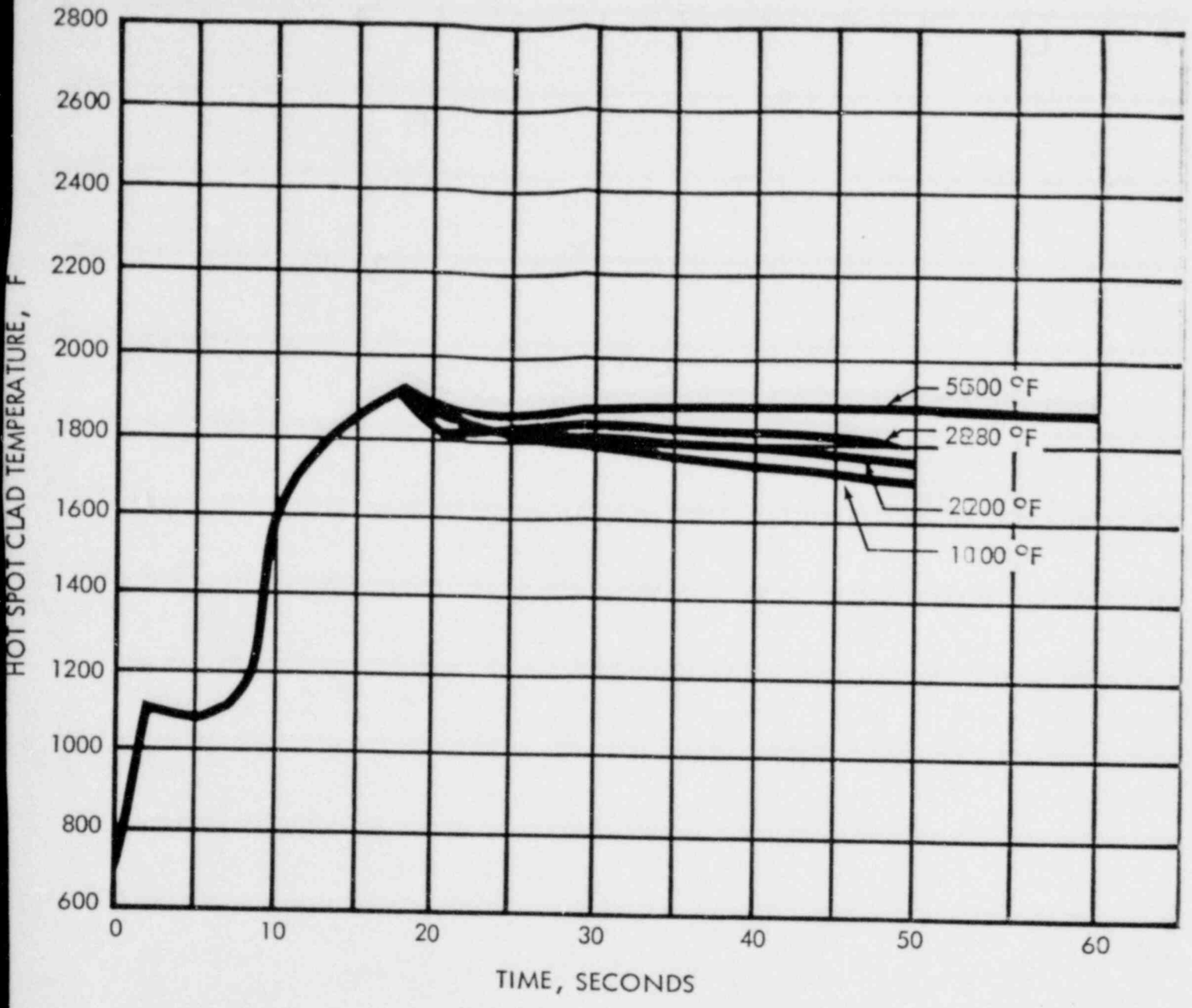

000 0275

FIGURE 14.2-226
HOT SPOT CLAD TEMPERATURES VERSUS TIME
FOR A 36-IN. ID, DOUBLE-ENDED, HOT-LEG
PIPE RUPTURE AND VARIABLE SINK TEMPERATURE

SMUD
SACRAMENTO MUNICIPAL UTILITY DISTRICT

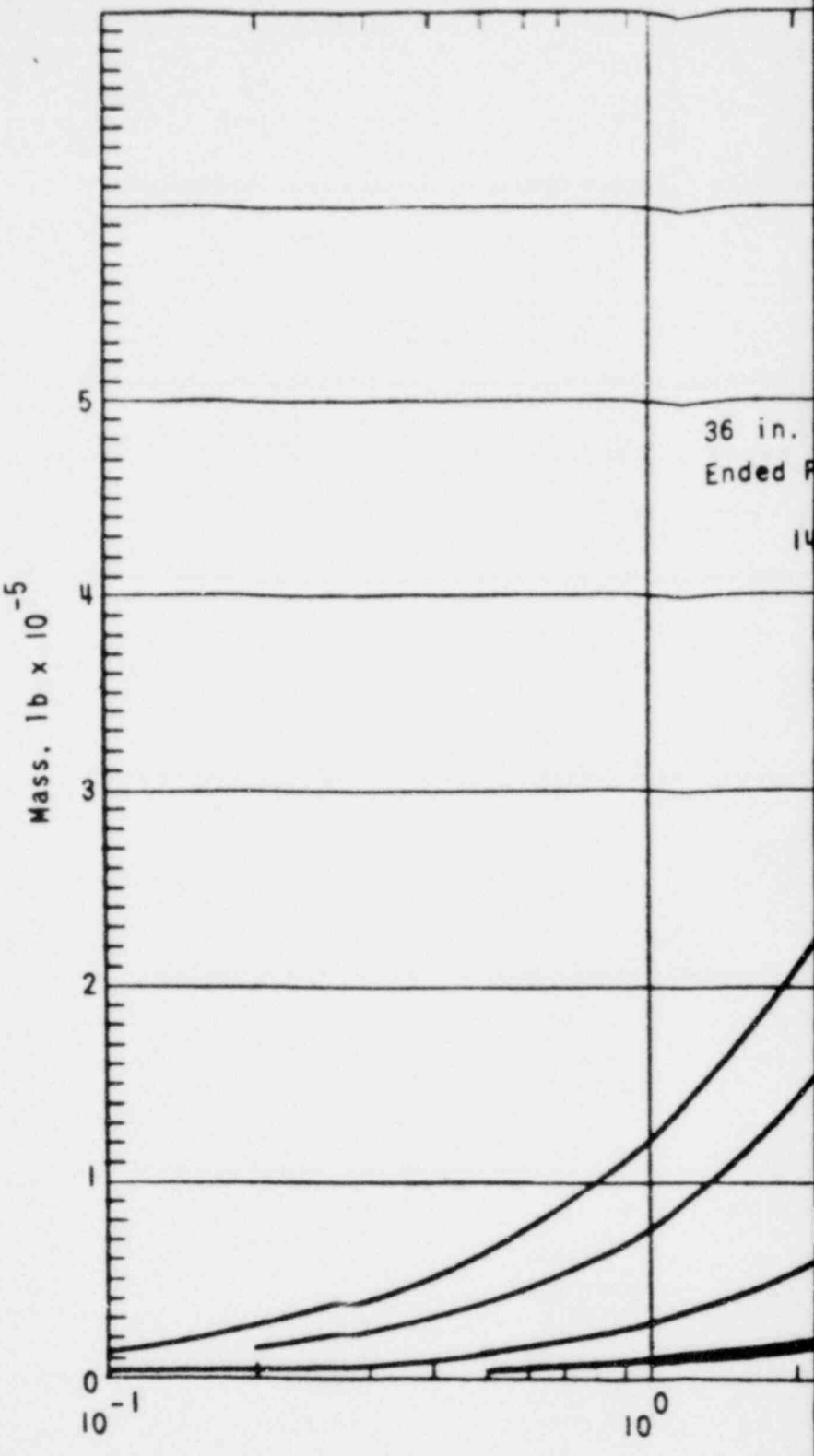

000 0276

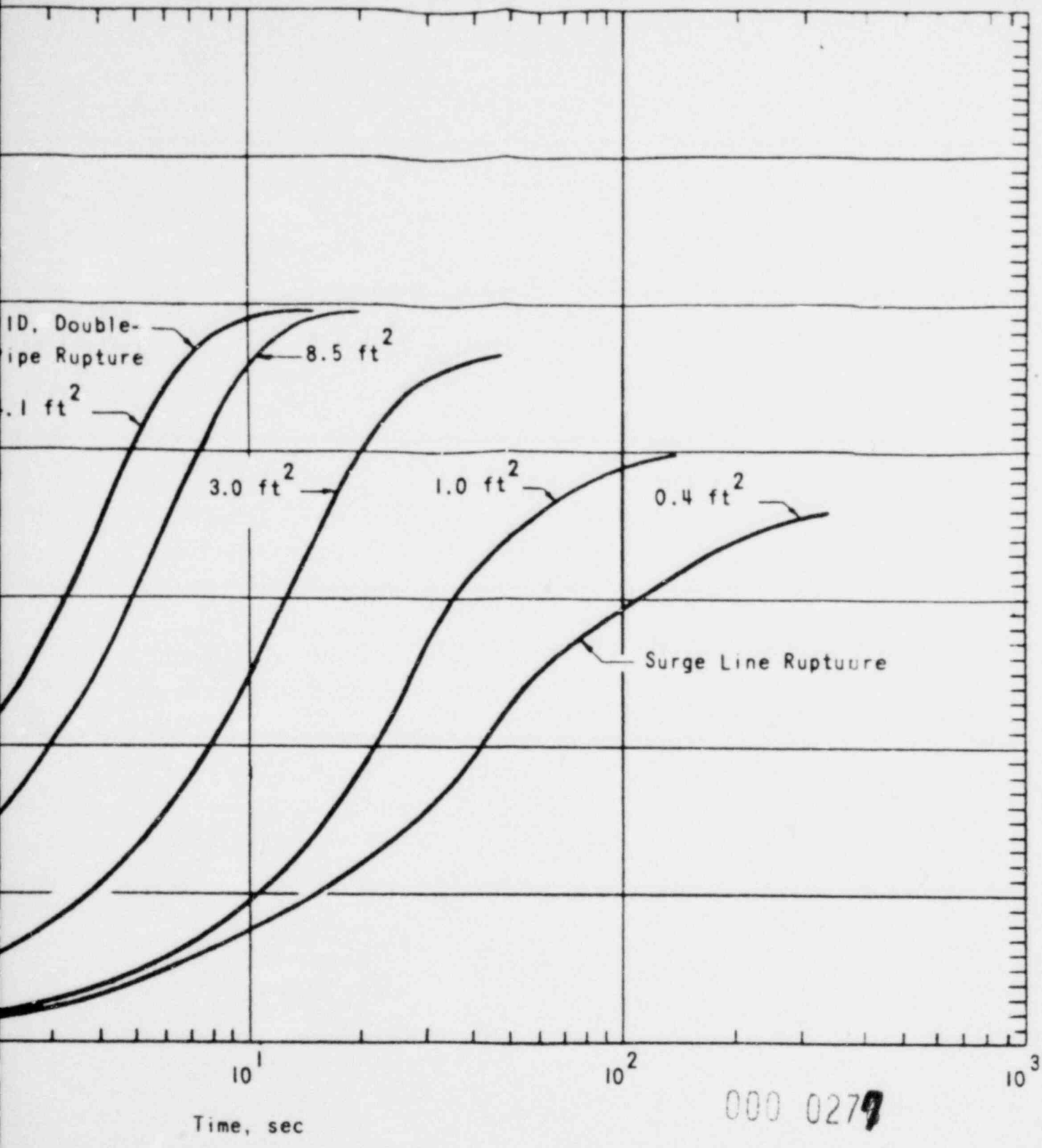

000 0279

FIGURE 14.2-27
MASS RELEASED TO REACTOR BUILDING
FOR THE SPECTRUM OF HOT-LEG RUPTURES

SMUD
SACRAMENTO MUNICIPAL UTILITY DISTRICT

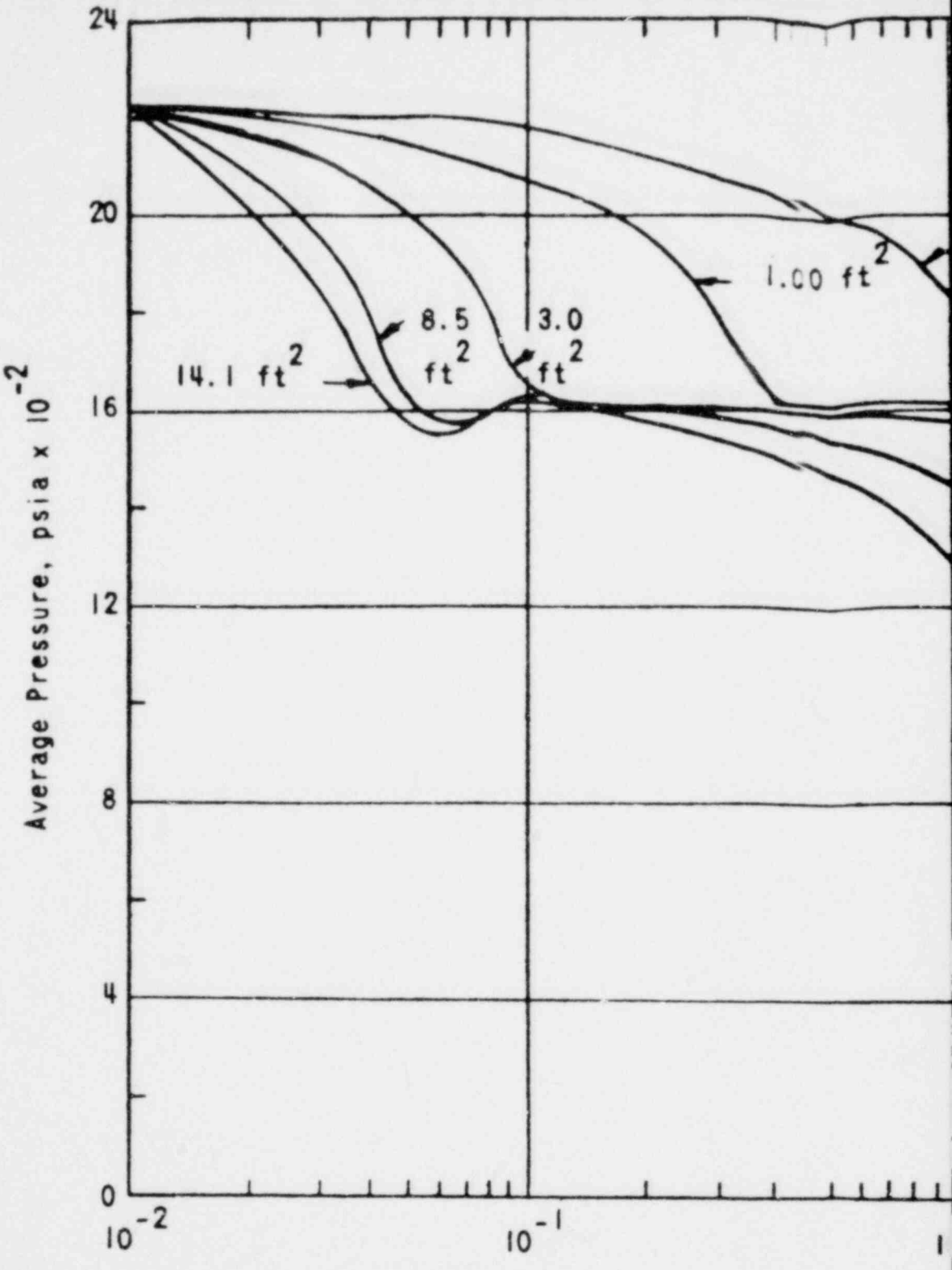
24
20
16
12
8
4
0
Average Pressure, psia x 10^{-2}
10^{-2}
10^{-1}
1
14.1 ft^2
8.5 ft^2
3.0 ft^2
1.00 ft^2

000 0278

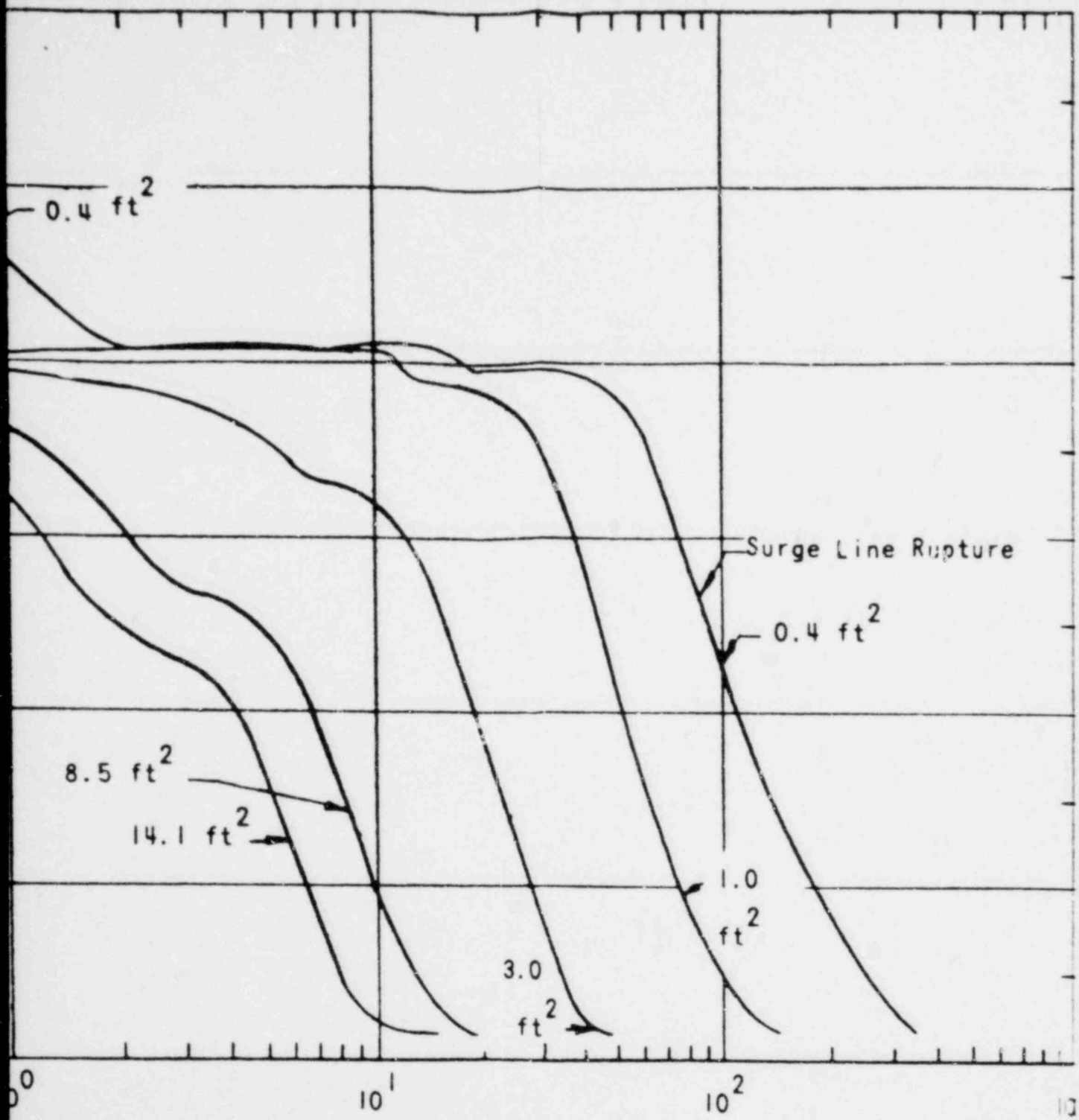

000 0279

FIGURE 14.2-28
REACTOR COOLANT AVERAGE PRESSURE FOR
THE SPECTRUM OF HOT-LEG RUPTURES

SMUD
SACRAMENTO MUNICIPAL UTILITY DISTRICT

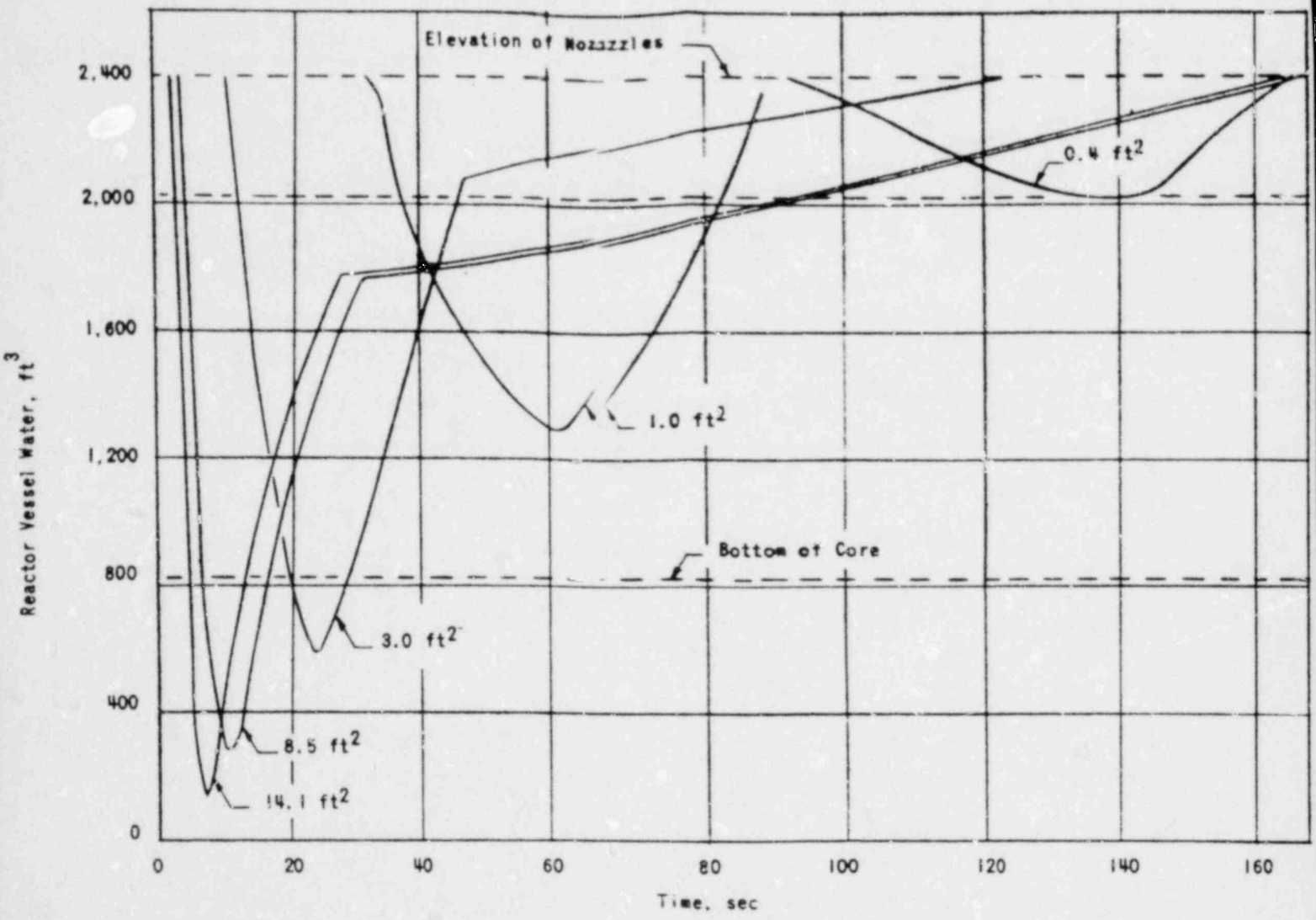

000 0280

FIGURE 14.2-29
HOT-LEG RUPTURES - REACTOR VESSEL WATER VOLUME VERSUS TIME INCLUDING EFFECTS OF BOILOFF AND INJECTION

SMUD
SACRAMENTO MUNICIPAL UTILITY DISTRICT

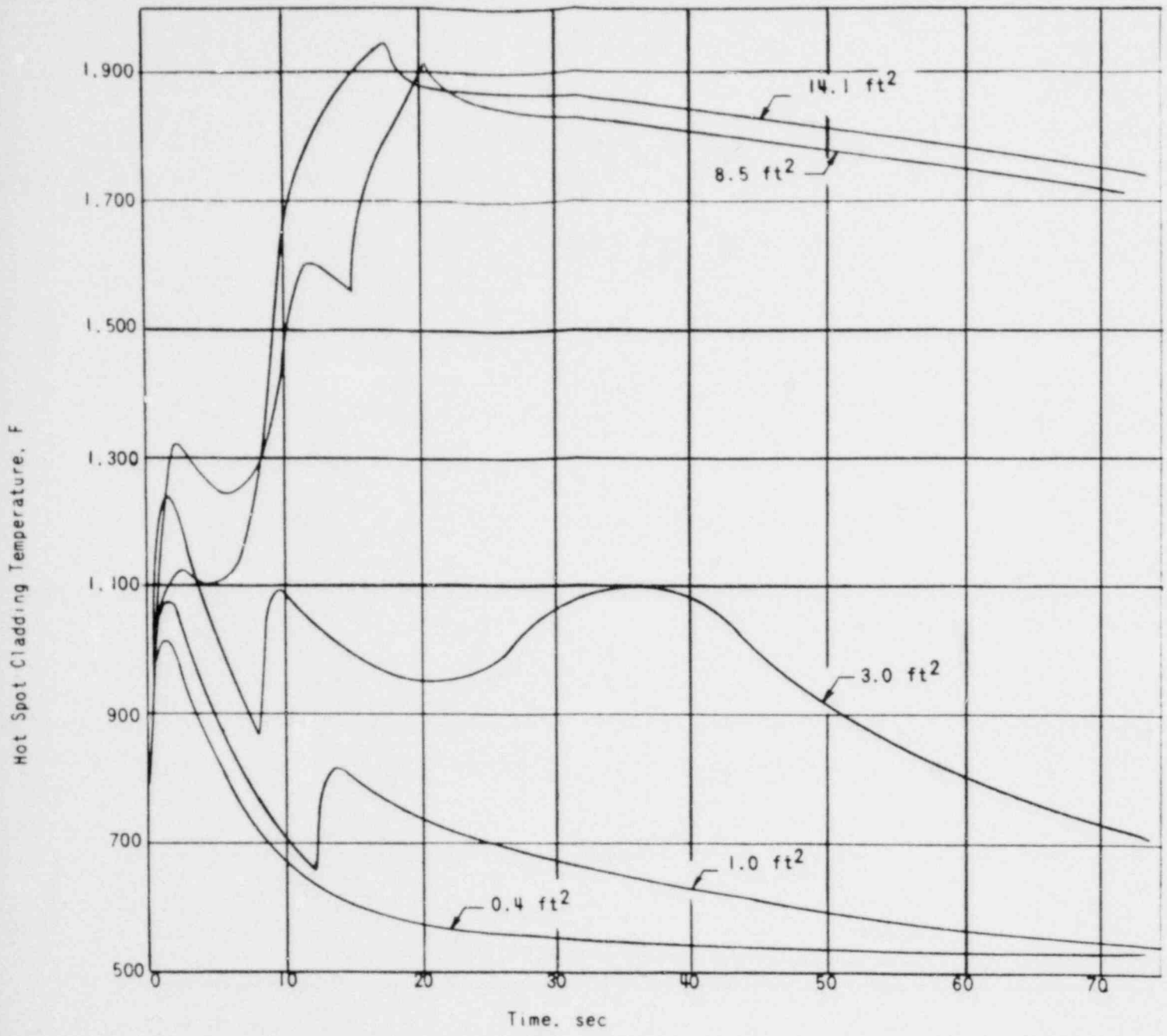

FIGURE 14.2-30
HOT SPOT CLAD TEMPERATURE VERSUS TIME
FOR SPECTRUM HOT-LEG LEAKS

000 0281

SMUD
SACRAMENTO MUNICIPAL UTILITY DISTRICT

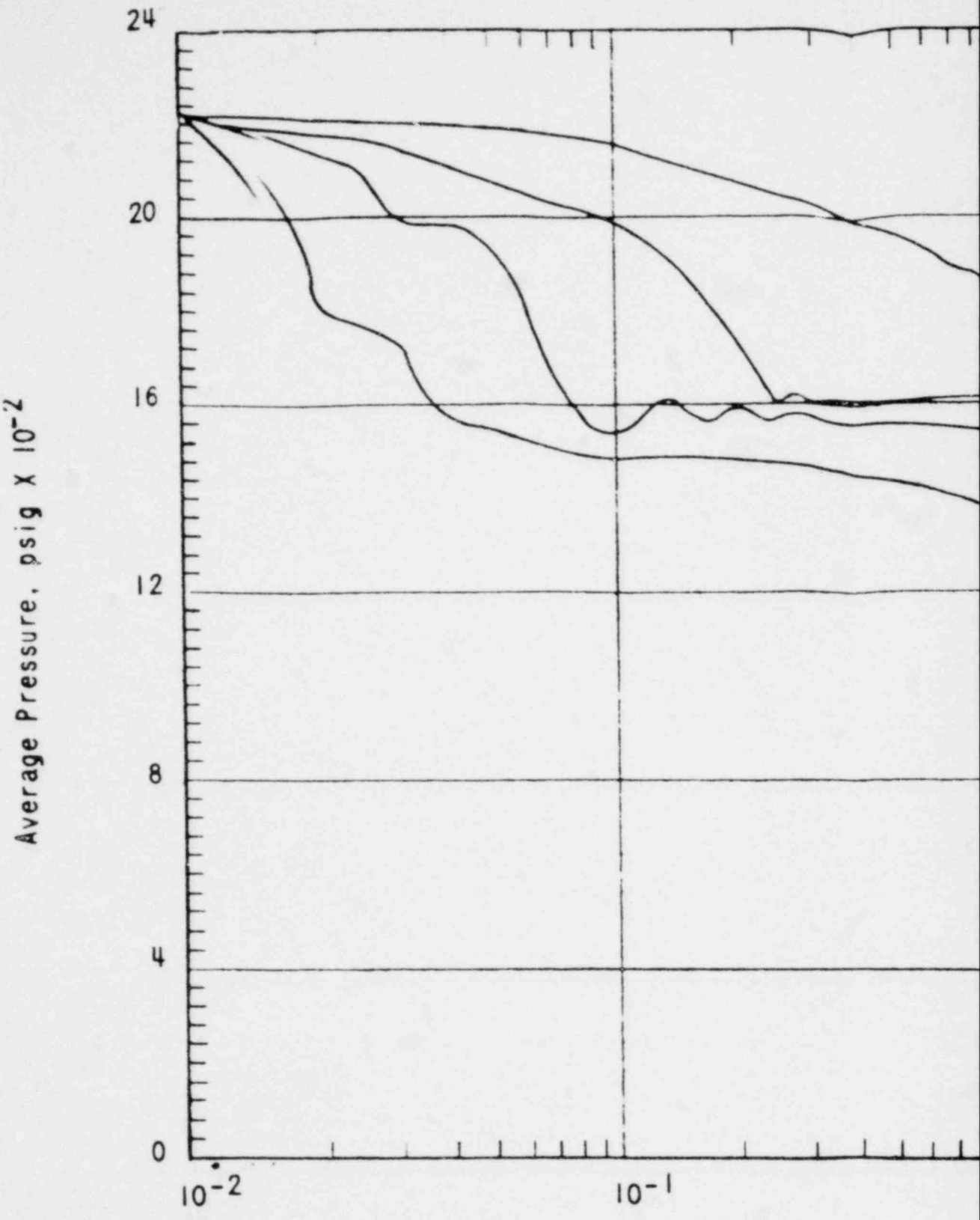

000 0282

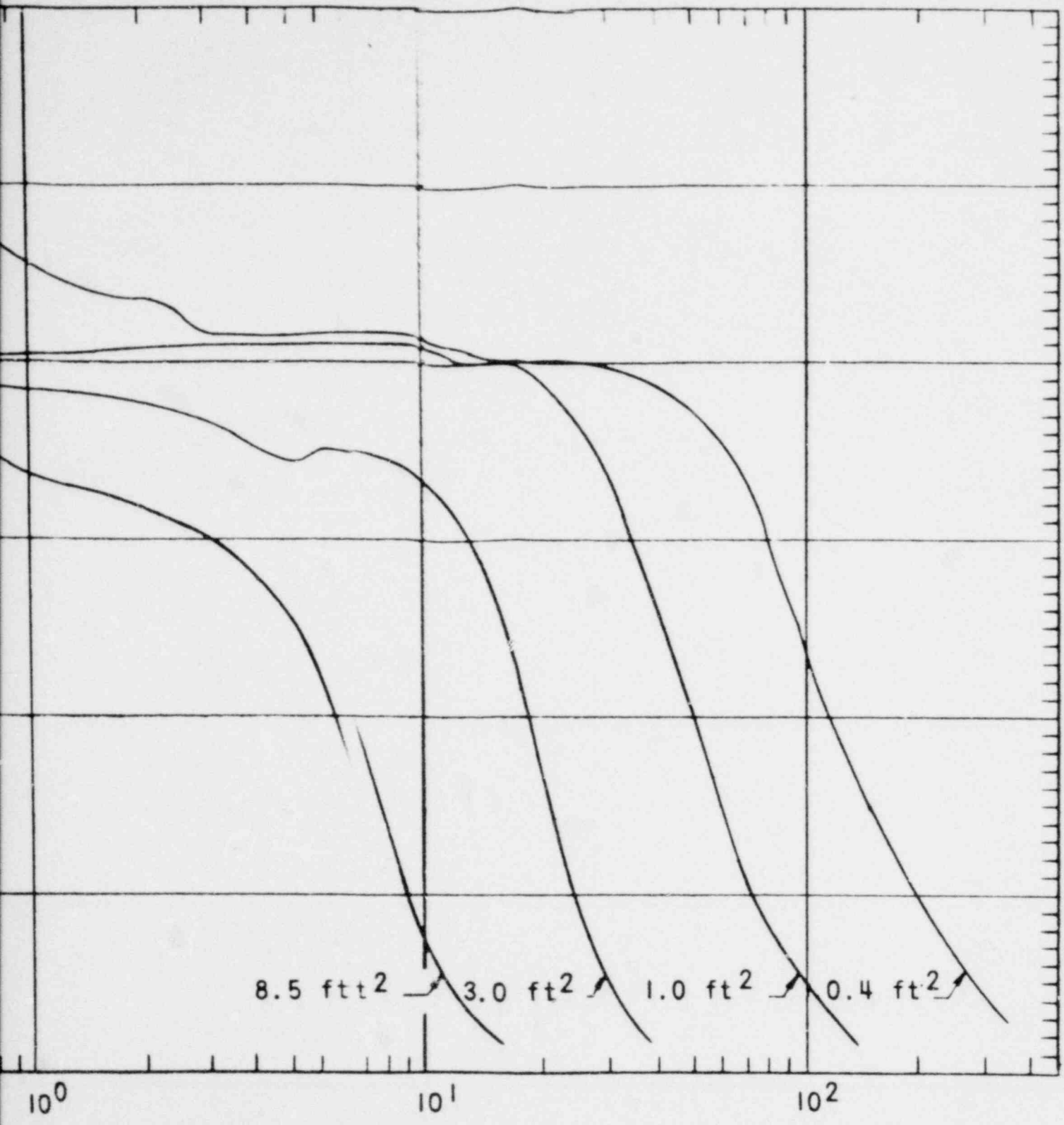

FIGURE 14.2-31
REACTOR COOLANT AVERAGE PRESSURE -
SPECTRUM OF COLD-LEG RUPTURE SIZES

000 0283

SMUD
SACRAMENTO MUNICIPAL UTILITY DISTRICT

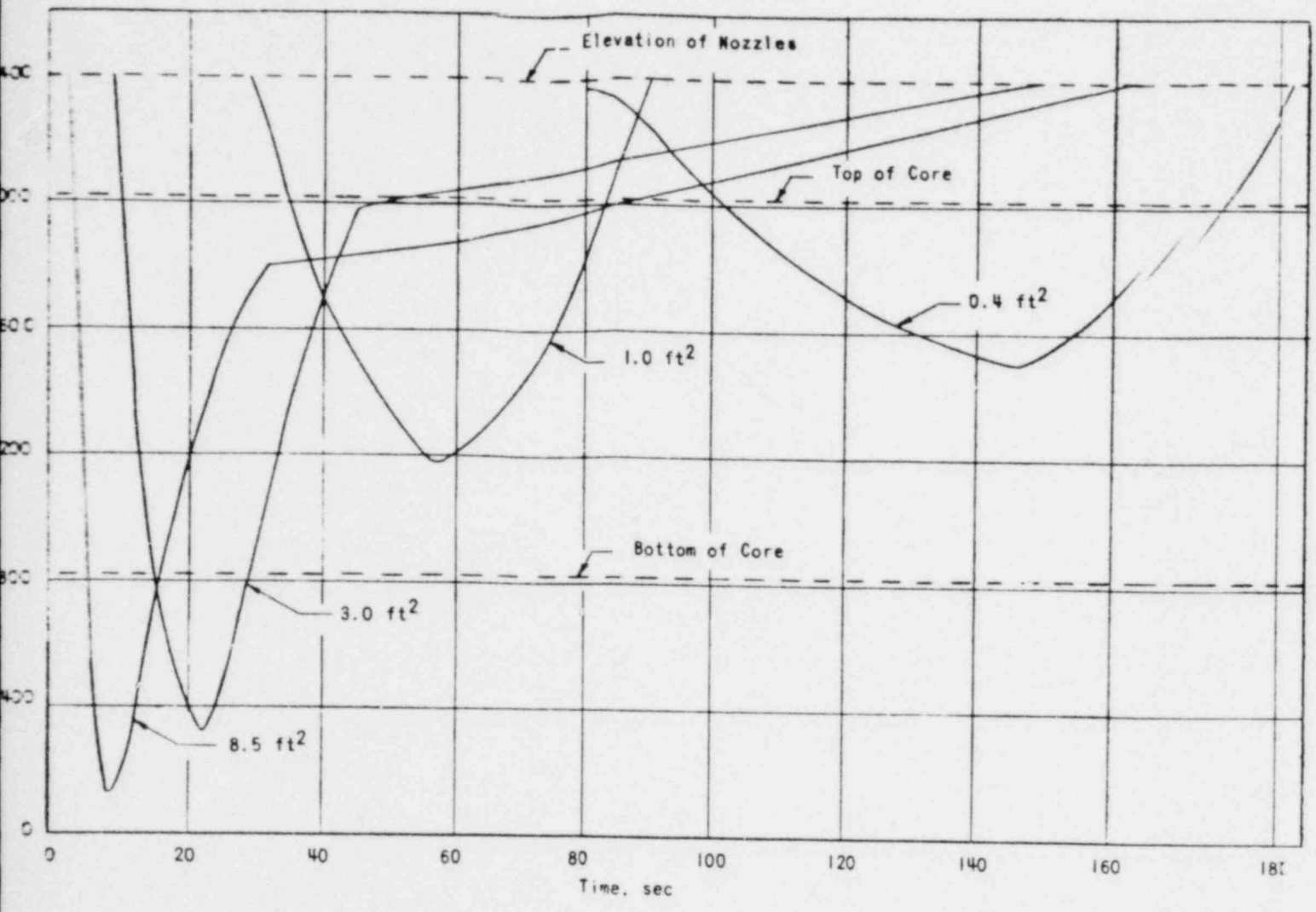

000 0284

FIGURE 14.2-32
COLD-LEG RUPTURES - REACTOR VESSEL WATER VOLUME VERSUS TIME, INCLUDING EFFECTS OF BOILOFF AND INJECTION

SMUD

SACRAMENTO MUNICIPAL UTILITY DISTRICT

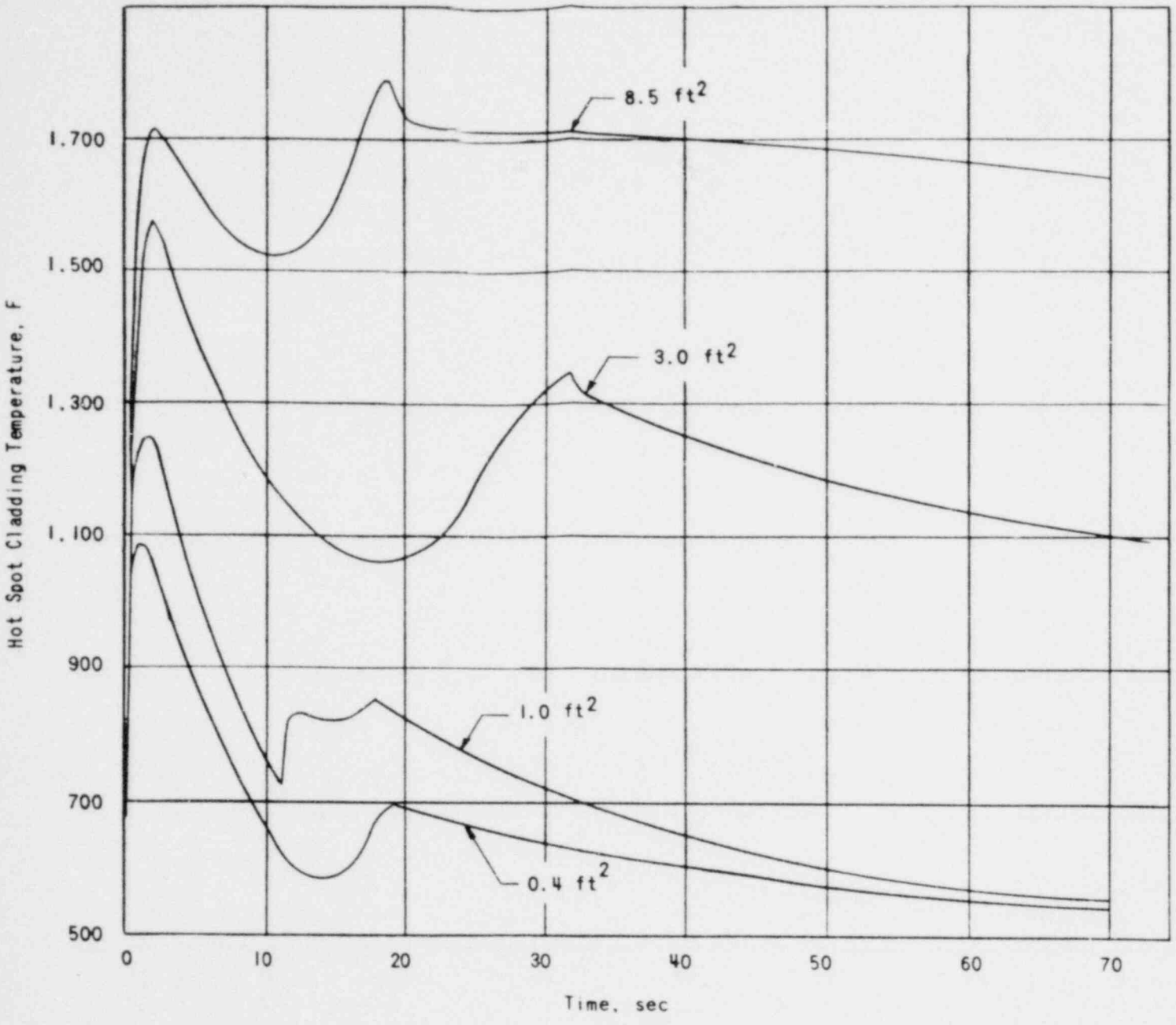

000 0285

FIGURE 14.2-33
HOT SPOT CLAD TEMPERATURE VERSUS TIME
FOR SPECTRUM OF COLD-LEG RUPTURES

00 1

SMUD
SACRAMENTO MUNICIPAL UTILITY DISTRICT

LEGEND:

HPI - HIGH PRESSURE INJECTION
LPI - LOW PRESSURE INJECTION

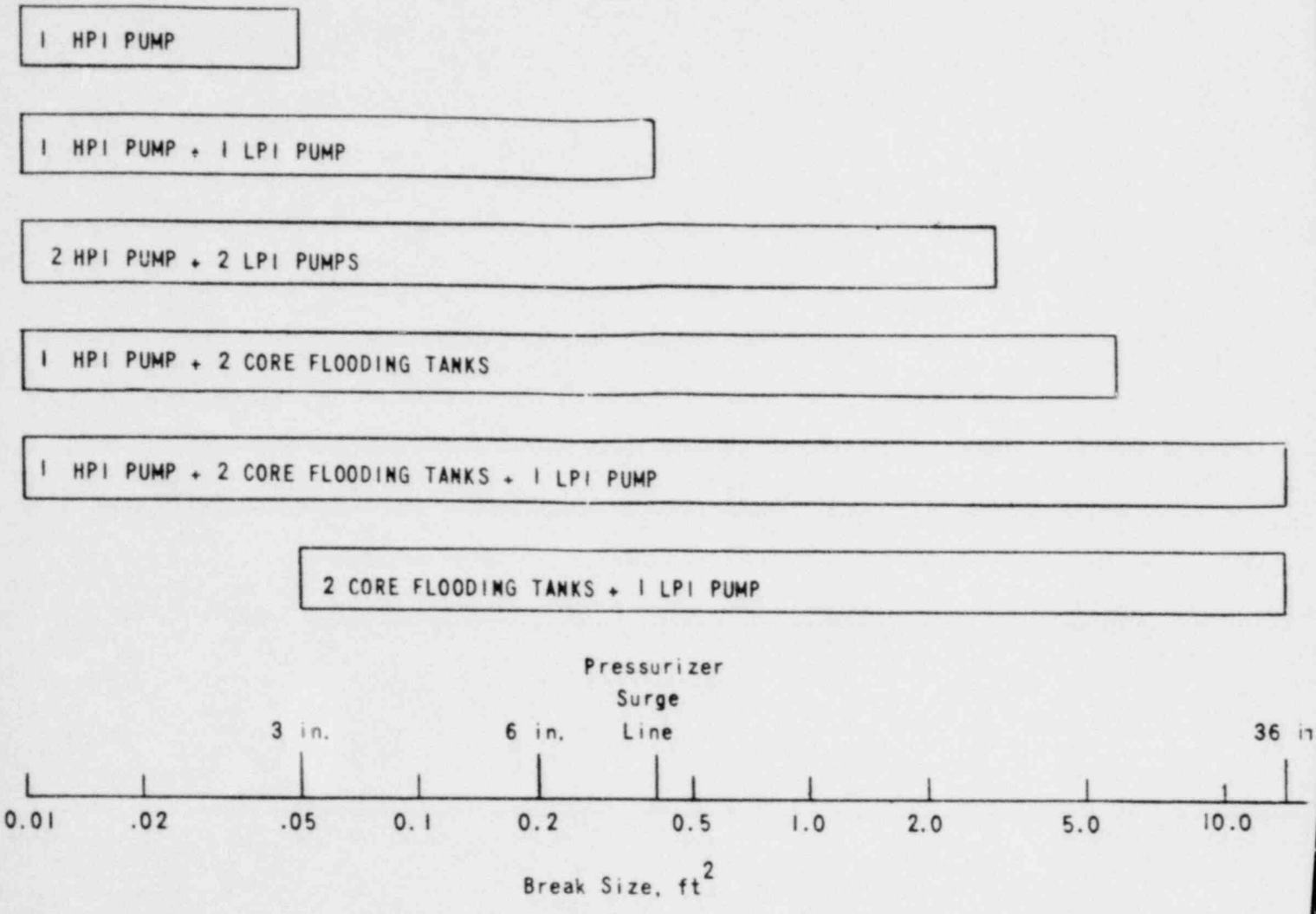

000 0286

FIGURE 14.2-34
EMERGENCY CORE COOLING
SYSTEMS CAPABILITY

SMUD

SACRAMENTO MUNICIPAL UTILITY DISTRI

Amendment

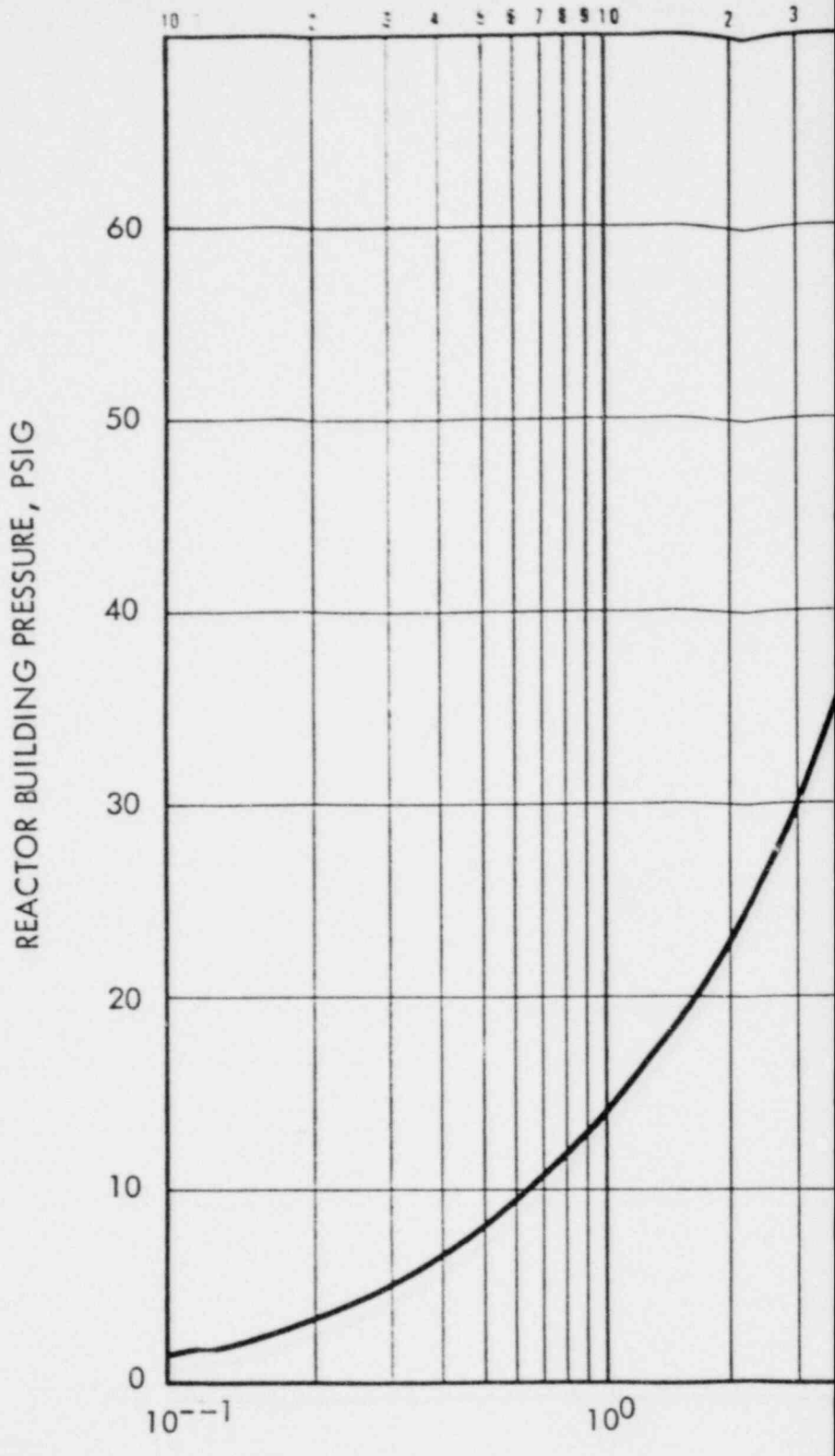

000 0287

00

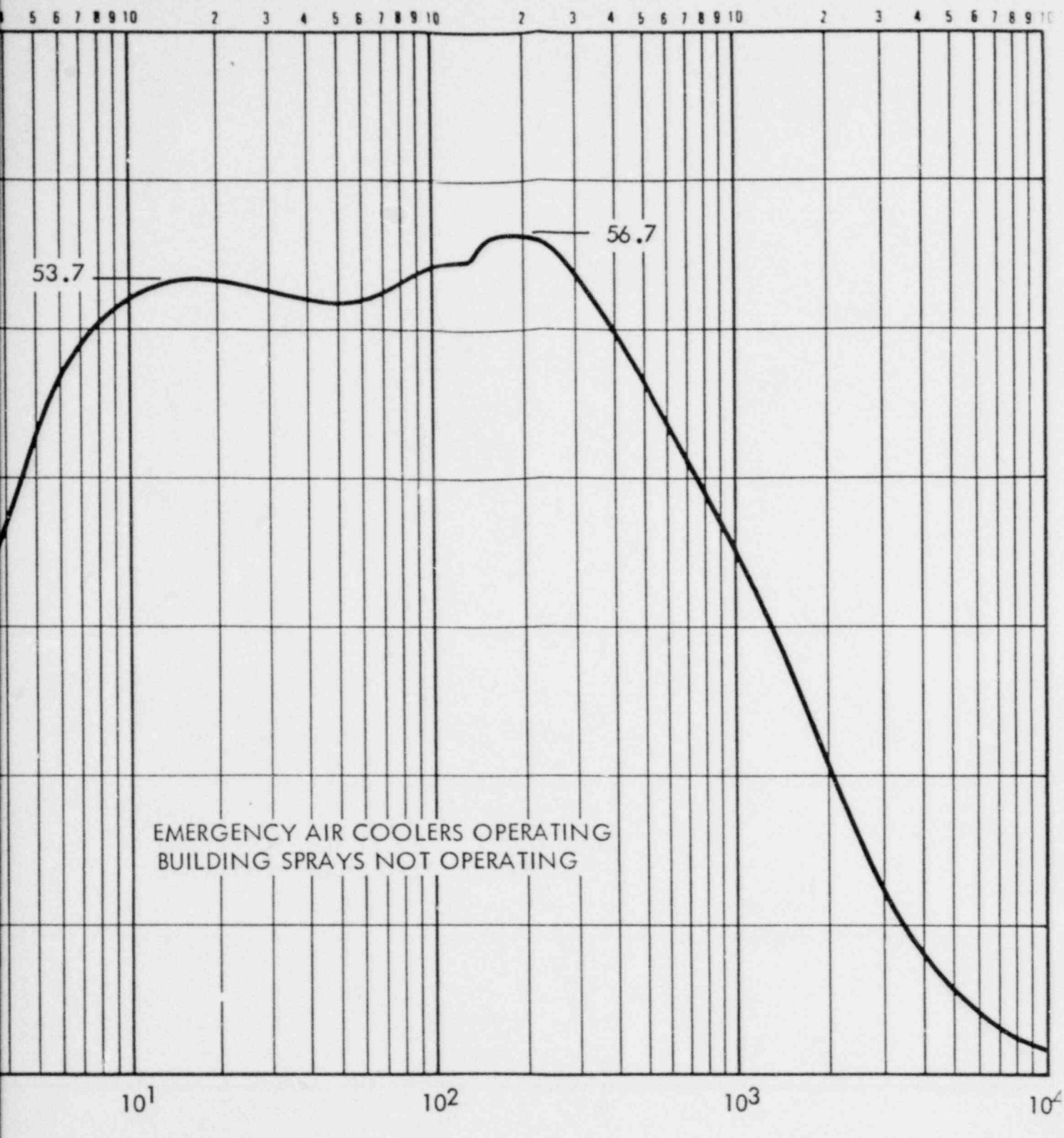

FIGURE 14.2-35
REACTOR BUILDING PRESSURE VERSUS
TIME AFTER A 14.1 FT^2
HOT-LEG PIPE RUPTURE

000 0288

SMUD
SACRAMENTO MUNICIPAL UTILITY DISTRICT

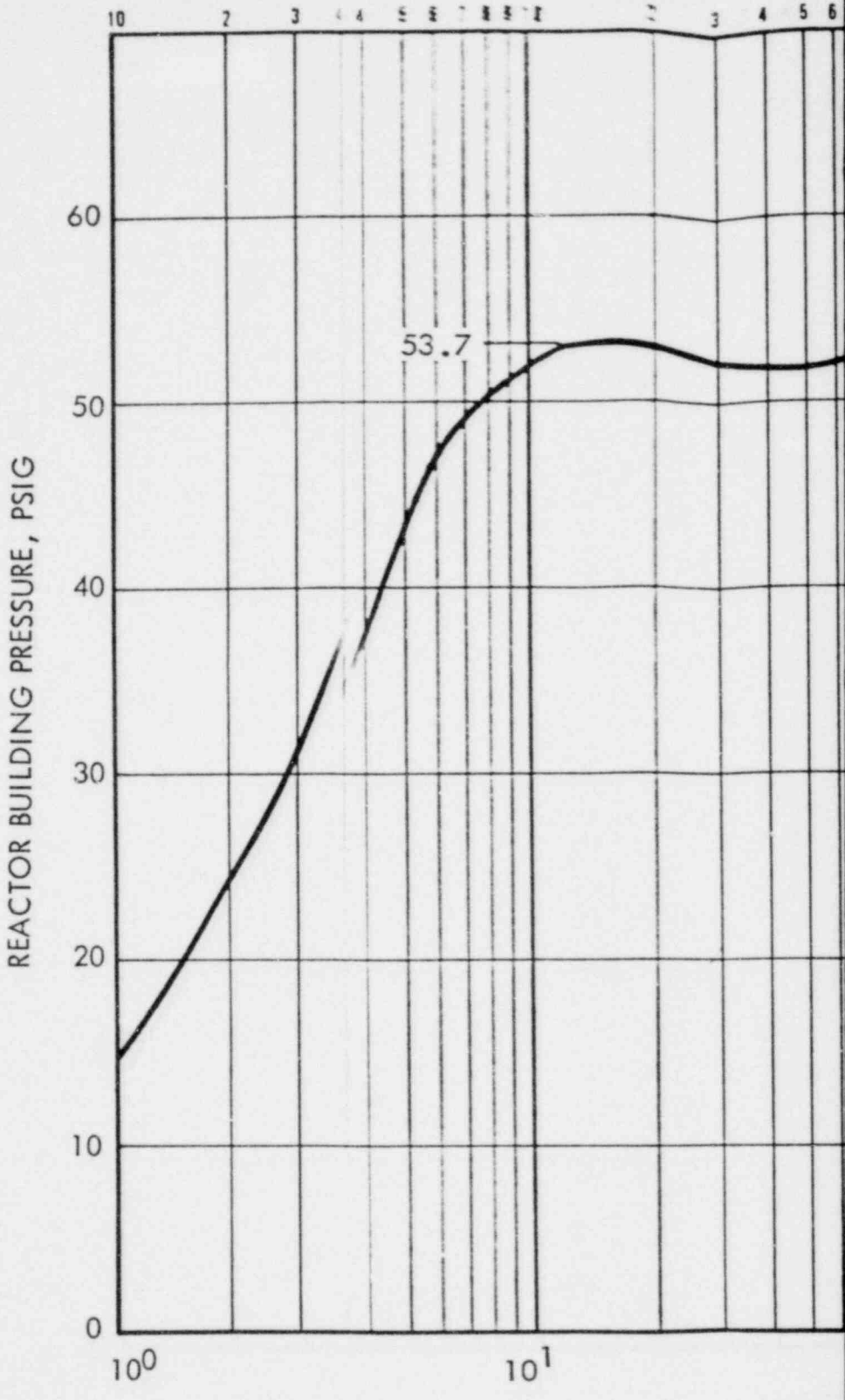

000 0289

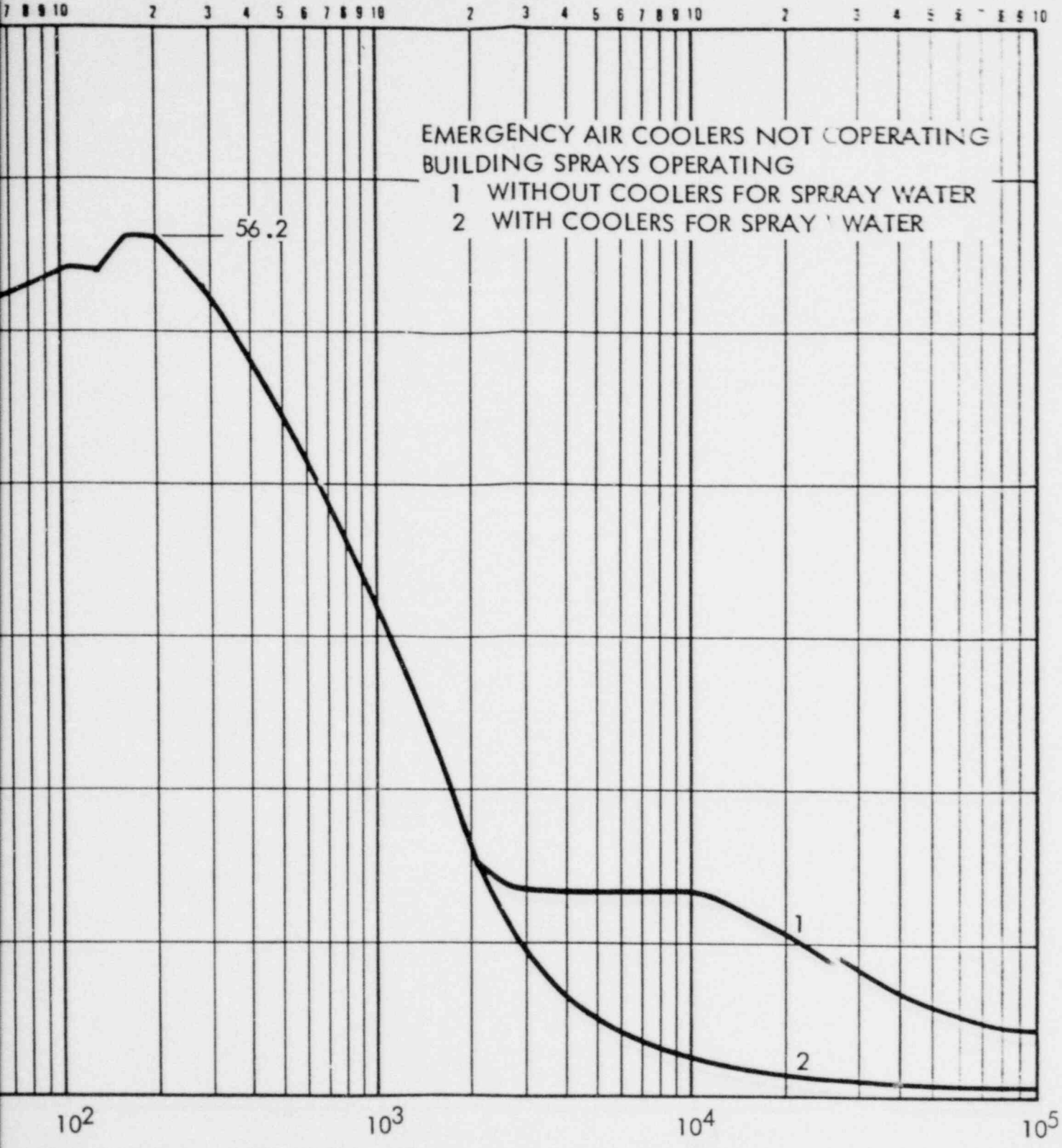

FIGURE 14...2-36
REACTOR BUILDING PRESSURE VERSUS TIME
FOR A 14.1 FT^2 HOT-LEG PIPE RUPTURE
WITH AND WITHOUT COOLING OF THE
RECIRCULATED SPRAY WATER

000 0290

SMUD

SACRAMENTO MUNICIPAL UTILITY DISTRICT

Amendment 1

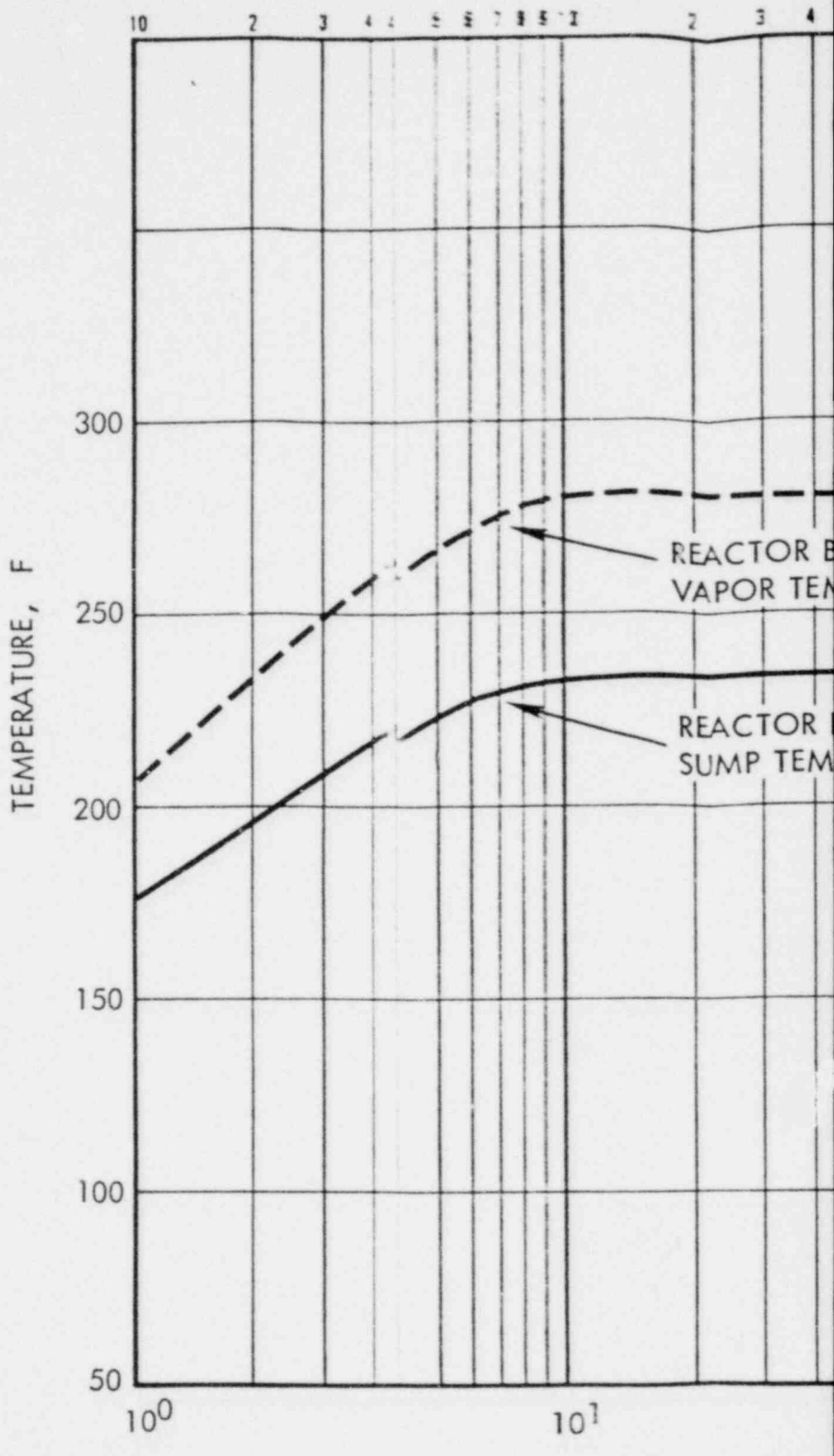
TEMPERATURE, F
300
250
200
150
100
50
10^0
10^1
REACTOR B
VAPOR TEM
REACTOR
SUMP TEM

000 0291

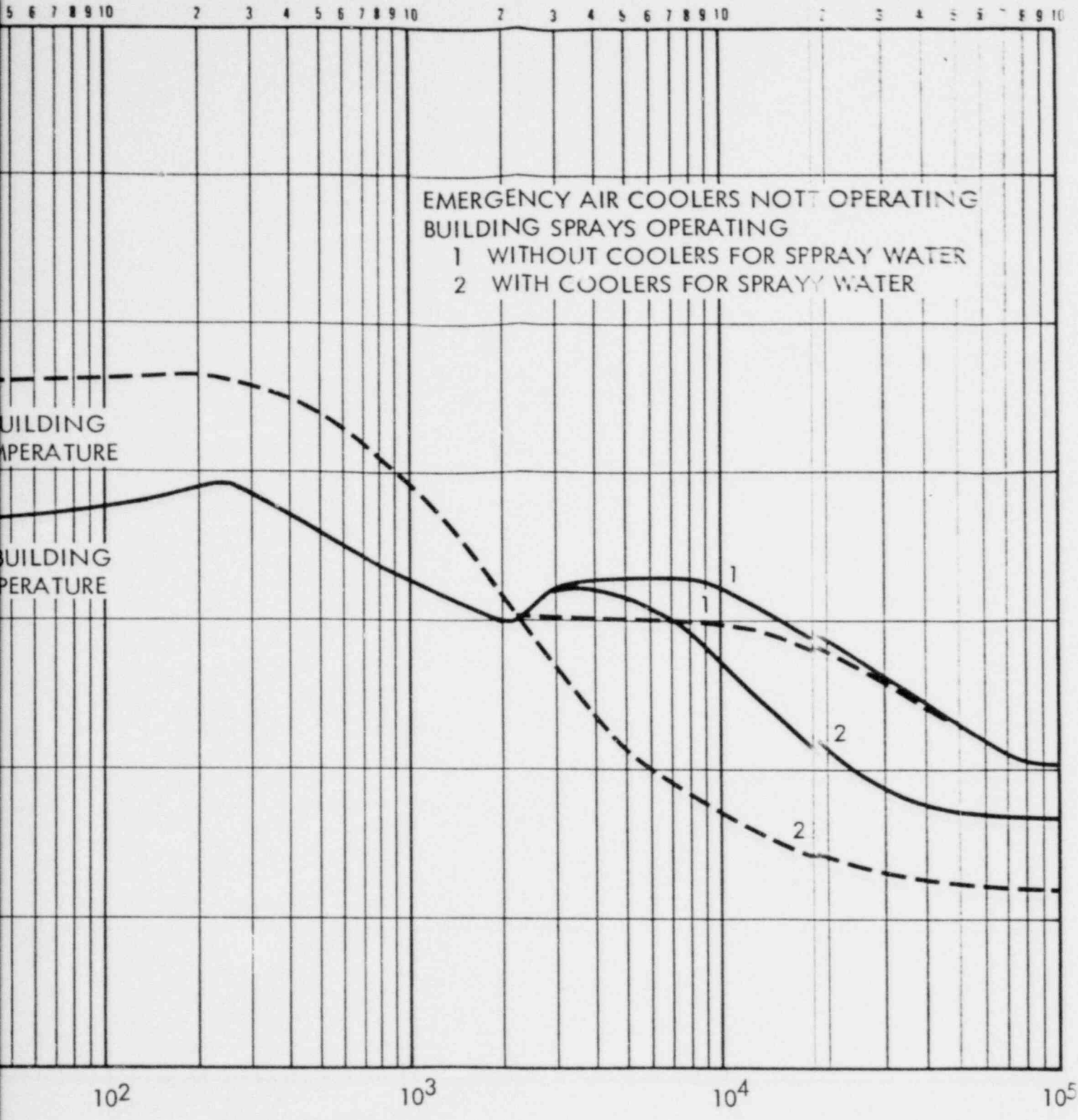

FIGURE 14.4.2-37
REACTOR BUILDING ATMOSPHERE AND SUMP COOLANT TEMPERATURES FOLLOWING A 14.1 FT^2 HOT-LEG PIPE RUPTURE

000 0292

SMUD

SACRAMENTO MUNICIPAL UTILITY DISTRICT

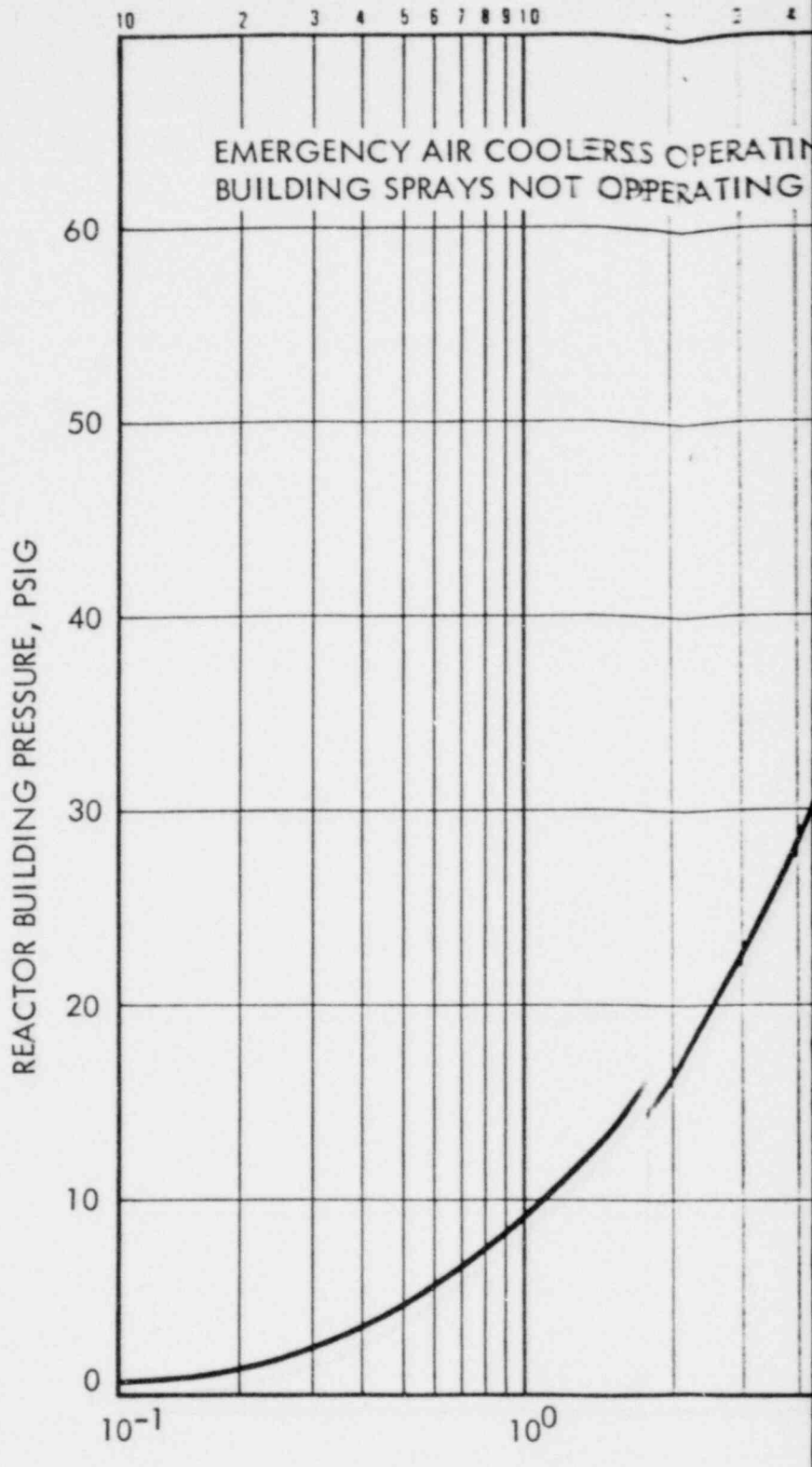
EMERGENCY AIR COOLERSS OPERATIN
BUILDING SPRAYS NOT OPPERATING
REACTOR BUILDING PRESSURE, PSIG
60
50
40
30
20
10
0
10^{-1}
10^{0}

000 0293

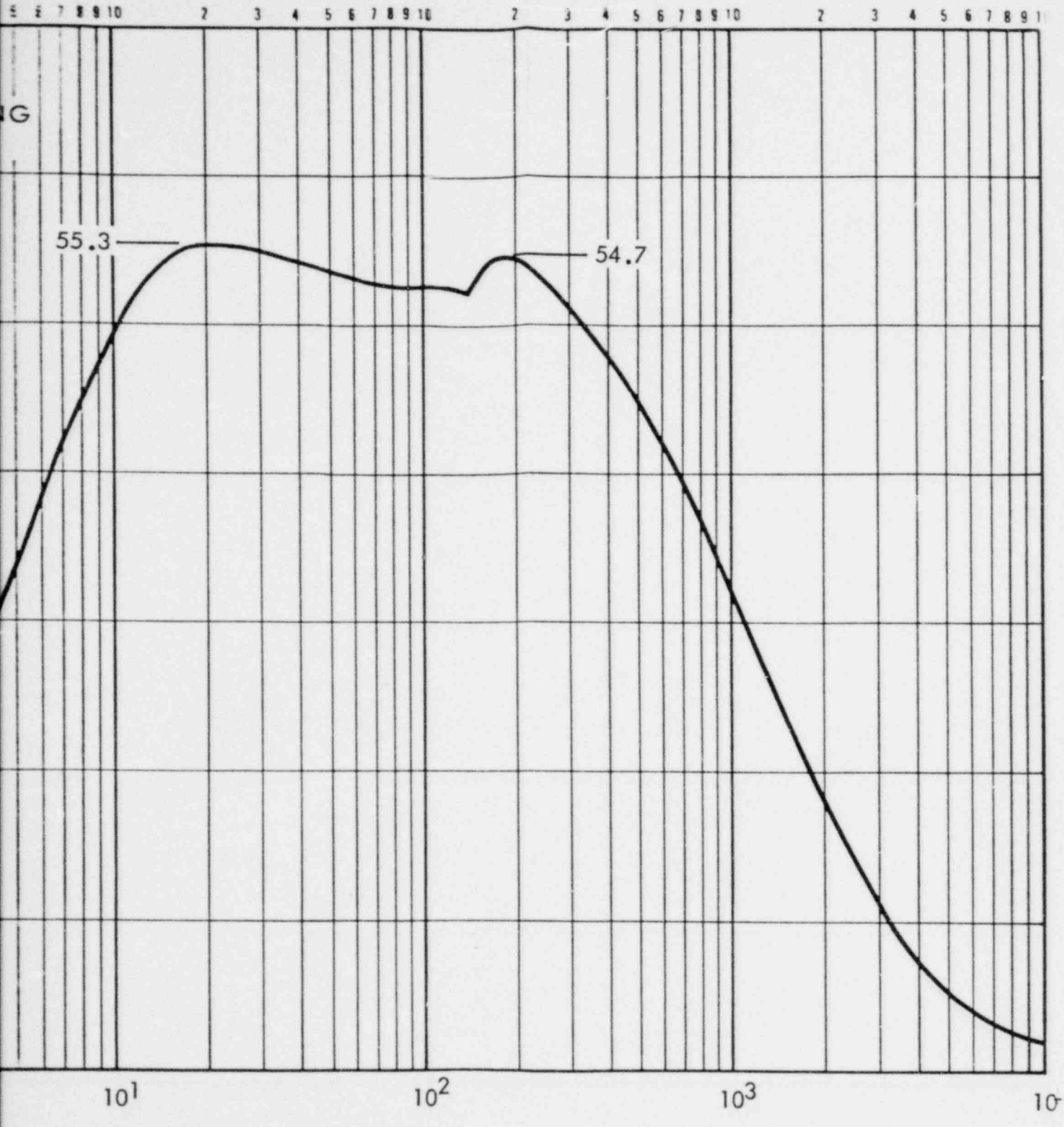

FIGURE 14.2-38
REACTOR BUILDING PRESSURE VERSUS
TIME AFTER RUPTURE (8.5 FT^2)

SMUD

SACRAMENTO MUNICIPAL UTILITY DISTRICT

000 0294

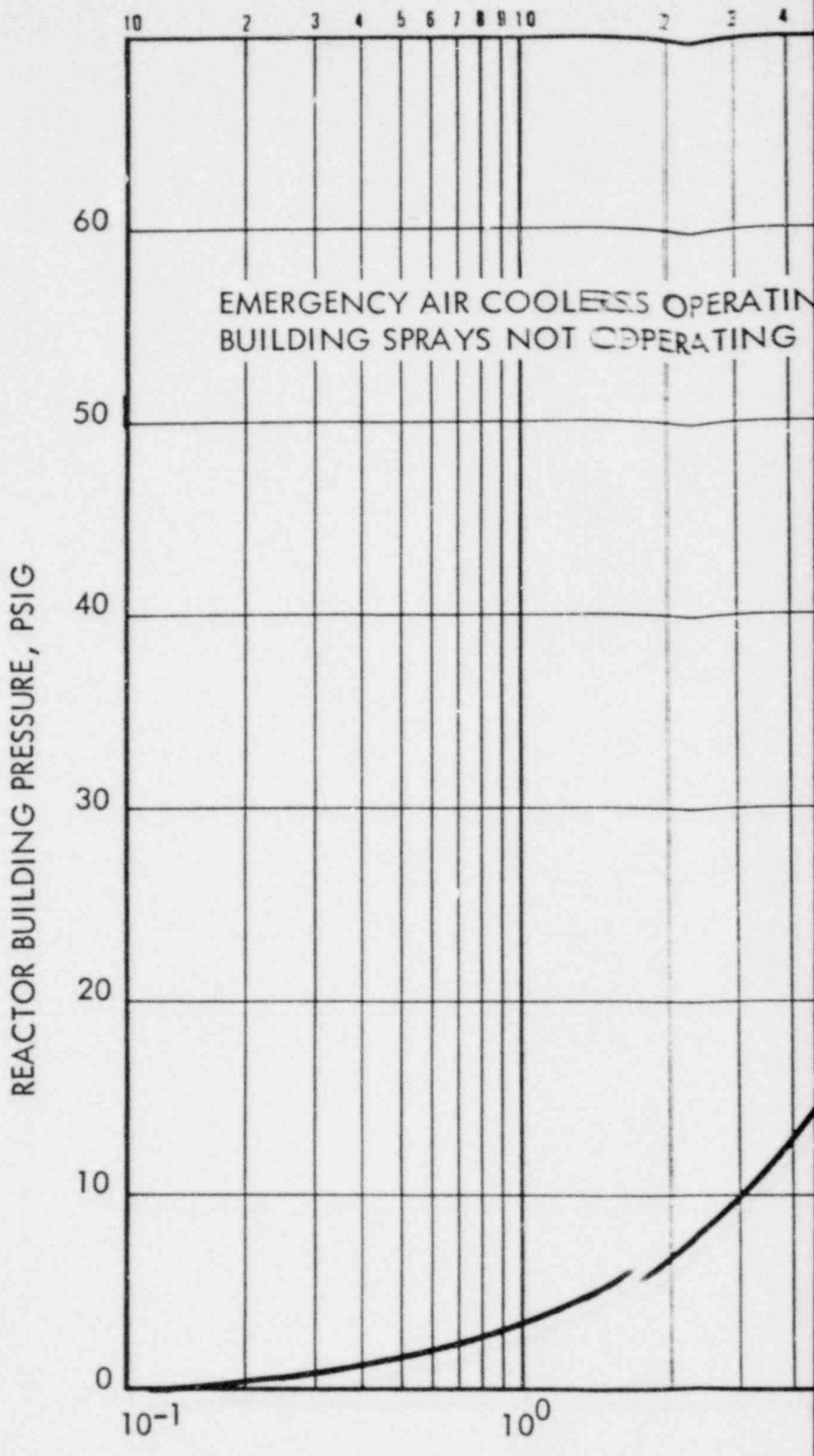
10 2 3 4 5 6 7 8 9 10 2 3 4
60
50
40
30
20
10
0
EMERGENCY AIR COOLERS OPERATIN
BUILDING SPRAYS NOT OPERATING
REACTOR BUILDING PRESSURE, PSIG
10^{-1}
10^{0}

000 0295

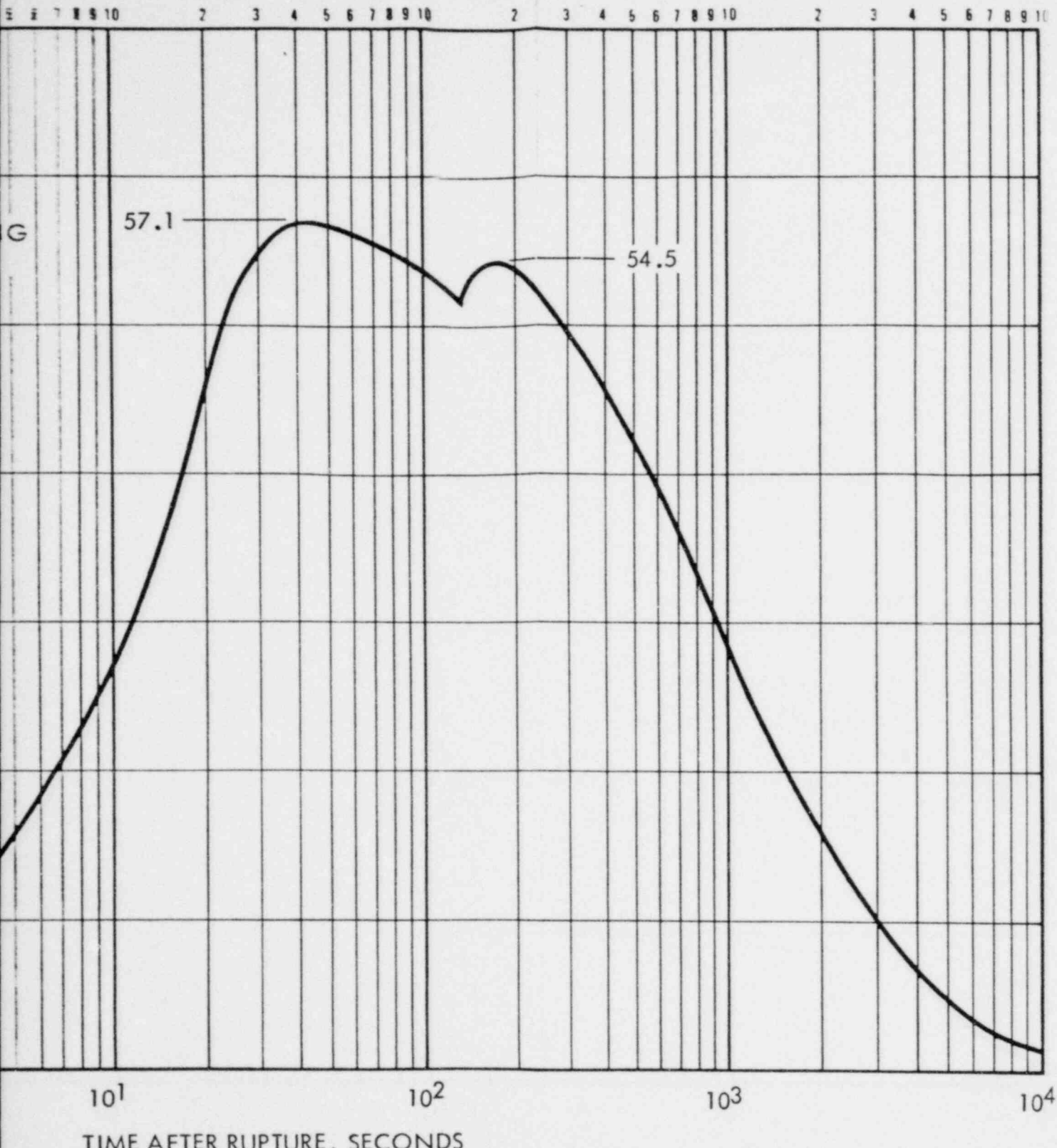

FIGURE 14.2-39
REACTOR BUILDING PRESSURE VERSUS
TIME AFTER RUPTURE (3.0 FT^2)

000 0296

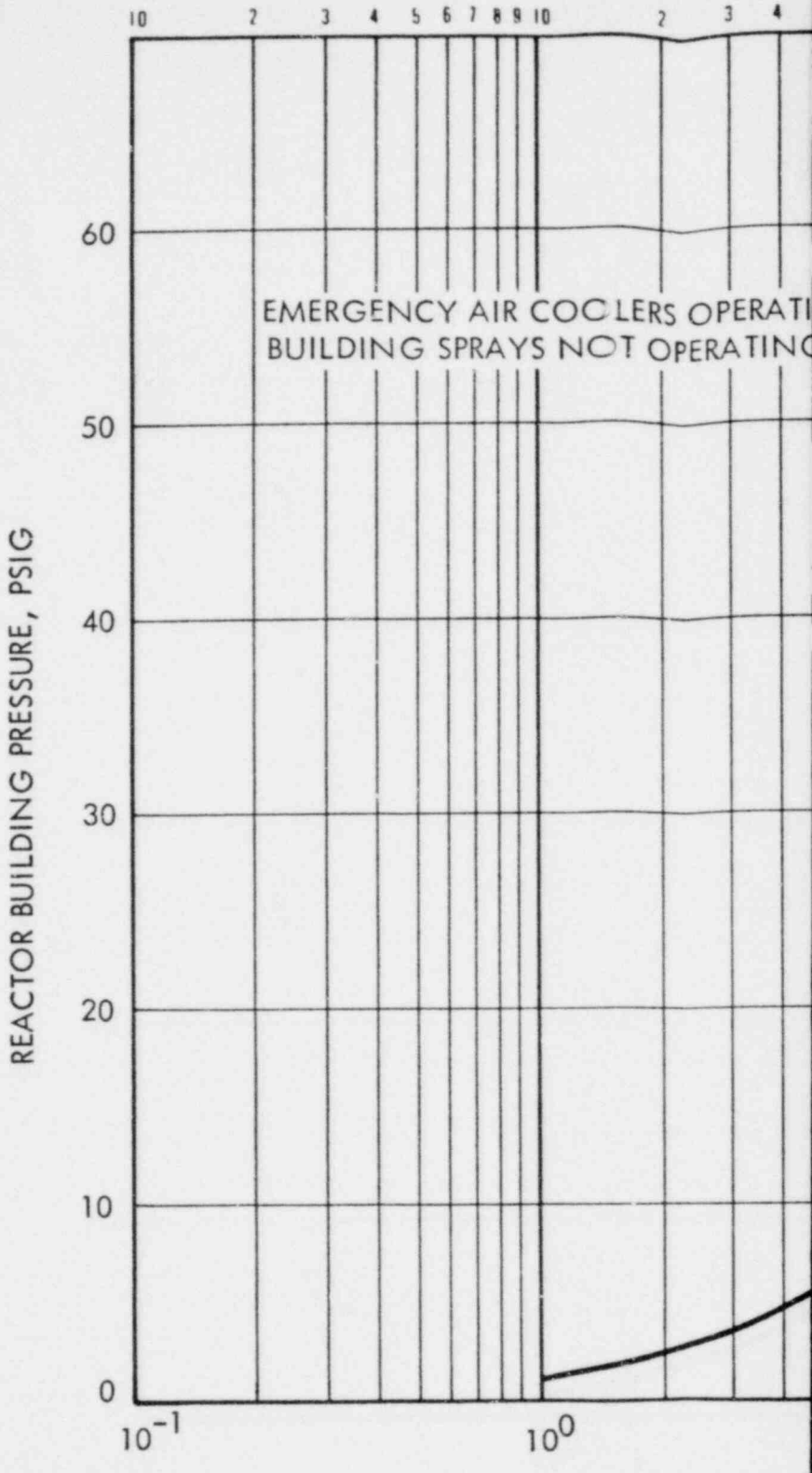
10 2 3 4 5 6 7 8 9 10 2 3 4
60
50
40
30
20
10
0
EMERGENCY AIR COOLERS OPERATI
BUILDING SPRAYS NOT OPERATING
REACTOR BUILDING PRESSURE, PSIG
10^{-1}
10^{0}

000 0297

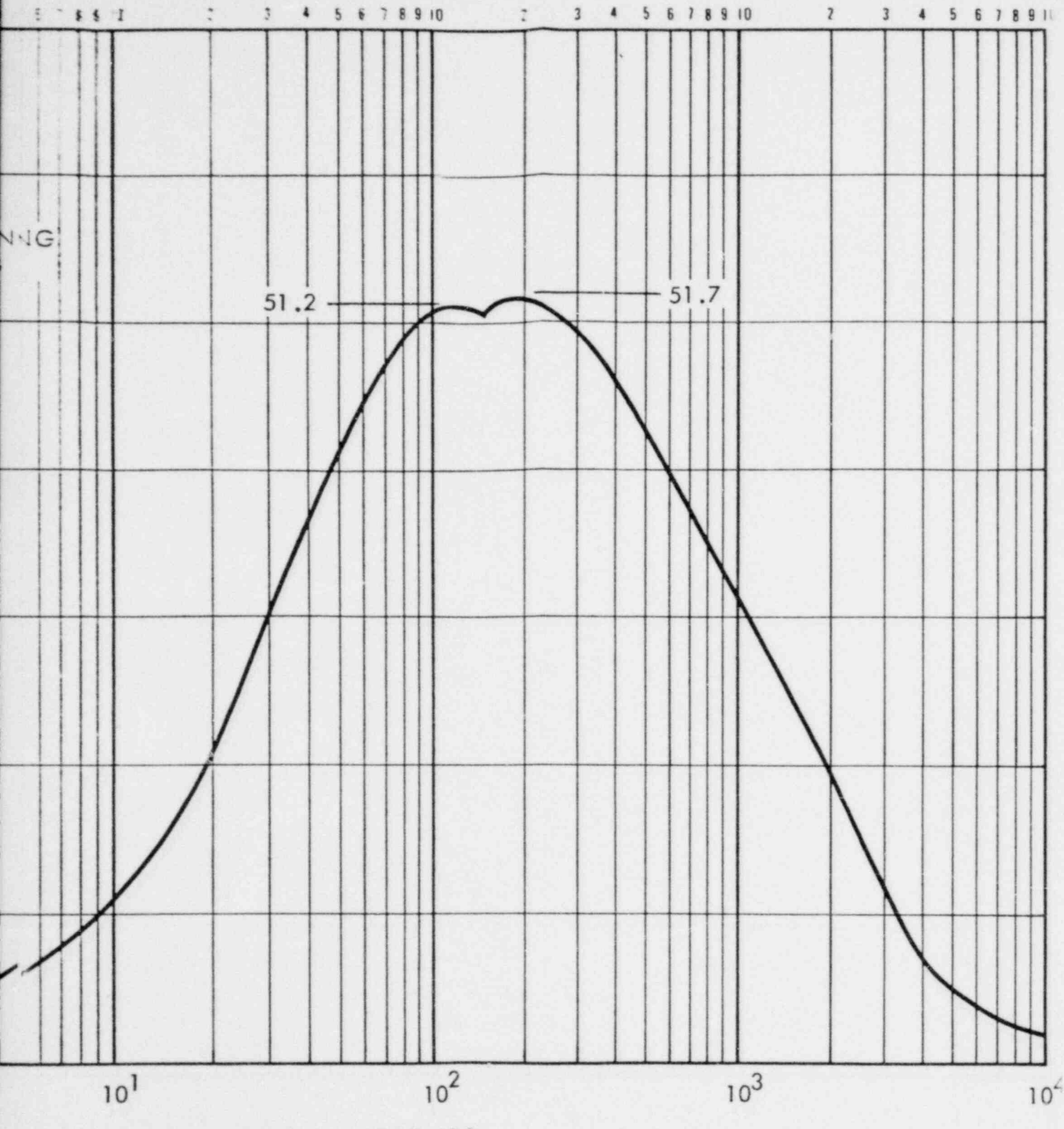

FIGURE 14.2-40
REACTOR BUILDING PRESSURE VERSUS
TIME AFTER RUPTURE (1.0 FT^2)

1298

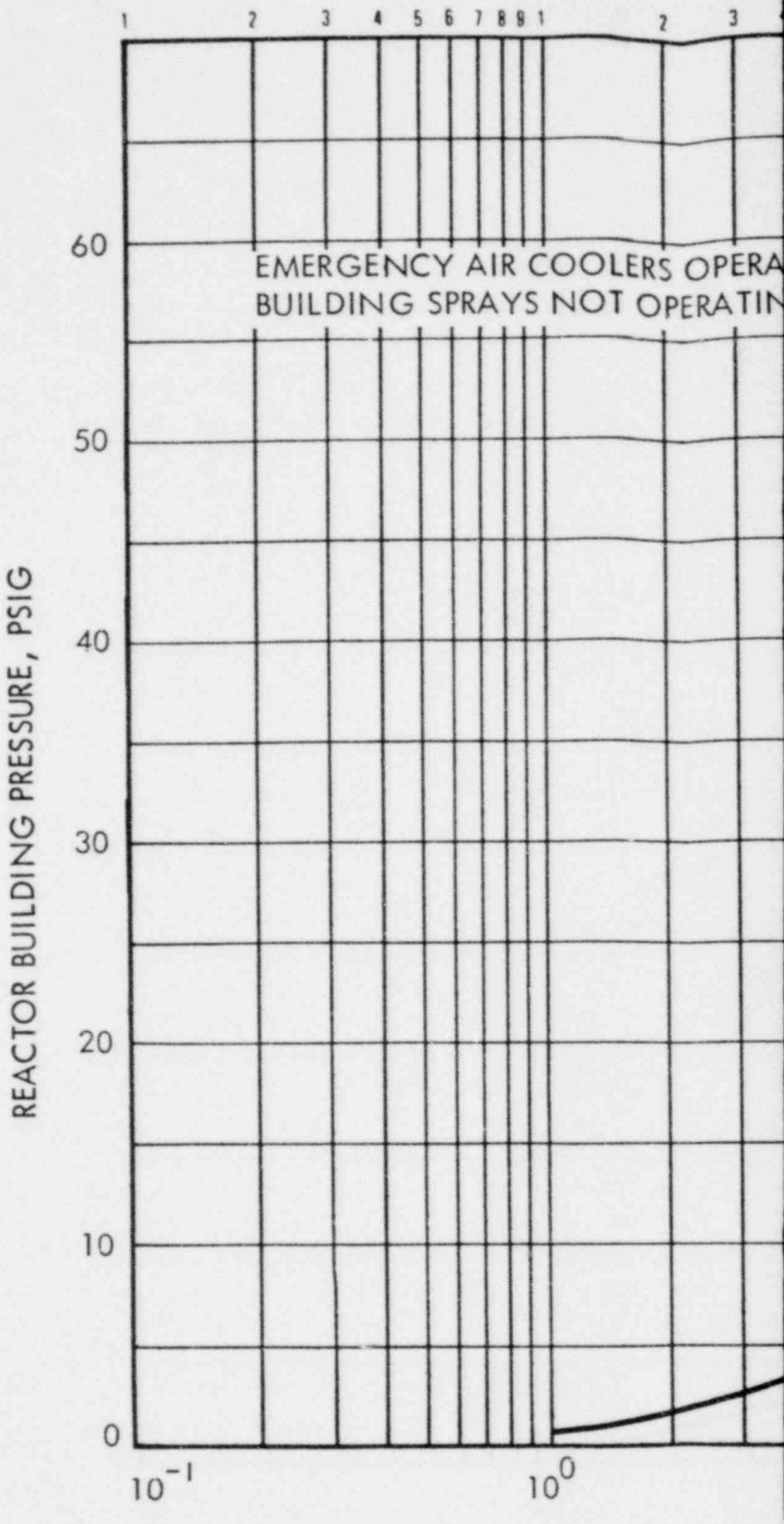
EMERGENCY AIR COOLERS OPERA
BUILDING SPRAYS NOT OPERATIN
REACTOR BUILDING PRESSURE, PSIG
60
50
40
30
20
10
0
10^{-1}
10^{0}

000 0299

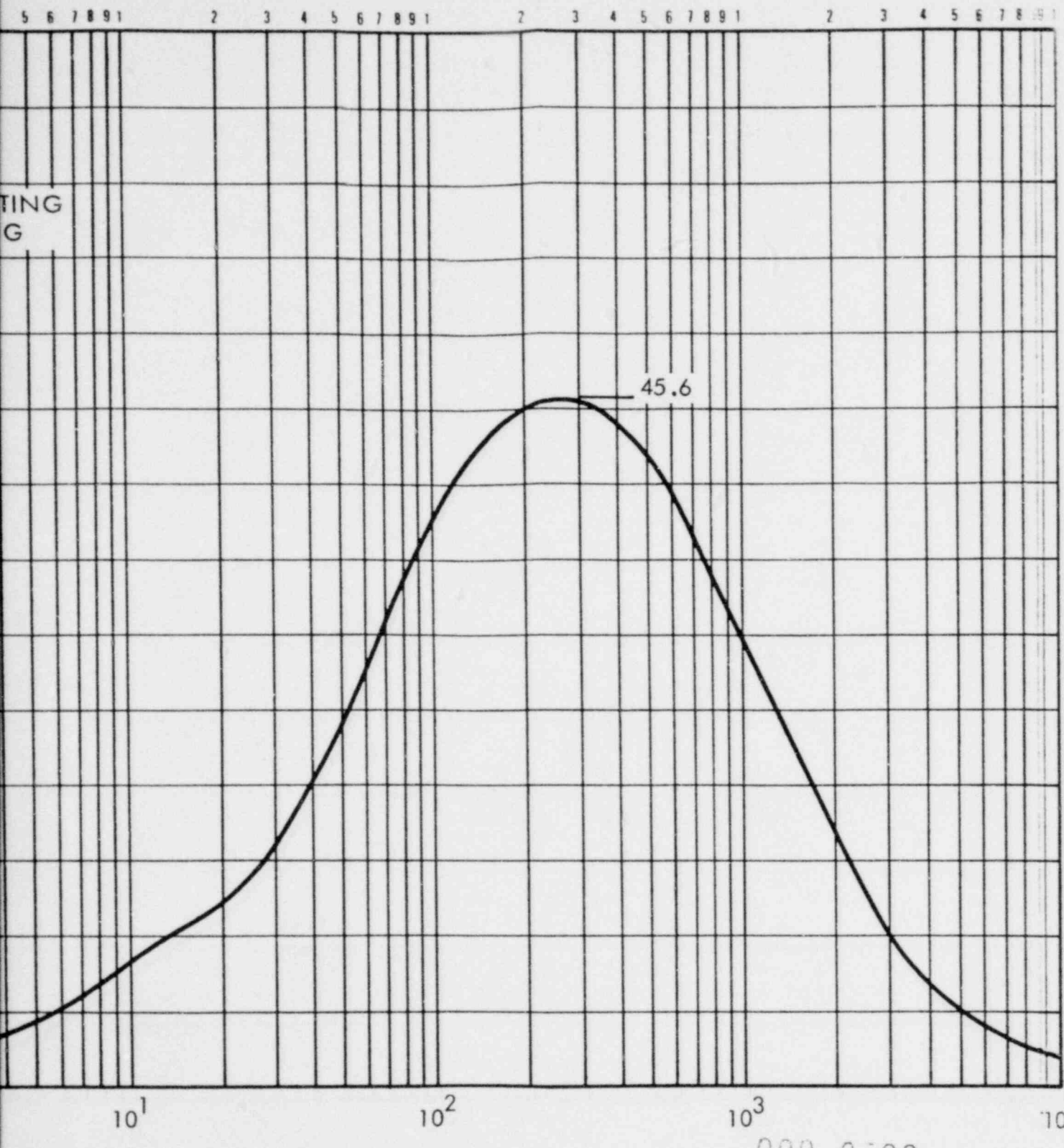

000 0300

FIGURE 14.2-41
REACTOR BUILDING PRESSURE VERSUS
TIME AFTER RUPTURE (0.4 FT^2)

SMUD 00216

SACRAMENTO MUNICIPAL UTILITY DISTRICT

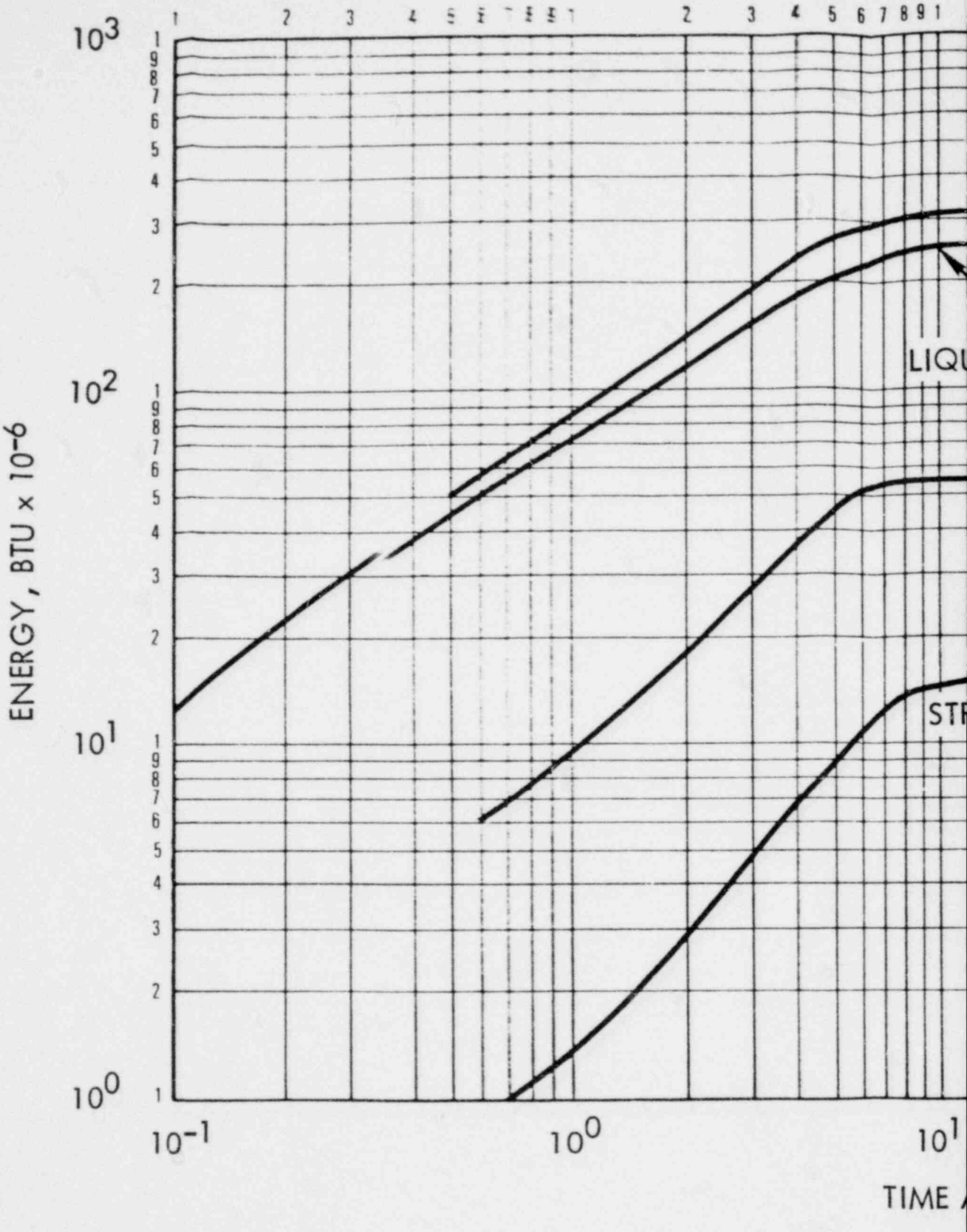

000 0301

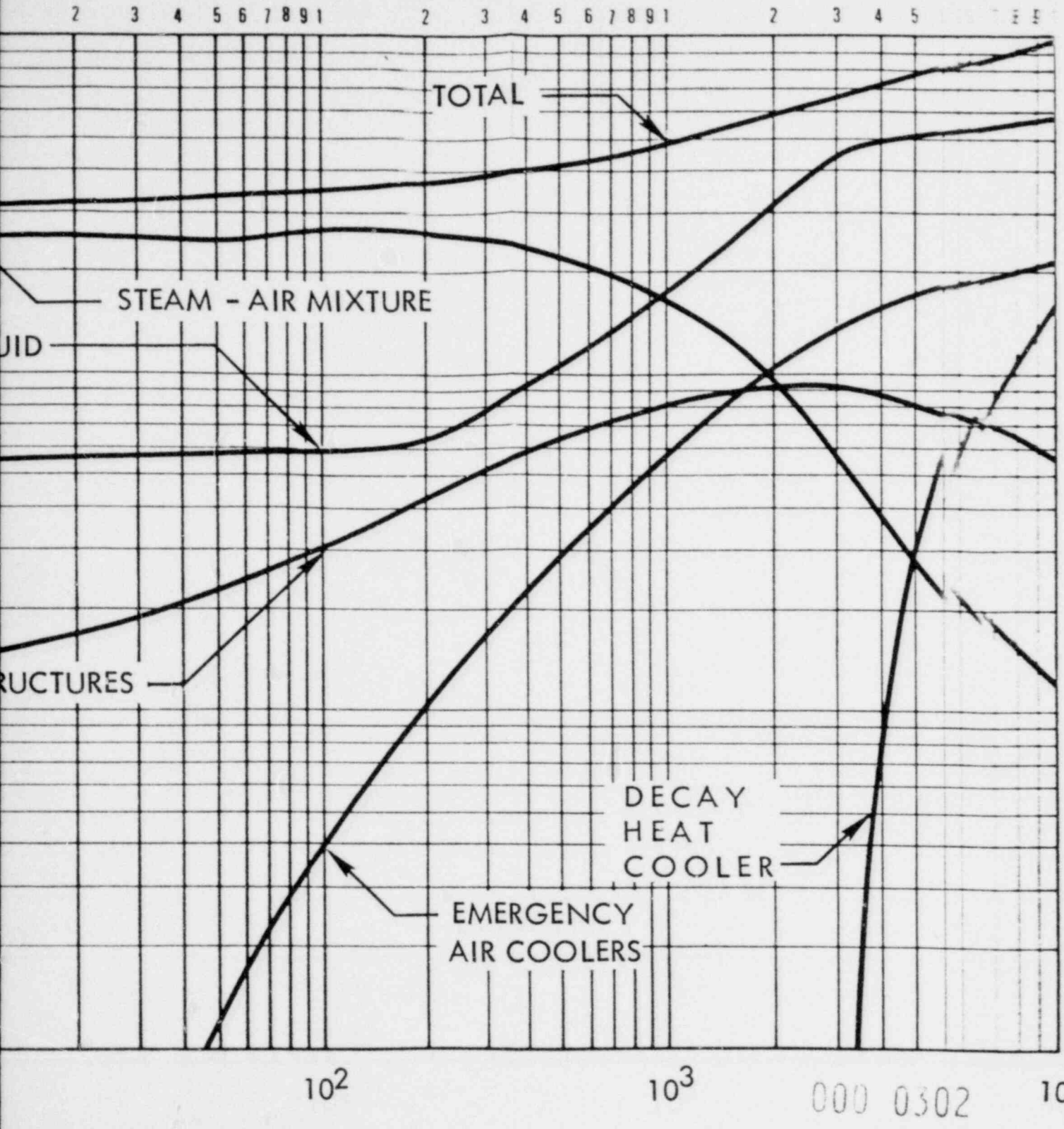

000 0302

FIGURE 14.2-42
REACTOR BUILDING ENERGY INVENTORIES
FOR 14.1 FT^2 HOT-LEG PIPE RUPTURE

SMUD
SACRAMENTO MUNICIPAL UTILITY DISTRICT

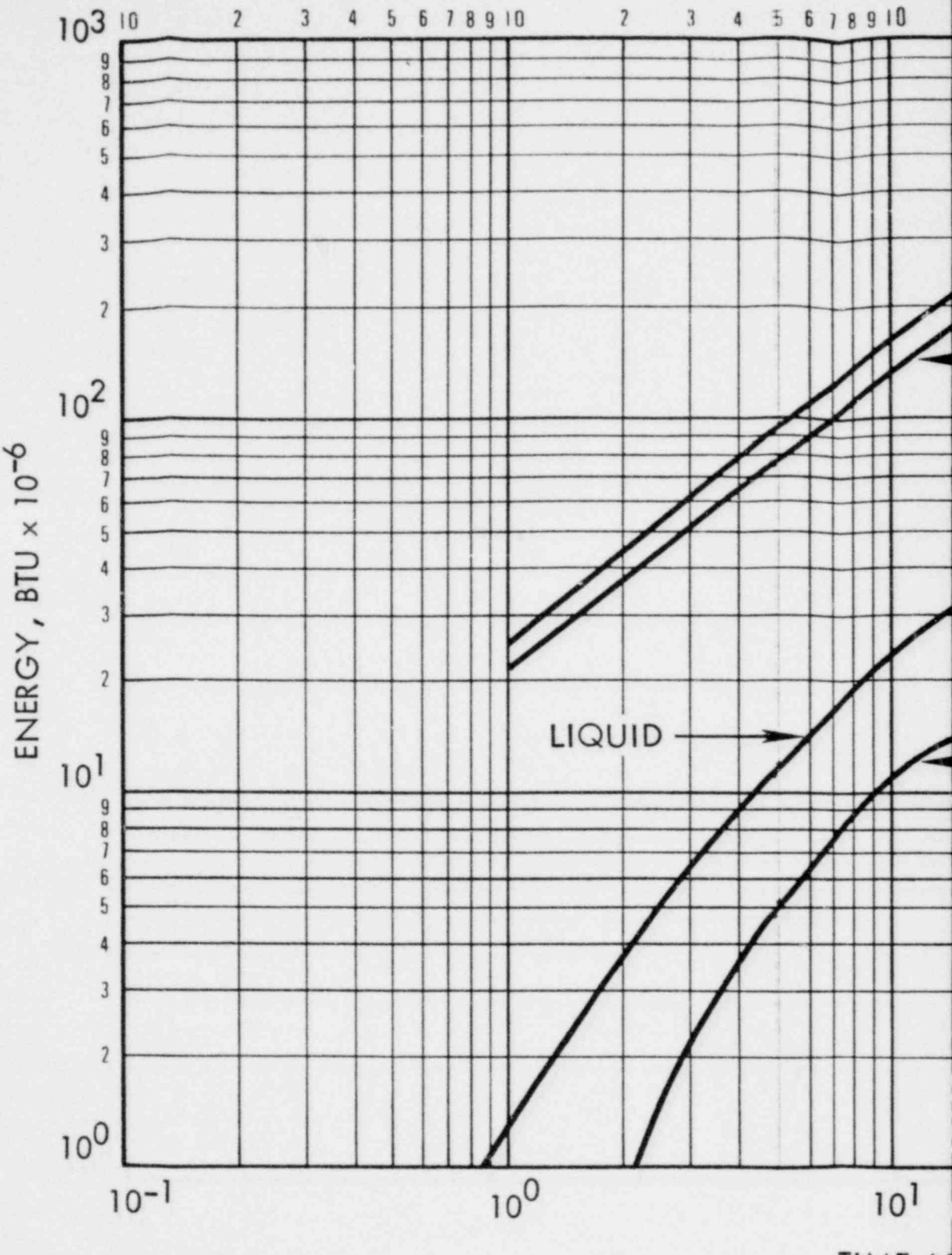

000 0303

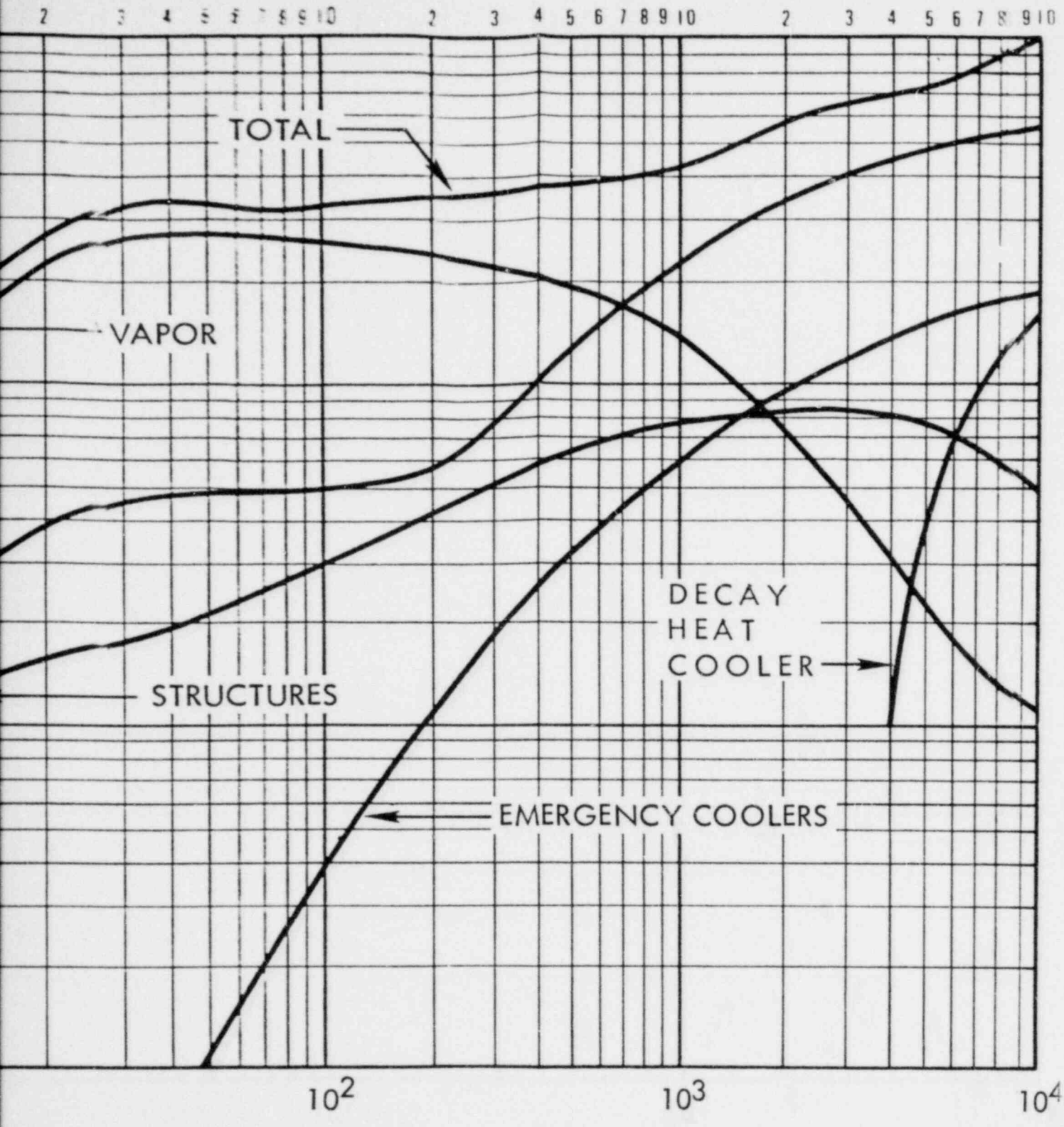

TER RUPTURE, SECONDS

FIGURE 14.2-43 000 0304
REACTOR BUILDING ENERGY FOR
INVENTORY FOR 3.0 FT^2 RUPTURE

SMUD 00
SACRAMENTO MUNICIPAL UTILITY DISTRICT

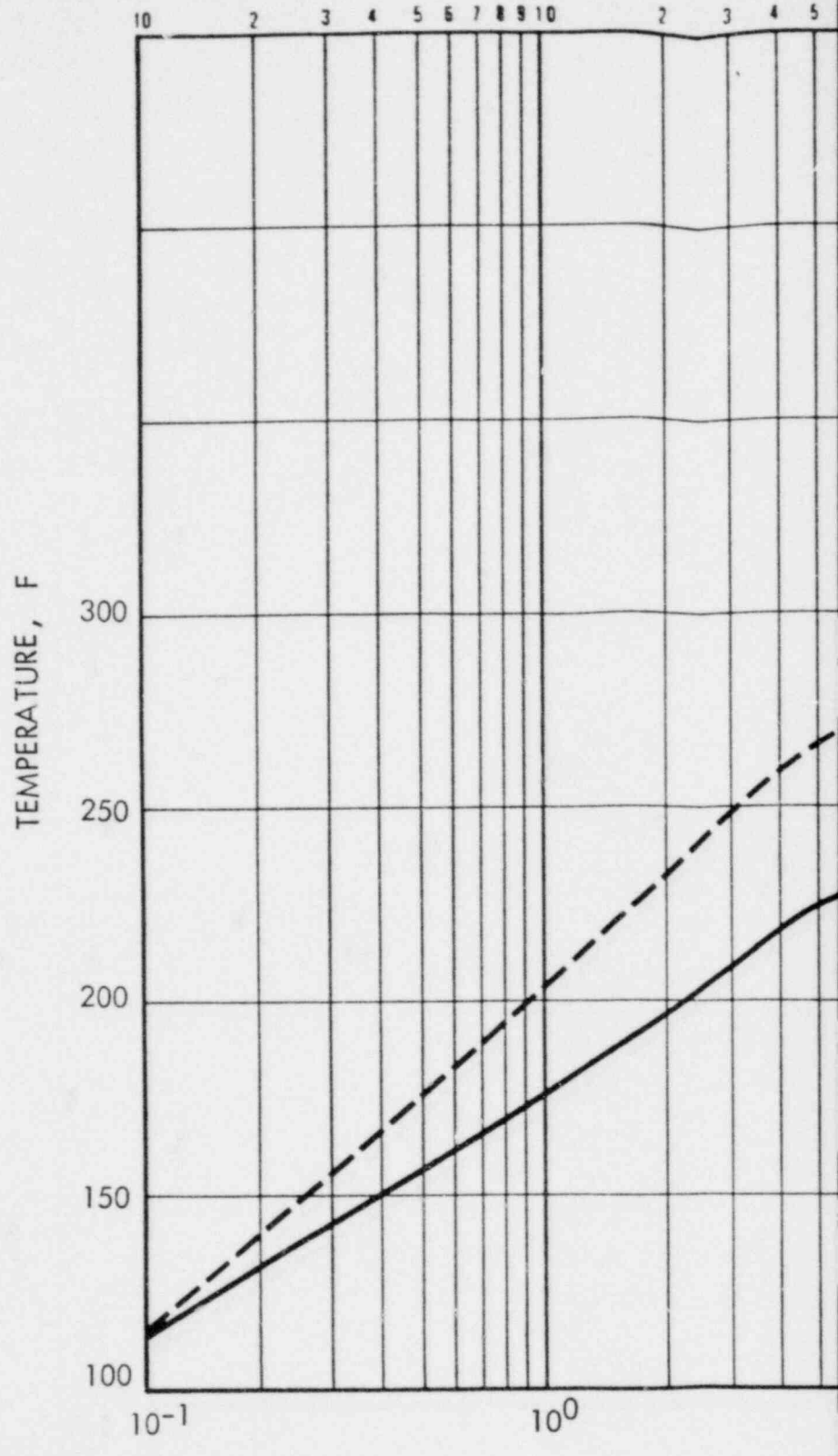

000 0305

00

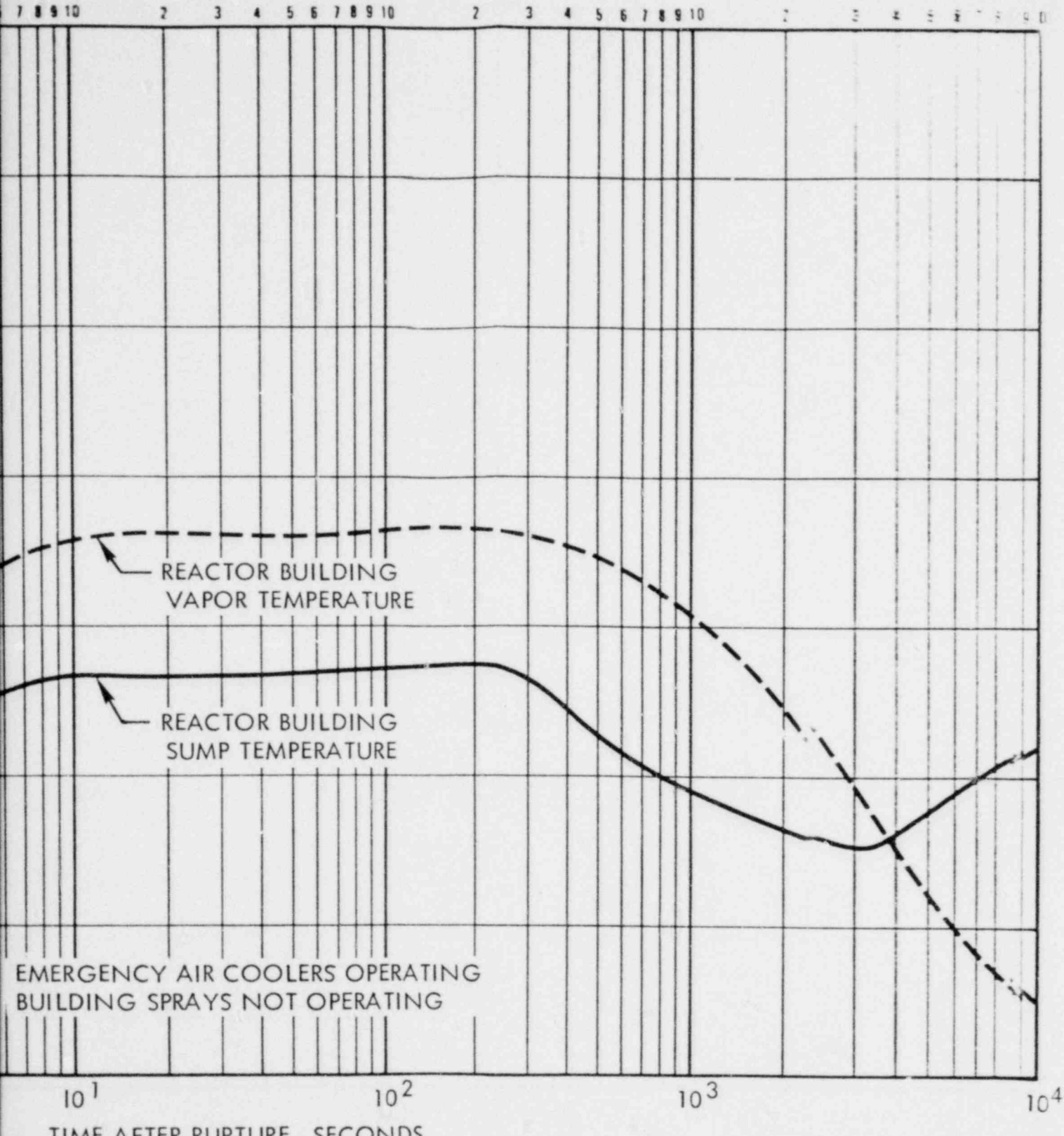

FIGURE 14.2-44
REACTOR BUILDING VAPOR AND SUMP TEMPERATURES VERSUS TIME AFTER A 14.1 FT^2 HOT-LEG PIPE RUPTURE

020 0306

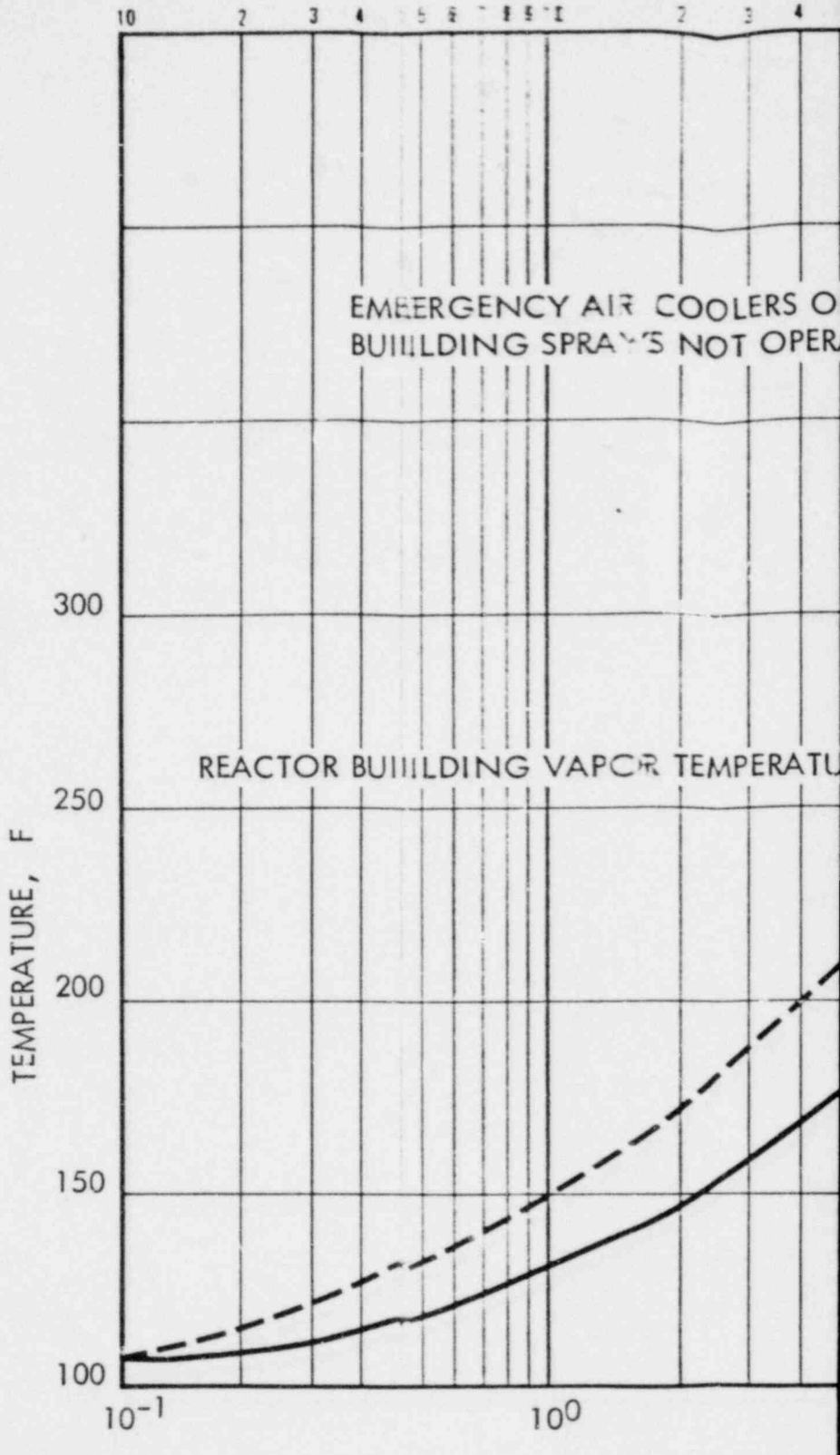
EMEERGENCY AIR COOLERS O
BUIIILDING SPRA'S NOT OPER
REACTOR BUIIILDING VAPOR TEMPERATU
TEMPERATURE, F
300
250
200
150
100
10^{-1}
10^{0}

000 0307

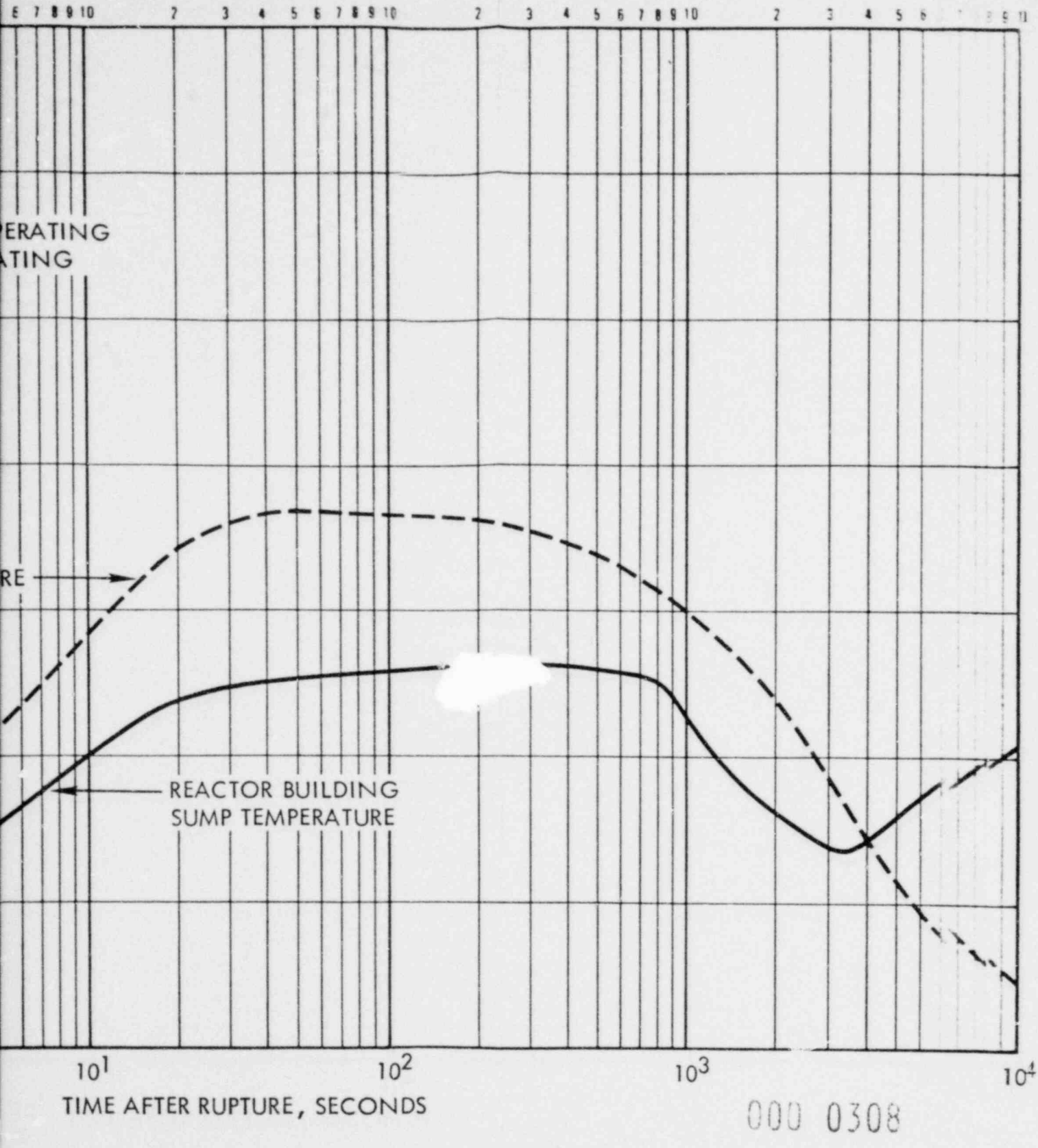

000 0308

FIGURE 14.2-45
REACTOR BUILDING VAPOR AND SUMP
TEMPERATURES VERSUS TIME AFTER
A 3.0 FT^2 RUPTURE

SMUD
SACRAMENTO MUNICIPAL UTILITY DISTRICT

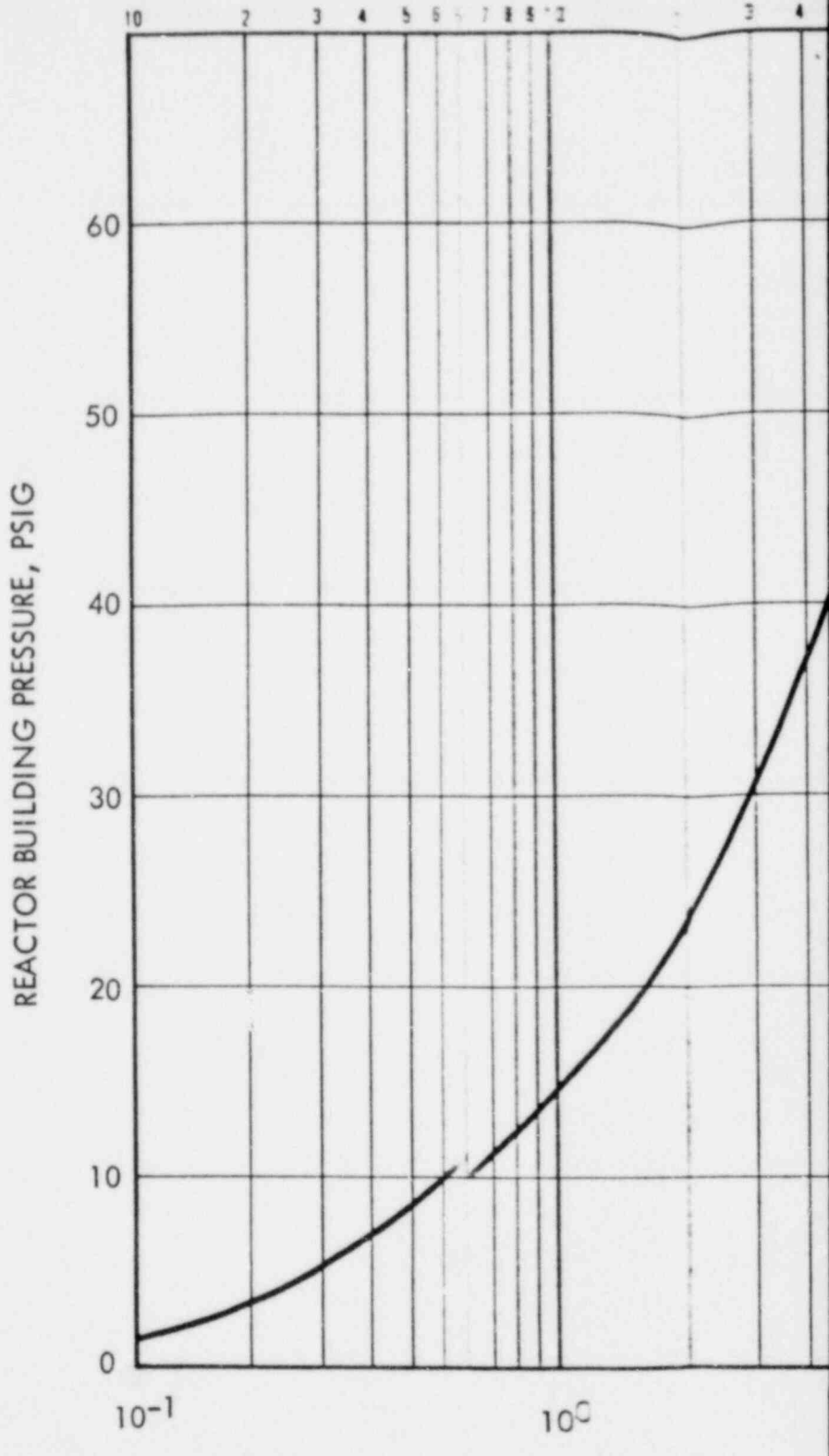

000 0309
0C

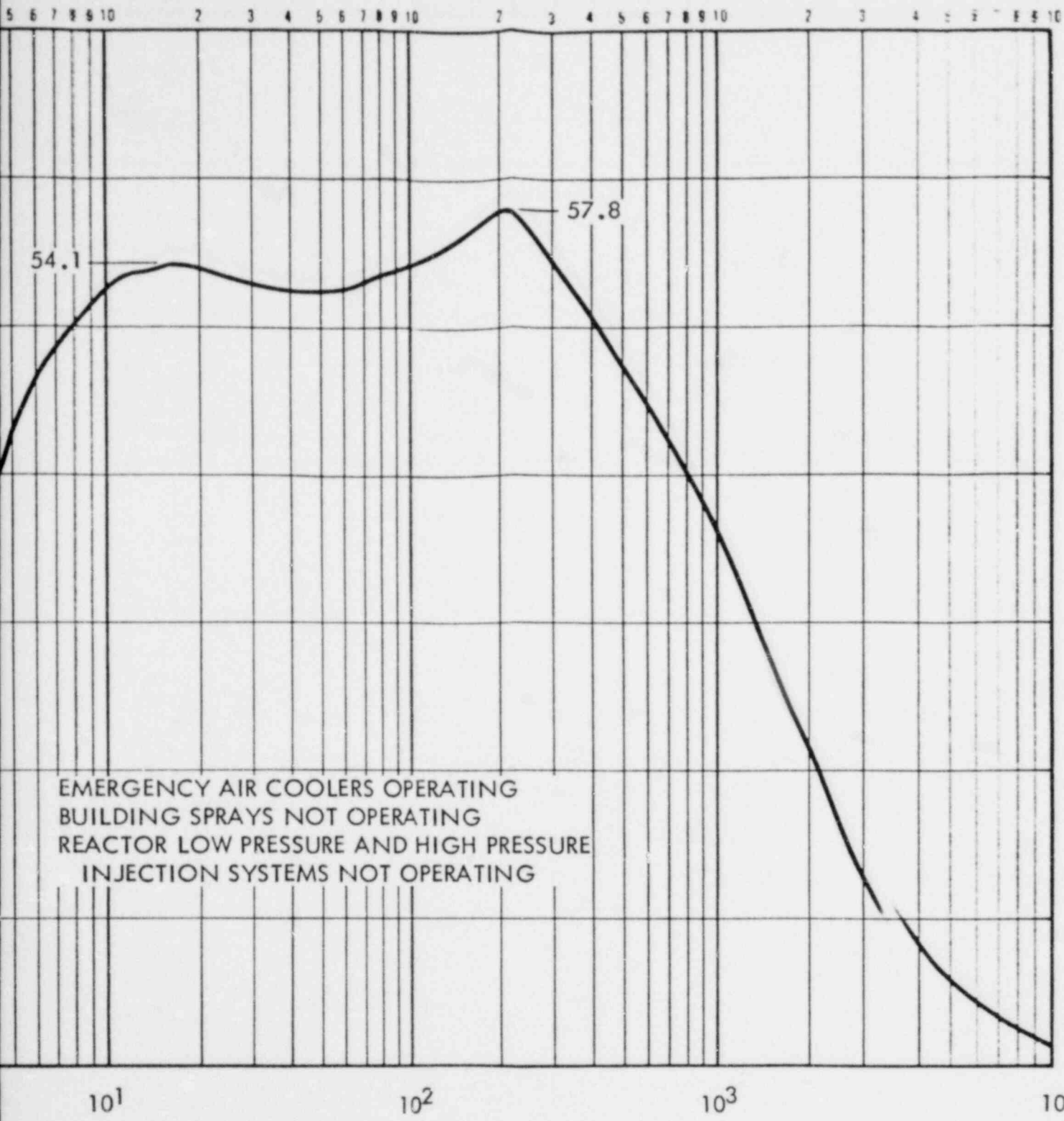

FIGURE 14.2-46
CRITERION 49 FOR A 144.1 FT^2
HOT-LEG PIPE RUPTURE

SMUD
SACRAMENTO MUNICIPAL UTILITY DISTRICT

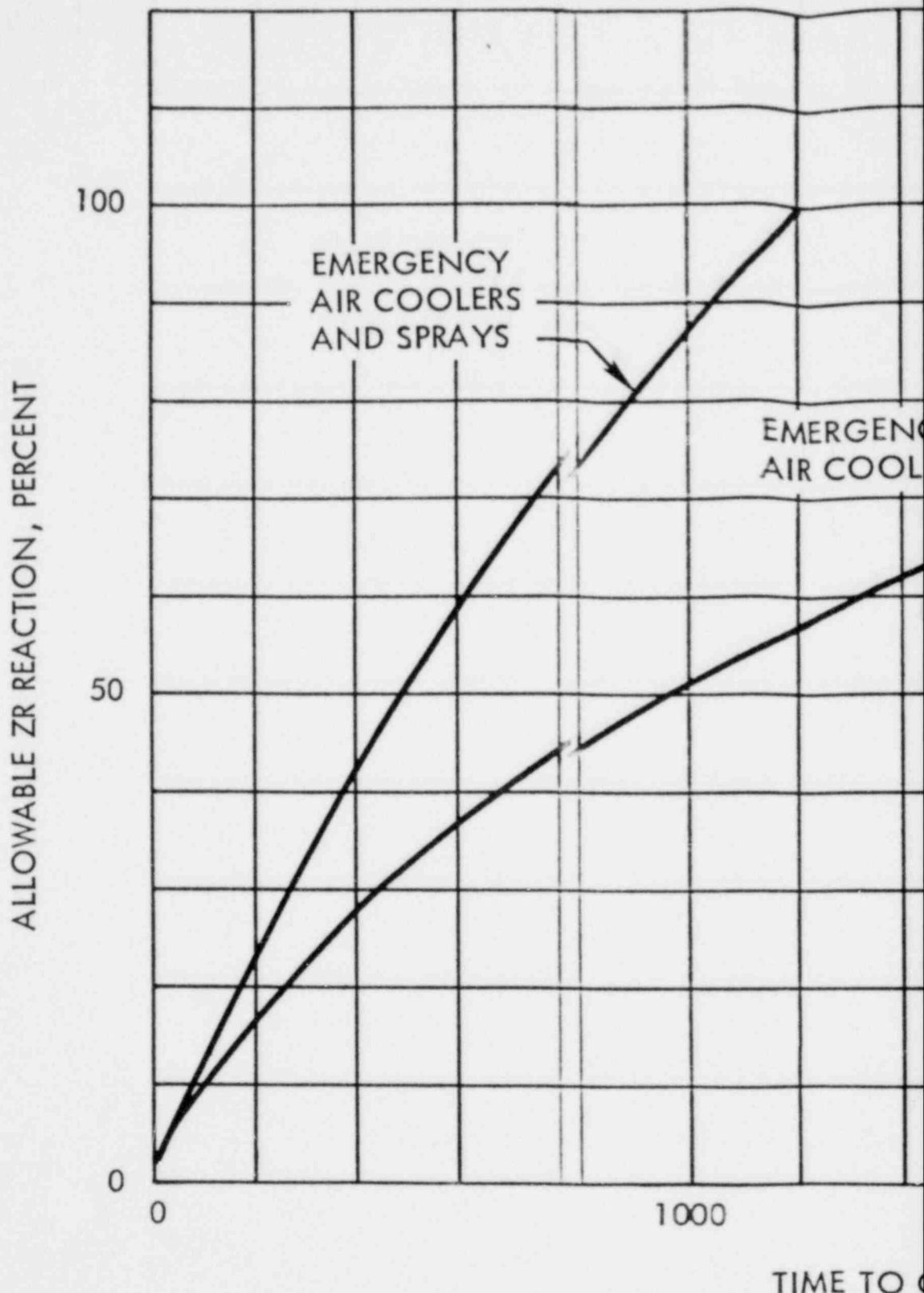
100
50
0
0
1000
ALLOWABLE ZR REACTION, PERCENT
EMERGENCY
AIR COOLERS
AND SPRAYS
EMERGENC
AIR COOL
TIME TO

311
0022B

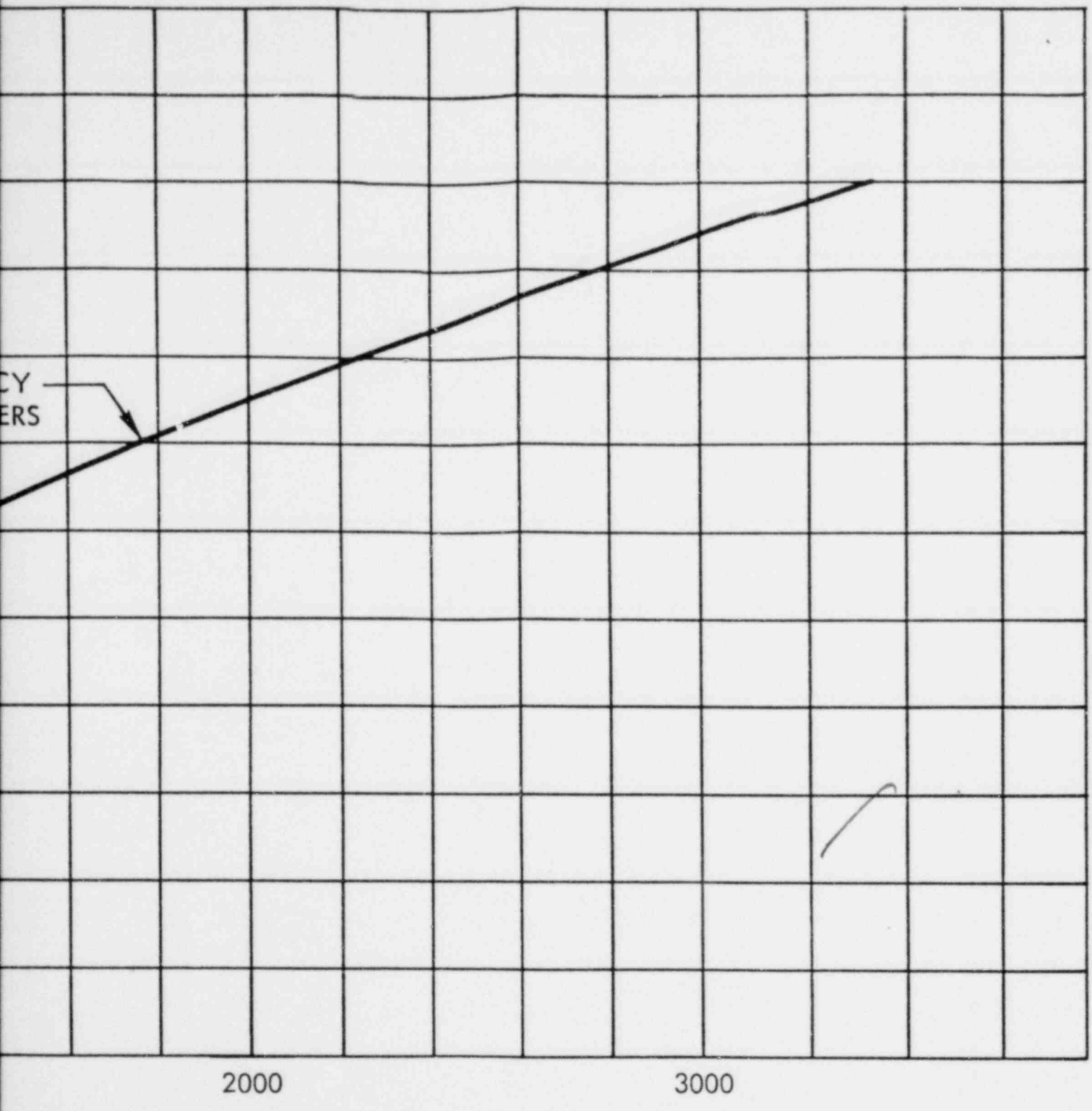

FIGURE 14.2-47
REACTOR BUILDING : ZR REACTION CAPABILITY
FOR 59 PSIG : DESIGN PRESSURE

SMUD
SACRAMENTO MUNICIPAL UTILITY DISTRICT

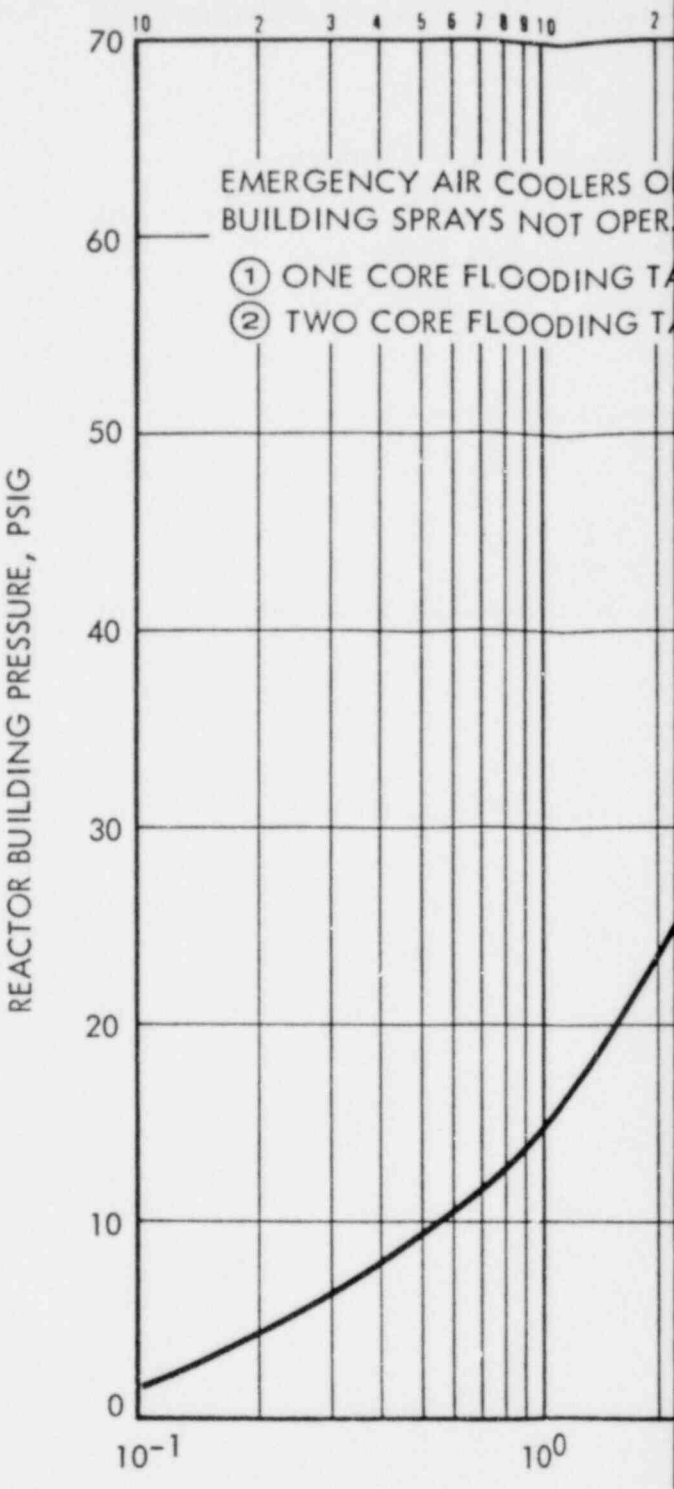
REACTOR BUILDING PRESSURE, PSIG
70
60
50
40
30
20
10
0
10 2 3 4 5 6 7 8 9 10 2
EMERGENCY AIR COOLERS O
BUILDING SPRAYS NOT OPER
① ONE CORE FLOODING TA
② TWO CORE FLOODING TA
10^{-1}
10^{0}

000 0313

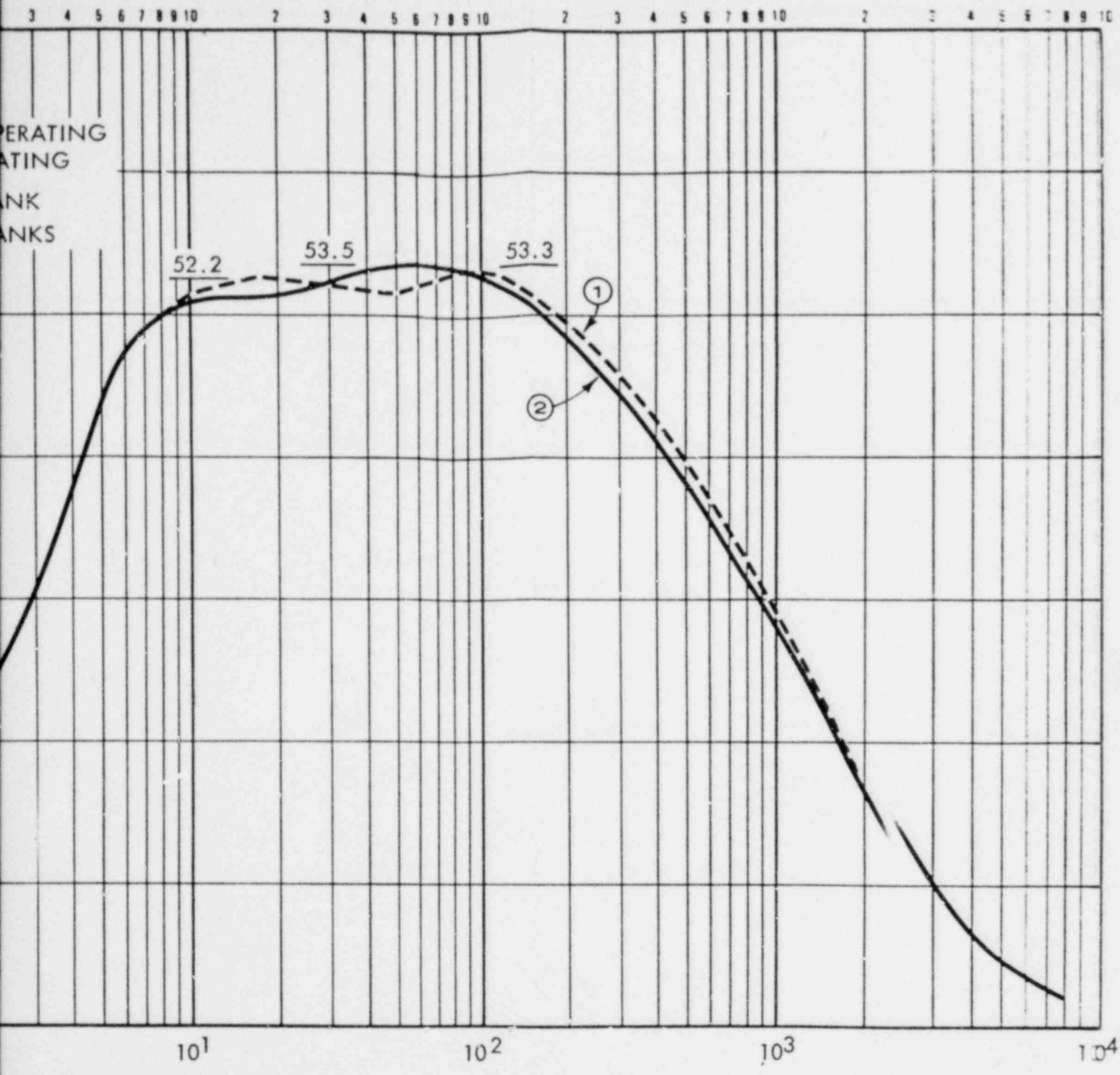

000 0314

FIGURE 14.2-48
REACTOR BUILDING PRESSURE VERSUS TIME AFTER A 14.1 FT^2 HOT LEG PIPE RUPTURE WITH ONE AND TWO CORE FLOODING TANKS OPERATING

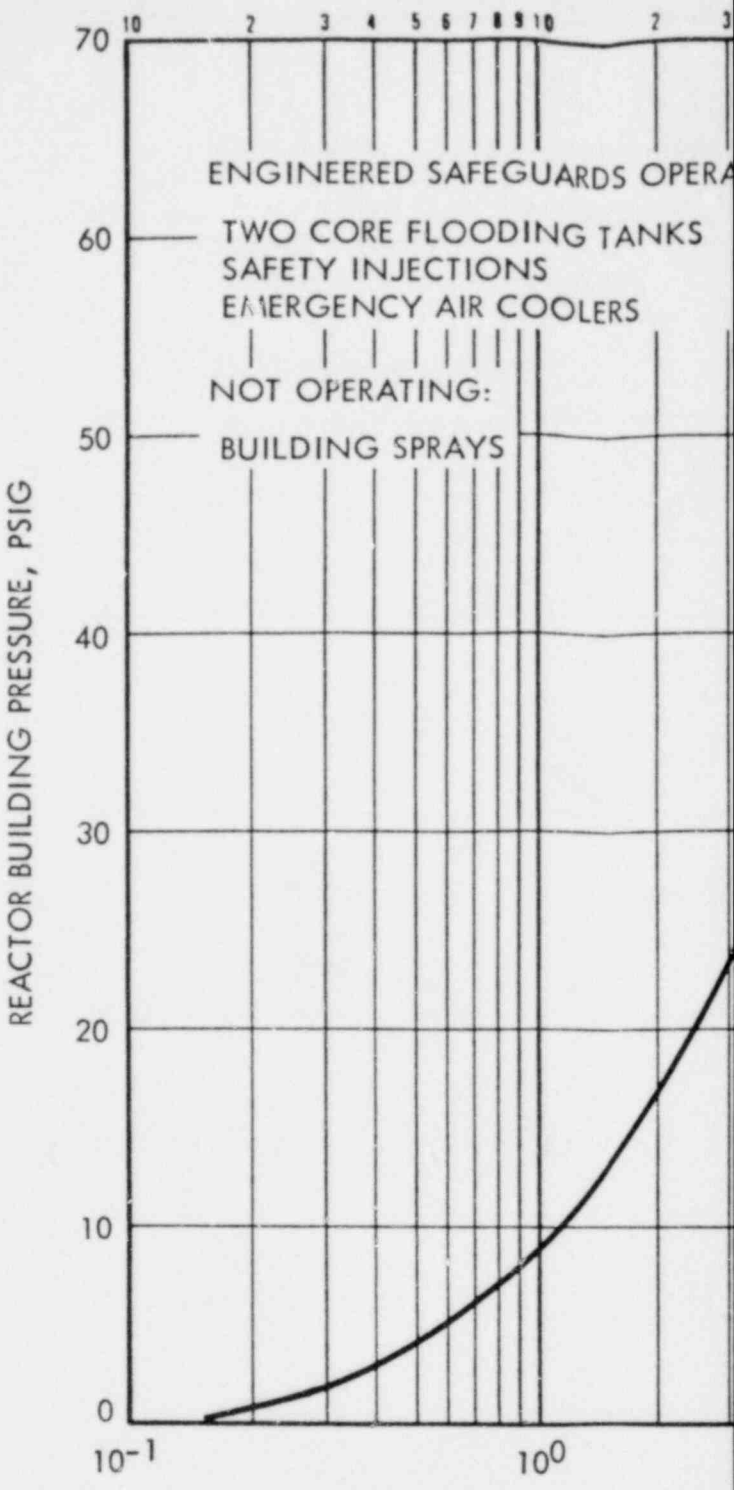
ENGINEERED SAFEGUARDS OPERA
TWO CORE FLOODING TANKS
SAFETY INJECTIONS
EMERGENCY AIR COOLERS
NOT OPERATING:
BUILDING SPRAYS
REACTOR BUILDING PRESSURE, PSIG
70
60
50
40
30
20
10
0
10
2
3
4
5
6
7
8
9
10
2
10^{-1}
10^{0}

000 0515 0

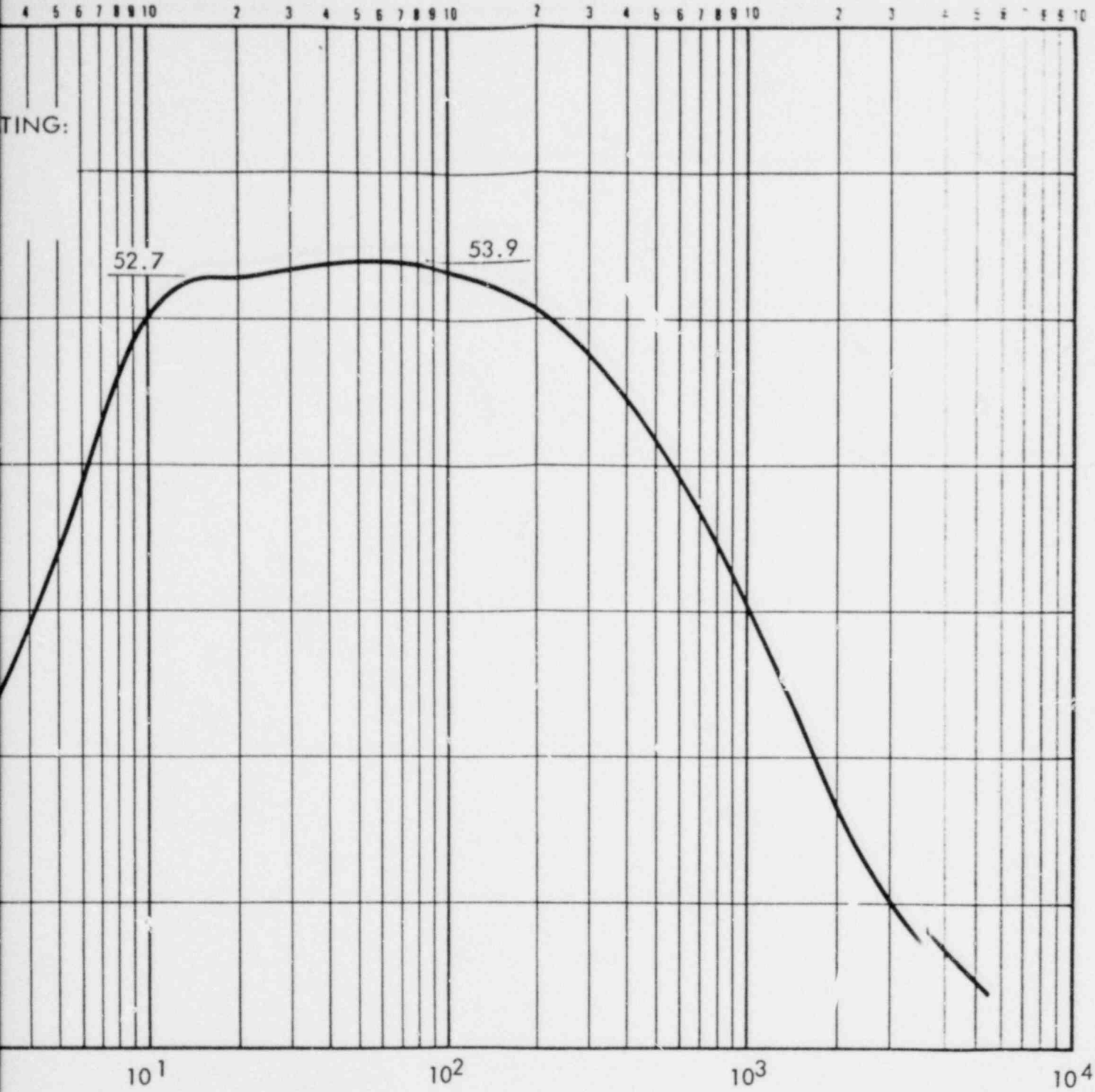

000 0316

FIGURE 14.2-49
REACTOR BUILDING PRESSURE VERSUS
TIME AFTER RUPTURE (8[illegible].5 FT^2)
WITH OPERATION OF CORE FLOODING TANKS

SMUD
SACRAMENTO MUNICIPAL UTILITY DISTRICT

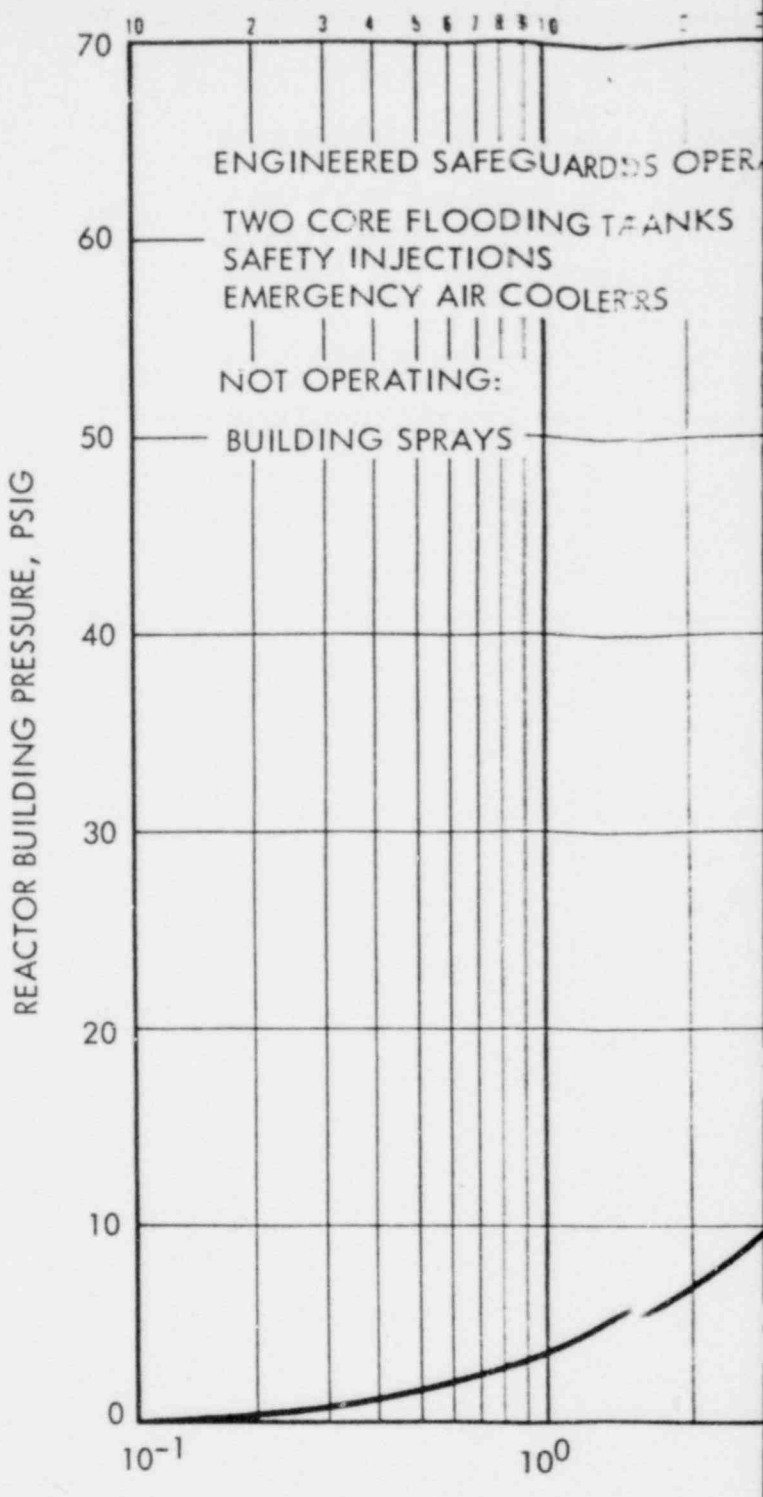
ENGINEERED SAFEGUARDS OPER
TWO CORE FLOODING TANKS
SAFETY INJECTIONS
EMERGENCY AIR COOLERS
NOT OPERATING:
BUILDING SPRAYS
REACTOR BUILDING PRESSURE, PSIG
70
60
50
40
30
20
10
0
10^{-1}
10^{0}

000 0317

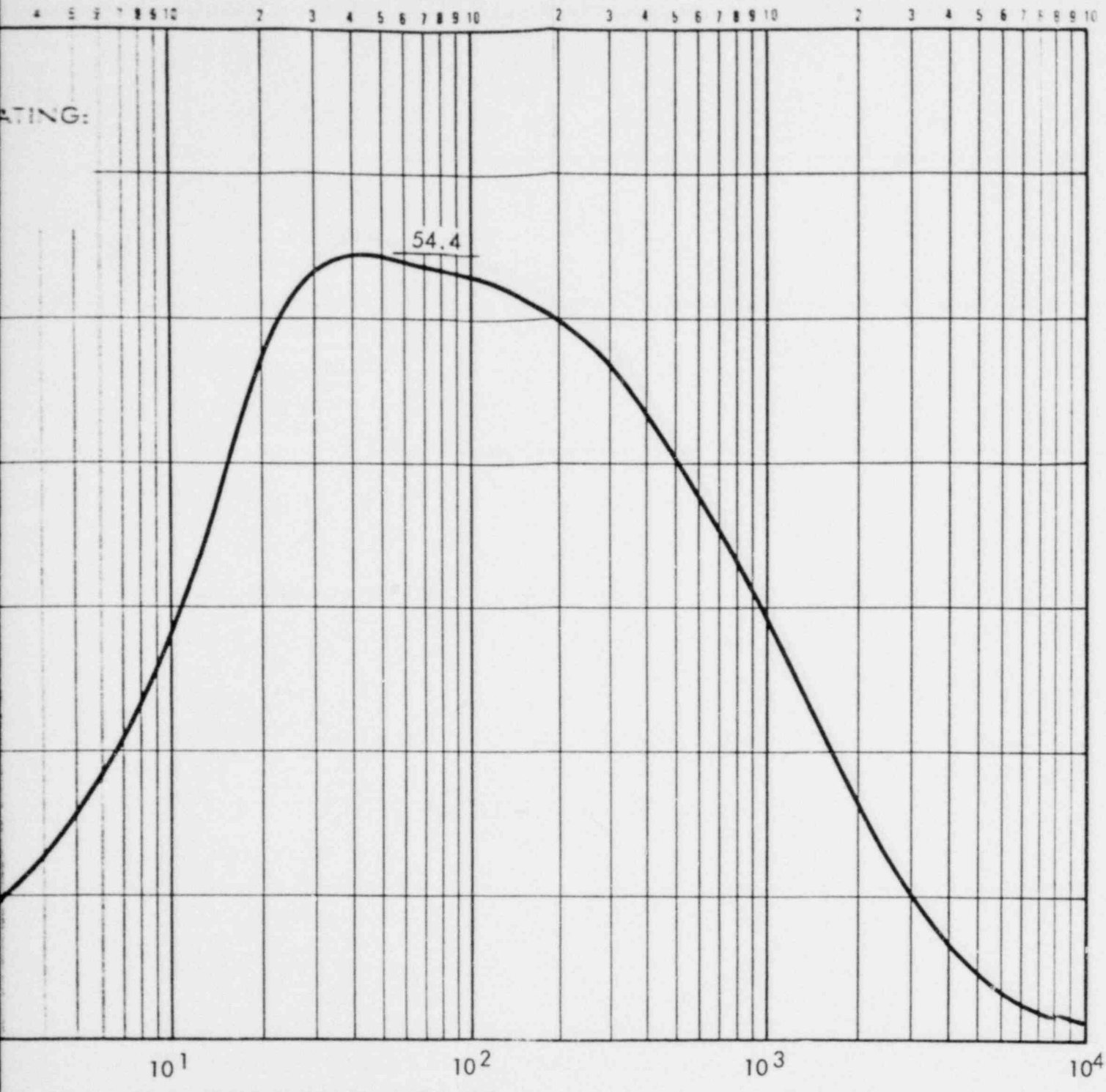

000 0318

FIGURE 14.2-50
REACTOR BUILDING PRESSURE VERSUS
TIME AFTER RUPTURE (3.0 FT^2) WITHH
OPERATION OF CORE FLOODING TANKS

OC

14.3 ENVIRONMENTAL CONSEQUENCES OF HYPOTHETICAL ACCIDENTS

14.3.1 GENERAL APPROACH

The descriptions of various accidents and accident results on plant operations and associated equipment were presented in preceding subsections. The environmental consequences are discussed here in terms of radiation doses to potential receptors. The calculated doses are summarized in Table 14.3-1.

14.3.2 STEAM GENERATOR TUBE FAILURE

This accident is described in 14.1.2.10. Briefly, it postulates that the steam generator tube failure occurs at a time when the reactor is operating with 1 percent failed fuel. The fission product contamination of the primary coolant is continuously removed by the purification system with the exception of fission gases, kryptons and xenons. A total of 1.6×10^8 cubic centimeters of primary coolant is assumed to leak into the secondary coolant. With 1 percent failed fuel, the primary coolant will carry approximately 306.2μ curies of xenon and 22.3μ curies of krypton isotopes per cubic centimeter of coolant. (Table 11.1-3) Consequently, 52,600 curies of noble gases are released into the secondary coolant and through the condenser vents to the atmosphere as indicated in 14.1.2.10. Essentially all iodine is retained in the condensate, only 0.05 curies of I-131 being released through the vents. Assuming conservatively semi-infinite cloud dimensions at the point of reception, a ground level release in the "wake" of the building rather than an elevated release from the vents, a downwind cloud concentration corresponding to the 2-hour dispersion factor listed in 2.3.4, and an average energy of the noble gases in the cloud of 0.4 Mev/dis., the resulting whole-body dose for this accident at the site boundary (0.4 mile) is calculated to be 0.770 rem. At the low population center (city of Lodi, 17 miles from the site) the whole-body dose is 0.016 rem. The thyroid dose is 0.007 rem at the site boundary and less than 1 millirem at the low population center.

14.3.3 LOSS OF ELECTRIC POWER

The description of this accident is in 14.1.3.8. In this accident, a portion of the secondary coolant steam is vented to the condenser through the by-pass valve or to the atmosphere through safety valves. Under normal operation, the secondary loop steam is clean and its venting to the atmosphere will not create any radiological hazard. However, if the loss-of-electric-power accident occurs when the unit is operating with one percent of fuel elements failed, and if simultaneously, a steam generator tube develops a leak, the noble gases in the primary system would escape to the atmosphere. The estimated time of steam relief as described in 14.1.2.8 is 2 minutes, compared to 1.7 hours of venting in the steam generator tube failure accident. Consequently, the whole-body dose at the site boundary from the noble gases released in this accident would be approximately 0.015 rem. The thyroid dose is less than 0.001 rem. Therefore, it is concluded that the loss-of-electric-power accident will not be a hazard to the public even under the most severe assumptions.

000 0319

TABLE 14.3-1
SUMMARY OF MAXIMUM INTEGRATED DOSES IN REMS

Accident	Reference Sections	Integrated Short-Term Exposure at 0.4 Miles		Integrated Short-Term Exposure at 17 Miles	
		Thyroid	Whole Body	Thyroid	Whole Body
Steam Generator Tube Failure	14.3.2	0.007	0.770	Negligible*	0.016
Loss of Electric Power	14.3.3	Negligible	0.015	Negligible	Negligible
Fuel Handling Accident	14.3.5	0.204	0.400	0.004	0.001
Waste Gas Tank Rupture	14.3.7	0	0.308	0	0.007
Steam Line Failure Outside Containment Building	14.3.4	0.306	0.003	0.007	Negligible
		Integrated 2-Hour Exposure at 0.4 Miles		Integrated 30-Day Exposure at 17 Miles	
Steam Line Failure within Containment Building	14.3.4	Negligible	Negligible	Negligible	Negligible
Rod Ejection Accident	14.3.6	0.040	0.002	0.001	Negligible
Loss-of-Coolant Accident	14.3.8	0.730	0.061	0.026	Negligible
Maximum Hypothetical Accident	14.3.9	12.3	1.0	0.420	0.007

*Describes an integrated dose less than 1 millirem

000 320

00

14.3.4 STEAM LINE FAILURE

The steam line failure accident is reported in 14.1.2.9. This accident can be postulated to occur inside or outside the containment building. A steam line failure within the containment building is evaluated first. Under normal operating conditions, there would be no radioactivity in the secondary loop. However, to evaluate environmental consequences of this accident, it is assumed that, at the time of the accident, the unit operated with 1 percent failed fuel and with a simultaneous steam generator tube leakage allowing the fission products from the primary loop to enter the secondary coolant system. As in the previously discussed accidents, the secondary loop contamination is principally through the noble gases which are not removed in the ion exchangers of the primary coolant purification system.

The estimated steam generator tube leakage for this accident is 6.81×10^5 cubic centimeters over a 3 hour period.

Since the noble gases activity of the primary coolant resulting from 1% of failed fuel elements is 328.5 μcuries/cc (Table 11.1-3), the total activity released to the contaiment is 224 curies. Similarly, the amount of curie-equivalents of I^{131} released is 4.22 curies. Assuming a containment leakage rate of 0.1 percent per day at the containment pressure of 10 psig, both the whole-body and the thyroid 2-hour doses at the site boundary are less than 1 millirem.

Using the above assumptions for a postulated steam line failure outside the containment building, the downwind doses will result from an essentially instantaneous and uncontained release. The calculated doses for this accident are 0.306 rem to the thyroid and 0.003 rem whole-body cloud dose at the site boundary. The thyroid dose at the low population center is 0.007 rem and the whole-body dose is less than 1 millirem.

Calculations were also carried out for primary coolant releases other than 6.81×10^5 cm (180 gal.). Figure 14.3-7 indicates that the thyroid dose at the site boundary as a function of the percent of the primary coolant release, always assuming an instantaneous escape to the atmosphere of all iodine present in the released fraction of the primary coolant. A 50% and 100% instantaneous release of primary coolant to the atmosphere would result in thyroid doses at the site boundary of approximately 55 and 110 rem respectively. 1

The above discussion should not be construed that 50% and 100% releases of primary coolant to the atmosphere are regarded as credible or that a mechanism for such a release exists. The inclusion of Figure 14.3-7 is only for the purpose of demonstrating that even under such extreme assumptions of releases of primary coolant to the atmosphere, the thyroid doses at the site boundary will not exceed 10 CFR 100 guideline values of 300 rem.

000 0321

14.3.5 FUEL HANDLING ACCIDENT

The fuel handling accident is postulated for the auxiliary building and is described in 14.2.2.1. In this accident, 28.4 curies of iodine and 2.79 x 10^4 curies of noble gases are released to the building from 56 ruptured fuel pins. The building is continuously ventilated through high efficiency and charcoal filters which will retain the particulate fission products and 90 percent of iodine. It is conservatively assumed that in this accident, the 2.79 x 10^4 curies of noble gases and 2.84 curies of iodine are released at ground level in the "wake" of the building rather than from the elevated vents. 3

The whole-body dose at the site boundary calculated for a semi-infinite cloud geometry is 0.400 rem. The thyroid dose at the site boundary is 0.204 rem. The thyroid dose is directly proportional to the amount of iodine released. Therefore, if all 28.4 curies of iodine are released to the atmosphere (no credit for filter-removal of iodine), the thyroid dose would then increase by a factor of 10 to 4.00 rem. Even this higher number is still well below the AEC guideline values for the emergency thyroid dose of 300 rem.

14.3.6 ROD EJECTION ACCIDENT

The rod ejection accident is discussed in 14.2.2.2. The rod ejection damages the rod housing creating an equivalent opening of 0.04 ft^2 through which the reactor coolant escapes into the containment. It is assumed that the power excursion resulting from the rod ejection accident damages fuel rods, releasing 166,000 curies of I^{131} and 1.45 x 10^6 curies of noble gases to the containment building. The environmental consequences evaluation assumes that the sodium thiosulfate sprays iodine removal time constant of 25 hr^{-1} applies. The evaluation further assumes that the containment building leakage will remain 0.1 percent of the containment volume per day without any reduction for 30 days.

Based on these conservative assumptions, the 2-hour dose at the site boundary is 0.074 rem. The 30-day thyroid dose at the low population center (17 miles) is 0.001 rem. The 2-hour whole-body dose at the site boundary is 0.002 rem. The 30-day whole-body dose at the low population center is negligible.

It may be noted that if no credit for iodine removal is taken, the doses will increase by a factor of approximately 20 but will be still well below the AEC guideline values.

14.3.7 WASTE GAS TANK RUPTURE

The possibility of releasing significant amounts of gaseous activity to the atmosphere from the gaseous waste disposal system is remote. However, to evaluate upper limits on environmental consequences in case of such an accident, it is assumed that the waste gas tank ruptures releasing its contents to the auxiliary building and through the vents to the atmosphere.

000 0324

00L

The maximum activity in a waste gas decay tank will occur following a boron dilution cycle during reactor startup just prior to switching to the deborating demineralizer for boron removal. The reactor coolant water activity used for the analysis assumes prior operation for an extended period with 1 percent of failed fuel rods. Approximately 72,000 gallons of reactor coolant would be let down at this time. Since the purification demineralizers will remove the particulate fission products and iodine only, noble gases will be present in the primary coolant. The gaseous activity will be carried with the water to the reactor coolant flash tank, where it is assumed that the gases are immediately released from the water and carried with the purge gases to the waste gas decay tank. It is conservatively assumed that the gases do not undergo radioactive decay after leaving the reactor coolant system whereas normally they would be subjected to a 30-day decay time in the waste gas decay tanks. With these assumptions, the following activity is calculated to exist in the waste gas decay tank:

Isotope	Total Curies
Kr 85m	544.0
Kr 85	4,200.0
Kr 87	300.0
Kr 88	1,000.0
Xe 131m	570.0
Xe 133m	870.0
Xe 133	79,000.0
Xe 135m	272.0
Xe 135	2,550.0
Xe 138	136.0

The auxiliary building is ventilated and activity which is released to the building will be eventually vented to the atmosphere. To evaluate this accident, it is assumed that the activity is released instantaneously in the wake of the building rather than at a relatively slow rate through elevated venting. Assuming the 2-hour atmosphere dilution values developed in 2.3.3 and semi-infinite cloud geometry, the whole-body 2-hour gamma dose at the site boundary is 0.308 rem. Using the 2-hour dispersion factor, the whole-body dose at the low population center is 0.007 rem.

14.3.8 LOSS-OF-COOLANT ACCIDENT

14.3.8.1 Environmental Consequences

The loss-of-coolant accident is described in 14.2.2.3. The safety analysis for the loss-of-coolant accident considers the release of radioactivity in the coolant based on 1 percent failed fuel rods plus the fuel rod gap activity as indicated in section 14.2.2.3. Other parameters, such as fission product inventory, iodine plate out, reactor building iodine spray removal, reactor building leak rate, dilution multipliers, etc., are the same as those used in the analysis for the maximum hypothetical accident as described in 14.3.9 which follows.

000 0323 00

For the loss-of-coolant accident, coolant activity is negligible compared to the gap activity. Thus, the gap activity governs the doses. Figure 14.3-1 shows the thyroid dose as a function of distance for 2-hour, 24-hour and 30-day exposures due to the loss-of-coolant accident. The 2-hour dose at the site boundary exclusion distance is 0.73 rem, which is well below the 10-CFR-100 limit.

The 2-hour whole-body immersion dose from the plume at the site boundary is 0.061 rem. The direct dose from the reactor building at the site boundary is 0.001 rem for a 2-hour exposure. These doses are several orders of magnitude below the 10-CFR-100 limit.

14.3.8.2 Effects of Reactor Building Purging

At times during the normal operation of the reactor, it may be desirable to purge the reactor building while the reactor is operating. In the event of a loss-of-coolant accident during purging operations, some activity would be released to the environment. The purge valves will be completely closed in 5 sec. During this time, assuming a 36-in. ID, double-ended rupture, essentially all of the reactor coolant will have been blown down. The activity in the reactor building is due to the reactor coolant activity after operation with 1 percent failed fuel. For this case, approximately 1/400 of the reactor building atmosphere will escape through the purge valves before they close, corresponding to a release of 3 curie-equivalents of iodine-131. This analysis assumes unrestricted flow through the purge line for the full 5-second closing time. No reduction in flow is assumed as the valve closes, and therefore the results are conservative. The release of this iodine results in a total integrated thyroid dose of 0.216 rem at the exclusion distance. This dose, when added to the thyroid dose for a loss-of-coolant accident without purging, is well below the 10-CFR-100 guidelines.

14.3.9 MAXIMUM HYPOTHETICAL ACCIDENT

14.3.9.1 The Source Term

The maximum hypothetical accident is described in 14.2.2.4. The environmental consequences from this accident are analyzed on the method and assumptions given in TID-14844. The inventory of fission products in the core and the release of fission products from the core are as stated in TID-14844.

Of the total core inventory, 100 percent of the noble gases, 50 percent of the halogens, and 1 percent of the solids are assumed to be released into the reactor building. Half of the iodines released are assumed to plate out to exposed surfaces in the reactor building. The other 50 percent of the released iodine is assumed to be airborne on the reactor building and available for leakage. Reactor building spray is utilized to further reduce the airborne iodines. A spray removal coefficient of 25 hr^{-1} is used to evaluate iodine washdown. It is conservatively assumed that when the airborne iodine concentration is reduced to 5 percent of the initial

000 0524

concentration, no further credit for spray is taken. This corresponds to 1.25 percent of the iodine core inventory. A sensitivity analysis of the iodine spray removal was made and is presented in 14.3.10.

The reactor building leakage rate is assumed constant at 0.1 percent per day for the duration of the accident. This is another conservative factor since the leakage is a function of pressure differential and the pressure in the containment will be brought down to approximately 5.5 psig in about 2 hours.

14.3.9.2 Thyroid Dose

In determining the dose to the thyroid, a breathing rate of 3.47×10^{-4} m^3/sec is assumed for the 2-hour exposure dose. For the 24-hour dose, the breathing rate is the rate suggested in TID-14844 of 3.47×10^{-4} m^3/sec for the first 8 hours and 2.32×10^{-4} m^3/sec for periods longer than 24 hours. For the time interval between the 8th and 24th hour after the accident, a weighted average breathing rate of 1.74×10^{-4} m^3/sec was assumed.

The dose to the thyroid for the 24-hour exposure is assumed to be the sum of the initial 2-hour dose which is based on the 2-hour dilution multiplier and a 22-hour incremental dose which is based on the 24-hour dilution multiplier. Similarly, the 30-day dose to the thyroid is assumed to be the sum of the 24-hour dose and a 29-day incremental dose which is based on the 30-day dilution multiplier. This method results in higher thyroid doses for the 24-hour and 30-day exposures than would be obtained by using the 24-hour and 30-day dilution multipliers respectively for the entire 24-hour and 30-day periods. The dilution multipliers for 2-hour, 24-hours, and 30-day periods are presented in 2.3.

Figure 14.3-2 presents the thyroid dose as a function of distance from the reactor building for 2-hour, 24-hour, and 30-day exposures. The results show that the 2-hour thyroid dose at the site boundary exclusion distance (2100 feet or approximately 0.4 mile) is 12.3 rem and at the low population center for a 30-day exposure is 0.420 rem. If no credit for iodine removal by sprays is taken, these doses will increase by a factor of 20, but still will be less than the 10-CFR-100 guideline values.

14.3.9.3 Direct Dose from Containment Building

The direct gamma dose at various distances from the reactor building due to fission products contained in the building is shown in Figure 14.3-3 for 2-hour and 30-day exposures. The source intensity in the reactor building as a function of time after the accident is based on radiological decay only, with no credit taken for leakage, filtration, or washdown. The direct 2-hour and 30-day whole-body doses at the site boundary were calculated using the GRACE II computer code[19] based on a uniform cylindrical source and 3.5 feet of concrete shielding and are 0.4 and 0.9 millirem, respectively. The sky-shine dose is negligible due to the 3.5-foot thick concrete walls of the containment building.

000 0325 00

14.3.9.4 Whole-Body Dose From the Cloud

The whole-body dose due to immersion in the leakage plume (Figure 14.3-4) is 1.00 rem for a 2-hour exposure at the exclusion distance. The whole-body dose from a 30-day exposure at the low population center is 0.007 rem. This result is for a receptor point located in a simi-infinite cloud geometry. The source intensity is based on a 0.1 percent per day leakage rate of available noble gases and iodines as stated in Section 3.9.1.

14.3.9.5 Effects of Radiation Source From Pump Leakage During the Maximum Hypothetical Accident

An additional source of fission product leakage during the maximum hypothetical accident can occur from leakage of the engineered safeguards equipment external to the reactor building during the recirculation phase for long-term core cooling. A detailed analysis of the potential leakage from these systems is presented in 6.3. That analysis demonstrated that the maximum leakage is about 5,000 cc/hr.

It is assumed that the water being recirculated from the reactor building sump through the external system piping contains 50 percent of the core saturation iodine inventory. This is the entire amount of iodine release from the reactor cooling system. The assumption that all the iodine escaping from the reactor coolant system is absorbed by the water in the reactor building is conservative since much of the iodine released from the fuel will be plated out on the building walls. The activity in the recirculation water is equal to 0.037 equivalent curies of I-131 per cc of water. Since the temperature of water in the reactor building sump will not reach boiling when recirculation occurs, the iodine release is calculated using a gas/liquid partition coefficient of 9×10^{-3}.

Leakage from the auxiliary building is caused by exfiltration. It is assumed that the building leaks at the rate of 100 percent per day with atmospheric dilution occurring in the wake of the building. For this building leak rate and the inversion condition, the iodine will produce an integrated dose to the thyroid of 0.020 rem in 2 hours at the exclusion distance.

14.3.9.6 Rainout

The extent of airborne activity which may be brought down by a sustained rain occurring at the time of the atmosphere release was calculated. It has been shown in 2.3 that most of the rainfall in the Great Central Valley of California is brought from the SE-SSE by Pacific storms. Based on the precipitation data at Sacramento, the following assumptions, believed to be conservative were made for the rainout analysis based upon data presented in Appendix 2A.

0326

a. Duration of rainout - 8 hours

b. Rain Intensity - 0.05 inches/hour (0.127 cm/hr)

c. Neutral Meteorological Conditions (Class D)

d. Average Associated Wind Speed - 4.7 m/sec

The probability of wind continuing in one direction for 8 hours is approximately 10 percent. According to Engelmann[20], the washout coefficient for a rainfall of 0.127 cm/hr is 0.85×10^{-5}/sec, however, for the purpose of this calculation, a value for $\Lambda = 1 \times 10^{-4}$ is conservatively assumed.

The effect of rainout after the maximum hypothetical accident has been performed for the nearest source of potable water which will be the future Folsom South Canal passing at a distance of approximately 5 miles from the Rancho Seco site. All the existing sources of potable water open to the atmosphere are at significantly greater distances (see Subsection 2.4). A continuous 8-hour contamination of the canal water by the released iodine based on a 20° sector width at 5 miles and an average cloud concentration equal to 2/3 of the centerline concentration shows that 0.1 curies of I^{131} could be deposited in the canal water surface. However, since the proposed canal flow rate will be 3,500 ft^3/sec, the downstream dilution of I^{131} is $3.64 \times 10^{-8}\mu$ curies/cc, well below the $(MPC)_w$ value of $3 \times 10^{-7}\mu$ curies/cc.

14.3.9.7 Doses in the Control Room Following the MHA

Doses in the control room following the MHA accident will originate from three possible sources, as follows:

a. Direct gamma dose from fission product in the containment building through the3.75-feet thick concrete wall and 1-foot thick concrete ceiling in the control room.

b. Direct gamma dose from the plume resulting from containment building leakage when it passes over the control room.

c. Direct gamma dose from fractional amounts of fission products which may reach the control room with the ventilation make-up air.

Direct gamma doses in the control room from the containment building and from the plume are essentially due to 2 Mev gammas from krypton-87, krypton-88 and 1.5 Mev iodine-135. Contributions from isotopes of lower energy gammas is negligible since these are effectively screened out by the concrete shielding. These three isotopes have, however, relatively short half-lives and decay rapidly. For example, at the end of 100 hours following the accident, the combined gamma dose from these three isotopes has decreased to approximately 1/40 of the dose during the first hour. The following are the integrated 30-day dose contributions from the three sources mentioned above:

2

000 0327

a. Containment building - 0.3 rem

b. Effluent plume - 0.02 rem

c. Contaminated ventilation air - negligible

The containment building dose assumes a separation distance between reactor building and the receptor of at least 30 meters and a total concrete shield thickness of 4.75 feet. The doses from the contamination of the ventilation air will be minimized by appropriate design of the ventilation system, positioning of the intake vents and the use of filters. The positioning of the intake vents will give due consideration to the prevailing wind directions.

In conclusion, in view of the calculated dose levels and the conservative assumption on which these doses are based, a permanent occupancy of the control room following an MHA accident will be possible without exceeding 10 CFR 100 dose guidelines.

14.3.10 IODINE REMOVAL SENSITIVITY ANALYSIS

The reactor building spray system has two major functions following a loss-of-coolant accident. One of these functions is to reduce the temperature and pressure in the reactor building below the design values. The other is to remove most of the elemental iodine (I_2) in the reactor building atmosphere in as short a period of time as is practical. For this reason, the spray system uses a sodium thiosulfate solution.

The analysis of the capability of the spray system to remove iodine from the atmosphere was based on the work of Griffiths[14]. As shown by Taylor[15] the transfer of iodine into drops of caustic soda solution is gas film controlled. The additional condition of low iodine concentration e.g., $<10^{-7}$ gm/cm^3, leads to the following equation:

$$V_g = \frac{D_v}{d} (2 + 0.6\ Re^{1/2}\ Sc^{1/3})$$

where V_g = velocity of deposition, cm/sec

D_v = diffusivity for iodine in containment atmosphere, cm^2/sec

d = diameter of drops from spray, cm

Re = Reynolds number, $\frac{dv\rho}{\mu}$, where v, ρ, and μ are the velocity, density and viscosity of the containment atmosphere, respectively (in consistent units). For v, the terminal velocity of the drop of diameter d is used.

Sc = Schmidt number, $\frac{\mu}{\rho D_v}$ (consistent units)

000 0328

The removal of elemental iodine from the reactor building due to the operation of the spray system is given by the exponential equation:

$$A = A_o\, e^{-\lambda_s t}$$

where A_o = initial amount of I_2 in reactor building atmosphere, curies or curies/m^3

λ_s = iodine removal time constant, sec^{-1}

The iodine removal time constant is given by

$$\lambda_s = (V_g)\frac{S_d}{V_R}\ sec^{-1} \qquad |1$$

where V_g = velocity of deposition defined previously, cm/sec

S_d = total surface area of drops in the reactor building volume, cm^2

V_R = reactor building volume covered by the spray, cm^3

The value of S_d may be found from the following equation:

$$S_d = \frac{A_d\, F\, \bar{t}}{V_d}\ cm^2 \qquad |1$$

where A_d = surface area per drop, cm^2

V_d = volume per drop, cm^3

F = spray flow rate, cm^3/sec

$\bar{t}$ = average residence time of drop in the atmosphere, sec

For spherical drops $\frac{A_d}{V_d} = \frac{6}{d}$ Therefore,

$$S_d = \frac{6\, F\, \bar{t}}{d}\ cm^2 \qquad |1$$

and λ_s is given by $\lambda_s = \frac{6V_g\, F\, \bar{t}}{V_R\, d}\ sec^{-1}$

7100 0329

01

Calculations were made assuming different temperatures and pressures and different drop sizes. Ten different cases were investigated and the results are given in Table 14.3-2.

The effect of steam in containment air was investigated in Case 1. For Case 1 the containment atmosphere was assumed to be an air-steam mixture. In all other cases, an air atmosphere was assumed. It can be noted that assuming no steam in the containment atmosphere leads to slightly conservative results (compare Cases 1 and 2). It can be also noted, comparing Cases 1 and 2, that the analysis is not sensitive to pressure changes in the examined pressure range.

Figure 14.3-5 gives the relation between the drop size and iodine removal time constant. Figure 14.3-5 shows how the iodine concentration in the atmosphere is reduced with time for different drop sizes.

This analysis reveals that for drop sizes smaller than 1500 microns, the iodine concentration in the reactor building atmosphere will be reduced to 1| 5 percent of its initial value within about 12 minutes. For drop sizes of 1000 microns or less, the same concentration reduction occurs for one-half the spray system out of operation (1500 gpm spray flow rate).

To ensure excess reagent, a (one) molar solution of sodium thiosulphate is used.

It is seen that for the drop size chosen, 700 microns, and half the spray system out of operation, the iodine removal time constant is approximately 35 hr^{-1}. A very conservative value of 25 hr^{-1} was used in all calculations. When the airborne iodine concentration reaches 5 percent of its initial value, no further credit is taken for the effect of the spray system in removing airborne iodine. This corresponds to 1.25 percent of the initial core inventory of iodine which is not removed by spray. This is an additional conservative assumption which accounts for the methyl iodine released during and produced after the accident.[21-26]

14.3.11 POPULATION DENSITY CONSIDERATIONS

The above discussion concerning the environmental consequences of various accident conditions has demonstrated that the plant engineered safeguards adequately protect persons at the site exclusion area and low population zone boundaries from radiation exposure in excess of guidelines set forth in 10-CFR-100.

A further objective of the siting criteria is to assure that the cummulative dose to large numbers of persons which could result from any nuclear accident is low in comparison with the AEC guideline values.

To illustrate that the population center distance criteria are effectively met, Table 14.3-3 has been prepared. This tabulation indicates the total man-rem exposures occurring in the Sacramento and Stockton sectors and is

000 0330

TABLE 14.3-2
SUMMARY OF THE SENSITIVITY ANALYSIS OF IODINE REMOVAL SHOWING THE EFFECTS OF PARAMETER VARIATIONS

Case No.	Drop Size (Microns)	Drop Fall Velocity cm/sec	Velocity of Deposition V_g cm/sec	Temp. ^oF	Press Psig	λs Hr^{-1}	Comments
1	1000	400	6.25	281	59	35.2* (17.6)**	Air-Steam Mix
2	1000	400	6.08	281	55	34.2 (17.1)	All Air
3	1000	400	7.72	212	25	43.5 (21.75)	All Air
4	1000	400	11.6	100	0	65.4 (32.7)	All Air
5	200	76	8.14	281	55	1200 (600)	All Air
6	600	237	6.41	281	55	101.5 (50.75)	All Air
7	800	320	6.2	281	55	54.4 (27.2)	All Air
8	1200	475	5.95	281	55	23.4 (11.7)	All Air
9	1400	550	5.89	281	55	17.2 (8.6)	All Air
10	1500	590	5.86	281	55	14.9 (7.45)	All Air

*Spray Flow Rate = 3000 GPM
**Spray Flow Rate = 1500 GPM

000 331

computed using the projected 1985 population distribution presented in Figure 2.2-6 and the calculated maximum hypothetical accident (MHA) thyroid dose versus distance curve shown in Figure 14.3-2. These two sectors are the most highly-populated sectors surrounding the Rancho Seco site. 2

TABLE 14.3-3
SMUD SITE POPULATION
DISTRIBUTION AND INTEGRATED
MAN-REM EXPOSURES

Distance (Miles)	22.5° Sector Thru Sacramento		22.5° Sector Thru Stockton	
	Population (2000)	Man-Rem	Population (2000)	Man-Rem
0-5	14	70	12	60
5-10	580	696	483	580
10-20	83,984	40,312	43,340	20,803
20-30	634,021	158,505	256,737	64,184
30-40	39,098	6,256	32,900	5,264
40-50	18,991	2,279	41,681	5,002
Total	776,688	208,118	375,153	95,893

The man-rem exposure limits implicit in the 10-CFR-100 population center criteria can be estimated by considering the residents of a population center of 25,000 persons (located 1-1/3 times the distance from the reactor to the outer boundary of the low population zone) receive an exposure from a cloud less than 300 rem at the nearest low population zone out boundary. This would give a corresponding dose of about 180 rem at the population center. An integrated 30-day thyroid dose of about 4.5×10^6 man-rem would result under these conditions.

The man-rem exposures indicated in Table 14.3-3 are considerably below the limiting values indicated in 10 CFR 100 and TID-14844 for population centers.

000 0332

00

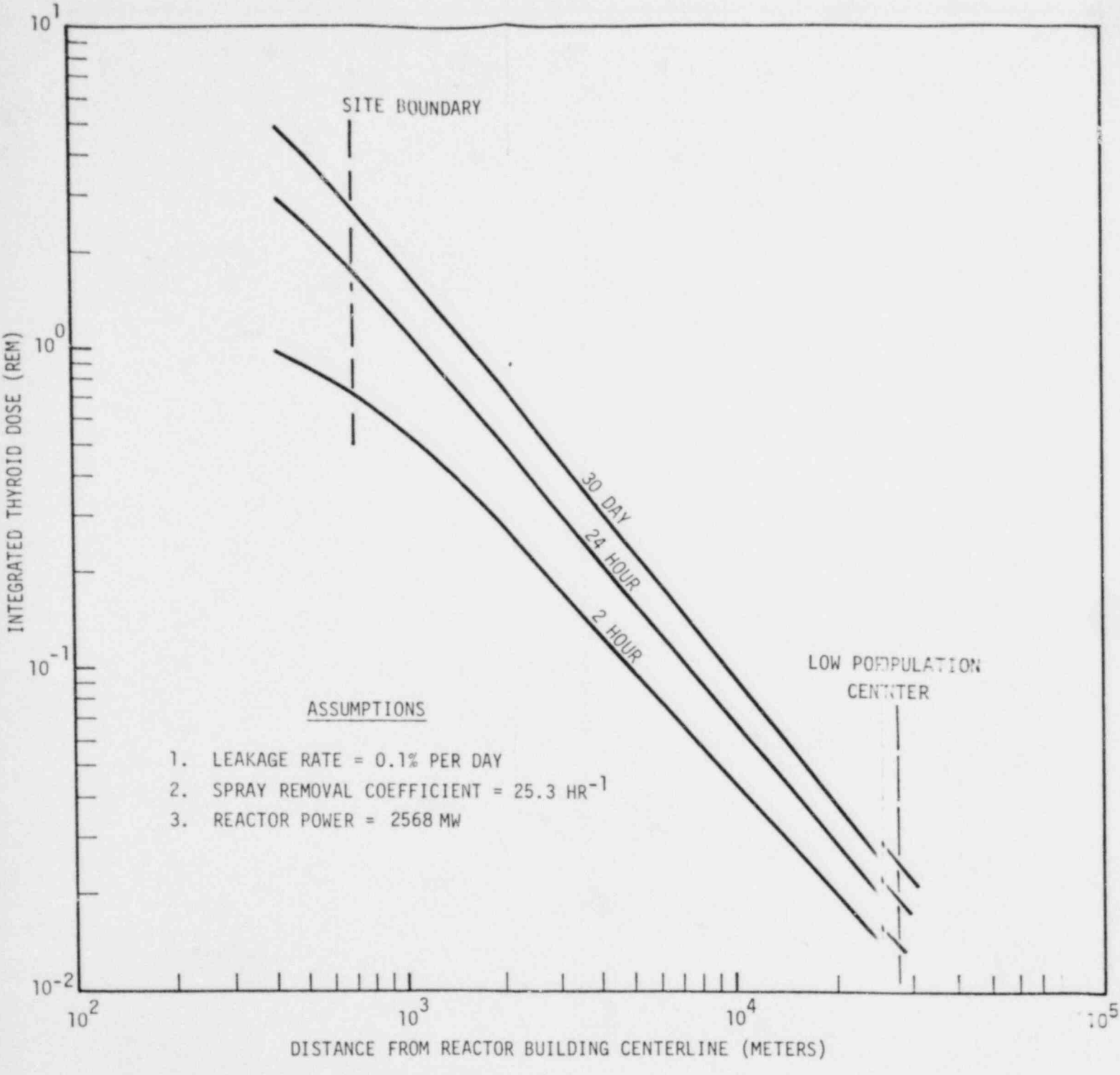

000 0333

FIGURE 14.3-11
THYROID DOSE FROM
LOSS-OF-COOLANT ACCIDENT

00

SMUD

SACRAMENTO MUNICIPAL UTILITY DISTRICT

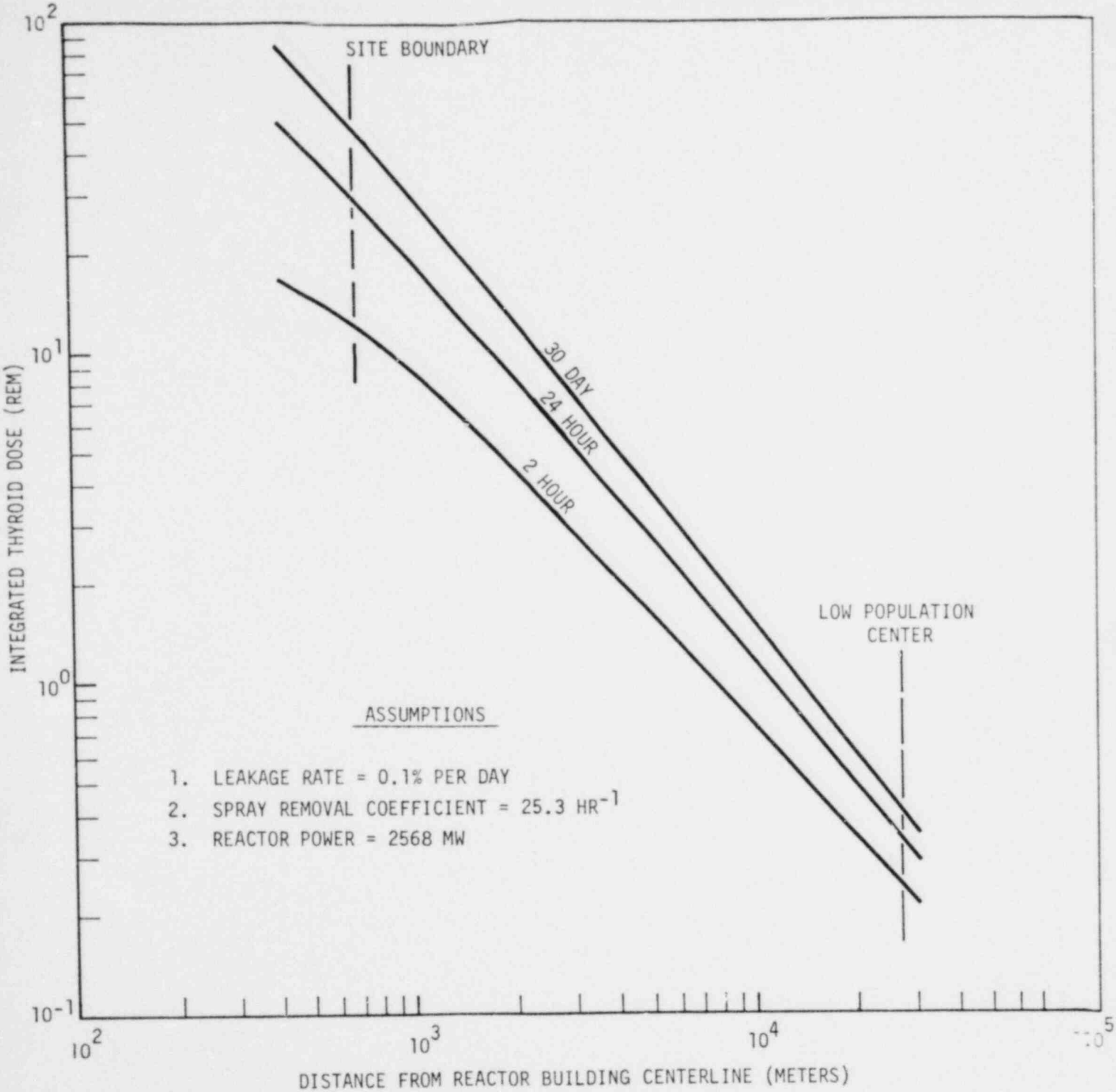

FIGURE 14.3-2
THYROID DOSE FROM THE
MAXIMUM HYPOTHETICAL ACCIDENT

000 0534

SMUD
SACRAMENTO MUNICIPAL UTILITY DISTRICT

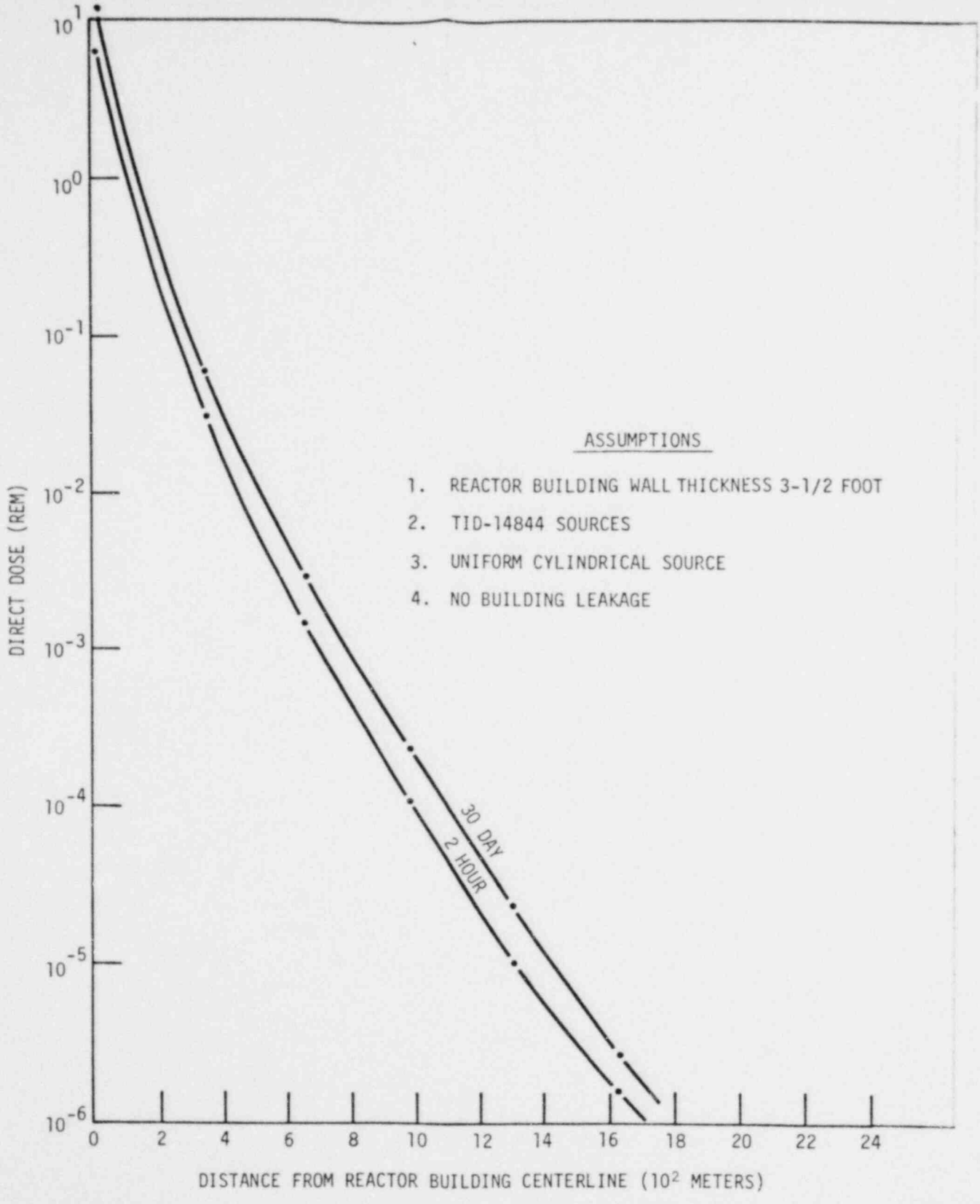

FIGURE 14.3-3
REACTOR BUILDING DIRECT
DOSE FOLLOWING MHA

000 0535

SMUD

SACRAMENTO MUNICIPAL UTILITY DISTRICT

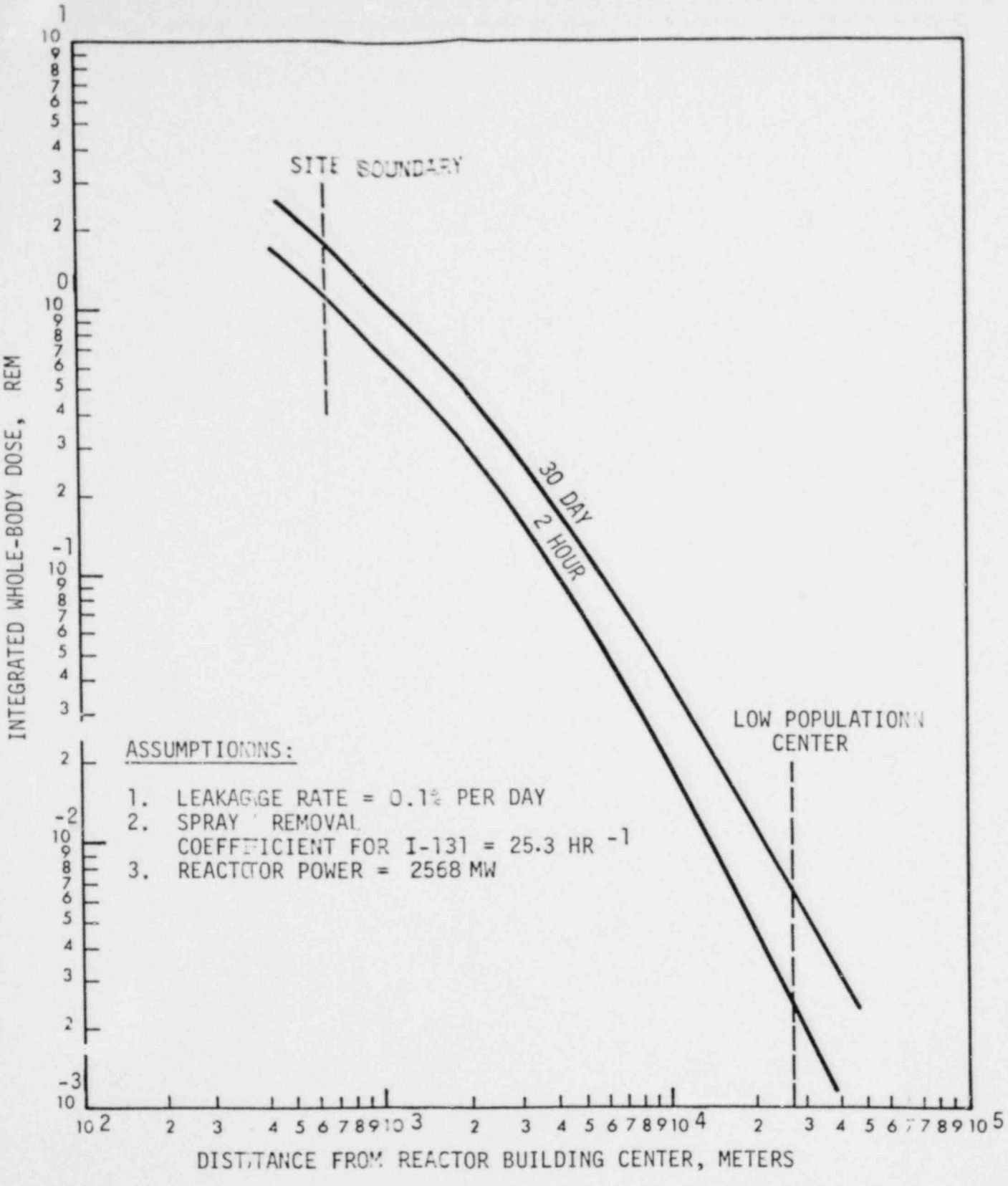

000 0336

FIGURE 14.3-4
WHOLE-BODY CLOUD DOSE
FOLLOWING MHA

SMUD
SACRAMENTO MUNICIPAL UTILITY DISTRICT

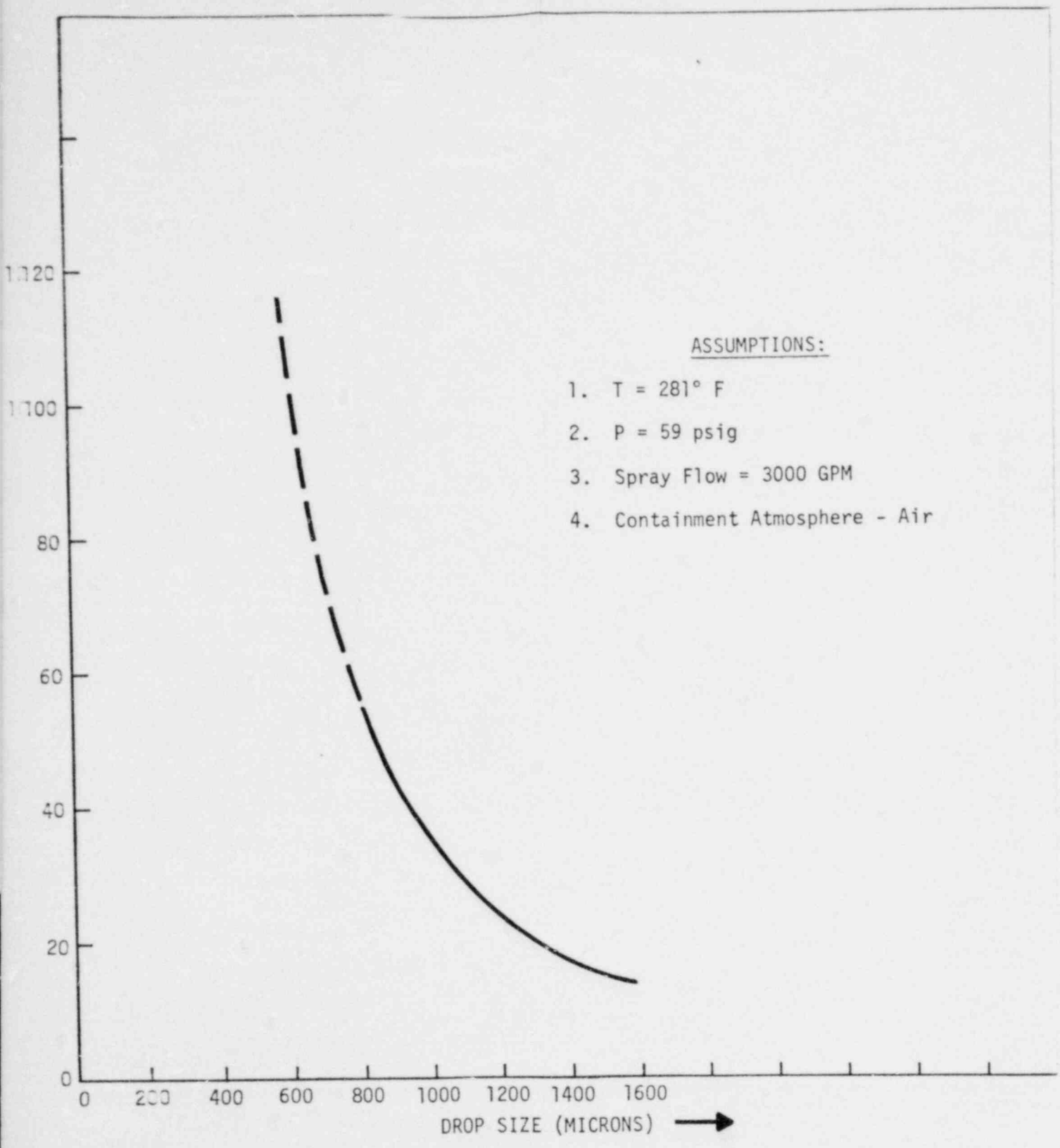

FIGURE 14.3-5
IODINE REMOVAL TIME CONSTANT

000 0337

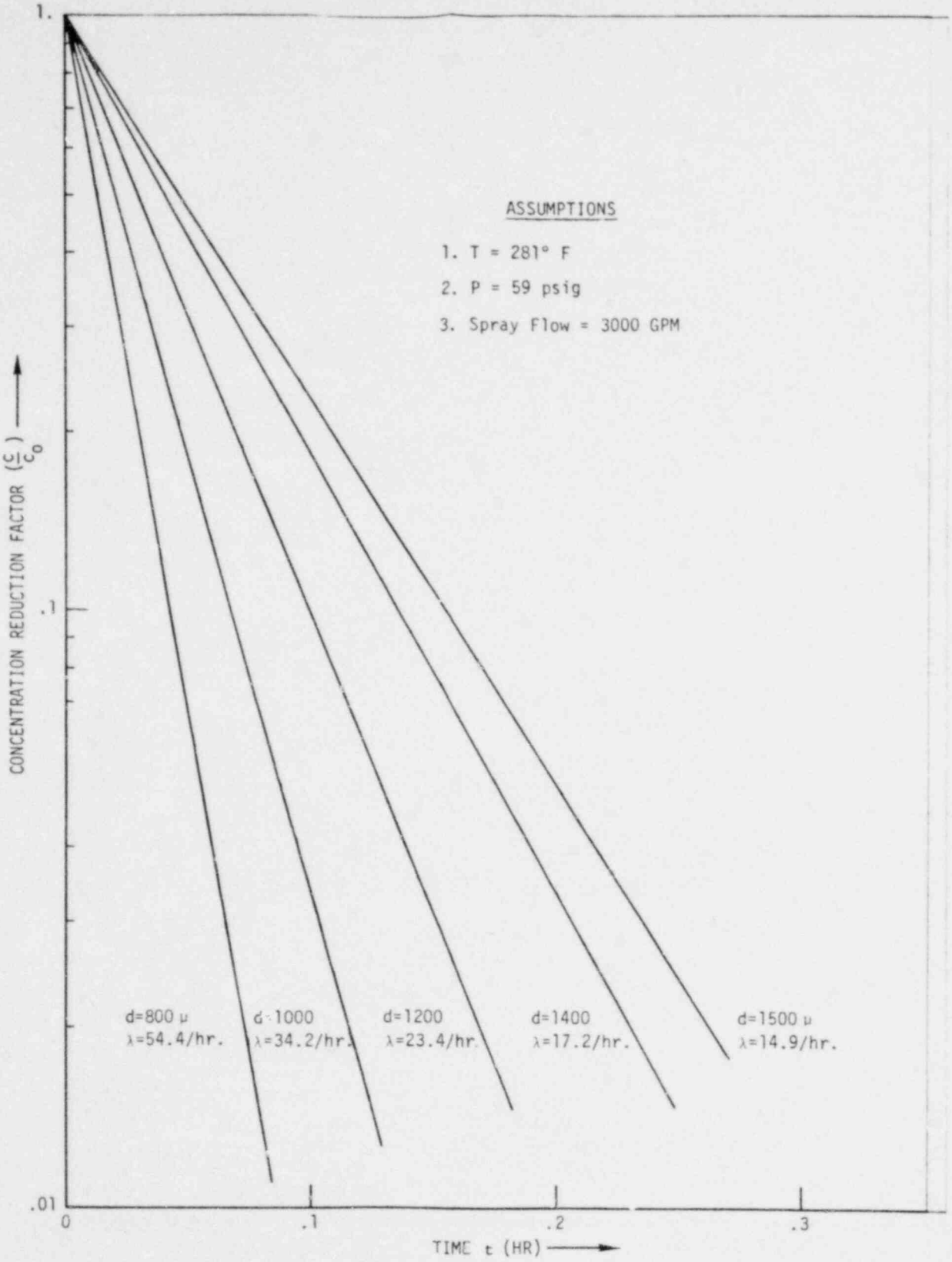

FIGURE 14.3-6
CLOUD CONCENTRATION REDUCTION FACTOR
AS A FUNCTION OF DROPLET SIZE

000 0338

00

SMUD
SACRAMENTO MUNICIPAL UTILITY DISTRICT

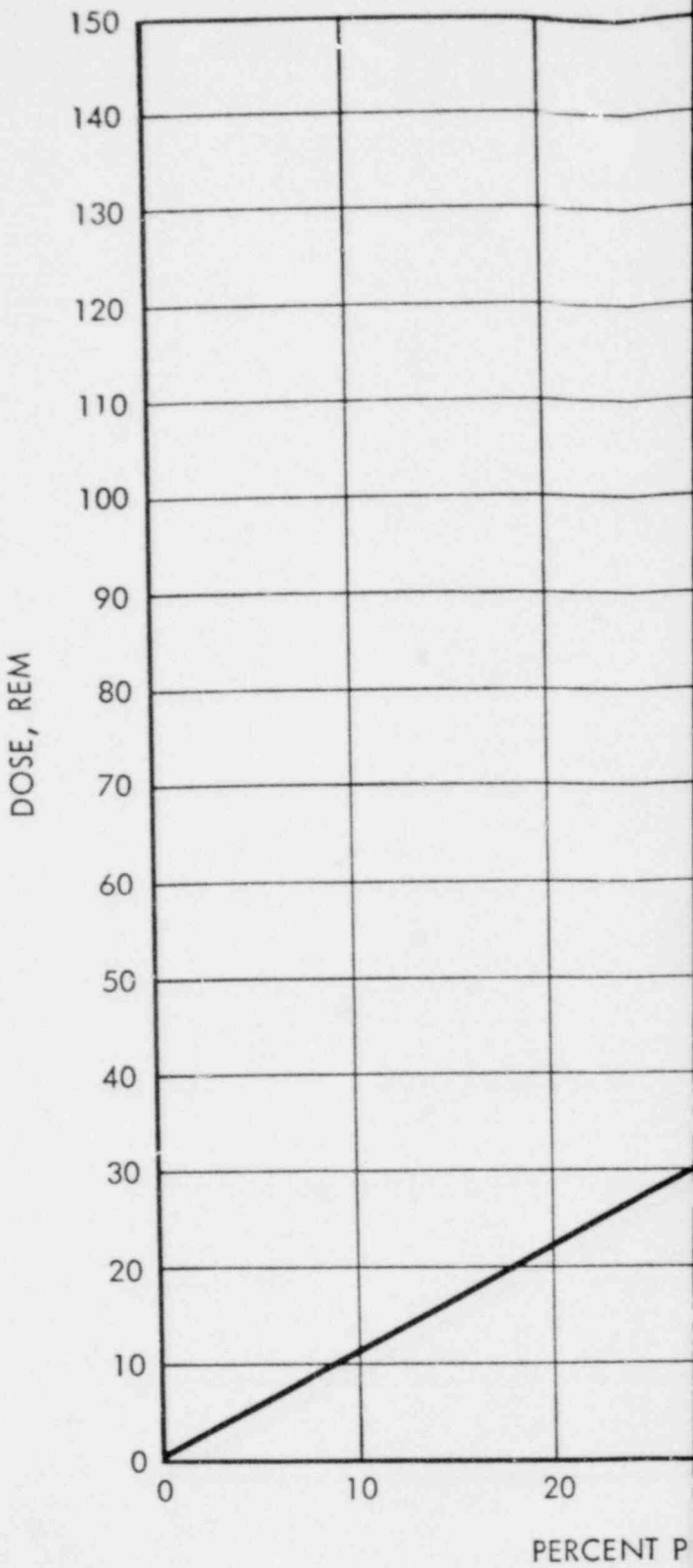
150
140
130
120
110
100
90
80
70
60
50
40
30
20
10
0
DOSE, REM
0
10
20
PERCENT P

000 0339

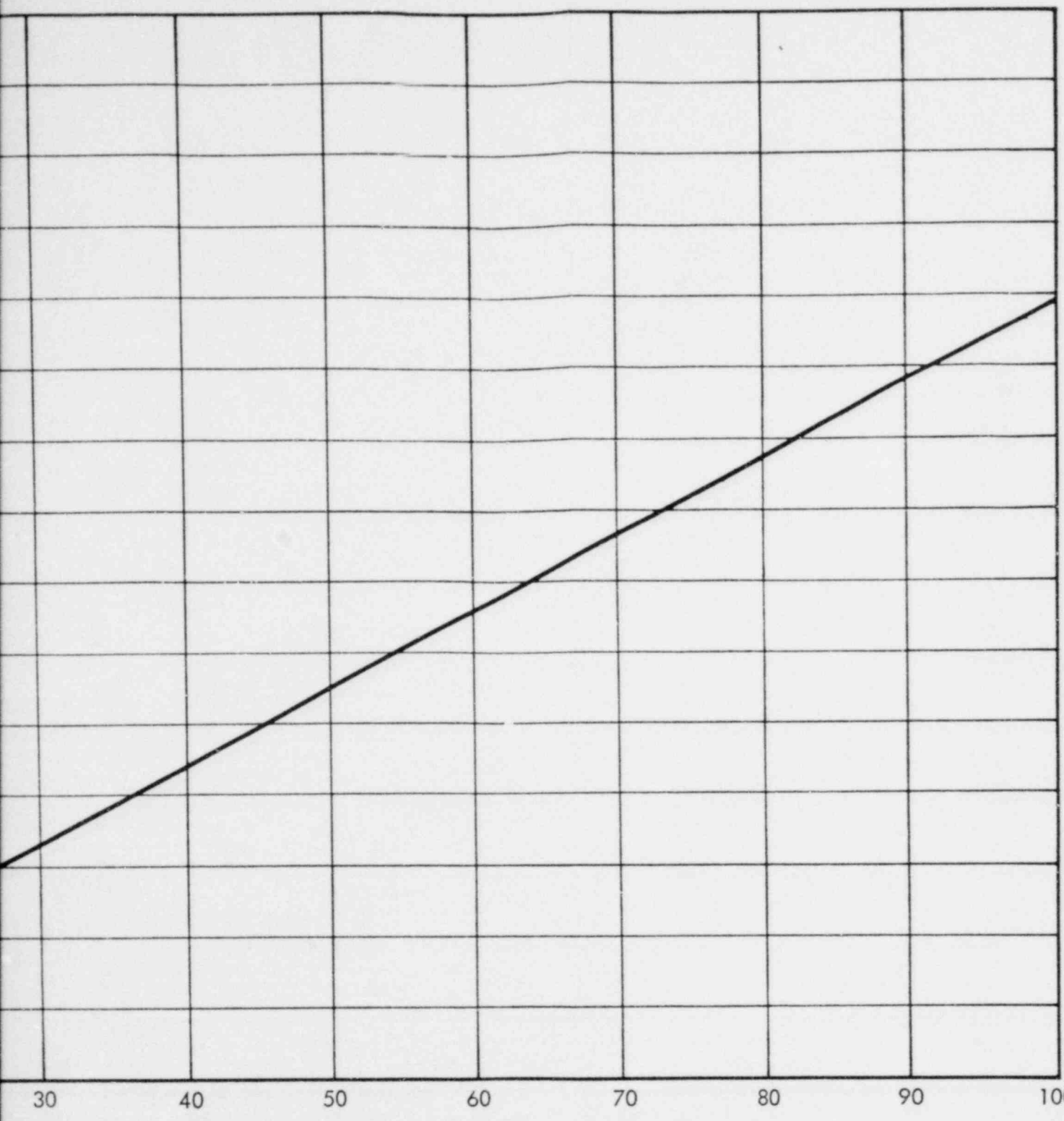

RIMARY COOLANT INSTANTANEOUSLY RELEASED TO THE ATMOSPHERE

FIGURE 14.3-7
THYROID DOSE AT THE SITE BOUNDARY

000 0340

14.4 REFERENCES

1. Watson, L. C., Bancroft, A. R., and Hoelke, C. W., Iodine Containment by Dousing in NPD-11, AECL-1130.

2. Styrikovich, M. A., et al., "Transfer of Iodine from Aqueous Solutions to Saturated Vapor", Soviet Journal of Atomic Energy 17, July 1964.

3. Disperson of Soluble Radioactive Material in Water, CF-58-3-109.

4. International Symposium on Fission Product Release and Transport Under Accident Conditions, Oak Ridge, Tennessee, April 1965.

5. Liimatainen, R. C., et al., Studies of Metal-Water Reactions at High Temperature, ANL-6250.

6. Ackerman, R., et al., "High Temperature Vapor Pressure of UO_2", Journal of Chemical Physics, December 1956.

7. Reactor Development Program Progress Report, ANL-6912, June 1964.

8. AEC Research and Development Reports, WIGL2 - A program for the Solution of the One-Dimensional Two-Group, Space-Time Diffusion Equations Accounting for Temperature, Xenon and Control Feedback, WAPD-TM-532, October 1965.

9. Margolis, S. G. and Redrield, J. A., FLASH: A Program for Digital Simulation of the Loss-of-Coolant Accident, WAPD-TM-534, May 1966.

10. Grenda, R. J. and Patterson, J. F., "The Velocity of Rising Steam in a Bubbling Two-Phase Mixture," Transactions of the ANS 5, No. 1, p 151, June 1962.

11. Possible Zirconium Water Reactions in Water Reactors, AEC Regulatory Staff Symposium, April 27, 1965.

12. Wagner, R. J. and Finnegan, L. J., "An Analytical Model for Predicting the Pressure-Temperature History Within a Containment Vessel in Response to a Loss-of-Coolant Accident," Phillips Petroleum Company, Atomic Energy Division, Idaho Falls, Idaho, Presented at ANS Meeting, Washington, D.C., November 1965.

13. Quinn, E. P., Forced-Flow Heat Transfer to High-Pressure Water Beyond the Critical Heat Flux, ASME 66WA/HT-36, November 27, 1966.

14. Griffiths, V., The Removal of Iodine from the Atmosphere by Sprays, AHSB (S) R 45, 1963.

15. Taylor, R. F., "Absorption of Iodine Vapor by Aqueous Solutions", Chem. Eng. Sa., X, No. 1/2, pp 68-80, April 1959.

16. Ranz, W. E. and Marshall, W. R., Chem. Eng. Progress, 48, 141, 173, 1952.

0341

17. R. A. Langley, Jr., COPATTA Program Description. To be published. Bechtel Corp., San Francisco.

18. A. Kolflat and W. A. Chittenden, "A New Approach to the Design of Containment Shells for Atomic Power Plants," Atomic Power Engineering Group, Sargent and Lundy, Engineers, Chicago.

19. D. S. Duncan and A. B. Speir, "GRACE II An IBM-709 Program for Computing Gamma-Ray Attenuation and Heating in Cylindrical and Sperical Geometries," NAA-SR-Memo-4649, November, 1959.

20. R. J. Engelmann, "Calculation of Precipitation Scavenging of Particulates and Gases from the Atmosphere," Nuclear Safety Vol. 7, No. 3 Spring 1966.

21. V. Griffiths, "The Removal of Iodine from the Atmosphere by Sprays." AHSB (S) R45, (1963).

22. R. F. Taylor, "Absorption of Iodine Vapor by Aqueous Solutions," Chemical Engineering Science, Vol. 10, p. 68-79, (1959).

23. E. W. R. Steacie and R. D. McDonald "The Kinetics of the Thermal Decomposition of Gaseous Methyl Iodine" J. A. C. S., Vol. 57, Part 1, page 488 (1935).

24. J. F. Croft, et. al. "Experiments on the Deposition of Airborne Iodine of High Concentration" AEEW-R265, June 1963.

25. J. D. McCormack and R. K. Hilliard "Natural Removal of Fission Products Released from UO_2 Fuel in Condensing Steam Environments," International Symposium of Fission Product and Transport Under Accident Conditions, CONF-650407, April 1965.

26. G. W. Parker, et. al. "Behavior of Fission Products Released from Simulated Fuels in the Containment Mockup Facility," p. 83, Nuclear Safety Program Semiannual Progress Report for Period Ending June 30, 1965, ORNL-3843.

27. J. F. Wilson, et. al., "The Velocity of Rising Steam in a Bubbling Two-Phase Mixture," Transactions of the ANS, Vol. 5, No. 1, p 151, June 1962.

000 0348

002